PHD COURSE IN EXPERIMENTAL MEDICINE

XXXII CYCLE

CURRICULUM OF PHARMACOLOGY AND TOXICOLOGY

DEPARTMENT OF PHARMACY

UNIVERSITY OF GENOA

Mesenchymal stem cell-derived exosomes and exosome-shuttled miRNAs ameliorate the reactive and neurotoxic phenotype of mouse SOD1^{G93A} astrocytes and human-derived SOD1^{A4V} astrocytes

---

PhD student: *Francesca Provenzano*

Tutor: *Professor Giambattista Bonanno*

PUBLICATIONS

The data described in this thesis represent the work done for my PhD project and are the matter of a manuscript in preparation. During my doctorate course I collaborated to other research of the group on ALS, that produced the following five papers:

Bonifacino T., Cattaneo L., Gallia E., Puliti A., Melone M., **Provenzano F**., Bossi S., Musante I., Usai C., Conti F., Bonanno G., Milanese M. In-vivo effects of knocking-down metabotropic glutamate receptor 5 in the SOD1^{G93A} mouse model of amyotrophic lateral sclerosis. Neuropharmacology 2017, vol. 123:433-445, doi: 10.1016/j.neuropharm.2017.06.020.

Ravera S., Bonifacino T., Bartolucci M., Milanese M., Gallia E., **Provenzano F**., Cortese K., Panfoli I., Bonanno G. Characterization of the mitochondrial aerobic metabolism in the pre- and perisynaptic districts of the SOD1^{G93A} mouse model of amyotrophic lateral sclerosis. Mol Neurobiol. 2018 Apr 14. doi: 10.1007/s12035-018-1059-z.

Bonifacino T., **Provenzano F.**, Gallia E., Ravera S., Torazza C., Bossi S., Ferrando S., Puliti A., Van Den Bosch L., Bonanno G., Milanese M. In-vivo genetic ablation of metabotropic glutamate receptortype 5 slows down disease progression in the SOD1^{G93A} mouse model of amyotrophic lateral sclerosis. Neurobiol Dis. 2019 May 15. doi: 10.1016/j.nbd.2019.05.007.

Ravera S., Torazza C., Bonifacino T., **Provenzano F.**, Rebosio C., Milanese M., Usai C., Panfoli I., Bonanno G. Altered glucose catabolism in the presynaptic and perisynaptic compartments of SOD1^{G93A} mouse spinal cord and motor cortex indicate that mitochondria are the site of bioenergetic imbalance in ALS. J Neurochem. 2019 Jul 8. doi: 10.1111/jnc.14819.

Bonifacino T., Rebosio C., **Provenzano F.**, Torazza C., Balbi M., Milanese M., Raiteri L., Usai C., Fedele E., Bonanno G. Enhanced function and overexpression of metabotropic glutamate receptors 1 and 5 in the spinal cord of the SOD1^{G93A} mouse model of amyotrophic lateral sclerosis during disease progression. Int J Mol Sci. 2019 Sep 13;20(18). doi: 10.3390/ijms20184552.

TABLE OF CONTENTS

ABSTRACT

Amyotrophic lateral sclerosis (ALS) is a fatal neurodegenerative disease affecting primarily motor neurons (MNs) but involving also non-neuronal cells. Nowadays, it is well recognised that astrocytes, microglia and oligodendrocytes play a central role in disease onset and progression. In particular, astrocytes acquire a toxic phenotype characterized by an abnormal proliferation and by the release of neurotoxic factors, including pro-inflammatory cytokines (Lee et al., 2016).

We have previously shown that the intravenous administration of mesenchymal stem cells (MSCs) in $SOD1^{G93A}$ mice prolonged survival, ameliorated motor skills and reduced gliosis and inflammation in spinal cord. These beneficial effects were not associated with MSC differentiation, being possibly mediated through paracrine mechanisms. We hypothesized that MSC-derived exosomes and exosome-shuttled miRNAs could mediate these positive effects. To verify our hypothesis we tested here the effects of exosomes derived from INFγ-activated MSCs on cultured astrocytes prepared from the spinal cord of 120 day-old late-symptomatic $SOD1^{G93A}$ mice.

The phenotype of $SOD1^{G93A}$ astrocytes and the efficacy of the exosome treatment were characterized by Western blotting, confocal microscopy and ELISA immunoassay.

Vimentin, GFAP and S100β, astrogliosis markers, were increased in astrocytes from 120 days-old $SOD1^{G93A}$ mice vs. age-matched WT astrocytes and their expression was reduced after exposure to exosomes. Nrf2, a booster of the response to oxidative stress, was decreased in $SOD1^{G93A}$ astrocytes vs. age-matched WT astrocytes. Exosome treatment normalized Nrf2 down-regulation both in the cytoplasm and nucleus.

The quantification of TNF-α, IL-1β, IL-6 and CCL2 expression and release showed that these four pro-inflammatory factors were more expressed in and more efficiently released from SOD1^{G93A} astrocytes and that the exposure to exosomes resulted in a significant decrease of their over-expression and release.

Conversely, the anti-inflammatory cytokine IL-10 was decreased in SOD1^{G93A} astrocytes and its expression was normalized after exposure to exosomes. Also NLRP3 expression, a marker of the multiprotein oligomer inflammasome, was increased in SOD1^{G93A} astrocytes and the increase was reversed by exosomes.

The amelioration of SOD1^{G93A} astrocyte phenotype had a positive impact on MN viability in astrocyte-MN co-cultures. We observed a constant decrease of MN survival during time, both in control and exosome-treated co-cultures; however, the viability of MNs seeded on exosome-treated SOD1^{G93A} astrocytes was always significantly higher when compared to co-cultures with untreated astrocytes.

Exosome cargo was analysed for miRNAs and potential mediators of exosome activity were identified. The selected miRNAs showed a significant efficacy to reduce GFAP, IL-1β and TNF-α expression. Computational analysis highlighted their possible involvement in the modulation of NFκB and MAPK pathway activation, affecting numerous kinases and transcription factors involved in the regulation of these inflammatory signalling pathways. qPCR analysis confirmed the ability of these four miRNAs to reduce MAPK11 expression and to regulate TNF-α synthesis.

Finally, we translated this study to human astrocytes derived from healthy donors and ALS patients carrying the A4V-SOD1 mutation. Human ALS astrocytes were treated with exosomes derived from human MSCs, activated with INFγ. We observed only a slight

amelioration of ALS astrocyte phenotype after the exosome treatment. Remarkably, analysis of MN viability showed an increased MN number in co-cultures with exosome-treated astrocytes compared to those co-cultured with untreated astrocytes.

These results indicate that exosomes and exosome-shuttled miRNAs can reduce astrocyte reactivity and that this effect has a positive impact on MN viability. The in-vitro exosome activity, both in mouse and human models, paves the way to translational preclinical *in-vivo* treatments in $SOD1^{G93A}$ mice.

1. INTRODUCTION

1.1 The ALS Disease

Amyotrophic lateral sclerosis (ALS) is a progressive neurodegenerative disease. Main feature of the pathology is the death of motor neurons (MNs) in the motor cortex and spinal cord (Brown, 1995). The mean age of onset is 55-60 years of age and within 3-5 years from clinical onset patients succumb to the disease (Williams and Windebank, 1991). The first clinical symptom is represented by muscle weakness, which evolves with the progression of the disease in severe muscle atrophy, paralysis and finally respiratory failure due to diaphragm denervation.

The first ALS cases were reported in 1824 by Charles Bell, but the first to discover the relationship between the clinical signs and the findings at autopsy was Jean-Martin Charcot. He deduced the correlation that links the deformity of limbs due to muscle spasticity with the corticospinal tract pathology. From this evidence he coined the name of the disease (Rowland, 2001), the etymology of which describes some characteristics of the disease: “amyotrophic” describes the peculiar muscle atrophy, weakness and fasciculation due to death of the lower MNs; “lateral sclerosis” indicates the hardness to palpation of the lateral columns of the spinal cord in autopsy specimens, which is determined by gliosis following the degeneration of the cortico-spinal tracts.

Currently, the incidence of ALS is 2-3 new cases per 100,000 inhabitants/year and the prevalence is about 7-9 cases/100,000 inhabitants in occidental countries (Hardimanet al., 2017). The disease affects men more commonly than women. There are some world areas where the incidence is 50-100 times higher compared to normal values (Steele e McGeere, 2008), such as in Japan, Guam Island, Kii peninsula and in south-west of New Guinea (Kurtzke, 1982; Kuzuhara et al., 2001). It is believed that this incidence augmentation

could be determined by environmental factors, in particular from a cyanotoxin, the β-N-Methylamino-L-Alanine (BMAA), contained in cycadales seeds that are used to produce flour. One of the hypothesis is that these populations are unable to prevent BMAA accumulation, causing an high concentration of BMAA in the organism, that can determine an abnormal activation of glutamate receptors and lead to excitotoxicity (Cox et al, 2018; Rao et al., 2006).

There a two different forms of ALS depending on the origin of the degeneration: bulbar ALS and spinal ALS. The bulbar form of ALS derives from secondary MN death. It is characterized by speech disorders, tongue atrophy, dysphagia and abnormal salivation. If the symptoms are due to primary MN degeneration ALS is consider pseudobulbar, in which patients can have problems to control emotions and they are affected by uncontrollable laugh and cry. In both forms muscle weakness occurs 1-2 years after first symptoms but the progression to respiratory failure is within 2-3 years, faster than spinal form of ALS. In the spinal form of ALS the disease arises in limb weakness that can affect both superior and inferior limbs. Moreover, spinal ALS patients can even develop bulbar symptoms during disease progression and respiratory failure occurs within 3-5 years. This form is characterized by asymmetric muscle atrophy and spasticity of hands, forearms, shoulders and legs.

Unfortunately, there is not a treatment able to efficaciously contrast the fast progression of ALS for both forms of the disease. The Food and Drug Administration (FDA), and then also the European Medicine Agency, approved two drugs for ALS treatment: Riluzole and Edaravone, which act on neuron excitability and oxidative stress, respectively. But, since these two drugs have only a modest impact on ALS symptoms and on life quality of patients, there is an urgent needed to investigate deeper the mechanisms underlying the

pathogenesis of ALS in order to identify potential new targets to modulate the disease. Of primary importance is the possibility of selecting early biomarkers of ALS, to stratify patients according to their specific disease signature and to intervene at an early stage of the disease.

1.2 Genetic bases of ALS

1.2.1 Familial and sporadic ALS

ALS patients can be divided in two groups, namely familial (fALS) and sporadic (sALS). Approximately 10% of the total ALS cases are familial and based on genetic mutations which are usually inherited in a mendelian autosomal dominant manner (Oskarsson et al. 2018).

The first ALS-linked mutation to have been discovered was on the gene encoding copper-zinc superoxide dismutase (SOD1) (Rosen, 1993). SOD1 mutations represent about 15% of fALS cases (Volk et al., 2018). The most common mutation identified is a hexancleotide GGGGCC (G_4C_2) repeat expansion in the chromosome 9 open reading frame 72 (C9orf72) gene. This mutation was described for the first time in 2006 in Scandinavian and Dutch patients presenting ALS and fronto-temporal dementia (Vance et al., 2006; Morita et al., 2006) and involves 30-40% of fALS (Oskarsson et al. 2018). Many other mutations have been described, such as in Trans-activation response (TAR) DNA-binding protein 43 (TDP-43 or TARDPB), Fused in sarcoma/translated in liposarcoma (FUS/TLS or FUS), vesicle-associated membrane protein associated B (VAPB), valosin-containing protein (VCP), alsin (ALS2), tumor necrosis factor (TNF) receptor-associated factor NF-κB activator (TANK)-binding kinase 1 (TBK1) (Mathis et al., 2019; Volk et al., 2018). During

the last years an increased number of mutations linked to ALS has been described; indeed, at least 30 fALS-related genes have been discovered.

On the contrary, the aetiology of sporadic ALS is still largely unknown. The main hypothesis at the basis of sporadic ALS pathogenesis is a higher genetic susceptibility to environmental factors. Some works determined a correlation between ALS risk and exposure to pesticides in patients with polymorphism of PON1, PON2 or PON3 genes (Slowik et al. 2006, Ticozzi et al. 2010) or with a reduction of their expression (Gagliardi et al. 2013). These genes codify for A-esterase paraoxonase, which is able to detoxify organophosphate pesticides and their activity is dependent on different genetic variants, which could determine a decreased detoxifying activity. Many studies reported a relationship between ALS and professional soccer activity. The cause of this supposed correlation is still unclear, there are many hypotheses trying to explain this epidemiological finding, such as an excessive physical activity, repeated head injuries, exposure to pesticides and dietary supplements or illegal substances. However, these results derived from retrospective studies that did not show a significant correlation between ALS and diverse environmental factors, therefore the role of these risk factors in ALS remains only a hypothesis, requiring further studies, possibly, over a long period of time (Chio et al., 2005; Chio et al., 2009; Bozzoni et al., 2016).

Even if the cause is different, fALS and sALS present indistinguishable clinical symptoms and biological features. Today it is well known that ALS is a multifactorial and non-cell autonomous disease. Indeed, many factors have been proposed to be at the basis of MN degeneration and cell types of central nervous system (CNS) other than neurons are subjected to alterations which promote the development of a toxic environment in ALS.

1.2.2 Genetic mutation in ALS

1.2.2.1 SOD1 mutations

A mutation of SOD1 was first discovered in 1993. Today, over 180 mutations have been identified, including single point mutations, deletions, insertions and truncations. The SOD1 gene is located on chromosome 21q22.11 and is composed of five exons encoding for 153 amino acids which generate the SOD1 enzyme protein. This enzyme is ubiquitously expressed and highly conserved across species and localizes in the cytoplasm, nucleus, lysosomes and intermembrane space of mitochondria, where it binds copper and zinc ions and forms a homodimer displaying dismutase function; thus removing dangerous superoxide radicals by metabolizing them to molecular oxygen and hydrogen peroxide, thus providing a defence against oxygen toxicity (Saccon et al., 2013).

The most common mutations of the SOD1 gene are the D90A (aspartic acid at codon 90 changed to alanine), the A4V (alanine at codon 4 changed to valine) and G93A (glycine at codon 93 changed to alanine). The D90A mutation is the most abundant mutation in SOD1 gene, the A4V mutation is linked to approximately 50% of fALS case in the U.S.A. population and the G93A mutation is more rare but it is one of the most studied in a transgenic model of the disease, because it is able to generate degeneration of MNs and ALS symptoms close to human disease (Pansarasa et al., 2018; Andersen 2006).

The mutations in SOD1 gene lead to an unknown gain of function of the enzyme that may determine increased production of reactive oxygen species (ROS). Moreover, the mutation in SOD1 gene determines the formation of misfolded SOD1 protein and the formation of aggregates, triggering abnormal mitochondrial function, endoplasmic reticulum (ER) stress, axonal transport defects, excessive production of extracellular superoxide, and

oxidative damage from aberrantly secreted mutant SOD1 (Illieva et al., 2009). In particular, mutated SOD1 is able to activate a cascade of events in different cellular pathways involving MNs, astrocytes and oligodendrocytes. Selective expression of mutated SOD1 in MNs determined changes in RNA expression at early stage of the disease, causing ER stress, synapse and metabolic abnormalities. Selective expression of mutated SOD1 in astrocytes stimulates RNA changes later in the disease, affecting gene involved in inflammation and metabolism (Sun et al., 2015).

Finally, early RNA changes, consisting mainly in the dysregulation of myelination and lipid signalling pathways, appeared when expressing selectively mutated SOD1 in oligodendrocytes. This analysis revealed that ER stress in motor neurons is an initiating event, after which a dysregulation of lipid signalling occurs in the three cell types, probably due to an abnormal association with membranes of misfolded SOD1. Since MNs produce high levels of SOD1 and have very low levels of ER chaperones, they represent the most vulnerable cells to misfolded SOD1 accumulation. The subsequent damage caused by mutated SOD1 in astrocytes and oligodendrocytes is essential to sustain and amplify the first toxic events within MNs (Sun et al., 2015).

New evidence shows that WT-SOD1 may be involved also in sALS pathogenesis. Gruzman and collegues (2007) detected a modified 32-kDa SOD1 polypeptide, characterized by a covalent bond between the two monomers, which is present, together with the well know 16-kDa SOD1 polipeptide, in spinal cord extracts from fALS and sALS patients but not in the control group (Gruzman et al., 2007). This discovery stimulated further studies on the role of SOD1 in sALS patients, which revealed that WT-SOD1 can acquire the toxic properties of mutant SOD1, thus determining the development of aggregates, in particular in the nuclei of astrocytes of spinal cords of ALS patients (Ezzi

et al., 2007; Forsberg et al., 2011). Finally, a loss of function of WT-SOD1 in sALS was observed. Indeed, the level of WT-SOD1 inside the nuclei of MNs and leukocytes is strongly reduced in sALS patients, leading to increase of DNA damage and, consequently, to a more severe disease progression (Cereda et al., 2013; Sau et al., 2007).

1.2.2.2 C9orf72 mutations

The C9orf72 mutation in ALS and FTD patients was identified for the first time in 2006, but only in 2011 it was revealed that this mutation is an expansion of G_4C_2 hexanucleotide repeat (HRE) in a non-coding region of the C9orf72 gene. The size of the repeats in ALS and FTD cases ranges between 700 and 1,600 as compared to 2-23 in control individuals. As for the majority of ALS-related mutations, also the C9orf72 mutation presents autosomal dominant inheritance (Hosler et al., 2000). ALS caused by C9orf72 mutation is characterized by early disease onset with bulbar involvement, cognitive and behavioural disorders, marked by psychosis and Parkinsonism in many cases (Kumar et al., 2017).

The C9orf72 protein functions are still unknown. From bioinformatic data, it seems to belong to the family of DENN (Differentially Expressed in Normal and Neoplastic Cells) proteins, which regulate membrane trafficking by activating RabGTPase proteins and control protein degradation through autophagy modulation (Leko et al., 2019). At the moment three different mechanisms have been described in C9orf72 patients leading to MN degeneration.

In the first hypothesis, C9orf72 mutation determines a loss of function. In humans, three transcript variants have been identified. Transcript variants 2 and 3 originate two identical protein isoforms of 481 amino acids, while variant 1 is truncated and generates an isoform of 222 amino acids. Many studies highlighted a reduced expression of long or short protein

isoforms in brain and spinal motor neurons, respectively (Frick et al., 2018; Xiao et al., 2015; Waite et al., 2014). Indeed, C9orf72 HRE induces DNA hyper-methylation leading to decreased C9orf72 transcripts (Gijselinck, 2016). In drosophila and zebrafish models the knock-out or knock-down of C9orf72 gene determined MN degeneration (Therrien et al., 2013; Ciura et al., 2013), but the human C9orf72 gene has only partial homology with its ortholog in these two models. In mouse, which has a C9orf72 gene more similar to human, the knockout or knockdown of C9orf72 gene did not determine the development of the ALS and FTD classic phenotype, suggesting that C9orf72 loss of function is not the true cause of the disease (Sudria-Lopez et al., 2016; Koppers et al., 2015).

The second possible mechanism of C9orf72-related neurodegeneration is represented by a gain of function. The sequence G_4C_2 is characterized by a high uniformity, determining the formation of high-order DNA structures, called G-quadruplex. These structures could increase the length of the repeats creating a heterogeneous mixture of G-quadruplexes through the DNA sequence (Fratta et al., 2012). When the G-quadruplexes are localized in the HRE region of the C9orf72 gene, they generate truncated RNA transcripts that are aborted in the hexanucleotide repeat region. In turn, this event can cause the formation of G-quadruplexes, RNA hairpin structures and hybrid structures between HRE-containing RNA and HRE-containing DNA (R-loops) (Hauesler et al., 2014; Reddy et al., 2014). All these high-order structures could promote and regulate the replication, transcription and translation of the surrounding region (Kendrick and Hurley, 2010), leading the cells to nucleolar stress and impeding the correct RNA processing (Hauesler et al., 2014). Indeed, one of the main biological features of ALS patients carrying HRE-C9orf72 mutation is the presence in the brain of nuclear aggregates of HRE-containing RNA (RNA foci) (DeJesus-Hernandez et al., 2011). Antisense RNA and several proteins, which specifically bind the

aggregates, such as nucleolin, Pur-α, Heterogeneous Nuclear RiboNucleoProtein (hnRNPs), double-stranded RNA-specific adenosine deaminase B2 (ADARB2), Serine/arginine Rich Splicing Factor 1 (SRSF1), SRSF2 and ALYREF have been found within RNA foci (Lee et al., 2013; Cooper-Knock et al., 2014). The sequestration of these proteins within the RNA foci leads to impairment of ribosome maturation and RNA transport and translation (Haeusler et al., 2014). To test this hypothesis, ALS mouse models carrying transgenic C9orf72, determining RNA and protein toxic gain of function, have been studied. However, signs of neurodegeneration were observed only in some cases, requiring deeper analysis on the cause of ALS in C9orf72 patients (Moens et al., 2018; Liu et al., 2016).

The last mechanism, the same related with a toxic gain of function of C9orf72, considers the accumulation of Dipeptide Repeat (DPRs) proteins translated by C9orf72 HRE-containing RNA (Ash et al., 2013). DPR proteins, in particular when enriched in Arginine, are able to disrupt the regular transport between nucleus and cytoplasm (Jovičić et al., 2015), thus interfering with RNA processing (Kwon et al., 2014), and to affect the ubiquitin proteasome system, followed by ER stress and formation of toxic amyloid fibrils (Zhang et al., 2014; Chang et al., 2016). Unexpectedly, even if there is clear evidence of DPR protein toxicity in C9orf72 mouse models, in ALS and FTD patients only low levels of DPRs were found in brain regions which are most involved in the disease (Mackenzie et al., 2013). Why of this discrepancy is still unknown, but the most accredited hypothesis sustains that, at the time of autopsy, the only survived neurons are the ones with lower levels of DPRs, while neurons containing high level of DPR proteins are more susceptible to degeneration and, therefore, precociously die (Wen et al., 2017).

In conclusion, many studies proposed a synergic toxic mechanism where the loss of function of C9orf72 makes cells more sensitive to its toxic gain of function (Maharjan et al., 2017).

1.2.2.3 TDP-43 mutations

TDP-43 is a ubiquitously expressed DNA-/RNA-binding protein. It is encoded by TARDBP gene, located in the short arm of chromosome number 1 at position 36.22 (1p36.22) (Buratti and Baralle, 2001). TDP-43 is predominantly a nuclear protein, but can move to the cytoplasm following physiological inputs or stress insults (Winton et al., 2008). Therefore, the main functions of TDP-43 are exerted in the nucleus, such as regulation of RNA splicing and modulation of microRNA (miRNA) biogenesis. Interestingly, TDP-43 is capable of autoregulating its own mRNA stability and consequently also the protein level. In cell cytoplasm, TDP-43 is essential for dendritic and somatodendritic RNA transport granules in neurons and for neuronal plasticity (Alami et al., 2014; Ayla et al., 2011). In ALS and FTD, TDP-43 is one of the major components of ubiquitinated neuronal cytoplasmic inclusions (Arai et al., 2006; Vance et al., 2009). It forms aggregates, containing both full-length and fragmented protein, that result to be detergent resistant and hyperphosphorylated. Moreover, it has been reported an enrichment of TDP-43 in cytosplasm and a consequent reduced level in the nucleus.

TARDBP gene presents numerous mutations related to ALS or FTD (Sreedharan et al., 2008). Among the most studied mutations we can mention A315T, Q331K, M337V, which originated ALS-disease mouse models (Buratti, 2015). Mutated TDP-43 has an increased propensity to aggregate, a high tendency to cytoplasmic mislocalization and alterations of binding interaction with other proteins (Prasad et al., 2019). The augmented translocation

of TDP-43 from the nucleus to cytoplasm causes a loss of function (Arai et al., 2006), characterized by a dysregulation of RNA processing (Freibaum et al., 2010). Although the precise sequence of events in TDP-43-linked ALS is still undefined, several findings sustain that TDP-43 loss of function and mislocalization are the first critical neutotoxic mechanisms, followed by the formation of insoluble aggregates (Ederle and Dormann, 2017). These latter represent the basis of TDP-43 gain of toxic functions. Indeed, the deposition of insoluble TDP-43 inclusions causes alteration of autophagy by adsorbing proteins related to autophagy pathways, such as microtubule-associated proteins 1A/1B light chain 3B (MAP1LC3B or LC3-II) and p62, and determines reduction of protein turn-over (Budini et al., 2017), impairment of endocytosis (Liu et al., 2017) and abnormal mitochondria morphology, transport and distribution (Wang et al., 2013; Magrane et al., 2014). Finally, the coexistence of all these elements leads to an impaired response of MNs to oxidative stress, excitotoxicity, Calcium (Ca^{2+}) homeostasis and protein degradation.

1.2.2.4 FUS/TLS mutations

FUS/TLS is a ubiquitously expressed RNA/DNA binding protein. It is located in the short arm of chromosome 16 at the position 11.2 (Ederle and Dormann, 2017). FUS is one of the components of the hnRNP complex. It is involved in several cellular processes, such as gene transcription and regulation, DNA repair, RNA shearing, transport and translation, processing of miRNAs, and maintenance of genomic stability (Lagiertourenne et al., 2010).

The first mutation in FUS gene was discovered in 2009 (Kwiatkowski et al., 2009). Then, several ALS-linked mutations have been identified, such as P525L, P525R and, recently, Y526C (Mackanzie et al., 2010; Corcia et al., 2017). It is recognized that mutated FUS

determines a severe and fast progressive form of ALS. In many cases the onset of the disease occurs before 40 years of age and for P525L and Y526C mutations first symptoms appear even at 20-25 years (Corcia et al., 2017). FUS mutations determine a mislocalization of the FUS protein, which translocates from the nucleus to the cytoplasm. In the cytoplasm, FUS causes the formation of stress granules during oxidative stress insults, mitochondrial dysfunction or viral infection (Gao et al., 2017).

FUS mutation can lead to cytotoxicity by two mechanisms. Gain of toxic function, due to translocation to the cytoplasm, an event that favours aggregate formation and sequestration of other proteins involved in several physiological pathways (Ramaswami et al., 2013), or loss of function, due to mRNA instability in particular in the spines of neurons (Neumann et al., 2009). Furthermore, astrocytes and microglia produce a strong inflammatory response, by secreting high level of IL-1β, TNF-α and IL-6 and by increasing transcription of inducible nitric oxide synthase (iNOS) and Prostaglandin E2 (PGE_2) (Ajmone-Cat et al., 2019).

A recent study, conducted on FUS iPSC-derived neurons and post-mortem tissue from FUS-ALS patients, demonstrated that FUS mislocalization determines an imbalance in RNA-binding protein (RBP) homeostasis [hnRNPA1, TATA-Box Binding Protein Associated Factor-15 (TAF-15), Ewing sarcoma breakpoint region 1(EWSR1),...], exacerbating FUS pathogenesis and accelerating neurodegeneration (Marrone et al., 2019). Since the level of p62 was increased in neurons with FUS mutations compared to control neurons, they hypothesized an impairment of the protein quality control system linked to a decreased clearance of FUS aggregates. Indeed, when they tested two different compounds, torkinib and PQR309, able to trigger autophagy, a decrease of FUS aggregate levels was observed, both *in vitro* and *in vivo* in Drosophila model, also RBP homeostasis

was rescued, increasing neuron survival and ameliorating Drosophila motor skills (Marrone et al., 2019).

1.2.2.5 Ubiquilin-2 and sequestosome 1 mutations

Ubiquilin-2 (UBQLN2) is a ubiquitin-linked protein involved in the protein quality control system at neuronal level. UBQLN2 gene is located on X chromosome at the position 11.21; mutations in this gene determine a rare form of X-linked ALS/FTD. UBQLN2 missense mutations have been identified in X-linked ALS and FTD, with most of the mutations occurring in or near a proline-rich repeat domain (Deng et al., 2011). UBQLN2 behaves as an adaptor protein, shuttling ubiquitinated proteins to the proteasome for degradation (Ko et al., 2004). Moreover, it also modulates autophagy and interacts with several molecular chaperones (Hjerpe et al., 2016). Mutations in UBQLN2 cause an increase propensity to self-assembly and promote the formation of insoluble inclusions, leading to an imbalance of the protein quality control system and cell homeostasis (Sharkey et al., 2018).

Sequestome 1 (SQSTM1), also known as the ubiquitin-binding protein p62, is an autophagosome cargo protein receptor required for selective macroautophagy. It acts as a bridge between polyubiquitinated cargo and autophagosomas (Clausen et al., 2010). It is located on chromosome 5 at the position 35.3. In the same way of UBQLN2, SQSTM1 forms toxic aggregates in cell cytoplasm and alters the normal protein turn-over. Silencing SQSTM1 affects mitochondrial membrane potential and consequently inhibits mitochondrial electron transport chain. Moreover, a recent paper described a link between SQSTM1 mutations and mitochondrial dysfunction. In fibroblasts of two ALS patients harboring two different point mutations (A381V and K238del), SQSTM1 was

significantly reduced. NADH and FAD redox index was measured to evaluate the energetic metabolism in mutant cells and an impairment in complex I function was detected, leading to a decrease production of ATP. On the other hand, also FAD level was reduced, suggesting a possible shift to complex II respiration to compensate the inhibition of complex I. These altered mitochondrial functions promote ROS production, determining oxidative stress damage (Bartolome et al., 2017). Impairment of ATP production, together with an increase ROS formation, is one of the main mechanism causing MN degeneration. This mechanism could be related also to sporadic ALS and other forms of familial ALS, indeed SQSTM1 positive inclusions are common in almost all patients (Hiji et al., 2008; Pikkarainen et al., 2008).

1.2.2.6 Optineurin mutations

Optineurin is a polyubiquitin-binding protein, which regulates several physiological cellular processes (Ryan and Tumbarello, 2018). Optineurin is highly conserved among species and is located on chromosome 10 at the position 13, encoding a 577 amino acid cytoplasmic protein, in humans. It is ubiquitously expressed, but higher expression was observed in brain, retinal ganglion cells, spleen, skeletal muscle, and heart (De Marco et al., 2006).

As anticipated, Optineurin has many functions: it controls signalosome assembly for NFκB activation, works as an autophagy adaptor; selectively binds to the cargo deputed to degradation of damaged mitochondria, protein aggregates, or intracellular pathogens and delivers them to autophagosomes. During autophagy, optineurin facilitates autophagosome maturation and its fusion to lysosomes, interacts with TBK1 to trigger the production of antiviral type I interferon (IFN) in response to viral infection, preserves the Golgi

apparatus structures and regulates post-Golgi transport and exocytosis, protects from nectroptosis and/or apoptosis during TNF-mediated NFκB stimulation (Markovinovic et al., 2017; Ryan and Tumbarello, 2018).

Mutations of optineurin have been identified in fALS and sALS patients and more than 20 ALS-linked missense optineurin variants have been reported (Maruyama et al., 2010; van Blitterswijk et al., 2012). The most accredited hypothesis for the toxic effects of optineurin mutations consists in a loss of function, due to the deletion of the transcriptional starting sites in exon 4 and exon 5 and non-sense mutations encoding truncated proteins lacking different portions of its C-terminus (G23X,Q165X, S174X, Q398X) (Maruyama et al., 2010, Beeldman et al., 2015), causing the loss of optineurin functional domain.

Because of the numerous functions of optineurin, its loss of function has disastrous consequences, such as autophagy impairment, mitochondrial dysfunction leading to energetic deficit, altered inflammatory response to damage-associated molecular patterns (DAMPs), incapacity to mitigate NFκB and necroptosis pathway activation in chronic stress condition, and imbalance of pro- and anti-inflammatory factors (Markovinovic et al., 2017; Markovinovic et al., 2018). Mouse models with mutations or knock-out for optineurin have been generate to validate the loss of function hypothesis. A detailed characterization of CNS features for optineurin$^{-/-}$ mice showed a massive axonal degeneration, sustaining the idea that the loss of function of optineurin can lead to ALS (Skarnes et al., 2011).

1.2.2.7 VCP mutations

VCP is a ubiquitously expressed protein involved in protein homeostasis, mitochondria quality control and apoptosis (Meyer et al., 2012). VCP gene is located on chromosome 9 at the position 13.3.

The 2% of fALS cases are caused by autosomic-dominat VCP mutations and more than 20 different mutations in VCP gene have been identified (Johnson et al., 2010). Recent *in vitro* and *in vivo* studies on transgenic models highlighted the pathologic mechanisms determined by VCP mutation. Hall and colleagues (2017) demonstrated that VCP-mutant neurons, derived from induced pluripotent stem cells (iPSCs), showed increased synapse loss, cell death, transcriptional perturbations of genes encoding for ion channels and synapse structural proteins, ER stress and uncoupled oxidative phosphorylation leading to ROS production (Hall et al., 2017).

Mutant VCP affects also skeletal muscle; one *in vivo* model generated by deleting VCP in differentiated skeletal muscle presented ALS symptoms, such as weight loss, weakness and reduced motor skills. The main cause for myofiber necrosis seemed to be the dysregulation of lysosomal homeostasis due to lack of VCP. Indeed, damaged endo-lysosomes are not recognized for autophagic degradation without VCP labelling, thus leading to damaged lysosome accumulation and consequently to mitochondria dysfunction and energetic impairment (Arhzaouy et al., 2019).

1.2.2.8 TBK1 mutations

TBK1, located on chromosome 12 (12q14.2), codes for a protein kinase involved in many pathways including immune response and autophagy. TBK1 is composed of 4 domains: a

kinase domain, responsible for its kinetic activity, an ubiquitin-like domain, a scaffold dimerization domain, and a C-terminal domain, involved in TBK1 association to binding partners such as OPTN (de Majo et al., 2018). TBK1 plays a key role in autophagy, through the phosphorylation of several autophagy adaptors including p62, OPTN and nuclear dot protein 52 kDa, enhancing their ability to link LC3-II and ubiquitinated cargoes. It regulates microtubule dynamics in mitosis and the cytoplasmic levels of dynein. Further, it is involved in the induction of interferons synthesis and release, modulating neuroinflammatory stimuli (Oakes et al., 2017).

Mutations in TBK1 have been recently linked with ALS and FTD by two independent whole exome sequencing/whole genome sequencing studies. Many ALS-linked TBK1 mutations generate premature stop codons, leading to non sense-mediated mRNA decay and haploinsufficiency that is predicted to impair autophagy (Cirulli et al., 2015; Freischmidt et al., 2015).

A recent work in a mouse model knock-out for TBK-1 further validated the hypothesis of a loss of function of TBK-1 related to ALS and FTD pathogenesis. These mice showed aggregates positive for TDP-43 and p62, motor impairment, astrogliosis and reduced number of synapses in the cortex, supporting the involvement of TBK-1 also in learning and memory activity (Duan et al., 2019). However, the role of TBK-1 in ALS and FTD disease is still unclear and further studies are necessary to clarify the functions of this kinase.

Table 1. Summary of the most common mutations linked to ALS.

Gene	Locus	Protein	Protein function	Loss/gain of function	% Frequency in FALS
SOD1	21q22.11	Cu/Zn Superoxide dismutase	Superoxide dismutase	Gain of toxic function	15%
C9ORF72	9p21-22	C9ORF72	Possible guanine nucleotide exchange factor	Gain of toxic function/Loss of function	30%
TARDBP	1p36.22	TDP-43	RNA-binding protein	Gain of toxic function/Loss of function	5%
FUS	16p11.2	FUS/TLS	RNA-binding protein	Gain of toxic function/Loss of function	5%
UBQLN2	Xp11.21	Ubiquilin 2	Autophagy adaptor	Gain of toxic function	>1%
SQSTM1	5q35.3	p62	Autophagy adaptor	Gain of toxic function	>1%
OPTN	10p13	Optineurin	Regulates autophagy and inflammation	Loss of function	4%
VCP	9p13.3	Valosin-containing protein	Ubiquitin segregase	Loss of function	1-2%
TBK-1	12q14.2	TANK-binding kinase 1	Regulates autophagy and inflammation	Loss of function	1%

1.3. Biomolecular aspects of ALS

Nowadays, it is well recognized that ALS is a multifactorial disease, in which several mechanisms take place and different cellular types are involved, contributing to MN degeneration. Thanks to transgenic mouse models, *in-vitro* systems able to mimic pathologic conditions, and post-mortem tissue analysis, several alterations in physiological cellular homeostasis have been partially revealed, even if the precise ALS causative mechanisms are still unclear. These toxic events are similar both in fALS and sALS.

1.3.1 Oxidative stress

Oxidative stress is one of the main events in ALS and also one of the best studied, because of the numerous disease models based on SOD1 mutation. Oxidative stress biomarkers have been found in urine, blood, cerebrospinal fluid (CSF), and individual tissue of ALS patients (Kikuchi et al., 2002; Mendez et al., 2015).

Oxidative stress derives from the imbalance between oxidants and anti-oxidants within a biological structure. An abnormal production of ROS or deficit in antioxidant systems could be at the basis of tissue damage and cell death (Singh et al., 2019).

Hydrogen peroxide (H_2O_2), superoxide anion (O_2^-) and hydroxyl radical ($HO^\bullet$), but also reactive nitrogens species (RNS), such as nitric oxide (NO), are physiologically produced during cell life cycle. Indeed, many cell functions, such as signal transduction, gene transcription, oxidative phosphorylation and ATP production in mitochondria, require oxygen as a substrate (Halliwell, 2006; Uday et al., 1990). If these reactive molecules are not detoxified by anti-oxidant enzymes, as glutathione peroxidase, SOD1, and catalase, they can damage cell structure by causing oxidation of different biomolecules, such as

lipids, protein, DNA/RNA, etc. (Yu et al., 2012). Lipids are highly susceptible to oxidation and a damage at this level leads to a perturbation of plasmatic membrane fluidity and permeability, that promotes the entrance of substances, in particular ions, inside the cell (Brown and Murphy, 2009). Lipid peroxidation promotes the propagation of oxidative damage that ultimately affects also proteins and RNA/DNA, determining structural and functional modifications with increased protein aggregation and proteolysis (Halliwell and Gutteridge, 1984).

The cell compartment in which most part of ROS/RNS originated is the mitochondrion, probably because mitochondria are enriched in redox enzymes (Halliwell, 2007). Mitochondria dysfunctions (e.g. due to mitochondria DNA damage) could improve ROS/RNS production, together with a reduced protective action from these reactive species. Since mitochondria are the main producers of the cell-needed energy, their malfunction leads the cells to apoptosis or senescence with catastrophic events, especially in non-proliferative cells, as neurons (Wang et al., 2013; Redza-Dutordoir and Averill-Bates, 2016).

Even if SOD1 mutations represent the direct link with oxidative stress in ALS, redox alterations have been found also in C9orf72, TDP-43 and FUS familial forms, suggesting a correlation between RNA metabolism dysregulation and oxidative stress. Cohen and Coll. demonstrated that oxidative stress causes TDP-43 delocalization from the nucleus to the cytoplasm and increases its tendency to aggregate (Cohen et al., 2015). Moreover, both TDP-43 and FUS co-localizes with stress granules, that represent one of the responses of cells to oxidative stress insults modulating gene expression by prioritizing translation of stress response-linked genes (Li et al., 2013; Bentmann, 2012). If stress granules persist, they can play a pivotal role in aggregate formation (Parker et al., 2012).

On the other hand, TDP-43, FUS and C9orf72 can co-localize with mitochondria and cause oxidative stress. Three hypotheses have been proposed to explain this mechanism. First, a direct damage may occur due to sequestration of mitochondrial proteins by RNA-binding proteins (Magranè et al., 2014; Deng et al., 2015). Second, through interaction with non-mitochondrial proteins that are involved in mitochondrial protein synthesis. Among these, FOXO3 acts by down-regulating many nuclear-encoded genes that control mitochondrial function. TDP-43 exerts a negative control on FOXO3 and in TDP-43-linked ALS, where it translocated from the nucleus to the cytoplasm, FOXO3 showed an increased inhibitory activity leading to a reduction of the mitochondrial functions (Ferber et al., 2012; Zhang et al., 2014). Finally, TDP-43 and FUS could be involved in the regulation of specific mRNAs coding for proteins preserving mitochondria physiology. This last hypothesis is sustained by a recent study which demonstrated the ability of mutant TDP-43 to alter the splicing pattern of nuclear-transcribed mRNA, coding for mitochondrial fission regulator-1 (Mtfr-1) and complex I subunits ND3 and ND6, causing complex I disassembly (Finelli et al., 2015; Wang et al., 2013).

A reduced efficiency of the anti-oxidant response has been reported in ALS patients, in association with the increased production of ROS and free radicals. In particular, the Nuclear factor erythroid 2-related factor 2 (Nrf2), a key player to stimulate the resistance of the cells to oxidative stress, was decreased in ALS patients (Sarlette et al., 2008). In normal condition Nrf2 is bound to the endogenous inhibitor Kelch-like ECH associated protein 1 (Keap1). Nrf2 is activated by endogenous or exogenous stressors, which cause increased levels of free radicals; then, it translocated from the cytoplasm to the nucleus, where forms heterodimers with other transcription factors and binds to the antioxidant response element (ARE), a regulatory enhancer region. The Nrf2-ARE interaction

promotes the transcription of several genes involved in the cellular antioxidant and anti-inflammatory defence, such as phase 2 detoxification enzymes [NAD(P)H quinone oxyreductase (NQO1), glutathione)], that are necessary for glutathione biosynthesis, extracellular superoxide dismutase, glutamate-6-phosphate-dehydrogenase, heat shock proteins and ferritin. Furthermore, Nrf2 promotes the synthesis of pro- and anti-inflammatory enzymes, such as cyclooxygenase-2 (COX-2), iNOS, and heme oxygenase-1 (HO-1) (Petri et al., 2012).

Because of the key role of Nrf2 in regulating antioxidant response, many studies focused on the administration of Nrf2 activator to slowdown the disease progression. Neymotin et al. (2011) tested two analogs of 2-cyano-3,12-dioxooleana-1,9-dien-28-oic acid (CDDO) in the $SOD1^{G93A}$ mouse model of ALS. In treated mice, Nrf2 expression was increased and function was recovered. Accordingly, the authors observed an upregulation of classical Nrf2-regulated genes. These positive effects at biomolecular level translated in an amelioration of motor performance, a reduction of weight loss and, finally, in a prolonged survival (Neymotin et al., 2011).

Other activators of Nrf2 have been tested, such as tert-butylhydroquinone, DL-sulphoraphane, lipoic acid, fumaric acid and curcumin (Petri et al., 2012). The unsuccessful results registered using these positive modulators have been ascripted to the low penetration of the blood brain barrier (BBB), but they were also related to the unclear mechanisms of action since it was reported that the expression of a large variety of non-Nrf2-dependent genes was modified from these substances (Kwak et al., 2010).

1.3.2 Mitochondrial dysfunctions

Mitochondria are cellular organelles that cover an essential role in different cellular processes, in particular in energy metabolism, Ca^{2+} homeostasis, lipid biosynthesis and apoptosis. They are fundamental for neuron survival and function. Indeed, neurons require the 20% of the body's resting ATP production (Engl and Attwell, 2015). For this reason mitochondrial dysfunction is one of the stronger hypothesis at the basis of ALS pathogenesis (Smith et al., 2017).

1.3.2.1 Mitochondrial structure

fALS and sALS patients showed structurally altered and aggregated mitochondria, with swollen and vacuolated morphology (Sasaki et al., 2007). The mitochondria morphology disruption can directly derive from mutated proteins, in particular mutations have been identified in the mitochondrial protein CHCHD10, which allows the contact between the inner and the outer mitochondrial membrane. Also other ALS-mutated proteins seem to be involved in the structure and function impairment of mitochondria. Mutant SOD1 aggregates within the intermembrane space, decreasing the electron transport chain complexes, affecting the activity of voltage-dependent anion channel-1 (VDAC1) and promoting pro-apoptotic signals through interaction with Bcl-2 (Ferri et al., 2006; Israelson et al., 2010; Pasinelli et al., 2004). TDP-43 co-localizes with mitochondria and binds the mRNAs coding for mitochondrial proteins, reducing energy metabolism (Wang et al., 2013). FUS co-localization with mitochondria reduces ATP production, probably due to an interaction with the mitochondrial chaperone heat shock protein of 60 kDa (HSP60) (Deng et al., 2015).

Mitochondrial fission and fusion, two essential functions for the auto-regulation of the mitochondrial dynamic network, were altered in diverse ALS models. Fusion permits mitochondrial exchange of metabolites, DNA and proteins and allows for dissipation of small changes in mitochondrial membrane potential. On the other hand, fission facilitates mitochondrial motility and determines the isolation of damaged parts of the network, before their degradation by mitophagy. Dynamin-related protein 1 (Drp1) and Fission 1 (Fis1) sustain the fission process; while mitofusin (Mfn) 1 and 2 and Optic atrophy 1 (Opa1) promote fusion (Chan et al., 2012; Westrate et al., 2014).

In ALS models, an increased expression of fission proteins respect to fusion proteins was reported (Liu et al., 2013; Xu et al., 2010). An abnormal mitochondrial fission in ALS could cause the formation of smaller mitochondria, which are less energetically stable and more susceptible to ROS accumulation, if they cannot fuse back to the network (Hoitzing et al., 2015). A proof of concept for this pathogenic mechanism has been provided by some studies on the beneficial effects of mitochondrial fission inhibition or mitochondrial fusion upregulation in ALS models, in which a reduced mitochondrial fragmentation and an increase of MN viability were observed (Song et al., 2013; Wang et al., 2013).

1.3.2.2 Mitochondrial axonal transport

Axonal transport is essential for MN survival. Indeed MNs are highly polarized cells and require membrane-bound vesicles, organelles, protein, lipids and RNA to transport mitochondria from the soma to the axon terminal and *vice versa.* In physiological condition, kinesin-1 and dynein allow the transport of mitochondria along the entire length of MN axons, the first from the soma to the axon terminal (anterograde transport) and the second from axon terminal to the cell body (retrograde transport) (Smith et al., 2017).

Diverse SOD1 mutations affect anterograde transport of mitochondria in cultured cortical neurons and in embryonic MNs (De Vos et al., 2007). Other mutations causing impaired mitochondrial axonal transport has been identified in VAPB, TDP-43 and TBK1 (Magranè et al., 2014; Wang et al., 2013; Oakes et al., 2017). Dysfunctions in mitochondrial axonal transport cause redistribution of mitochondrial in axons, in particular MNs showed a decreased number of axonal mitochondria, already at an early stage of the disease, which, in addition, assume a cluster pattern (Sasaki et al., 2007).

1.3.2.3 Mitochondria and calcium homeostasis

In addition to an energetic deficit, mitochondria changes determine an alteration of intracellular Ca^{2+} levels. Loss of Ca^{2+} homeostasis has been detected in several ALS animal models and also in ALS patients, already at an early symptomatic stage of the disease (Stoica et al., 2016; Damiano et al., 2006; Mòrotz et al., 2012).

One of the causes of Ca^{2+} dysregulation could be the loss of communication between mitochondria and the ER. Indeed these two organelles interact through protein complexes, such as Mnf1, Mnf2, inositol 1,4,5-trisphosphate receptor (IP3R) and VDCA1 (Manfredi et al., 2016). This interaction, that allows the exchange of Ca^{2+} between mitochondria and ER, has been found impaired in mutant SOD1-, TDP-43- and FUS-related ALS (Stoica et al., 2016; Bernard-Marissal et al., 2015; Stoica et al., 2014).

Notably, MNs are more sensible to Ca^{2+} homeostasis disruption compared with other neuronal cells. They express a higher number of permeable Ca^{2+} receptors at the postsynaptic level, determining a massive Ca^{2+} influx during excitatory neurotransmission, and, at the same time, they suffer of impaired cytosolic buffering capacity, as they express low level of parvalbumin and calbindin, two essential Ca^{2+} buffering proteins. This make

MNs highly dependent from mitochondria to control the intracellular Ca^{2+} level (Van den Bosh et al., 2000).

Loss of Ca^{2+} homeostasis can trigger numerous toxic events: elevated concentration of cytosolic Ca^{2+} directly impacts axonal transport of mitochondria by interacting with the mitochondrial kinesin-1 receptor Miro1 (Wang et al., 2009), increases ROS production and oxidative stress due to Ca^{2+} overload in mitochondria (Carriedo et al., 2000), activates calpain-1 leading to a massive proteolitic activity of specific substrates, such as nNOS, αII-spectrin, NR2B subunit of NMDA receptor (Stifanese et al., 2014; Stifanese et al., 2010), cleaves and activates pro-apoptotic proteins (Ashkenazi and Salvesen, 2014).

Sigma-1 receptor (Sig1R), highly expressed at the mitochondria-associated ER membranes, has been found mutated in rare forms of ALS (Al-Saif et al., 2011) and downregulated in $SOD1^{G93A}$ mice and in patients with fALS and sALS. Its downregulation seems to be strictly related with the severity of disease progression (Mavlyutov et al., 2013; Prause et al., 2013). Thanks to Sig1R role in Ca^{2+} homeostasis maintenance, Tadić and colleagues tested diverse agonists for Sig1R to restore mitochondria-ER communication. The SA4503 and PRE-084 compounds have been tested in non-transgenic and in $SOD1^{G93A}$ MNs from mice embryos. Only the Sig1R agonist SA4503 exerted a positive effect on motor neuron survival, by accelerating Ca^{2+} cytosolic clearance after the activation of α-Amino-3-hydroxy-5-methyl-4-isoxazolepropionic acid (AMPA)-type glutamate receptors or bradykinin stimulus and up-regulating Sig1R expression (Tadić et al., 2017).

1.3.2.4 Mitochondria and skeletal muscles

Mitochondrial abnormalities were observed also in skeletal muscles of fALS and sALS patients, already at an early stage of disease progression. The first studies reported changes in the number and in the morphology of mitochondria, that appeared elongated and large; moreover, they form aggregates able to undermine the integrity of the sarcolemma membrane in subsarcolemma regions (Chung et al., 2002; Napoli et al., 2011). The altered morphology denotes also a functional impairment. Indeed, a lot of evidence showed a reduced efficiency of mitochondrial respiration and ATP production, probably due to decreased activity of several enzymes, among these the NADPH dehydrogenase (complex I) and cytochrome c oxidase (complex IV) (Crugnola et al., 2010; Echaniz-Laguna et al., 2006). Subsequent studies, by microarray and qPCR analysis, revealed that also the mRNA for several proteins involved in mitochondrial biogenesis and dynamics were down-regulated in skeletal muscles of ALS patients (Russell et al., 2013). As for MNs, muscle mitochondrial malfunction leads to an imbalance of intracellular Ca^{2+} concentration. Indeed, sodium (Na^{+}) permeant nicotine receptors produce depolarization at the neuromuscular junction that allows a massive Ca^{2+} influx and muscle contraction (Fucile, 2004). If mitochondria are not able to efficiently uptake Ca^{2+} from the cytosol, a cascade of toxic events, such as incapacity to generate an electric potential, can be triggered (Yi et al., 2011). Oppositely, mitochondrial Ca^{2+} overload will induce abnormal ROS production in mitochondria (Muller et al., 2007) and excessive Ca^{2+} will exacerbate mitochondrial damage (Saotome et al., 2008; Yi et al., 2004). The final consequence of these events is represented by an interruption of the cross-talk between motor neurons and skeletal muscles and, finally, to muscular atrophy (Rasola et al., 2010).

1.3.3 Excitotoxicity

1.3.3.1 Increased glutamate availability

Excitotoxicity, that is the toxicity mediated by an abnormal concentration of glutamate in the synapses, is a well-studied feature of ALS. In 1996, Excitatory Amino Acid Transporter 2 (EAAT2) modifications were linked with ALS pathogenesis. Indeed, a deficit in the uptake of glutamate from the synapses was reported in cortex and spinal cord of ALS patients (Bristol and Rothstein, 1996). A further study revealed that EAAT2 functional alterations derived from aberrant truncated transcripts of EAAT2 gene (Lin et al., 1998). Other factors able to affect EAAT2 transcription, translation and activity have been reported, such as oxidative stress, fatty acids, growth factors and cytokines (Rao et al., 2003; Gegelashvili et al., 1997; Trotti et al., 1995). The reduced clearance of glutamate leads to an increased activation of MNs, with an abnormal influx of Ca^{2+}. As described above, Ca^{2+} homeostasis dysregulation determines fatal changes in cell physiology, inducing ER stress, mitochondria overload and, finally, cell death (Van Damme et al., 2005).

Not only glutamate clearance but also an abnormal release of glutamate was observed in *in vitro* models of ALS. Synaptosomes prepared from spinal cord of $SOD1^{G93A}$ mice showed increased release of glutamate both in basal conditions and after the application of depolarizing stimuli, already at a presymptomatic stage of the disease (Milanese et al., 2011; Bonifacino et al., 2016). Moreover, Group I metabotropic glutamate autoreceptors (mGluR1 and mGluR5) in the $SOD1^{G93A}$ mouse model resulted more sensitive to the glutamate released in synaptic space, compared to control mice, causing an increased

activation of these receptors and allowing excessive Ca^{2+} influx and glutamate release (Giribaldi et al., 2013, Bonifacino et al., 2019).

1.3.3.2 AMPA receptor hyperfunction

AMPA receptors are a class of ionotropic glutamate receptors permeable for Ca^{2+} or Na^{+}, depending on the expression and the post-transcriptional editing of the mRNA of the different subunits that form the receptor (Lorenzini et al., 2018). Numerous findings support the involvement of this receptor in ALS pathogenesis and progression. Even if autoradiography binding did not show differences between AMPA receptor in ALS patients and in healthy controls (Allaoua et al., 1992), MNs are differentially vulnerable to toxic levels of kainic acid, an agonist of both AMPA and kainate receptors, *in vitro* (Carriedo et al., 1996; Bar-Peled et al., 1999) and *in vivo* (Sun et al., 2006). Therefore, it has been hypothesized that alteration of AMPA receptors are due to modifications in its composition. Indeed, the expression of GluR2 AMPA subunit, which normally blocks Ca^{2+} entry through the receptor channel, was decreased in spinal cord of mutant SOD1 mice and ALS patients (Van Damme et al., 2005; Takuma et al., 1999). However, the most validated hypothesis bases on changes in GluR2 AMPA subunit mRNA editing. In healthy condition, GluR2 mRNA is subjected to a post-transcriptional Q/R substitution, in which a glutamine is replaced with an arginine, making the receptor impermeable to Ca^{2+} (Swanson et al., 1997). Instead, in ALS the GluR2 mRNA editing resulted incomplete and AMPA receptor becomes permeable to Ca^{2+} (Takuma et al., 1999; Kawahara et al., 2004). The discovery of ALS-linked mutations in proteins regulating RNA processing further supports a possible alteration in GluR2 mRNA editing. Interestingly, C9orf72, TDP-43 and FUS sequestrate RNA transcript variants of adenosine deaminase 2 (ADAR2), which catalyzes

GluR2 mRNA editing, determining a reduction of the receptor activity and an increase of Ca^{2+} permeability in ALS MNs (Donnelly et al., 2013; Aizawa et al., 2010).

A recent study on AMPA receptor expression and function reported differences between iPSC-derived MNs carrying C9orf72, SOD1, TDP-43 or FUS mutation (Bursch et al., 2019). Although AMPA receptor mRNA did not change in C9orf72 MNs, these showed higher Ca^{2+} peaks following receptor activation compared to healthy controls. In mutated SOD1 and FUS MNs the Ca^{2+} peak amplitudes decreased when compared to healthy controls. Also in TDP-43 MNs the AMPA expression level was unchanged compared with healthy control. However, also in this case MNs displayed higher intracellular basal level of Ca^{2+} and increased Ca^{2+} peaks after AMPA receptor activation, compared to control MNs. These mutation-specific differences could explain the diverse responses to the pharmacological treatment with riluzole between ALS patients characterized by distinct disease aetiology (Bursh et al., 2019).

1.3.3.3 Hyperexcitability

Neuronal hyperexcitability represents a leading mechanism to explain excitotoxicity in ALS. Several studies in patients showed an alteration of MN excitability already at an early stage of the disease. Indeed, the MN-evoked potential and the resting threshold, measured in abductor pollicis brevis, were increased and decreased, respectively. These results suggest that a lower stimulus should be sufficient to generate a response in MNs at the beginning of the disease (Vucic and Kiernan, 2006). In accordance, the analysis of GABAergic interneurons, which strictly regulate neuronal signalling, revealed a decrease of their inhibitory action in the motor cortex of ALS animal models (Moser et al., 2013;McGown et al., 2013). Of note, a reduction of mRNA for $GABA_A$ receptor subunit α,

which could directly impair GABAergic transmission reducing GABA binding to its receptors, has been observed in post-mortem tissue from ALS patients (Petri et al., 2003). This phenomenon can determine the generation of a MN response even if they receive a sub-threshold stimulus (Wagle-Shukla et al., 2009).

Another mechanism, to explain hyperexcitability, is emerged in $SOD1^{G93A}$ mouse model of ALS. Cortical neurons from $SOD1^{G93A}$ mice showed unchanged fast transient Na^+ currents and increased persistent Na^+ currents; in particular the amplitude resulted higher, compared to control cortical neurons (Pieri et al., 2009). Persistent Na^+ currents are essential to sustain and generate prolonged depolarization; thus, an alteration of their amplitude may represent a possible mechanism leading to hyperexcitability. As proof of concept to validate the involvement of persistent Na^+ currents in hyperexcitability, Pieri and Colleagues tested the effect of riluzole on $SOD1^{G93A}$ cortical neurons. A low dose of riluzole significantly reduced the persistent Na^+ currents and the firing frequency, but did not modify the resting membrane potential.

The unaltered resting membrane potential suggests that persistent Na^+ currents exert only a modest role and that other mechanisms can sustain hyperexcitability, such as alteration of potassium (K^+) currents. Shibuya and Colleagues reported a decrease expression of Kv1.1, Kv1.2 and Kv7.1 K^+ channels in ALS patients, compared to controls. A decrease of K^+ outward currents causes a higher level of extracellular K^+, increasing the resting membrane potential and the firing frequency in MNs (Shibuya et al., 2011; Kanai et al., 2006).

1.3.4 Axonal transport dysfunction

Axonal transport allows the exchange of mitochondria and vesicular or non-vesicular cargoes (lysosomes, signalling endosomes, amyloid precursor protein-containing vesicles,

AMPA receptor-containing vesicles, mRNA/protein complexes) between the MN soma and the axon terminals. We can distinguish axonal transport in fast axonal transport or slow axonal transport. Both typologies are mediated by the same molecular motors that move cargoes along microtubules and the different speed is determined by prolonged pauses between movement in slow axonal transport.

Microtubules are polymers constituted of heterodimers of α-tubulin and β-tubulin. They are polarised with a fast growing plus end and a slow growing minus end, because of tubulin heterodimer head to tail rearrangement. The microtubule polarity defines the direction of the movement of the molecular motors along them. Two families of microtubule-based molecular motors are involved in axonal transport: kinesin family and dynein family. The first family mediates the anterograde transport and the second the retrograde transport (De Vos et al., 2017).

As already mentioned in a previous paragraph, there is a lot of evidence supporting a defect of axonal transport in ALS. Indeed, accumulations of phosphorylated neurofilaments, mitochondria and lysosomes in the proximal axon of large MNs in the form of axonal spheroids are well documented in ALS animal models and in post-mortem tissues from ALS patients (Hirano et al., 1984a; Hirano et al., 1984b; Corbo and Hays, 1992). Moreover, pre-symptomatic $SOD1^{G37R}$ mice showed a significant decrease in the slow anterograde transport of cytoskeletal components (Williamson and Cleveland, 1999), pointing at a key role of axonal transport impairment in neurodegeneration.

The causes of axonal transport impairment are only partially understood. A large number of genetic mutations in proteins of axonal transport machinery has been found. Among these mutant proteins, we can list ALS2, which alters Rab5-dependent endosome

trafficking, AMPA receptor trafficking and retrograde neurotrophin trafficking (Lai et al., 2009); charged multivesicular body protein 2B (CHMP2B) which fails in the recruitment of Rab7 to endosomes, determining a defects in retrograde transport of neurotrophin (Urwin et al., 2010); mutated Dynactin 1 (DCTN1), a subunit of the dynactin complex, that shows a loss of function leading to an impairment of axonal transport and vesicle trafficking (Puls et al., 2003).

Recently, a new mutation in kinesin family member 5A (KIF5A) has been associated with ALS. It is part of a multi-subunit complex that acts as a microtubule motor in intracellular protein and organelle transport, including mitochondria (Hirokawa et al. 2009). Both mutation in the C-terminal and N-terminal of KIF5A leads to its loss of function. Mutation affecting the N-terminal tail causes a reduced binding of cargoes to KIF5A, leading to a severe form of ALS; instead, mutation affecting the N-terminal tail results in the decrease of axonal transport velocity and flux. This latter mutation is associated with mild pathologies, such as Charcot-Marie-Tooth disease type 2 and hereditary spastic paraplegia, but currently there is no evidence of its involvement in ALS (Brenner et al., 2018).

One of the proposed mechanisms to explain axonal transport impairment includes the alteration of mitochondrial Rho GTPase 1 (Miro1) expression level. Miro1 allows the binding of mitochondria with kinesin-1 or cytoplasmic dynein and their transport along MN axons. Miro1 activity depends from Ca^{2+} concentration. Indeed, Ca^{2+} binding to Miro1 modifies its interaction with kinesin-1 and through this alteration prevents kinesin-1-microtubules binding or determines the release of kinesin-1 from mitochondria (Wang and Scharz, 2009). However, also mitochondria damage determines changes in Miro1, which is subjected to phosphorylation by phosphatase and tensin homolog (PTEN)-induced putative kinase 1 (PINK1), which targets Miro1 for parkin-dependent proteasomal degradation.

Obviously, Miro1 degradation leads to an irreversible detachment of molecular motors from the mitochondrial surface (Shlevkov et al., 2016). A study on rat cortical neurons transfected with WT-SOD1 or $SOD1^{G93A}$, revealed a correlation between mutant SOD1 and expression of Miro1. Indeed, the transfection with $SOD1^{G93A}$ determined a decrease of Miro1 in neurons, compared to WT-SOD1-transfected neurons. Miro1 degradation was caused by PINK1/parkin pathway activation; indeed, knock-down of PINK1 rescued the toxic effects of $SOD1^{G93A}$ on mitochondrial axonal transport (Moller et al., 2017).

Nowadays, it is well demonstrated that $SOD1^{G93A}$ exerts its toxic function through the activation of specific kinase cascades, such as p38 mitogen-activated protein kinase (MAPK). MAPK was found to be activated in the spinal cord of pre-symptomatic $SOD1^{G93A}$ mice compared to wild type and WT-SOD1 controls. Interestingly, p38 MAPK activity was highest in early symptomatic $SOD1^{G93A}$ mice (Bisland et al., 2010). Gibbs and Colleagues demonstrated that the abnormal activation of p38 MAPK in $SOD1^{G93A}$ MNs determines an impairment of axonal transport and that its inhibition completely restores axonal transport of signalling endosomes. In particular, they observed that p38 MAPKα inhibits axonal anterograde transport through direct phosphorylation of kinesin-1, thus reducing the ability of the molecular motors to move along axonal microtubule of primary $SOD1^{G93A}$ MNs (Gibbs et al., 2018).

In a TDP-43 mouse model of ALS has been observed a decreased number of mitochondria and lysosomes at the axon terminal level, suggesting an impairment of vesicular trafficking along the axon (Shan et al., 2010). Therefore, many studies have been done to discover the mechanisms underlying axonal transport deficit in TDP-43-related ALS. Since TDP-43 binds mRNAs regulating brain development and synaptic stability and facilitates their trafficking from the nucleus to the axon terminal, one of the most convincing hypothesis is

a loss of function of mutant TDP-43 due to modifications in the prion-like domain of TDP-43, which normally mediates the assembly of RNA granules (Alami et al., 2014). A second toxic mechanism could be related to mislocalization and aggregation of TDP-43, which determines a lack of TDP-43 activity in mRNA translation and splicing. For instance, TDP-43 stabilises neurofilament light chain mRNA, one of the major components of MN cytoskeleton (Strong et al., 2017). Moreover, a reduction of axonal growth and disruption in cytoskeleton morphology have been observed in TDP-43 related ALS, suggesting a massive involvement of TDP-43 in the regulation of translation and stabilization of several cytoskeletal proteins, included tubulin, microtubules and neurofilaments (Triphati et al., 2014; Baskaran et al., 2018; Kreiter et al., 2018).

Also, mutant FUS protein showed a gain of toxic function mechanism, which leads to a reduction of mitochondria trafficking along the axons. Guo and Colleagues demonstrated a direct correlation between mutant FUS and mitochondrial axonal transport impairment in iPSC-MNs derived from ALS patients carrying FUS mutations. Moreover, this observation was validated in iPSC-MN after mutant FUS correction by CRISP-Cas9 technology and by the over-expression of mutant FUS in H9-hESC lines following the induction with doxycycline. In the first case, the correction of the mutation in FUS gene rescued axonal transport; on the contrary, when mutant FUS over-expression was induced in hESC-derived MNs a strongly reduction of mitochondria motility was recorded (Guo et al., 2017).

The mitochondria transport defect seems to be related to mitochondria-associated with the ER membranes, rather than to mitochondria morphological alteration or cytoskeletal changes. Indeed, the physiological overlapping between mitochondria and ER, which is involved in several crucial functions included intracellular trafficking, was reduced in

iPSC-MNs carrying FUS mutation compared to controls, indicating a general problem in axonal transport. To rescue axonal transport, inhibitors of histone deacetylase 6 (HDAC6) were tested on FUS iPSC-MNs. HDAC6 is a cytoplasmic deacetylase which modulates the acetylation state of α-tubulin, regulating its ability to bind molecular motor proteins to microtubules (Guo et al., 2017). It has also been reported that FUS and TDP-43 regulate mRNA transcript of HDAC6 (Kim et al., 2010). However, the amelioration of axonal transport in FUS iPSC-MNs after the inhibition of HDAC6 by pharmacological treatment or ASO silencing was due to increased acetylation of α-tubulin in the microtubules and not directly related to an effect on mutant FUS (Guo et al., 2017). In accordance with this hypothesis, the genetic deletion of HDAC6 in $SOD1^{G93A}$ mice prolonged survival probability by protecting the integrity of MN axons (Taes et al., 2013).

1.3.5. Neuroinflammation

Neuroinflammation is recognized as one of the main factors which affect ALS progression. A lot of evidence supports a toxic role of neuroinflammation in the late stage of the disease. Indeed, studies on mutant SOD1 mice described a protective role of microglia and astrocytes at the disease onset, when these two cell types attempt to protect MNs from degeneration by secreting anti-inflammatory cytokines and trophic factors, such as interleukin-4 (IL-4), interleukin-10 (IL-10), insulin-like growth factor-1 (IGF-1), brain-derived neurotrophic factor (BDNF). On the contrary, at the late stage of the disease microglia and astrocytes shift to a pro-inflammatory negative phenotype, that exacerbates MN degeneration (Beers et al., 2011).

An activated inflammation state is present also at the systemic level, involving the innate immune system. For instance, peripheral blood monocytes exert a pro-inflammatory action

in ALS patients; in particular, they are more active in fast progressing ALS (Zhao et al., 2017). In addition, a dysregulation of T lymphocytes has been reported in ALS patients. The number of regulatory T lymphocytes (Tregs) and the expression of their specific transcriptional factor FOXP3 were reduced in ALS patients, who showed a fast progressive form of ALS. Moreover, Tregs isolated from the blood of ALS patients were not able to suppress responder T lymphocytes *in vitro*, suggesting a dysfunction and not only a decreased number of Tregs in ALS patients (Beers et al., 2017).

Major histocompatibility complex I (MHCI) is a key molecule of the immune system for the antigen presentation to $CD8^+$ T lymphocytes. Recently, MHCI has been found also in the CNS, where it regulates long-term plasticity of excitatory synaptic transmission (Chiarotto et al., 2017), where it has a relevant role in axon regeneration. In a mouse model knocked-out for β2 microglobulin (β2m), a subunit of MHCI, axonal regrowth after axotomy of peripheral sciatic nerve was impaired compared to WT mice (Oliveira et al., 2004). On the other hand, transgenic mice with enhanced neuronal MHCI expression recovered more efficiently the locomotor function after spinal cord injury when compared to WT mice (Joseph et al., 2011), validating the importance of functional MHCI in CNS homeostasis. In $SOD1^{G93A}$ mice, an altered distribution of MHCI has been reported already at the beginning of the disease. In control animals, MHCI was localized in lumbar spinal cord MN perikarya, while in $SOD1^{G93A}$ mice it moved in efferent axons and axon terminals (Nardo et al., 2016). In addition, a higher expression level of β2m and Lmp7 immunoproteasome subunits, responsible for antigenic peptides production, was detected in $SOD1^{G93A}$ mice, suggesting the ability of MNs to produce and expose MHCI linked with antigenic peptides to be presented to cytotoxic T cells, that infiltrate peripheral nervous system (PNS). This mechanism seems to be protective for MNs at an early stage of the

disease. Indeed, SOD1^{G93A} mice knock-out for β2m showed an anticipation of motor performance decline, associated with an earlier axonal impairment and denervation of hind limb muscles (Staats et al., 2013). In contrast, MHCI overexpression at the late stage of the disease exerted a detrimental effect, due to the strongly activation of pro-inflammatory microglia, accelerating denervation and atrophy of forelimbs in SOD1^{G93A} mice. On the contrary, the β2m deletion promoted the maintenance of forelimb innervations and prolonged mouse survival (Nardo et al., 2018).

A loss of MHCI exposure on MN cell membrane has been reported at a late stage of the disease, probably due to ER stress and its dysfunction. MHCI are assembled in ER, but at the late stage of the disease ER works to maintain unfolded protein homeostasis (unfolded protein response to cell stress) and MHCI heavy chains move from ER membrane to the cytosol where they are degraded by the proteasome (Lilley and Ploegh, 2005).

In astrocytes, silencing of MHCI regulates their state of activation and the production of pro-inflammatory cytokines *in vitro*, but no MHCI activation was detected in spinal cord of SOD1^{G93A} mice during the disease progression (Rojas et al., 2014). Instead, microglia cells expressed high level of MHCI in spinal cord of SOD1^{G93A} mice and recruited cytotoxic CD8+ T lymphocytes, which exacerbated inflammation in spinal cord of SOD1^{G93A} mice and promote MN death (Nardo et al., 2016). A further demonstration supporting the role of MHCI in microglia activation derives from SOD1^{G93A} mice knock-out for β2M, a component of MHCI, in which the inflammatory response was reduce both *in vitro* and *in vivo* (Nardo et al., 2018).

NFκB is considered the first player in the development of the inflammatory response. It regulates the expression of genes of cytokines, chemokines, enzymes, adhesion molecules,

pro- and anti-apoptotic proteins. NFκB is formed by two of five DNA-binding proteins (p50, p52, p65 RelA, c-Rel, RelB) and a different assembly determines specific transcriptional activity. When inflammatory mediators bind their respective receptor, a signalling cascade is initiated that leads to phosphorylation and activation of I-Kappa-B Kinase (IKKB), which, in turn, phosphorylates the NFκB inhibitory protein IκBα and determines its proteasomal degradation. Finally, NFκB (p65/p50) can translocate to the nucleus where it modulates gene transcription (Ghosh and Karin, 2002).

In glial cells derived from fALS and sALS patients, NFκB has been found up-regulated, confirming the involvement of neuroinflammation in ALS and the relevant role of astrocytes and microglia in disease progression (Haidet-Phillips et al., 2011; Swarup et al., 2011). Frakes and Colleagues demonstrated that the selective partial deletion of IKKB and, consequently, NF-κB inhibition in microglia cells of $SOD1^{G93A}$ mice significantly increased the survival of these mice. The knock-down of IKKB in $SOD1^{G93A}$ microglia reduced typical markers of pro-inflammatory microglia (M1), such as CD68, CD86 and iNOS. A general analysis for GFAP and Iba1 revealed a lower astrogliosis and microgliosis in $SOD1^{G93A}$ mice. Unexpectedly, the same deletion in astrocytes did not produce an improvement in disease symptoms, suggesting different mechanisms for astrocyte-mediated toxicity (Frakes et al., 2014).

p50 and p65 RelA subunits can assembly to form NFκB, which can have neuroprotective or neurotoxic effects, depending on the acetylation state of RelA (Lanzillotta et al., 2010). RelA subunit is highly expressed in mutant SOD1 MNs *in vitro* models and in ALS patients (Lanzillotta et al., 2013; Jiang et al., 2005). A following study demonstrated that RelA presents an aberrant acetylation state, represented by global lysine deacetylation and enhanced acetylation of a specific residue of lysine in position 310 (K310). This latter

promotes the transcription of pro-apoptotic factors inducing neurodegeneration (Schiaffino et al., 2018; Lanzillotta et al., 2013). The administration of MS-275, an HDACs inhibitors, and resveratrol, mediating the selective deacetylation of K310, reverted the aberrant acetylation state of RelA and increased the expression of Bcl-xL, an anti-apoptotic protein, in lumbar spinal cord of $SOD1^{G93A}$ mice. These biochemical read-outs translated in a delay of disease onset, an amelioration of motor skills and an increase of survival (Schiaffino et al., 2018).

Cytosolic nucleotide-binding oligomerization domain (NOD)-like receptor (NLR) pyrin domain containing 3 (NLRP3; inflammasome) is recognized as one of the main mediators of neuroinflammation development in ALS and in other neurodegenerative diseases and during brain aging. NLRP3 is formed by three components: a cytosolic pattern recognition receptor (PRR), pro-caspase 1 and apoptosis-associated speck-like protein (ASC) containing a caspase recruitment domain. Its assembly can be triggered by toll-like receptors (TLRs) activation, following pathogen-associated molecular patterns (PAMPs) and DAMPs binding, or by endogenous cytokines. TLRs and cytokines, through the NFκB pathway, promote the transcription of NLRP3, pro-IL-1β and pro-IL-18. After this first step, NLRP3 binds ASC and this latter recruits and activates caspase 1. The activation of caspase 1 leads to the proteolitic cleavage of pro-IL-1β and pro-IL-18 in their respective active forms, mediating the innate immune response (Singhal et al., 2014; Davis et al., 2011; He et al., 2016).

In $SOD1^{G93A}$ rat brain, increased level of NLRP3 and active caspase 1 were reported. This augmentation was associated with a higher expression of TLR4 and NFκB (Gugliandolo et al., 2018). Other studies described NLRP3 activation as an early event in ALS pathogenesis. Johann and Colleagues detected higher concentrations of inflammasome and

IL-1β in spinal cord of 60 days-old SOD1^{G93A} mice and in post-mortem tissue from ALS patients (Johann et al., 2015). A next paper hypothesized that one of the causes of increased NLRP3 expression is protein nitration. As already described, ROS and RNS are hallmarks of ALS and these reactive species determine damage to proteins, such as protein tyrosine nitration. The treatment of SOD1^{G93A} microglia with iNOS and NOX2 inhibitors reduced nitrotyrosine levels and, consequently, caspase 1 and NLRP3 activation, supporting the involvement of protein nitration in neuroinflammation spread (Belleza et al., 2018).

Recently, a new neurotoxic mechanism mediated by TDP-43 has been uncovered. Microglial cells derived from cerebral cortex showed an increased activation of NLRP3, caspase 1 and caspase 3 after the exposure to exogenous TDP-43, which was internalized by microglia. Therefore, TDP-43 could promote TNF-α, IL-1β and IL-18 production and secretion, determining the genesis of a chronic inflammatory state. The internalization of TDP-43 aggregates and their toxic effects seem to depend on the chaperon HSP-27, which has been found up-regulated in CSF and spinal cord of ALS mouse models and in brain samples from ALS patients. HSP-27 exacerbated the pro-inflammatory response in TDP-43-exposed microglia and induced the activation of caspase 3, ultimately leading to active IL-18 levels increase through an alternative pathway respect the classical NFκB/NLRP3 (Leal-Lasarte et al., 2017).

1.4 Non-cell autonomous aspects of ALS

The first studies aimed to unveil pathogenic mechanisms at the basis of ALS onset were focused on MNs, since they are the damaged cells leading directly to ALS symptoms. However, in the last decades a pivotal role in disease onset and progression also of non-neuronal cell, such as astrocytes, microglia and oligodendrocytes, has been recognised. This change of viewpoint derives from many observations made after histological assessments and transcriptomic profiling of disease tissue, which highlighted a strong non-neuronal signature in ALS and other neurodegenerative diseases (Lee et al., 2016; Chen et al., 2018).

1.4.1 The role of astrocytes in ALS

Nowadays, astrocytes are recognised as the main cell type regulating homeostasis of the CNS. They preserve an ancillary defensive response, i.e. astrogliosis, which is essential for neuroprotection and tissue regeneration and repair. However, astrogliosis response can worsen and cause several forms of neuropathologies.

Astrocytes are electrically non-excitable, even if they express a large number of excitable molecules and mechanisms, such as plasmalemmal ion channels and receptors for neurotransmitter, neuromodulators and neurohormones, cytoplasmic structure modulating second messenger stimuli. Intracellular fluctuation of ions mediates astrocytes excitability through the modulation of ion channel opening, in particular Ca^{2+} and Na^{+} channels. These ion changes will balance homeostatic cascade signalling, including the monitoring of ion and neurotransmitter concentration, pH homeostasis, neutralization of ROS by secreting ROS scavengers.

Astrocytes play a fundamental role in synapse regulation. Perisynaptic astrocytes are enriched in various transporters which maintain neurotransmitter homeostasis in the synaptic space. This class of astrocytes are characterized by a high plastic capacity; indeed, they participate to synaptogenesis, synaptic maturation and synaptic extinction.

In response to a damaging insult, astrocytes shift from a rest phenotype to a high reactive and proliferative one, in order to repair the damage and supply trophic factors to neurons and reduce neuronal degeneration. In many neurodegenerative disease this mechanism results impaired and it leads to neurotoxic events (Verkhratsky and Zorec, 2019).

A recent analysis described the behaviour of astrocytes following a transient ischemia, induced by occluding the middle cerebral artery (MCAO) or after a treatment with the bacterial endotoxin lipopolysaccharide (LPS) to generate an inflammatory response. Both MCAO and LPS stimulated astrogliosis in brain cortex. However, mRNA analysis revealed two diverse population of astrocytes, depending on the causative stimulus. After MCAO, most of upregulated genes were associated with the production of neurotrophic factors and cytokines, including Cardiotrophin-like cytokine factor 1 (CLCF1), Leukemia inhibitory factor (LIF), IL-6, IL-10 and thrombospondines that may facilitate the regeneration of lost synapses. On the other hand, LPS-treated astrocytes showed an increased transcription of genes related to classical complement cascade activation (C1r, C1s, C3 and C4), playing a critical role in synapses pruning during development and, likely, leading to synapses loss in neurodegenerative diseases. Therefore, on the basis of this different transcriptional pattern we can divide astrocytes in A2, supporting neuronal repair, and A1 astrocytes, which exacerbate the damage and trigger a strong inflammatory response (Zamanian et al., 2012).

A deeper study on the mechanisms leading to A1 astrocytes activation highlights the role of microglia. LPS stimulation polarized microglia to M1 phenotype, characterized by high secretion of IL-1α, IL-1β, TNF-α and C1q, mediators of inflammatory response. When astrocytes were grown with medium derived from LPS-stimulated microglia, they shifted to A1 phenotype. Notably, if they were grown with unstimulated-microglia medium any change was detected. Moreover, a cytokine cocktail, containing IL-1α, TNF-α and C1q, was able to induce A1 astrocytes, validating the starting hypothesis. A1 astrocyte toxicity derives from secretion of soluble toxins, able to rapidly kill neurons. In ALS and in most neurodegenerative diseases the presence of neuroinflammation and M1 activated microglia has been reported; thus, suggesting astrocyte activation in the A1 manner. Indeed, complement component 3 (C3), highly up-regulated in A1 astrocytes and absent in A2 astrocytes, was massively represented in post-mortem tissues from ALS, Alzheimer's disease, Huntington's disease, Parkinson's disease and multiple sclerosis. This evidence demonstrates that A1 astrocytes are present in most neurodegenerative diseases, where, probably, they cover a non-marginal role in neuron death (Liddelow et al., 2017).

The role of astrocytes in the regulation of innate immunity in CNS is currently well recognised. Astrocytes express TLRs, type I membrane glycoproteins characterized by leucine-rich-repeat motifs in the extracellular domain. TLR1, TLR2 and TLR6 recognise bacterial lipoproteins; TLR3, TLR7, TLR8 and TLR9 specifically bind nucleic acids; TLR5 identifies flagellin; TLR4 presents a wide spectrum of ligands, including LPS and fungal zymosan. The main TLR expressed on astrocyte membrane is TLR3. In particular, it has been reported that TLR3 expression can be induced by stimulating astrocytes with pro-inflammatory cytokines, such as IL-1β and IFN-β or IFN-γ. Also TLR2 and TLR4 are expressed in astrocytes, although at lower levels.

The major signalling pathway activated by TLRs starts with the binding of MyD88 with the toll-interleukin 1 receptor (TIR) cytoplasmic domain, leading to the recruitment of the IL-1 receptor-associated kinase (IRAK4). This latter dissociates from MyD88, binds to and activates the TNF receptor associated factor 6 (TRAF6), promoting to the formation of Complex-1. Then, this triple association dissociates from TLR and mediates the recruitment of several proteins, including TGFβ related kinase (TAK-1), and TAK-1 binding protein (TAB) 1-3, forming core components of Complex-2. These processes determine the phosphorylation of TAK-1 and induce the activation of IKK complex which in turn phosphorylates IκB protein, causing its degradation and allowing the translocation of NFκB to the nucleus. On the other hand, Complex-2 can activate MAPKs, ERK1/2, p38 and JNK via phosphorylation, which in turn modulate the activation of several transcription factors.

The activation of these two different pathways leads to an increased transcription of iNOS, inducible COX-2, and stimulates the release of major inflammatory cytokines, such as IL-1β, IL-6, and TNF-α (Rahimifard et al., 2017). These mechanisms are essential for the development of an appropriate response to pathogens. Indeed, mice that were knock-out for TLR3 were unable to activate the inflammatory response after Theiler's murine encephalomyelitis virus (TMEV) and, therefore, to block its replication (So et al., 2006; Farina et al., 2007).

The activation of NFκB in astrocytes highlights their involvement in neuroinflammatory response regulation and recovery function modulation after injury. A mouse model knock-out for NFκB showed a reduced production and secretion of cytokines and chemokines, reducing the recruitment of leukocytes and macrophages to the lesioned area. This less-activated environment promoted functional recovery and tissue regeneration (van Loo et

al., 2006). On the other hand, the absence of inflammatory responses can be detrimental in CNS. Mouse model knock-out for IL-6 or IL-1β showed a delayed astrocyte activation and increased BBB permeability, causing an incapacity of astrocytes to reduce the lesioned area. Moreover, a decreased synthesis of the neurotrophic factors CNTF (Ciliary neurotrophic factor) and IGF-1, both helpful in tissue regeneration (Herx et al., 2001; Swartz et al., 2001), was registered. A strictly regulation of the inflammatory responses is essential to preserve the physiological homeostasis of CNS and a dysregulation of the balance between pro- and anti-inflammatory responses can be harmful for the organism.

The first evidence of astrocyte alteration in ALS derived from animal models in which mutant SOD1 was selectively expressed or deleted in astrocytes. First experiments were carried out on chimeric animals composed of mixtures of normal cells and cells that express a human mutant SOD1 polypeptide at levels sufficient to cause fatal motor neuron disease. Researchers reported that the presence of wild-type non-neuronal cells in the $SOD1^{G37R}$ and $SOD1^{G85R}$ chimeras delayed disease onset and prolonged their survival. In accordance, chimeric animal characterized by the expression of mutant SOD1 in non-neuronal cells but not in MNs showed histological signs of neurodegeneration, caused by the accumulation of ubiquitinated epitopes, that were never seen in age-matched wild-type littermates (Clement et al., 2003). Some years later, similar experiments using Cre-Lox recombination to delete mutant SOD1 gene selectively in microglia or astrocytes were performed. The reduction of mutant SOD1 expression in astrocytes of $SOD1^{G37R}$ or $SOD1^{G85R}$ mice did not delay disease onset and early disease progression, but it slowed the late disease course extending significantly mouse survival (Boille et al., 2006; Yamanaka et al. 2008; Wang et al., 2011). These experiments highlighted the non-neuronal

component of ALS and, moreover, identified astrocytes and microglia as pivotal players of disease progression rather than of disease onset.

Another approach to validate the astrocyte role in neurodegeneration consisted in cell transplantion. Transplantation of WT astrocyte precursors in cervical spinal cord of ALS mice slowed the disease progression and prolonged survival probability (Lepore et al., 2008). In accordance, transplantation of astrocyte precursors carrying $SOD1^{G93A}$ gene mutation promoted local degeneration in spinal cord and caused motor dysfunction in WT mice (Papadeas et al., 2011). Finally, Nagai and Colleagues confirmed by in-vitro co-culture studies the detrimental role of ALS astrocytes: mutated astrocytes were able to induce neurodegeneration both in ALS MNs and healthy MNs, supporting the hypothesis of a gain of toxic functions of astrocytes in ALS (Nagai et al., 2007).

During the last decades many studies tried to understand which are the toxic factors released by astrocytes in ALS. The first papers were focused on the role of astrocytes in excitotoxicity, because of the down-regulation of EAAT-2 in astrocytes membranes, that leads to a reduced uptake of glutamate from the synapses (Brujin et al. 1997), and their loss of control of the GluR2 AMPA-subunit editing, causing an abnormal influx of Ca^{2+} in MNs (Van Damme et al., 2007).

Astrocytes represent one of the major sources of energy for MNs, in particular through the shuttle of lactate (Pellerin and Magistretti, 1994). MNs are able to promote aerobic glycolisis in astrocytes by glutamate release. This latter induces the activation of the Na^+/K^+ -ATPase pump that consumes the ATP produced by phosphoglycerate kinase (Pgk), triggering glucose uptake and its glycolytic processing, leading to the release of lactate from astrocytes. Lactate can then contribute to the activity-dependent fuelling of the

neuronal energy demands associated with synaptic transmission (Pellerin et al., 2007). However, gene expression analysis in $SOD1^{G93A}$ astrocytes revealed an impairment of many proteins involved in lactate shuttle, such as Glutamate Aspartate transporter-1 (GLAST-1), Na^+/K^+ -ATPase, Pgk and the lactate efflux transporter Solute carrier 16a4 (Slc16a4).

The quantification of lactate level in the spinal cord of $SOD1^{G93A}$ transgenic mice validated the gene analysis results. $SOD1^{G93A}$ mice showed a significant reduction of lactate shuttle between astrocytes and MNs already at an early stage of the disease, followed by a further decrease during disease progression. $SOD1^{G93A}$ derived astrocytes showed the same impairment of lactate shuttle when co-cultured with transgenic or WT mouse MNs. Moreover, the expression of the lactate transporter Slc16a4 was down-regulated in spinal cord astrocytes isolated from three patients with ALS carrying SOD1 mutations, in comparison to control individuals. The impairment of the lactate shuttle leads to MN energetic deficit, causing alteration of membrane potential and imbalance of ion concentration (Ferraiuolo et al., 2011).

Astrocytes secrete many trophic factors, including nerve growth factor (NGF). Mature NGF modulates neuronal differentiation and survival by binding Tyrosine receptor Kinase A (TrKA). On the other hand, Pro-NGF preferentially binds the p75 receptor, which determines axonal growth and remodelling during development, although its expression is barely detectable in adult. Notably, p75 expression increases in pathological condition, where it promotes the activation of apoptosis pathways by boosting NFκB, p53 and Bax. Ferraiuolo and Colleagues demonstrated that astrocytes derived from $SOD1^{G93A}$ mice expressed higher amount of NGF compared to WT astrocytes and, at the same time, p75 receptor and its pro-apoptotic associate protein (Ngfrap1) were up-regulated in $SOD1^{G93A}$

astrocytes. This alteration, together with a reduction of mature NGF, leads to a decrease MN viability in ALS mice (Ferraiuolo et al., 2011).

The metabolism of nucleosides was also altered in astrocytes from C9orf72 and sporadic ALS patients. ALS models showed an increased release of ATP from MNs, determining microglia activation and increased astrogliosis and neuroinflammation. Moreover, adenosine, the last step of ATP metabolism, was also higher in ALS. An increased concentration of adenosine causes activation of low affinity receptors on astrocytes, promoting astrocyte proliferation and activation, reducing glutamate uptake and stimulating Ca^{2+}-dependent glutamate release (Rothstein et al., 1996). The up-regulated levels of adenosine were related to a lower expression in ALS astrocytes of adenosine deaminase (ADA), an ubiquitously expressed enzyme that converts adenosine in inosine. Further evidence sustaining the detrimental role of low levels of ADA in ALS was collected by inhibiting ADA in control astrocytes. The inhibition of ADA in control astrocytes caused an impairment of MN viability in the co-culture model. In addition, exposure of ALS astrocytes to inosine was able to partially rescue MN survival, validating the relevant function of adenosine and inosine in ALS (Allen et al., 2019).

Astrocytes are key players in neuroinflammation development. They are able to produce and secrete cytokines, thus they can actively modulate the inflammatory response in CNS. Increased serum/plasma and CSF levels of TNF-α, IL-6, IL-8, and IFN-β, have been detected in ALS patients when compared to controls (Philips and Robberecht, 2011; Hu et al., 2017). These findings promoted the study of the cytokine function and of inflammation in ALS.

Transforming growth factor βs (TGF-βs) are pleiotropic cytokines that exert key functions in immune homeostasis, neurotrophic response and microglia development. In ALS patients, TGF-β1 levels are elevated in serum, plasma and CSF (Houi et al.,2002). Endo and Colleagues detected high levels of TGF-β1 in astrocytes from sporadic ALS patients and from $SOD1^{G93A}$ mice. The over-production of TGF-β1 caused a faster disease progression, while the deletion of SOD1 mutation from ALS mice determined a reduction of TGF-β1 production and decreased disease severity. This neurotoxic effect seems to derive from a TGF-β1-dependent alteration of the balance between INF-γ and IL-4 production in T cells and microglia. The pharmacological treatment with a TGF-β signalling inhibitor after the disease onset prolonged survival of $SOD1^{G93A}$ mice, rescuing INF-γ/IL-4 dysregulation and decreasing the number of activated microglial cells. Moreover, the correlation between TGF-β1 level and disease progression suggested the use of TGF-β1 as a predictive biomarker for disease progression and severity (Endo et al., 2015).

TGF-β1 is also involved in protein aggregation. Indeed the increased secretion of TGF-β1 by astrocytes activates the mammalian target of rapamycin (mTOR) signalling pathway, which causes an impairment of autophagic function in MNs. In particular, TGF-β1 activated mTOR pathway in MNs, inducing aggregation of p62 and LC3-II, the main proteins involved in autophagy (Tripathi et al., 2017).

TNF-α is one of the main cytokines that have been found overexpressed in blood and CSF of ALS patients (Tateishi et al., 2010; Poloni et al., 2000). High concentrations of TNF-α, together with the up-regulation of TNF-α receptors (TNFRs), have also been reported in spinal cord of $SOD1^{G93A}$ mice before symptom onset (Brambilla et al., 2016; Yoshihara et al., 2002).

TNF-α can be differentiated in two diverse forms: membrane-bound TNF-α (mTNF-α) and soluble TNF-α (sTNF-α). The two forms of TNF-α act through TNFR1 and TNFR2. Both are able to mediate the cytotoxic and apoptotic effects of TNF-α. TNRF1 contains a death domain, while TNRF2 acts through a cell-to-cell interaction. In particular, TNRF2, by binding mTNF-α, can induce tumor and neuronal cell death. This second mechanism seems strongly involved in ALS. Indeed, a study on spinal cord astrocytes-MN co-cultures from $SOD1^{G93A}$ mice reported an increase of mTNF-α in MNs and the reduction of TNRF2, but not of TNRF1, completely rescued MNs. The same positive effects on MN survival were observed in $SOD1^{G93A}$ mice knock-out for TNFR2 (Tortarolo et al., 2015).

On the contrary, the ablation of TNRF1 exacerbated the detrimental effects of TNF-α. Indeed, when TNRF1 is expressed on the astrocyte membrane, it promotes the production and secretion of glial-derived neurotrophic factor (GDNF), which supports neuron growth and survival (Brambilla et al., 2016). Another study demonstrated that both receptors exert their functions through activation of the ASK1/p38MAPK pathway, which resulted detrimental for MNs. The inhibition of p38 MAPK prevented MN death in $SOD1^{G93A}$ co-cultures, suggesting the essential role of the TNFRs/ASK1/p38MAPK pathway in neurodegeneration (Dewil et al., 2007). TNF-α exerts its toxic function also in other models of ALS. For instance, astrocytes expressing mutant FUS secreted TNF-α as main toxic factor mediating MN death through NFκB pathway activation. Moreover, TNF-α modulated the expression of AMPA receptors and GluA2 AMPA-subunit in MNs, determining an increase permeability to $Ca^{2+}$and leading to excitotoxity (Kia et al., 2018).

Finally, modifications of miRNA expression level were reported. Cortical astrocytes from $SOD1^{G93A}$ mice showed a down-regulation of miR-146a, miR-125 and miR-21 compared to control astrocytes. miR-146a works as negative-feedback regulator of TLR

inflammatory pathway (Iyer et al., 2012), while miR-125 and miR-21 are modulators of neurite outgrowth (Le et al., 2009; Kang et al., 2019). $SOD1^{G93A}$ astrocytes presented higher level of HMGB1 and NFκB, leading to an increase of cytokines production. In accordance, the down-regulation of these three miRNAs caused a reduction of MN viability (Gomes et al., 2019).

At the same time, also the pattern of miRNAs released from astrocytes through extracellular vesicles (EVs) has been found altered.

miRNAs secreted by astrocytes regulate a number of transcripts, encoding proteins involved in axonal growth and maintenance. EV cargo was found modified in C9orf72 astrocytes and was able to induce MN toxicity. In particular miR-494-3p was strongly down-regulated in EVs derived from C9orf72 human astrocytes, determining an impairment of axonal development and inducing neurite retraction and MN death, by increasing Semaphorin-3A (SEMA3A) levels (Varcianna et al., 2019).

As described above, astrocytes represent an essential support for MN survival and, in ALS and other neurodegenerative disease, they are subject to a shift from a supportive to a neurotoxic phenotype, causing metabolic alteration, loss of trophic function, secretion of toxic factors and development of a chronic inflammatory response. The totality of these alterations makes astrocytes good targets to modulate disease progression and rescue MNs in ALS. In particular, astrocytes are largely used for a first drug screening to select promising molecules (Gorshkov et al., 2018). Moreover, some drugs targeting astrocytes have been tested in patients. For example, ceftriaxone, which exhibits effectiveness in boosting EAAT2 expression, was tested in rodent models and then in ALS patients.

Unfortunately, the clinical trial failed in Phase III because of its lack of efficacy (Cudkowicz et al., 2014).

1.4.2 The role of microglia in ALS

Microglial cells are the sentinels of the CNS, playing a main role both in physiological and pathological conditions. Microglial cells fulfil crucial functions in embryonic and postnatal formation of CNS, promoting neuronal survival by releasing several neurotrophic factors, such as IGF-1 and CX3CL1. Moreover, microglia regulates CNS homeostasis through cellular pruning via NGF-induced cell death, removal of cellular debris and apoptotic cells by phagocytosis and lysosome degradation (Nayak et al., 2014).

In many acute and chronic diseases characterized by a neuroinflammatory component, microglia cells show altered morphology and transcription pattern, classified in the following specific phenotypic profile M0, M1 and M2. M0 corresponds to a resting state, in which microglia receives inhibitory signals from the CNS environment. When these inhibitory signals are replaced by activating stimuli, microglia can undergo three different fates: classical M1 activation stimulated by IFN-γ, alternative M2a and M2b phagocytic/neuroprotective activation stimulated by IL-4 and IL-13, and, finally, acquired deactivation M2c stimulated by TGF-β and IL-10. The balance between these different activation states is essential for the maintaining of CNS integrity. In CNS pathology the strictly regulation of microglia phenotype can fail and cause deleterious immune response exacerbating neuronal death (Hammond et al., 2018).

In *post-mortem* ALS patient tissue, a prominent microgliosis has been observed in the regions surrounding degenerated MNs, including motor cortex, in portions along the corticospinal tract and in ventral horn of the spinal cord. In adding, *in vivo* positron

emission tomography (PET) imaging showed microglia activation also at different stages of the disease and correlated the stronger microglia activation with the worse ALS clinical outcome (Chen et al., 2018). However, the role of microglia is not univocal in ALS. For instance, microglia isolated from $SOD1^{G93A}$ mice displayed a peculiar phenotype that differs from the commonly characterized M1/M2 phenotypes and from those obtained after activation with LPS or with other stressors. Indeed, $SOD1^{G93A}$ microglia cells at pre-onset stages reduce immune response and exhibit an anti-inflammatory behavior, marked by high expression levels of BDNF and CD163; while, at later stages of the disease, the phenotype shifts to a highly proliferative pro-inflammatory one, accompanied by increased levels of ROS production and glutamate release, which are detrimental for MNs (Volontè et al., 2019).

Evidence for microglia involvement in ALS progression derives from different mutated-SOD1 animal models, which demonstrated that the deletion of mutant SOD1 in microglial cells significantly increased the survival of $SOD1^{G37R}$ mice (Boillée et al., 2006) and that the administration of WT microglia in $SOD1^{G93A}$ mice slowed MN loss and extended lifespan compared to WT mice receiving $SOD1^{G93A}$ expressing cells or to $SOD1^{G93A}$ mice (Beers et al., 2006).

More recent studies investigated the influence of microglia phenotype modulation on disease progression. For instance, NFκB or IL-1β inhibition in microglia suppressed inflammatory toxicity to MNs (Frakes et al., 2014; Meissner et al., 2010); inhibition of colony stimulation factor 1 receptor (CSF1R), supporting microglia differentiation and proliferation, reduced microglia growth and slowed disease progression in $SOD1^{G93A}$ mice (Martìnez-Muriana et al., 2016); CNS-delivery of IL-4 via a gene therapy strategy in $SOD1^{G93A}$ mice determined an amelioration of clinical symptoms at an early stage of the

disease, by inducing a slowly proliferating microglia expressing genes typical of embryonic microglia (Rossi et al., 2018).

These results support the involvement of microglia in ALS onset and progression. However, the dual role of microglia in ALS makes it difficult to have a clear scenario of its beneficial function or detrimental effects.

1.4.3 The role of oligodendrocytes in ALS

Oligodendrocytes are the myelinating cells of the CNS, which origin from oligodendrocytes precursor cells (OPCs), deriving from the caudal region of the neural tube in the ventral midline, and secondly during development, from dorsal spinal cord. The main studied function of oligodendrocytes is the generation of myelin sheaths around target axons that results in enhanced rates of axonal conduction through the establishment of saltatory conduction (Tognatta et al., 2016).

Another main function of oligodendrocytes consists in providing metabolic support to neurons. Indeed, the lactate produced by oligodendrocytes is transferred, through the monocarboxylate transporter-1 (MCT-1), to myelinated axons, in order to maintain their structure and function. Interestingly, the expression of MCT-1 is particularly high in oligodendrocytes compared to other glial cells, suggesting a crucial role of oligodendrocytes in furnishing energy to neuron. Notably, the expression of MCT-1 is reduced in oligodendrocytes from patients with ALS and from the $SOD1^{G93A}$ mice, indicating that MCT-1 may play a role in ALS pathogenesis (Lee et al., 2012).

The contribution of oligodendrocytes to the disease has been demonstrated by deleting SOD1 from oligodendrocytes in the $SOD1^{G37R}$ mouse model. These mice showed a

significant delay of disease onset and an increase of survival, and did not exhibit motor neuron degeneration at the time of death. This evidence has suggested a more complex scenario in which each cell type plays a specific role in onset or progression of the disease (Yamanaka et al., 2008).

In ALS patients, a reduction of gray matter myelin and reactive changes in $NG2^+$ cells have been reported in the motor cortex and spinal cord. In accordance, an extensive degeneration of gray matter oligodendrocytes was observed also in $SOD1^{G93A}$ mice, already before the onset of the symptoms of the disease. These early alterations suggest that a loss of functions of oligodendrocytes, in particular in providing lactate to MNs, can lead to neurodegeneration. However, the mechanisms are still to be elucidated and the degeneration of oligodendrocytes before MN death remains an hypothesis. Among the proposed mechanisms affecting oligodendrocyte functions, we can list the formation of protein aggregates inducing ER stress and the strong pro-inflammatory environment characterized by a high level of IFN-γ; indeed, both conditions were capable to induce cell apoptosis (Kang et al., 2013).

In-vitro studies with oligodendrocyte-MN co-cultures validated the crucial role of mutated SOD1 in oligodendrocyte functions. Ferraiuolo and colleagues analysed the viability of mouse MNs co-cultured with mature oligodendrocytes prepared from $SOD1^{G93A}$ mice, from iPSCs of three sporadic and one familial patients carrying a mutation in FIG4 or from iNPCs of four sporadic, three C9orf72, one SOD1 and one TARDBP patients. In all the experimental conditions, they observed a significant reduction of MN survival compared to co-cultures with control oligodendrocytes. The impaired MN survival was due to a decreased production and transport of lactate in oligodendrocytes, leading to energetic deficit in MNs, except for C9orf72-derived oligodendrocytes in which there was no

variation in lactate level. In accordance, MN viability was rescued by adding lactate to the medium. To elucidate the mechanisms determining the malfunction of oligodendrocytes, SOD1 was silenced in the different cell lines and MN viability was evaluated. The reduction of misfolded SOD1 in mouse and human oligodendrocytes determined a restoration of MN survival, supporting the hypothesis of a SOD1-dependent toxic mechanism. This amelioration, upon SOD1 silencing, was not detected in C9orf72 oligodendrocytes, suggesting the involvement of different toxic pathways (Ferraiuolo et al., 2016).

Another study on a zebrafish ALS model, in which mutated SOD1 was selectively overexpressed only in mature oligodendrocytes, confirmed the ability of misfolded SOD1 to induce disruption of myelin sheaths and downregulation of MCT1, causing MN death. In adding, this model presented behavioural abnormalities, such as thigmotaxis, freezing behaviours, erratic movement and learning impairments, possibly due to myelin defect-induced diminution of axonal conduction. The administration of 4-aminoprydine and 4-aminopyridine-3-methanol, two potassium channel inhibitors already used in spinal cord injury and multiple sclerosis to restore axonal conduction, rescued motor deficits and behavioural changes, but MCT-1 expression remained unvaried, indicating the involvement of other still unknown mechanisms (Kim et al., 2019).

1.5 ALS treatment

As widely described above, ALS presents a pathophysiology extremely complex and the disease phenotype is highly variable between patients. These aspects of ALS can explain the absence of efficacious drugs and the poor success of clinical trials. In addition, the triggering events that determine MN degeneration are still unknown. It is still hard to differentiate the triggers of the disease from the secondary consequences shaping the evolution of both the sporadic or genetic ALS types.

The complexity of ALS determined the lack of a completely reliable animal model. The most studied is the SOD1 mouse model, which describes only a restricted part of ALS patients and showed limitations for translational research. During the last decade, more efforts have been dedicated to better clarify the clinical phenotypes related to ALS course and prognosis. ALS is now viewed as a syndrome rather than a pure disease. In the broad field of MN diseases (MNDs) is essential to stratify wisely patients for the clinical trials and, many studies aimed at identifying biomarkers, to allow a precocious diagnosis of ALS, or to indicate the prognosis of the disease. For instance, the AMBRoSIA project, funded by the Motor Neuron Disease Association (MNDA), was devoted to the discovery of specific biomarkers that characterize the genetic forms of MNDs by genetic blood, urine and skin cell analyses, looking for genetic mutations known to be linked to these pathologies.

Finally, the newly identified genetic mutations, such as the C9orf72 mutation, opened a new area of research on the mechanisms of selective degeneration that will further help to increase the knowledge of ALS pathophysiology. On the other hand, nevertheless the

increased knowledge of this disease obtained during the last 20 years, only weak progresses have been done in finding an effective therapy (Mathis et al., 2016).

1.5.1 Approved drugs for the treatment of ALS

Currently, there are only two drugs approved from FDA for the treatment of ALS: riluzole and edaravone.

Riluzole was approved in 1995 by FDA and it was the first drug for ALS treatment. The first studies of ALS pathogenesis highlighted a strong excitotoxic component, therefore riluzole was selected and tested in virtues of its anti-excitotoxic ability (Miller et al., 2012). Riluzole is a sodium channel blocker, and its neuroprotective effects in the spinal cord are exerted on neurons and axons to reduce the increase of intracellular Na^+ ion concentration and to reverse operation of the axonal sodium Ca^{2+} exchangers (Schwartz et al. 2002). In addition, riluzole acts as an anti-glutamatergic agent via the prevention of glutamate receptor function, the increase of glutamate uptake, by activating glutamate transporters, and by reducing the release of glutamate (Wang et al., 2004). Unfortunately, the beneficial effects are only modest: it was observed a prolonged survival from three to six months, in particular in patients affected from bulbar-onset ALS. However, symptom amelioration was not significant since there was no improvement of muscle strength and only a small positive effect on quality of life of patients (Miller et al., 2012). One possible reason to explain, at least in part, the modest effects of riluzole, is that the blockade of Na^+ channels affects the excitability of all neurons, thus reducing the release of both excitatory and inhibitory neurotransmitters.

Edaravone was approved in 2017 by FDA in U.S.A. and in 2018 in Canada. Edaravone acts as a ROS scavenger and inhibits peroxyl radical (LOO•)-induced peroxidation. One of

the most interesting findings suggests that edaravone scavenges H_2O_2 and protects cells against oxidative stress via upregulation of Peroxiredoxin-2, downregulation of protein disulfide isomerase A3, and inhibition of apoptosis. Edaravone traps •OH and inhibits OH^--dependent lipid peroxidation or tyrosine nitration induced by $ONOO^-$ (Jaiswal, 2019). Unfortunalely, the beneficial effects are weak also with edaravone and there are limitations to the use, being the drug efficacious when administered timely in diagnosed patients. The need to act at an early phase of the disease, the repeated intravenous administration and the lack of data about edaravone side effects in a long-term therapy make the prescription of edaravone difficult for clinicians (Hardiman and van den Berg, 2017).

New therapeutic approaches are continuously studied. Between the new drugs we can list: anti-apoptotic substances, such as ursodeoxycholic acid and tauroursodeoxycholic acid, which acts on mitochondrial dysfunction and abnormal Ca^{2+} concentration, and Masitinib, that targets the inflammatory component of ALS, slowing ALS progress by 27% in preliminary results in a recent phase III study in combination with riluzole treatment (Nowicka et al., 2019).

1.5.2 Cell therapy in ALS

To date, most of the drugs tested for ALS did not show a significant efficacy in slowing disease progression, the attention has been moved also to innovative therapies, such as transplantation of human neural stem cells (hNSCs) and mesenchymal stem cells (hMSCs).

hNSCs therapy is currently studied by two different clinical trials in Phase I and II. In one of the study hNSCs are produced by Neuralstem Inc.; they were isolated from fetal spinal cord and grown as an adherent monolayer in the presence of the fibroblast growth factor-2

(FGF-2). The other clinical trial uses hNSCs produced by Azienda Ospedaliera Santa Maria (Terni). Cells were derived from foetal brain and expanded as floating neurospheres with the support of endothelial growth factor (EGF) and FGF-2 (Mazzini et al., 2019).

Preclinical results with neural progenitor lines showed a good tolerability and survival of several months after the transplantation. They may exert their beneficial action on MN degeneration, motor symptoms and survival through the integration into the tissue, the differentiation into astrocytes, oligodendrocytes and neurons and the formation of synapses with host neurons (Xu et al., 2006).

A recent study showed that hNPCs expressing GDNF, that differentiate *in vivo* into astrocytes, ameliorated the health of upper MNs, supported lower MN survival, delayed paralysis and extended lifespan when transplanted in the cortex of $SOD1^{G93A}$ rats. This cells have been approved from FDA to proceed with clinical trials to explore their safety and efficacy in ALS patients (ClinicalTrials.gov Identifier: NCT02943850) (Thomsen et al., 2018).

The study of the stem cell efficacy in the treatment of ALS and other neurodegenerative diseases started 20 years ago thanks to their potential advantages, such as the wide range of actions, the possibility to differentiate into neuron-like cells and the ability to release neuroprotective factors (Ciervo et al., 2017). There are different types of stem cells, depending on their source. The most studied at present are mesenchymal stem cells (MSCs) that can derive from umbilical cord, bone marrow, adipose tissue and peripheral blood and can differentiate in components of mesodermal origin, as cartilage, bone, fat, muscle and stroma. Bone marrow-derived (BM)-MSCs have been administrated by intravenous, intrathecal or intraparenchymal injection in the $SOD1^{G93A}$ rodent model by

several research groups. The results support the beneficial impact of MSC injection in ALS rodent models on disease onset, survival, MN viability and neuroinflammatory markers (Ciervo et al., 2017).

The first clinical trial was conducted in 2001, even if there were not preclinical data. This study demonstrated the safety of BM-MSC transplantation, but it did not give clear results about the efficacy (Mazzini et al., 2003). Other studies validated the safety of BM-MSCs in patients, reporting the absence of tumorogenesis also in long-term analysis (Blanquer et al, 2012; Karussis et al., 2010). In 2015, Oh and Colleagues evaluated the clinical feasibility and safety of two repeated injection of autologous MSCs into CSF of ALS patients. CSF samples of two patients were collected before the first and the second injection in order to analyse cytokine content. Unexpectedly, IL-10, TGF-β and IL-6 were increased after MSC treatment, while the level of CCL2 was reduced. A phase II clinical trial is on-going to evaluate also the efficacy of the treatment (ClinicalTrial.gov Identifier: NCT01363401) (Oh et al., 2015).

In 2016 a promising clinical trial was conducted to evaluate the efficacy of BM-MSCs secreting enhanced levels of multiple neurotrophic factors (NTFs), including GDNF, BDNF, vascular endothelial growth factor (VEGF) and hepatocyte growth factor (HGF). MSC-NTF cell (NurOwn®) injection in patients with ALS was safe and well tolerated. Moreover, preliminary data showed a slower disease progression, characterized by a decreased decline of muscle volume and of the compound muscle action potentials (CMAPs), that were most prominent in the right (injected) arm and in the IM-treated cohort (Petrou et al., 2016). A Phase III clinical trial is currently on-going to test the safety and efficacy of repeated administration of NurOwn® therapy. The autologous NurOwn® are back-transplanted into the patient intrathecally by standard lumbar puncture

where neurons and glial cells are expected to take up the neurotrophic factors secreted by the transplanted cells (ClinicalTrial.gov identifier: NCT03280056).

The isolation of stem cells from adipose tissue (ADSCs) is easier and less invasive for the patients. Nevertheless, there are only few studies about ADSC treatment in ALS. In accordance with the results collected with BM-MSCs, ADSCs were able to delay disease onset and to extend the lifespan of $SOD1^{G93A}$ mice. Moreover, they presented a strong immunomodulatory function and determined an up-regulation of neurotrophic factors, such as VEGF and IGF-1 (Han et al., 2014). A recent work demonstrated that the administration of ADSC conditioned medium to $SOD1^{G93A}$ mice is sufficient to reduce neuromuscular junction denervation, highlighting the essential role of paracrine mechanisms in mediating beneficial effects of ADSC (Walker et al., 2018).

The treatment with ADSC has been recently translated to patients: a first clinical trial evaluated the safety of a single or repeated intrathecal injections of ADSC in ALS patients. They reported classical adverse effects that appeared after the injection and became milder or absent within 1-3 weeks post-treatment, such as headache, low back and leg pain. The treatment with ADSCs resulted safe, but the efficacy is still debated. Indeed, treated patients presented a slight and temporary improvement of bulbar function, increased limb strength, decreased fasciculations, decreased stiffness, and improved energy (Staff et al., 2016). At present, a new Phase II clinical trial is on-going to elucidate deeper the efficacy of ADSCs in the treatment of ALS (ClinicalTrial.gov identifier: NCT03268603).

Another active clinical trial is sponsored by The Andalusian Initiative for Advanced Therapies. It is a multicentre phase I/II Clinical trial, randomized, controlled with placebo, triple blinded to evaluate the safety of the intravenous administration of 3 doses of

autologous MSCs from adipose tissue in ALS patients (ClinicalTrial.gov identifier: NCT02290886).

1.5.3 Gene therapy in ALS

Gene therapy is a new attractive approach to modulate ALS progression by modifying the expression of genes, that have been reported altered in ALS. In order to modulate gene expression, antisense oligonucleotides (ASOs) and viral-direct gene delivery strategies have been developed.

ASOs are synthetic single-stranded DNA sequence that complemented selected sequences of target mRNA, determining mRNA degradation through RNase H enzyme recruitment. ASOs can also be modified to promote alternative splicing instead of mRNA degradation (Ly et al., 2018).

The first ASO targets SOD1 mRNA and preclinical studies demonstrated a good distribution of ASO in CNS and an efficacious knock-down of SOD1 which lead to an extension of survival (Smith et al., 2006). A first clinical trial reported the safety of intrathecal injection of ASO 333611 (ISIS-SOD1$_{RX}$) in SOD1-related ALS patients (Miller et al.,2013). Following these initial promising results, a clinical trial with a second generation SOD1-targeting ASO, BIIB067 (IONIS-SOD1$_{RX}$), started in January 2016 and is still on-going (ClinicalTrial.gov identifier: NCT02623699).

After the discovery of C9orf72 mutation in ALS, ASOs were designed to bind C9orf72 mRNA in the downstream region of the expansion. In fact, an ASO produced by Ionis Pharmaceutical that recognised the region within or immediately upstream of the intronic expansion did not show efficacy in reducing C9orf72 expression (Donnelly et al., 2013). *In*

vivo preclinical studies of C9orf72 ASO effectiveness demonstrated that a single intraventricular administration of ASO could attenuate RNA foci and dipeptide aggregates and improve the behavioural and cognitive deficits associated with the C9orf72 repeat expansion (Jiang et al., 2016).

Finally, another ASO tested in ALS was directed against ataxin-2, a protein that regulates stress granule formation of TDP-43 aggregates. Administration of anti-ataxin-2 ASO in mice expressing human TDP-43 reduced formation of TDP-43 aggregates, slowed disease progression, and extended lifespan (Becker et al., 2017).

The most common viral vector is the adeno-associated virus (AAV). This type of technology can provide greater ease in drug administration because it is able to readily cross the BBB when given systemically and can be manipulated to promote tropism to specific cell types and structures (Ly et al., 2018).

Nowadays, there are only preclinical results about the use of gene modulation through AAV injection. Thomsen and Colleagues suppressed mutant SOD1 in motor cortex and reported a significant delay in disease onset and extension in survival in transgenic $SOD1^{G93A}$ rats. In addition, they observed an increase survival of spinal MNs and an amelioration of neuromuscular junction (NMJ) healthy (Thomsen et al., 2014).

The same research group tried the systemic injection of AAV9-GDNF in $SOD1^{G93A}$ rats. However, in these experiments they registered only a modest functional improvement of motor performance and any effects on survival in $SOD1^{G93A}$ rats. Moreover, AAV9-GDNF administration caused side effects, including slowed weight gain, reduced overall activity levels and impaired working memory (Thomsen et al., 2017).

Finally, AAV5-mediated delivering of a miRNA (AAV5-miC) that targets C9orf72 mRNA was tested *in vitro* in astrocytes, frontal brain-like neurons derived from FTD patients and in human-derived iPSCs neurons. A reduction of sense intronic transcripts of C9orf72 was observed in all the *in-vitro* models, where a lower dipeptide aggregation and RNA foci formation were determined. AAV5-miC was administrated by intra-striatal injection in C9orf72 mice. Also in these *in-vivo* experiments, a significant decrease of C9orf72 mRNA and of the sense intronic transcripts was achieved in injected area and surrounding regions, suggesting a potential ability in reducing the toxic aggregation of dipeptides and disease severity also in *in vivo* ALS models (Martier et al., 2019a, Martier et al., 2019b).

2. AIM OF THE STUDY

In a previous study my research group reported that a single intravenous administration of MSCs, derived from bone marrow of 6 to 8 week-old female C57Bl/6J mice, in $SOD1^{G93A}$ mice extended lifespan, ameliorated motor performance and reduced astrogliosis and inflammation in spinal cord (Uccelli et al., 2012).

They analysed survival of MSC-injected SOD^{G93A} mice compared to saline-injected $SOD1^{G93A}$. These latter had a survival probability of 116.1 ± 3.4 days, while MSC administration prolonged the lifespan to 133.4 ± 3.8 days. Moreover, the performance of MSC-treated $SOD1^{G93A}$ mice in extension reflex of hind limbs, gait test and Rotarod task was significantly ameliorated compared to saline-treated $SOD1^{G93A}$ mice.

The beneficial effects on survival probability and motor skills were related to a decreased number of cells which were positive for ubiquitin, reduced astrocytes and microglia activation, lower levels of IL-1β and TNF-α mRNA, normalization of oxidative stress response and, finally, to an increase in GLT-1 mRNA expression and a rescue of abnormal glutamate release.

The distribution of MSCs after intravenous injection was tracked by transfecting MSCs with a Luciferase gene reporter vector. Luciferase positive cells were detected 24h and 48h after injection throughout the entire spinal cord. However the number of labelled MSCs appeared small; moreover, it significantly decreased 20 days after injection and was barely detectable 35 days after injection.

These results highlighted that only a small number of MSCs can migrate into the CNS of $SOD1^{G93A}$ mice after intravenous administration and suggested that the positive read-out could be driven by paracrine mechanisms rather than long-term MSC engraftment. Indeed, it has been reported that MSCs release different cytokines and chemokines, including IL-

10, CCL2, TGF-β, IL-6 and IL-7, growth factors (LIF, HGF), which can activate the regenerative potential of resident stem cells, promote angiogenesis and remodel stroma, anti-inflammatory factors, such as PGE_2 and TSG6 and, finally, extracellular vesicles (exosomes, microvesicles) (Shi et al., 2018).

Exosomes are nanovesicles with a diameter of 40-100 nm and constitute one of the main subclasses of EVs. The biogenesis of exosomes occurs via the endocytosis-exocytosis pathway when cells adsorb small amounts of intracellular fluid in a specific membrane region and form early endosomes. The early endosomes mature and expand into late endosomes, then intraluminal vesicles or multivesicular bodies (MVBs) are formed by internal budding of endosomal membrane and are released into the extracellular environment. Exosome exocytosis is regulated by p53 and under the control of the cytoskeleton activation pathway but not affected by calcium.

Exosomes contain a cargo of genetic material (mRNA, miRNA, pre-miRNA, and other non-coding RNA) and of proteins, that are transferred to and released into target cells. Exosomes can interact with cells via three pathways: they may enter cell via the endocytic uptake, by direct fusion of the vesicles to the cell membrane or by transferring their contents through adhesion to the cell surface mediated by the interaction with a lipid ligand receptor (Keshtkar et al., 2018).

It has been suggested that exosomes may be a way for the elimination of toxic substances from the affected cells and this may represent a mode for disease spreading, also in ALS. Mutant and misfolded WT-SOD1 can propagate from different cells to recipient cells, in association with vesicles which are released into the extracellular environment (Silverman et al., 2016) and it has been shown that exosomes derived from primary astrocytes, isolated

from SOD1^{G93A} mice, contain abnormal amount of mutant SOD1 and spread it, provoking MN death (Basso et al., 2013). Similarly, exposure of Neuro2a cells to exosomes from the brain of TDP-43^{A315T} mice, but not from control brain, caused cytoplasmic redistribution of TDP-43, suggesting that secreted exosomes contribute to propagation of TDP-43 proteinopathy. However, blocking exosome production *in-vivo* exacerbated the disease progression of mice expressing human TDP-43^{A315T}. The *in-vivo* data suggest that exosome secretion plays an overall beneficial role in neuronal clearance of pathological TDP-43 (Iguchi et al., 2016). In addition to TDP-43 and SOD1, other ALS-related proteins have been characterized in exosomes, such as FUS and C9Orf72, as well as non-coding miRNAs characteristic for the pathology (Roy et al., 2019).

Therefore, although it was thought initially that exosomes contained unwanted 'junk' RNA, instead, nowadays, it is recognised that cells selectively sort specific non-coding RNAs into exosomes for active transport to neighbouring cells. In particular, miRNAs, which regulate the expression of approximately 30–70% of human genes through base-pairing of their "seed" sequences with complementary mRNA, make up an important fraction of exosomal content, contributing to the overall biological functions of exosomes (Ferguson & Nguyen, 2016). Exosomes derived from MSCs substantially contain miRNAs that affect genes involved in specific processes related to cardiovascular development, angiogenesis and tube formation, pathways related to cell death and growth, and pathways related to fibrosis, such as platelet derived growth factor (PDGF) and TGF-β (Ferguson et al, 2018). Moreover, MSCs release exosomes containing miRNAs that are able to mitigate the inflammatory response, as miR-15a, miR-15b and miR-16, which act inhibiting the expression of CX3C-chemokine ligand 1 (CX3CL1), a potent macrophage chemoattractant, and miRNAs that suppress TLR signalling, causing the translocation of

NFκB to the nucleus, and hampering macrophage activation by engulfed mitochondria (Maffioli et al., 2017; Phinney et al., 2015).

The potential role of exosomes for therapeutic intervention in neurological and neurodegenerative disease, is well known (Croese and Furlan, 2018). Exosomes can transfer biological information over long distance and they are able to cross the BBB, they were then investigated as a potential therapeutic tool in ALS (Bonafede and Mariotti, 2017). Exosomes derived from adipose stromal cells may increase NSC-34 cell line viability, protecting from oxidative damage and inducing anti-apoptotic pathway activation (Bonafede et al., 2016; Bonafede et al., 2019). Moreover, exosomes derived from adipose stromal cells ameliorated the aggregation of SOD1 in the $SOD1^{G93A}$ mouse model of ALS (Lee et al., 2016). In a recent study, exosomes from the NSC-34 neuronal cell line, previously transfected with the mutant $SOD1^{G93A}$ protein, which were enriched of miR-124, caused a switch in the recipient N9 microglial cell line from a preferential M1 to a mixed M1 and M2 polarization (Pinto et al., 2017).

Starting from these findings describing the pivotal role of exosomes in cell-to-cell communication and of the selective effects on cellular function due to their unique miRNA cargo, we hypothesized that exosomes could be one of the major mediators of MSC immunoregulatory function. Moreover, we wanted to elucidate the role of miRNAs shuttled by exosomes as the effectors of their functions. To validate our hypothesis I studied the effectiveness of exosomes derived from MSCs primed with IFN-γ, in order to increase their anti-inflammatory and immunomodulatory properties (Vigo et al., 2016), in modulating the altered phenotype of ALS astrocytes, isolated from spinal cord of $SOD1^{G93A}$ mice at 120 days of life, representing a late stage of the disease and, in turn MN survival. Characterization of INF-γ-primed MSCs through microarray analyses revealed

that nine miRNAs were up-regulated compared to unstimulated MSCs and these miRNAs were present in exosomes. In my study I analysed the contribution of these selected miRNAs, which are contained in exosomes, to the modulation of the astrocyte phenotype by transfecting the cells with single synthetic miRNA (mimic) and I elucidated some of the pathways affected from the nine up-regulated miRNAs to pave the way to a possible treatment using specific miRNAs.

3. MATERIALS AND METHODS

3.1 Animals

B6SJL-TgN SOD1/G93A1Gur mice expressing high copy number of mutant human SOD1 with a Gly93Ala substitution (SOD1/G93A) and (WT) (Gurney et al., 1994) were originally obtained from Jackson Laboratories (Bar Harbor, ME, USA) and bred at the animal facility of the Pharmacology and Toxicology Unit, Department of Pharmacy in Genoa, where they were kept until experiments were carried out. Transgenic animals were crossed with background-matched B6SJL wild-type females, and selective breeding maintained each transgene in the hemizygous state.

All transgenic mice were identified by analysing tissue extracts from tail tips as previously described (Bonifacino et al. 2017). Tissue was homogenized in phosphate-buffered saline (PBS), freeze/thawed twice and centrifuged at 23,000 x g for 15 min at 4°C, and human SOD1 was evaluated by staining for its enzymatic activity after 10% non-denaturing polyacrylamide gel electrophoresis.

Animals were housed (6/7 per cage) at constant temperature (22 ± 1°C) and relative humidity (50%) with a regular 12 h -12 h light cycle (light 7 AM -7 PM). Food (type 4RF21 standard diet obtained from Mucedola, Settimo Milanese, Milan, Italy) and water were freely available. The number of animals of each sex was balanced in each experimental group to avoid bias due to intrinsic sex-related differences. For experimental use, animals were sacrificed at 120 days old, a late stage of the disease.

Experiments were carried out in accordance with the guidelines established by the European Communities Council (EU Directive 114 2010/63/EU for animal experiments published on September 22nd, 2010) and the Italian D.L. n. 26/2014 and were approved by the local Ethical Committee and by the Italian Ministry of Health (Project Authorization

No.97/2017-PR). All efforts were made to minimize animal suffering and to use only the number of animals necessary to produce reliable results. In particular, the use of primary cell cultures leads to a reduction in the number of utilized animals; indeed, our optimised protocol permitted the isolation of astrocytes from adult mouse spinal cord with a yield that allowed to study diverse parameters through multiple techniques starting from cells prepared from a single mouse. Moreover, we obtained, at least, two dishes of $SOD1^{G93A}$ astrocytes from a single mouse spinal cord, thus gave us the possibility to treat primary astrocytes from the same mouse with vehicle or MSC-derived exosomes, decreasing the number of animals necessary to perform the experiments, but improving also the experimental design.

3.2 Preparation of primary cultures of astrocytes

WT and $SOD1^{G93A}$ mice (120 days old) were euthanized by cervical dislocation, without prior anaesthesia by personnel well-trained with this technique, and spinal cords were rapidly removed. Primary astrocytes were prepared from spinal cord of adult mice with a protocol optimised in our laboratory. The tissue was chopped with a scalpel to act a first mechanical breaking up and to facilitate the next step of homogenization of the spinal cord.

The chopped spinal cord was transferred in a sterile 15ml falcon with 1 ml of Dulbecco's Modified Eagle Medium (DMEM; Euroclone, Cat# ECM0728L) containing 10% Fetal Bovine Serum (Euroclone, Cat# ECS0180L), 1% glutamine (Euroclone, Cat# ECB3004D) and 1% Penicillin/Streptomycin (Euroclone, Cat# ECB3001D), then, with a P1000 pipette the tissue was further disintegrated until reaching a homogeneous preparation, which was seeded at the optimal density of two 35mm Petri dishes, pre-coated with poly-L-ornithine hydrocloride (1.5µg/ml; Sigma-Aldrich, Cat# P2533) and laminin (3µg/ml; Sigma-Aldrich,

Cat# L2020), for SOD1^{G93A} spinal cord, and of one pre-coated 35mm Petri dish for WT spinal cord.

The preparation was placed at 37°C in humidified 5% CO_2 incubator for 5 days, then the medium containing tissue fragments was replaced with fresh complete DMEM. After 10DIV astrocytes were detached by incubation at 37°C for 15 minutes with Trypsin-EDTA 1X (Euroclone, Cat# ECB3052B). The trypsin solution was then neutralized with a volume of DMEM equal to four times the volume of trypsin and centrifuged for 5 minutes at 500 x g at room temperature. The cell pellet was re-suspended and re-plated on pre-coated 35 mm Petri dishes, at the optimal density of 10^5 cells, for qPCR, Western blot and astrocyte-MN co-culture analysis; while the astrocytes were re-plated on pre-coated glass coverslips placed in 24-wellplate, at a density of $3x10^4$ cells per well for confocal microscopy studies.

After 20DIV,when astrocytes reached the confluence and a proper degree of maturation, exosome treatment was started and, after 24 hours, samples were collected for the analyses.

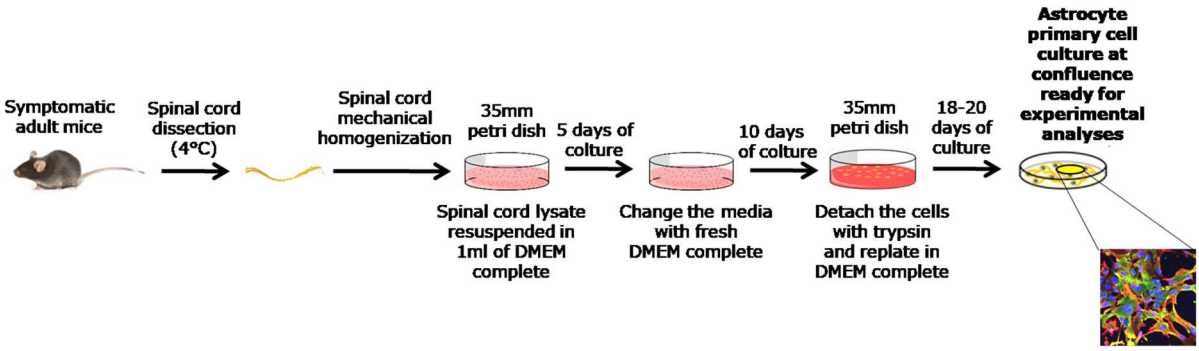

3.3 Human-fibroblast derived astrocytes

Fibroblasts derived from healthy donor and ALS patients, carrying the SOD1 mutation, were converted in induced Neural Progenitor Cells (iNPCs) by exposure to retroviral vectors (Oct3/4, Sox2, Klf4, and c-Myc) for 24 hours and then, after recovery in regular

fibroblast medium, a NPC conversion medium was added to cells and it was changed every day.

When cells changed shape and formed sphere-like structures, they were collected and expanded in individual wells of a six-well plate. As soon as the NPC culture was established, the medium was switched to NPC medium consisting of DMEM/F12 (Gibco, Waltham, MA, USA), Glutamax (Gibco, Waltham, MA, USA) 1% N2 (Gibco, Waltham, MA, USA), 1% B27 (Gibco, Waltham, MA, USA), 20 ng/ml FGF2 (Peprotech, Rocky Hill, NJ, USA), 20 ng/ml EGF (Peprotech, Rocky Hill, NJ, USA) and 5 ng/ml heparin (Sigma, St. Louis, MO, USA). The protocol for the conversion of fibroblasts in iNPCs lasts 4 weeks.

For astrocyte differentiation, iNPCs were seeded in NPC medium at low density in a fibronectin-coated 100mm Petri dish. The day after, the medium was switched to DMEM (Fisher Scientific, Hampton, NH, USA), 10% FBS (Life science production, Bedford, UK), 0.2% N2 (Gibco, Waltham, MA, USA). Astrocytes were allowed to mature for at least 7 days.

3.4 Isolation and expansion of mouse and human mesenchymal stem cells

Mouse bone marrow from 6- to 8-week-old C57BL/6J mice was flushed out of tibias and femurs. After 2 washes by centrifugation at 352 x g for 5 minutes in PBS, cells were plated in 75-cm^2 tissue-culture flasks at the concentration of 0.3 to 0.4 × 10^6 cells/cm^2 using Murine Mesencult as medium (Stem Cell Technologies, Cat# 05513). Cells were kept in a humidified 5% CO_2 incubator at 37°C, and the medium was refreshed every 3 to 4 days, for about 4 to 5 weeks; only adherent cells were collected following 10-minute incubation at 37°C with Trypsin-EDTA 1X.

After the first cut and for the subsequent 4 or 5 passages, the cells were plated in 25-cm^2 flasks at 1.2 to 2.0 × 10^4 cells/cm^2. For the following passages, cells were routinely seeded at 4 to 10 × 10^3 cells/cm^2 reaching confluence after 4 to 5 days. Mature MSCs were defined by their ability to differentiate into bone, cartilage and fat and by the expression of CD9+, Sca-1+, CD44+ and CD73+ and the lack of hematopoietic markers CD45-, CD34- and CD11b-, as previously reported (Zappia et al., 2005).

Human bone marrow stem cells were obtained from marrow aspirates of bone marrow donors (Divisions of Hematology, San Martino Hospital, Genoa, Italy). From approximately 1000 ml of marrow aspirate, ready for transplantation, 10 ml aliquots were taken and centrifuged on a Ficoll separating solution (Seromed, Berlin, Germany) for 20 minutes at 800 x g. The cell fraction was recovered, counted, suspended in complete MesenCult^{TM} Medium (StemCell Technologies, Cat# 05411) and plated at 5 × 10^6 cells in 75 cm^2 flask. The medium was changed after 3 days and then three times a week. When cells reached confluence (after 14DIV), they were detached by means of Trypsine-EDTA 1X, counted, and reseeded in 75 cm^2 flasks at a density of 1 x 10^5 MSCs per flask.

3.5 Isolation of MSC-derived exosomes and treatment of astrocytes

Exosomes were isolated from mouse or human MSCs. At confluence, MSC medium plus supplement was substituted with 10 ml MesenCult^{TM} serum-free medium and then primed with 10nM IFN-γ (Recombinant Mouse IFN-gamma Protein, R&D systems, Cat#485-MI; Recombinant Human IFN-γ, R&D, 285-IF). Cells were incubated for 24 hours at 37°C and 5% CO_2 in O_2. Next day, 1mM Adenosine 5′-triphosphate disodium salt hydrate (ATP, Sigma-Aldrich, Cat# A6419) was added to the medium for 20 minutes in order to promote

the release of exosomes by increasing the exposition on cytoplasmic membrane surface of phosphatidylserine, due to the activation of ATP P2X7 receptor (Wilson et al., 2004).

Medium was collected in 15ml falcon tubes and centrifuged 20 minutes at 2000 x g to remove debris and added with 5 ml of Total Exosome Isolation Kit (Invitrogen, Cat# 4478359) per 10 ml MSC-medium and stored overnight at 4°C. The day after, this mix was centrifuged 12,000 x g 1 hour. The supernatant was discarded and the exosome-pellet suspended in DMEM. MSCs were detached with Trypsin-EDTA 1X and counted by Neubayer Chamber to determine the exosome amount to be added in astrocyte medium. In each experiment, the ratio 1:6 between astrocytes and MSC derived-exosomes was maintained.

Mouse SOD1^{G93A} astrocytes and iAstrocytes were treated with MSC-derived exosomes for 24 hours in DMEM without FBS or knockout serum, respectively. After 24 hour treatment, mouse astrocytes were collected as cell pellet for Western blotting, or fixed with paraformaldehyde (PFA) for quantitative immunofluorescence experiments. Instead, after exosome treatment, human astrocytes required a wash-out period of 24 hours. Then iAstrocytes were detached and the cell pellet store at -80° for Western blot experiments. To study MN viability, medium containing exosomes was removed after 24 hours and MNs were seeded immediately on treated astrocytes, both in mouse and human experiments.

3.6 Confocal microscopy experiments

Astrocytes, seeded on 12mm diameter glass coverslips, were fixed with 4% PFA (Sigma-Aldirich, Cat# 47608) for 20 minutes at room temperature, protected from light. After fixing, PFA was removed and astrocytes were washed 3x with PBS 1X. Then, cells were permeabilized with methanol for 5 minutes at -20°C and washed 3x with PBS 1X. A

solution of 0.5% bovine serum albumin (BSA) in PBS was used as blocking solution for 15 minutes at room temperature.

All primary antibodies were diluted in 3% PBS-BSA blocking solution. Incubation was performed overnight at 4°C with the primary antibodies at the proper working dilution (Table 2).

The day after, cells were washed 3x in 0.5% PBS-BSA before the incubation of 1 hour at room temperature with the secondary antibody, diluted 1:3000 in PBS containing 3% BSA (Table 2).

Then, cells were washed 3 times in PBS and the coverslip was assembled on a microscopy glass slide through Fluoroshield™ with DAPI (Sigma-Aldrich, Cat# F6057). Fluorescence image (512 x 512 x 8 bit) acquisition was performed by a three-channel Leica TCS SP5 laser-scanning confocal microscope equipped with 458, 476, 488, 514, 543 and 633 nm excitation lines through a plan-apochromatic oil immersion objective 63x/1.4. Light collection was optimized according to the combination of the chosen fluorochromes, and sequential channel acquisition was performed to avoid cross-talk. The Leica "LAS AF" software package was used for image acquisition. The quantitative analyses of co-localization and the relative protein expression level were performed by calculating co-localization coefficients (Manders et al. 1992).

Table 2. List of primary and secondary antibodies with the respective working dilution, the supplier company and the catalog number.

PRIMARY ANTIBODIES	WORKING DILUTION	PRODUCER AND CATALOG NUMBER
rabbit polyclonal anti-Glial fibrillary acid protein (GFAP) antibody	1:1000	Sigma-Aldrich, Cat# G4546
mouse monoclonal anti-Vimentin antibody	1:1000	Sigma-Aldrich, Cat# V2258
mouse monoclonal anti-S100β antibody	1:500	Chemicon International, Cat# MAB079-1
rabbit recombinant monoclonal anti-NLRP3 antibody	1:100	Abcam, Cat# ab210491
rabbit polyclonal anti-Nrf2 antibody	1:500	Abcam, Cat# ab31163
goat polyclonal anti-IL1β antibody	1:1000	Sigma-Aldrich, Cat# I3767
goat polyclonal anti-TNF-α antibody	1:300	Sigma-Aldrich, Cat# T0938
chicken polyclonal anti-IL-6 antibody	1:500	Sigma-Aldrich, Cat#GW22495
rat monoclonal anti-monocyte chemotactic protein-1 (MCP-1) antibody	1:500	Abcam, Cat# ab8101
rabbit polyclonal anti-IL-10 antibody	1:500	Abcam, Cat# ab996995
monoclonal anti-glyceraldehyde-3-phosphate dehydrogenase (GAPDH) antibody	1:1000	Sigma-Aldrich, Cat# G8795
chicken polyclonal anti-GAPDH antibody	1:1000	Abcam, Cat# ab83957
SECONDARY ANTIBODIES		
donkey anti-rabbit Alexa Fluor A488-conjugated	1:3000	Thermo Fisher Scientific, Cat# R37118
donkey anti-mouse Alexa Fluor A488-conjugated		Thermo Fisher Scientific, Cat# A21202
donkey anti-goat Alexa Fluor A488-conjugated		Thermo Fisher Scientific, Cat# A11055
goat anti-chicken Alexa Fluor A488-conjugated		Thermo Fisher Scientific, Cat# A11039
donkey anti-mouse Alexa Fluor A467-conjugated		Thermo Fisher Scientific, Cat# A31571
goat anti-chicken Alexa Fluor A467-conjugated		Thermo Fisher Scientific, Cat# A21449

3.7 iAstrocyte immunofluorescence experiments

Cells were fixed with 4% PFA for 15 minutes and washed 3× with PBS before the blocking and permeabilizing solution, consisting of PBS with 10% horse Serum and 0.1% Triton X-100, was applied for 1 hour. All primary antibodies were diluted in blocking solution. Incubation was performed overnight at 4 °C with the following primary antibodies: rabbit polyclonal anti-GFAP (1:1000), chicken polyclonal anti-vimentin (1:1000) and rabbit polyclonal anti-CD44 (1:500). The day after, cells were washed 3× in PBS before the secondary antibody (anti-rabbit Alexa Fluor 488, anti-chicken Alexa Fluor 488, anti-rabbit Alexa Fluor 568) and DAPI, diluted in blocking solution (1:2000), were applied for 1 hour at room temperature. Then, cells were washed 3× in PBS. Astrocytes were analyzed by Opera Phenix High-Content Screening System (PerkinElmer).

3.8 Western blot experiments

The samples for Western blot analysis were collected by detaching cells with trypsin-EDTA and re-suspended them in PBS. Cells were centrifuged at 17,000 x g for 1 minute and PBS was removed. Cell pellets were stored at -80°C. Pellets were lysed by IP lysis buffer [150mM NaCl, 50mM HEPES, 1mM EDTA, 1mM DDT, 0,5% (v/v) Triton X-100, protease inhibitor cocktail (PIC), pH 8.0] + phosphatase inhibitors. Lysates were incubated for 15 minutes in ice, then they were centrifuged 17,000 x g for 5 minutes at 4°C. The lysate supernatant which contains soluble proteins was stored. Protein concentration was determined by BCA protein assay.

Appropriate amount (15 µg) of total proteins was separated by SDS-polyacrylamide gel electrophoresis using 4–20% precast gels (Bio-Rad, Cat# 4568094) and transferred to nitrocellulose membranes. Non-specific membrane binding sites were saturated in 5%

skimmed-milk solution and membranes were incubated overnight at 4 °C with the primary antibodies (Table 3).

After incubation with appropriate peroxidase-coupled secondary antibodies, protein bands were detected by a Western blotting detection system (SuperSignalTM West Femto Maximum Sensitivity Substrate, Thermo Fisher Scientific, Cat# 34095). Bands were detected and analysed for density using an enhanced chemiluminescence system (Alliance 6.7 WL 20 M, UVITEC, Cambridge, UK) and UV1D software (UVITEC). Bands of interest were normalized for GAPDH or β-actin level in the same membrane. The concentration of proteins felt in the linear portion of the curve.

Table 3. List of primary antibodies used to perform Western blot analysis, reporting the working dilution, the supplier company and the catalog number.

PRIMARY ANTIBODIES	WORKING DILUTION	PRODUCER AND CATALOG NUMBER
rabbit polyclonal anti-GFAP	1:1000	Sigma-Aldrich, Cat# G4546
mouse monoclonal anti-Vimentin antibody	1:1000	Sigma-Aldrich, Cat# V2258
mouse monoclonal anti-S100β antibody	1:100	Chemicon International, Cat# MAB079-1
rabbit recombinant monoclonal anti-NLRP3 antibody	1:100	Abcam, Cat# ab210491
rabbit polyclonal anti-Nrf2 antibody	1:500	Abcam, Cat# ab31163
rabbit polyclonal anti-NQO1 antibody	1:1000	Abcam, Cat# ab34173
rabbit monoclonal anti-phospho-NFκB p65 (Ser536) antibody	1:500	Cell Signalling Technology, Cat# 3033P
rabbit polyclonal anti-NLRP3 antibody	1:500	Sigma-Aldrich, Cat# SAB1410191
mouse monoclonal anti-β-actin antibody	1:5000	Sigma-Aldrich, Cat# A2228
mouse monoclonal anti-GAPDH antibody	1:1000	Sigma-Aldrich, Cat# G8795

3.9 Enzyme-linked immunosorbent assay

Astrocytes, cultured in 35mm Petri dish, were treated with MSC-derived exosome for 24 hours in DMEM serum free. Then, DMEM containing exosomes was replaced with complete fresh DMEM and astrocyte-conditioned medium was collected 48 hours after exosome withdraw.

Cell-conditioned medium was filtered with 0.22μm sterile filter. Then, TNF-α, IL-1β, IL-6 and CCL2 concentrations were measured with a specific enzyme-linked immunosorbent assay (ELISA) kit (R&D Systems, Cat# DY401, DY410, DY406 and DY479, respectively) according to the manufacturer's protocol. ELISA 96-wellplate was pre-treated for 24 hours at room temperature with the capture antibody for TNF-α (1:50), IL-1β (1:50), IL-6 (1:50) or CCL2 (1:500), then the excess of antibody was washed using the Wash buffer (R&D systems, Cat# WA126) and the plate was blocked by 1 hour incubation with Reagent Diluent (R&D systems, Cat# DY995).

At this point it was possible to add the standard and samples. Standard solution was prepared by diluting recombinant TNF-α, IL-1β, IL-6 or CCL2 in Reagent Diluent to have a concentration of 1000 pg/ml, 2000 pg/ml, 1000 pg/ml or 250 pg/ml as first point of the standard curve, respectively. A seven-point standard curve was generate using 2-fold serial dilutions in Reagent Diluent. 100 μl of standard at the diverse concentrations was added to each well and for each concentration of standard point was done a triplicate.

To collect the appropriate amount of cytokines for the analysis, 150-200 μl of medium per well was added. Each sample was loaded in duplicate. Three wells were used as blank, and were loaded with 100 μl filter water. Wells were incubated for 2 hours at room temperature to allow the binding of the specific cytokine with the antibody.

Then, the medium was aspirated and wells were washed 3x with Wash buffer and incubated for 2 hours with 100 µl of the detection antibody for TNF-α, IL-1β, IL-6 and CCL2 per well, each diluted 1:60 in Reagent Diluent. Wells were washed 3x with Wash buffer and 100 µl Streptavidin-HRP (1:40 in Reagent Diluent) were added to each well for 20 minutes, protected from light.

Streptavidin-HRP was washed 3x with Wash buffer and re-placed with 100 µl of Substrate Solution [1:1 mixture of Color Reagent A (H_2O_2) and Color Reagent B (Tetramethylbenzidine); R&D systems, Cat# DY999)]. The plate was incubated 20 minutes at room temperature, protected from light. Finally, 50 µl of Stop Solution (2N H_2SO_4, R&D systems, Cat# DY994) were used to block the reaction and the plate was ready for the acquisition.

Absorbance was measured at 450 nm with a microplate reader (SpectraMax 340PC Microplate Reader, Molecular devices, San Jose, California, USA). The standard curve was constructed by plotting the mean absorbance for each standard on the y-axis against the concentration on the x-axis and by drawing the best fit curve trough the points on the graph. The concentration of the samples can be obtained from the absorbance by regression analysis on the basis of the standard curve.

3.10 Motor neuron preparation from SOD1^{G93A} embryos and co-cultures with SOD1^{G93A} astrocytes

MNs were prepared from spinal cord of SOD1^{G93A} E13.5 mouse embryos (Vandenbergheet al., 1998; Wiese et al., 2009). Spinal cord was isolated from embryos by microscopy dissection, then meninges and the dorsal root ganglia were removed. The tissue was digested with 0.5% trypsin (Sigma-Aldrich, Cat# T4799) in Hank's Balance Salt Solution

(HBSS) for 20 minutes at 37°C. Then, trypsin solution was replaced with a mix of 0.4% BSA (Sigma-Aldrich, Cat# A3311) in Leibovitz-15 medium (Sigma-Aldrich, Cat# L5520) and 0.02 mg/ml Deoxyribonuclease I (DNAse; Sigma-Aldrich, Cat#DN25) and gently triturated with P1000 pipette.

The tissue homogenate was stratified on 6.2% OptiPrep (Sigma-Aldrich, Cat# D1556) cushion and centrifuged 500 x g for 15 minutes at room temperature. After centrifuging, the motor neuron-enriched cell population was localized at the interface between the OptiPrep solution and the medium. The MN band was collected and re-suspended in 3 ml of MN medium: Neurobasal medium (Gibco, Cat# 21103-049), 2% B27 supplement (Gibco, Cat# 17504044), 2% horse serum (Gibco, Cat# 16050130), 0.5mM stable L-Glutamine (Gibco, Cat#35050038), 25µM Mercaptoethanol (Sigma-Aldrich, Cat# M6250), 10 ng/ml ciliary neurotrophic factor (CNTF; Sigma-Aldrich, Cat# C3835), 100 pg/ml glial-derived neurotrophic factor (GDNF; Sigma-Aldrich, Cat# G1401), 5µg/ml Penicillin/Streptomycin.

Motor neurons were centrifuged at 75 x g for 20 minutes to remove Optiprep impurity. The pellet containing MNs was diluted in 1 ml of MN medium plus 50µl of Chick Embryo Extract (US Biological, Cat# C3999).

MNs were seeded at a density of 5 x 10^4 MNs in a 35mm Petri dish on confluent adult astrocytes prepared from 120 days-old $SOD1^{G93A}$ mice, previously treated or not with exosomes. After 3 days the medium was removed and replaced with fresh MN medium and then it was changed three times a week. On day 4 after seeding, MNs in an area of 1 cm^2 were counted to asses viability. The number of MNs was recorded three times a week for 14 days. The number of MNs at day 4 were considered as 100% of survival. The

percentage of survival at the other time-points was calculated as % of the number of MNs at day 4, in the same Petri dish.

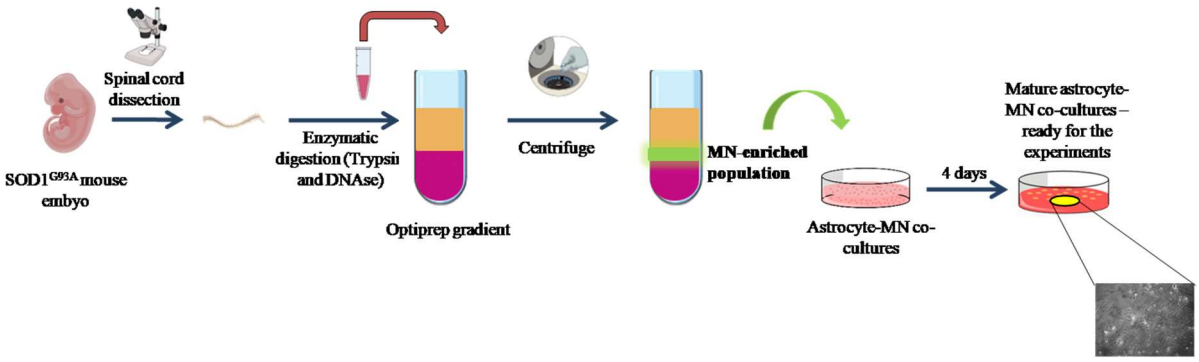

3.11 Immunofluorescence experiments on astrocyte-MN co-cultures

The co-culture system was prepared as described above. At day 7 after seeding, when MNs were completely mature and the number of cells was still enough high, astrocytes and MNs were fixed with 4% PFA for 20 minutes at room temperature, protected from light. The fixing solution was removed and cells were washed 3x with PBS 1X. Cells were then permeabilised with methanol for 5 minutes at -20°C and washed 3x with PBS 1X. A solution of 0.5% BSA in PBS was used as blocking solution for 15 minutes at room temperature.

All primary antibodies were diluted in 3% PBS-BSA blocking solution. Incubation was performed overnight at 4°C with the following primary antibodies: rabbit polyclonal anti-Homebox9 antibody (Hb9, 1:800; Abcam, Cat# ab92606), rabbit polyclonal anti-Islet-1 antibody (1:100, abcam, Cat# ab109517) or chicken polyclonal anti-β-Tubulin III (1:1000; Chemicon International, Cat# AB9354).

The day after, cells were washed 3x in 0.5% PBS and incubated for 1 hour at room temperature with the secondary antibodies. The following secondary antibodies were used:

donkey anti-rabbit Alexa Fluor A488-conjugated (Thermo Fisher Scientific, Cat# R37118) and goat anti-chicken Alexa Fluor A467-conjugated (Thermo Fisher Scientific, Cat# A21449). Antibodies were diluted 1:3000 in PBS containing 3% BSA. Finally, the cells were washed again 3x with PBS 1X and covered with a glass coverslip, fastened with the prolong reagent Fluoroshield™ containing DAPI. Fluorescence image acquisition was performed by an Olympus BX41 microscope through a 40x objective.

3.12 Motor Neuron Differentiation from mouse embryonic stem cells and co-culture of Motor Neurons and Astrocytes

Mouse embryonic stem cells expressing GFP under the MN-specific promoter HB9 were cultured on primary mouse embryonic fibroblasts (Merck, Burlington, MA, USA). For differentiation into MNs, cells were harvested with trypsin and suspended in DFK10 culture medium consisting of knock-out DMEM/F12 (Gibco, Waltham, MA, USA), 10% knockout serum replacement (Gibco, Waltham, MA, USA), 1% N2 (Gibco, Waltham, MA, USA), 1 mM L-glutamine (Gibco, Waltham, MA, USA), 0.5% glucose (Sigma, St. Louis, MO, USA) and 0.0016% 2-mercaptoethanol (Sigma, St. Louis, MO, USA).

Cells were seeded on non-adherent Petri dishes to allow the formation of embryoid bodies. After 1 day of recovery, 2 μM retinoic acid (Sigma, St. Louis, MO, USA) and 1 μM smoothened agonist (SAG; Millipore, St. Louis, MO, USA) were added freshly every day in new medium from day 2 to day 7 post-seeding to induce mouse embryo stem cell (mESC) differentiation into MNs. After 7 days of differentiation, embryoid bodies were dissociated using 200UI/ml papain (Sigma, St. Louis, MO, USA) and sorted using FACS.

Human astrocytes were plated in 96-well plates coated with human fibronectin (2.5 μg/mL) at a density of 10,000 per well. Two days later, FACS sorted GFP-positive MNs were

suspended in MN media consisting of DMEM/F12, 5% horse serum, 2% N2, 2% B27 plus GDNF (10 ng/mL), BDNF (10 ng/mL), and CNTF (10 ng/mL) and added to astrocytes at a density of 10,000 per well.

Each plate was scanned every day, until day 3 after MN seeding, with the fully automated IN CELL 6000 confocal plate reader to capture GFP-positive cells. The IN CELL Developer and Analyzer softwares were used to create whole-well pictures and count.

3.13 Transfection of mouse astrocytes with single synthetic miRNA (mimic)

$SOD1^{G93A}$ astrocytes were plated in 24-wellplates on 12mm coverslips for confocal microscopy or in 35mm Petri dishes for qPCR. Cells were transfected with the following miRNA mimics: miR-466q, mirR-467f, miR-466m-5p, miR-466i-3p, miR-466i-5p, miR-5126, miR-467g, miR-3082-5p, and miR-669c-3p (Qiagen, Hilden, Germany). To demonstrate the specificity of the mimic effect on its mRNA target, cells were always transfected also with a negative control (scramble). Astrocytes were transfected with miRNA mimics at a final concentration of 5 nM using HiPerFect Transfection Reagent (Qiagen, Cat# 301704) according to the manufacturer's instructions. HiPerFect Transfection Reagent enables highly efficient miRNA transfection, allowing translation repression of target mRNA using low miRNA concentration. After 48 hours incubation at 37°C in humidified 5% CO_2, astrocytes were fixed with 4% PFA for confocal microscopy or were detached with Accutase® (Euroclone, Cat# ECB3056D) and the cell pellet resuspended in 500 µl of QIAzol Lysis reagent (Qiagen, Cat# 79306).

3.14 qPCR experiments

$SOD1^{G93A}$ astrocytes, after transfection with single synthetic miRNA mimics, were collected for qPCR analysis as described above. RNA was isolated by the phenol-chloroform extraction procedure, using QIAzol Lysis Reagent. The purity of the RNA was evaluated by spectrophotometric analysis at the absorbance 230, 260 and 280 nm, to exclude the presence of peptides, phenols, aromatic compounds, or carbohydrates and proteins. The cDNA was synthesized according to the instructions provided by the kit used (Transcriptor First Strand cDNA synthesis kit, Roche Diagnostics, Germany).

Quantification of the gene expression was evaluated in duplicate, in a final volume of 20 µl containing 50 ng cDNA, 1 µl of each pair of forward and reverse primers (20 µM) (synthetized by Tib Molbiol, Genova, Italy) and 10 µl of FastStart Essential DNA Green Master (Roche, Cat# 06402712001), using the LightCycler 480 (Roche) amplifier. The amplification of GAPDH gene was adopted as housekeeping gene to normalize data.

Gene expression was expressed as relative mRNA amount (fold induction) compared with the control sample.

3.15 Statistical analysis

Data are expressed as the mean ± s.e.m., and p value < 0.05 was considered significant. Statistical comparison of two means were performed by unpaired two-tailed Student's *t*-test while multiple comparisons were performed using the analysis of variance (one-way ANOVA) followed by the Bonferroni's post hoc test. Analyses were performed by means of Sigma Stat software (Systat Software, Inc., San Jose, CA, USA).

4. RESULTS

4.1 Mouse astrocyte characterization and treatment with exosomes derived from mouse mesenchymal stem cells

4.1.1 Characterization of MSC-derived exosomes

Exosomes were isolated from the medium of MSCs stimulated or not with IFN-γ. The purity of the exosome preparation was analysed by measuring the expression of Alix and CD9, high-enriched proteins of exosomes, using Western blot analysis. Alix represents one of the accessory protein which is associate with the endosomal sorting complex for transport (ESCRT). This latter is involved in membrane budding and scission of vesicles from multi-vesicular bodies, playing a potential role in exosome formation. CD9 belongs to tetraspanin protein family, that are composed of four transmembrane domains and resulted enriched >100-fold in exosomes (Raposo and Stoorvogel, 2013).

Both markers were significantly elevated in exosome samples, validating our isolation method to obtain a population of microvesicles enriched in exosomes (Figure 1A).

Moreover, in order to verify the morphology of isolated microvesicles, we performed electron microscopy experiments. The most part of microvesicles ranged between 40 and 100 nm range, in accordance with literature data describing the exosome size (Figure 1B).

FIGURE 1.

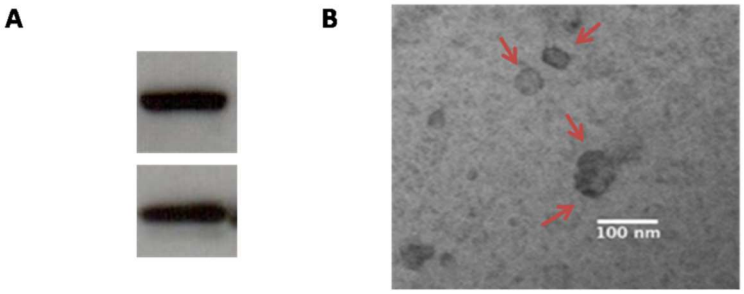

Figure 1. Characterization of exosomes isolated from MSC medium through Invitrogen Exosome Isolation Kit.

A) Representative bands for ALIX and CD9, exosome selective markers. **B)** Electron microscopy image showing that the most part of the isolated microvesicles size ranged between 40 and 100 nm.

miRNA expression was analysed in order to select possible mediators of exosome functions. Microarray analysis on MSCs and IFN-γ-primed MSCs was carried out by LC-Sciences company (Houston, TX, USA). The miRNA panel highlighted nine miRNAs (miR-466q, miR-467f, miR-466m-5p, miR-466i-3p, miR-466i-5p, miR-467g, miR-5126, miR-3082-5p, and miR-669c-3p) that were significant up-regulated in MSCs after IFN-γ stimulation compared to non-primed MSCs (data not shown). Then, the expression of these nine up-regulated miRNAs was quantified in MSC- and IFN-γ-primed-MSC- derived exosomes.

qPCR experiments on exosomes revealed that the expression of miR-466q, miR-467f, miR-466m-5p, and miR-466i-3p was significantly increased also in exosomes from IFN-γ-primed MSCs compared to untreated MSCs. On the contrary, the expression of miR-466i-

5p, miR-467g, miR-5126, miR-3082-5p, and miR-669c-3p was down-regulated in exosomes from IFN-γ-primed MSC compared to untreated MSCs (Figure 2).

FIGURE 2.

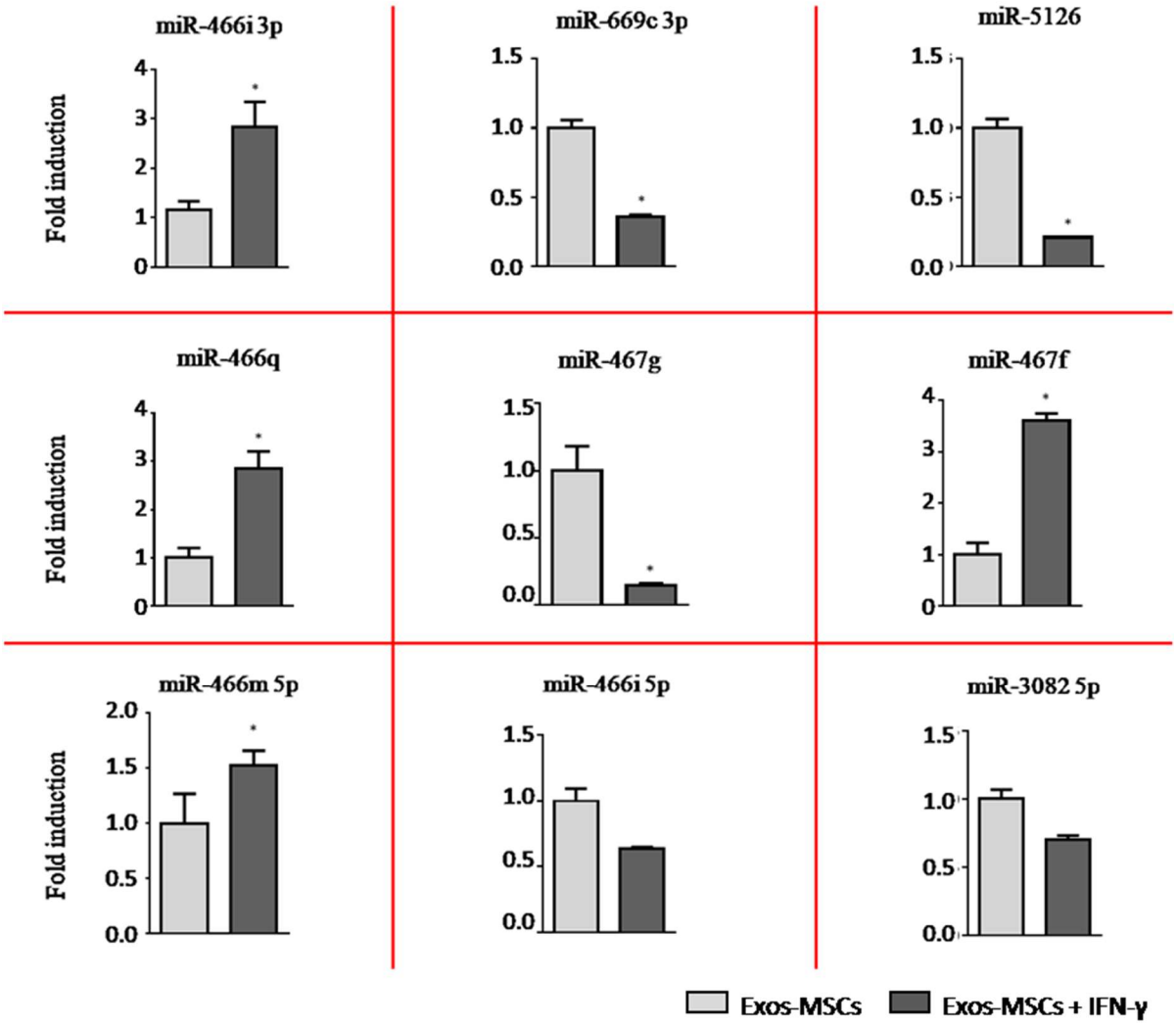

Figure 2. RT-PCR quantification of selected miRNAs present in exosomes derived from MSCs pre-treated or not with IFN-γ

Quantitative analyses of miRNAs contained in exosomes derived from mouse untreated- and IFN-γ-primed- MSCs. Data represent the mean ± SEM of three independent experiments run in triplicate. The miRNA expression of exosomes isolated from unstimulated-MSCs is reported as 1. *P < 0.05 at least vs. IFN-γ-primed- MSC-derived exosomes (two-tailed Student's t-test).

4.1.2 Exosome treatment reduces astrogliosis in SOD1^{G93A} astrocytes

GFAP, Vimentin and S100β are markers identifying reactive astrocytes. GFAP and Vimentin are structural component of astrocyte cytoskeleton. In particular, GFAP represents the essential subunit which constitutes type III intermediate filaments in astrocytes (Tardy et al., 1990).

Also Vimentin belongs to a protein family of intermediate filaments and plays a crucial role in supporting and anchoring the organelles in the cytosol. It is involved in cell shape maintaining, integrity of cytosol preservation and cytoskeletal interaction stabilization, both in physiological condition and in response to stress stimuli (Goldman et al., 1996). It has been reported that GFAP and vimentin are over-expressed in ALS in relation to a reactive and strongly proliferative state of astrocytes in the disease (Benninger et al., 2016; Schiffer et al., 1996).

S100β is a calcium binding protein expressed selectively in glial cells. It is involved in several homeostatic functions, such as microtubule assembly, axonal proliferation, astrogliosis, calcium concentration, inflammation. There is a lot of evidence of its dysregulation in ALS. Indeed, in patients, S100β is increased in brain cortex astrocytes, and in astrocytes and motor neurons in the spinal cord and its level, which resulted higher in the CSF of ALS patients, is directly correlated with worsing of prognosis of the disease (Serrano et al., 2017).

We quantified the expression level of GFAP, Vimentin and S100β by western blot (Figure 3). The three markers of astrogliosis were significantly up-regulated in SOD1^{G93A} astrocytes compared to WT astrocytes [1148% increase ($P < 0.05$, $F_{(2,7)}=13.362$), 180% increase ($P < 0.05$, $F_{(2,12)}=10.998$), 185% increase ($P < 0.05$, $F_{(2,15)}=6.751$), respectively]. The treatment of SOD1^{G93A} astrocytes with exosomes for 24 hours was able to reverse the

up-regulation of GFAP [66% decrease ($P < 0.05$, $F_{(2,7)}=13.362$)], vimentin [72% decrease ($P < 0.05$, $F_{(2,12)}=10.998$)], and S100β [77% decrease ($P < 0.05$, $F_{(2,15)}=6.751$)] compared to untreated SOD1^{G93A} astrocytes.

FIGURE 3.

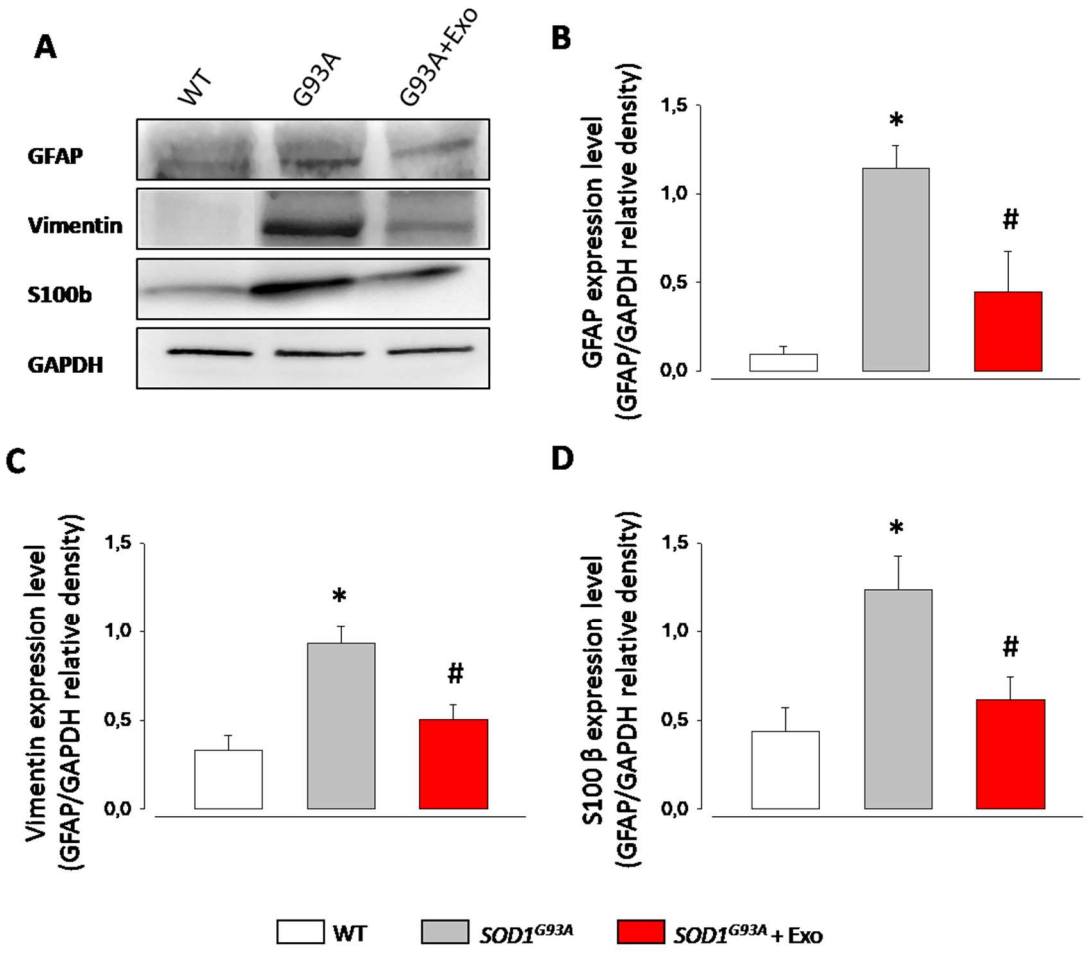

Figure 3. Western blot quantification of GFAP, vimentin and S100β expression in cell lysates from primary cultures of spinal cord astrocytes from WT and SOD1^{G93A} adult mice.

(A) Representative immunoreactive bands for GFAP, vimentin, S100β, and GAPDH; (**B**, **C**, **D**) Quantification of protein expression as per scanned band density in WT astrocytes, untreated SOD1^{G93A} astrocytes and SOD1^{G93A} astrocytes treated for 24h with exosomes. Protein expression

level was calculated as relative density, normalized to the housekeeping protein GAPDH. Data presented are means ± SEM of 4 independent experiments. *$P < 0.05$ vs. WT astrocytes; $^{\#}P < 0.05$ vs. untreated SOD1^{G93A} astrocytes (One-way ANOVA followed by Bonferroni post hoc-test).

The same expression trend of GFAP, Vimentin and S100β was observed by confocal microscopy analyses, confirming a higher expression of the three reactive astrocytic markers in SOD1^{G93A} astrocytes compared to WT astrocytes [GFAP: 51% increase ($P < 0.001$, $F_{(2,30)}=90.452$); Vimentin: 21% increase ($P < 0.01$, $F_{(2,22)}=50.181$); S100β: 25% increase ($P < 0.001$, $F_{(2,12)}=39.622$), respectively], and the positive effects of exosome treatment on GFAP [45% decrease ($P < 0.001$,$F_{(2,30)}=90.452$)], vimentin [77% decrease ($P < 0.001$, $F_{(2,22)}=50.181$) and S100β [132% decrease ($P < 0.001$, $F_{(2,12)}=39.622$)] over-expression (Figure 4).

FIGURE 4.

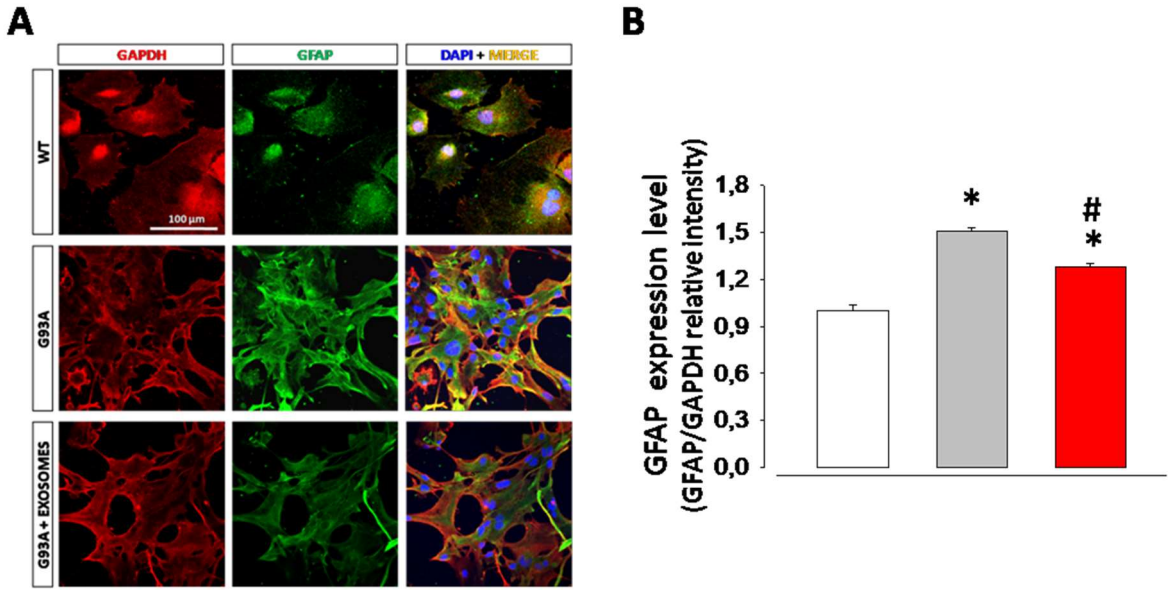

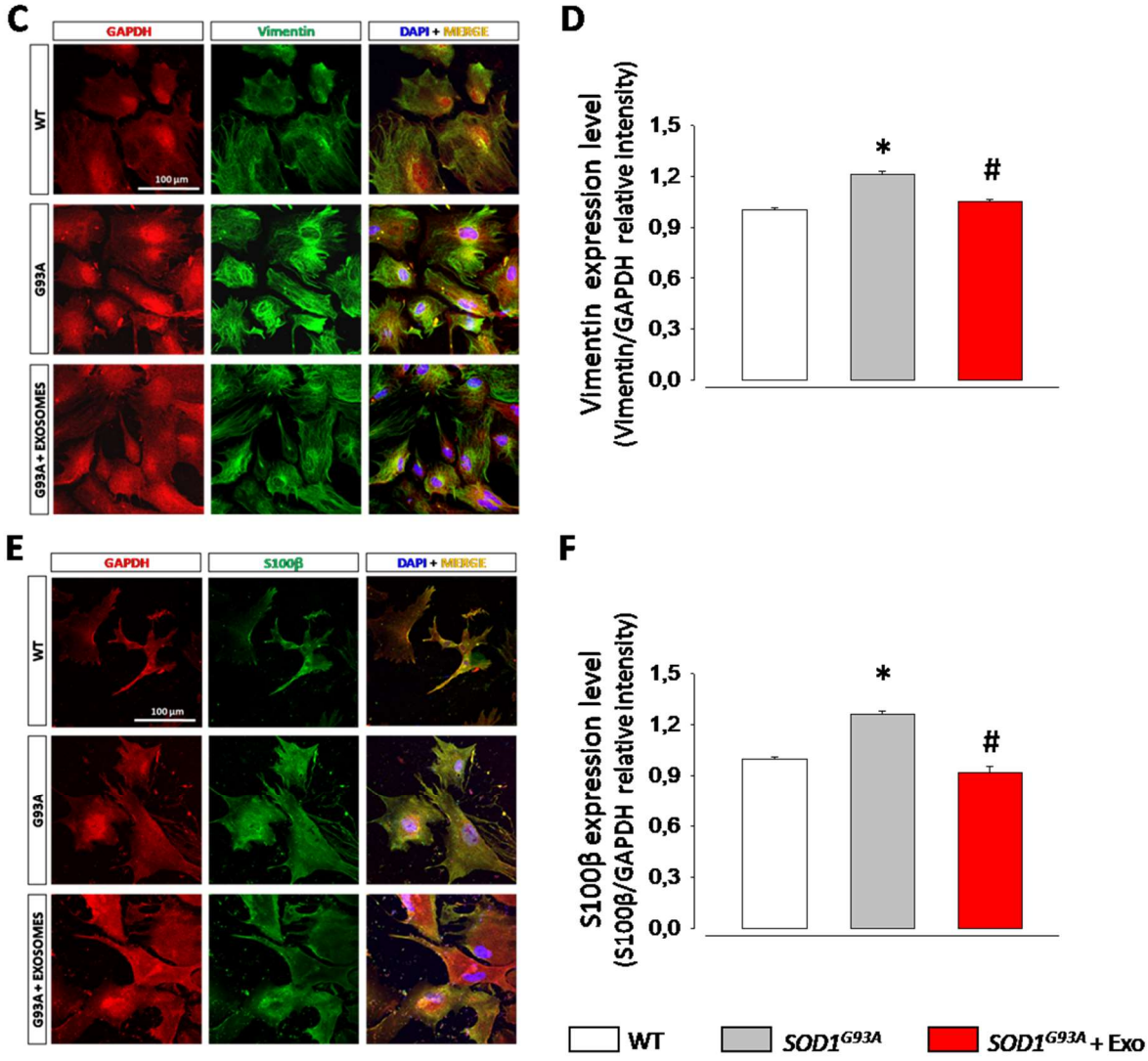

Figure 4. Immunocytochemical quantification of GFAP, vimentin and S100β expression in primary cultures of spinal cord astrocytes from WT and SOD1^{G93A} adult mice.

(A, C, E) Representative confocal microscopy immunocytochemical images for GAPDH (red) and GFAP (green) (upper panel), GAPDH (red) and vimentin (green) (middle panel) and for GAPDH (red) and S100β (green) (lower panel) in WT astrocytes, untreated SOD1^{G93A} astrocytes and SOD1^{G93A} astrocytes treated for 24h with exosomes. Nuclei were stained with 4',6-diamidin-2-fenilindolo (DAPI, blue). The merge panels represent the co-expression of GFAP and GAPDH, of vimentin and GAPDH, or of S100β and GAPDH, respectively. Scale bar: 100 µm. **(B, D, F)** Quantification of protein expression, as per relative fluorescence intensity, was performed calculating the co-localization coefficients (Manders et al., 1992) using Image-J software analyses. Data are expressed as relative fluorescence intensity of GFAP, vimentin or S100β normalized respect to the fluorescence intensity of the housekeeping protein GAPDH. The relative intensity of

control WT astrocytes is reported as 1. Data presented are means ± SEM of n=3 experiments run in triplicate (three different coverslips for each experimental condition); statistical analysis was performed by one-way ANOVA followed by Bonferroni post hoc-test. *$P < 0.001$ vs. WT astrocytes; $^{\#}P < 0.001$ vs. untreated SOD1^{G93A} astrocytes.

4.1.3 The over-expression and the abnormal release of pro-inflammatory cytokines in SOD1^{G93A} astrocytes are partially rescued upon exposure to MSC-derived exosomes

Astrocytes secrete various pro-inflammatory cytokines and chemokines. It has been observed a dysregulation of cytokine production and secretion in several neurodegenerative diseases and also in ALS (Farina et al., 2007; Holden 2007). To verify possible effects of the exosome treatment on the pro-inflammatory phenotype of SOD1^{G93A} astrocytes, we analysed the expression of the cytokines TNF-α, IL-1β, IL-6, and of the chemokine CCL2 by confocal microscopy.

The expression level of TNF-α, IL-1β, IL-6, and CCL2 was significant increased in SOD1^{G93A} astrocytes compared to WT astrocytes [TNF-α: 32% increase ($P < 0.001$, $F_{(2,27)}=65.648$); IL-1β: 63% increase ($P < 0.001$, $F_{(2,24)}=434.190$); IL-6: 46% increase ($P < 0.001$, $F_{(2,21)}=69.674$); CCL2: 37% increase ($P < 0.001$, $F_{(2,18)}=90.554$)].

The treatment with MSC-derived exosomes was able to reverse the up-regulation of TNF-α [79% decrease ($P < 0.001$, $F_{(2,27)}=65.648$)], IL-1β [64% decrease ($P < 0.001$, $F_{(2,24)}=434.190$)], IL-6 [66% decrease ($P < 0.001$, $F_{(2,21)}=69.674$)], and CCL2 [115% decrease, ($P < 0.001$, $F_{(2,18)}=90.554$)] compared to untreated SOD1^{G93A} astrocytes (Figure 5).

FIGURE 5.

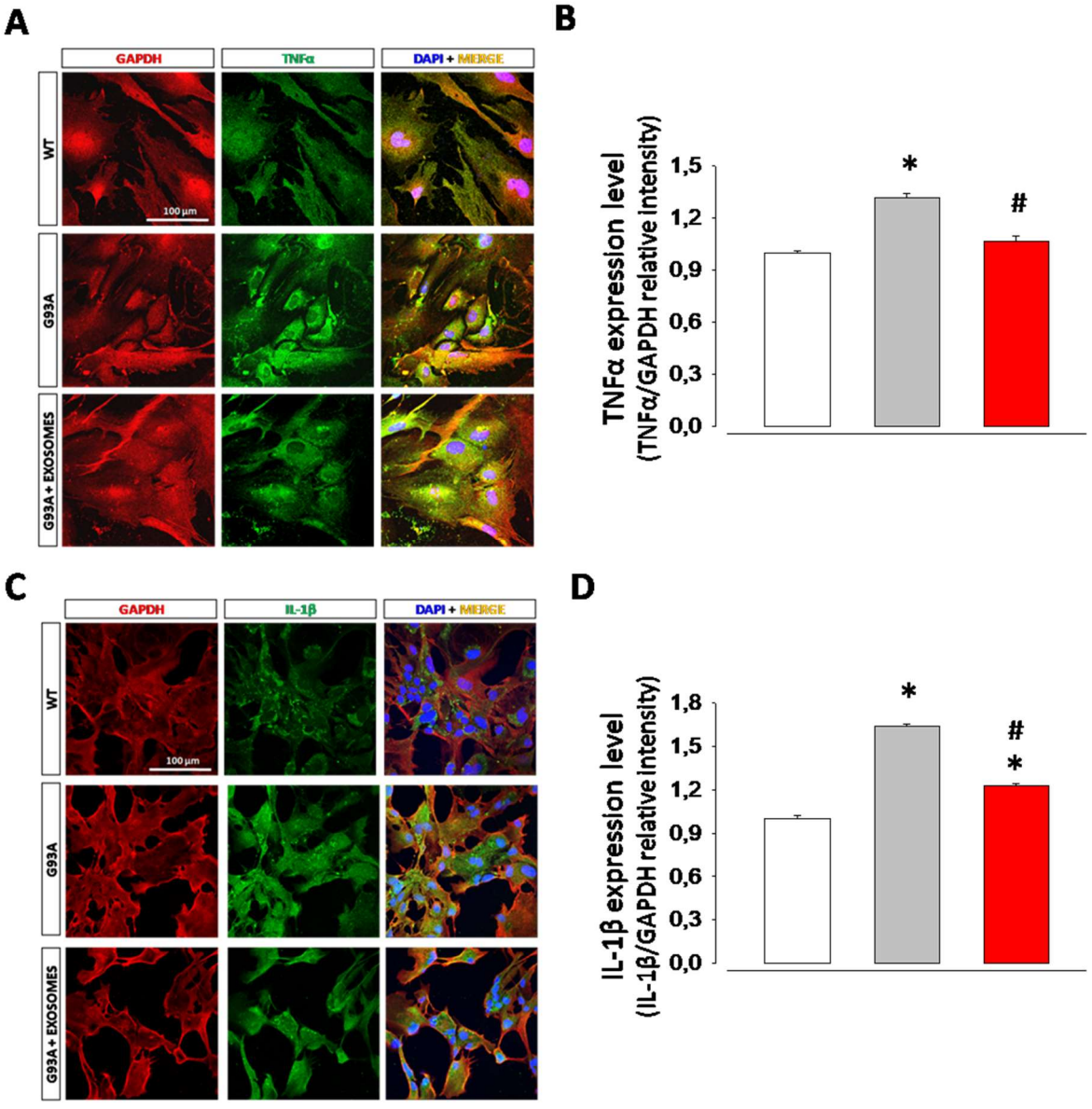
A
GAPDH
TNFα
DAPI + MERGE
WT
G93A
G93A + EXOSOMES
100 µm
B
TNFα expression level
(TNFα/GAPDH relative intensity)
1,5
1,2
0,9
0,6
0,3
0,0
*
#
C
GAPDH
IL-1β
DAPI + MERGE
WT
G93A
G93A + EXOSOMES
100 µm
D
IL-1β expression level
(IL-1β/GAPDH relative intensity)
1,8
1,5
1,2
0,9
0,6
0,3
0,0
*
#
*

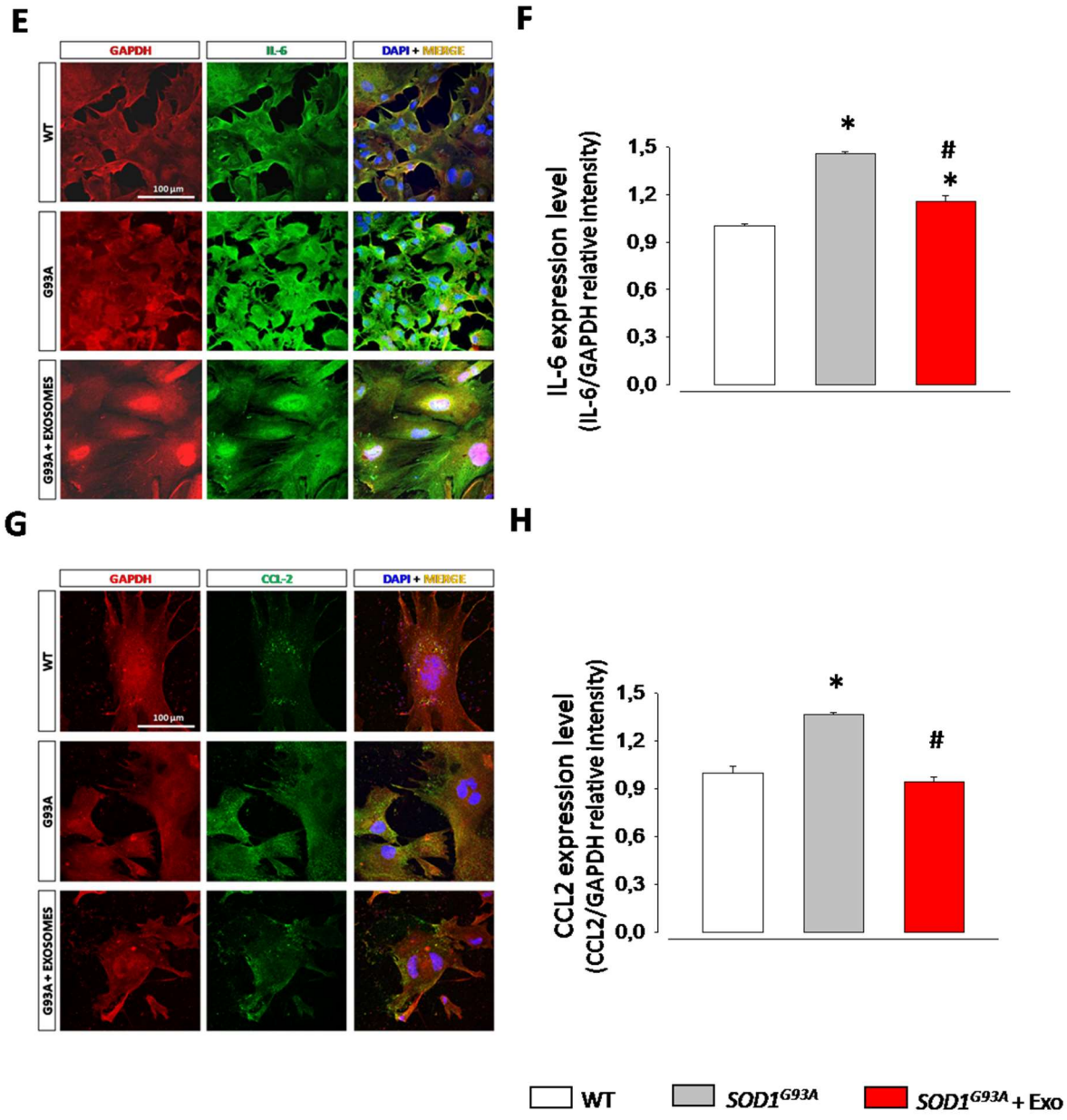

Figure 5. Immunocytochemical quantification of IL-1β, IL-6, TNFα and CCL2 expression in primary cultures of spinal cord astrocytes from WT and SOD1^{G93A} adult mice.

(A, C, E, G) Representative confocal microscopy immunocytochemical images for GAPDH (red) and TNF-α (green), GAPDH (red) and IL-1β (green), GAPDH (red) and IL-6 (green), or GAPDH (red) and CCL2 (green) in WT astrocytes, untreated SOD1^{G93A} astrocytes and exosome-treated SOD1^{G93A} astrocytes. Nuclei were stained with DAPI (blue). The merge panels represent the co-expression of TNF-α, IL-1β, IL-6, or CCL2 with GAPDH. Scale bar: 100 µm. **(B, D, F, H)** Quantification of protein expression, as per relative fluorescence intensity, was performed calculating the co-localization coefficients (Manders et al., 1992) using Image-J software analyses.

Data are expressed as relative fluorescence intensity of TNF-α, IL-1β, IL-6, or CCL2, normalized to the fluorescence intensity of the housekeeping protein GAPDH. The relative intensity of control WT astrocytes is reported as 1. Data presented are means ± SEM of 3 experiments run in triplicate (three different coverslips for each experimental condition). *P < 0.001 vs. WT astrocytes; $^{\#}$ P <0.001 vs. untreated SOD1^{G93A} astrocytes (One-way ANOVA followed by Bonferroni post-hoc test).

Then, we quantified the release of TNF-α, IL-1β, IL-6, and CCL2 in the culture medium collected from WT-, SOD1^{G93A}- and exosome-treated SOD1^{G93A} astrocytes. The release of TNF-α, IL-1β, IL-6, CCL-2 was massively augmented in SOD1^{G93A} astrocytes compared to WT astrocytes [TNF-α: 571% increase ($P < 0.001$, $F_{(2,6)}$=170.073); IL-1β: 351% increase ($P < 0.001$, $F_{(2,6)}$=542.972); IL-6: 758% increase ($P < 0.001$, $F_{(2,6)}$=481.467); CCL2: 96% increase ($P < 0.001$, $F_{(2,6)}$=44.549)].

TNF-α, IL-1β, IL-6 and CCL2 release was significantly reduced by 40% ($P < 0.001$, $F_{(2,6)}$=170.073), 12% ($P < 0.05$, $F_{(2,6)}$=542.972), 20% ($P < 0.05$, $F_{(2,6)}$=481.467), and 56% ($P < 0,05$, $F_{(2,6)}$=44.549), respectively, in SOD1^{G93A} astrocyte-conditioned medium 48 hours after the exposure to exosomes (Figure 6).

FIGURE 6.

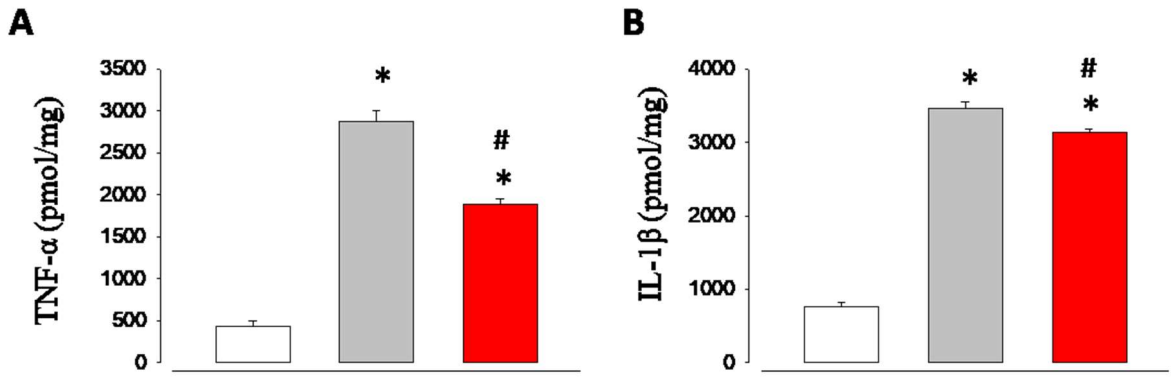

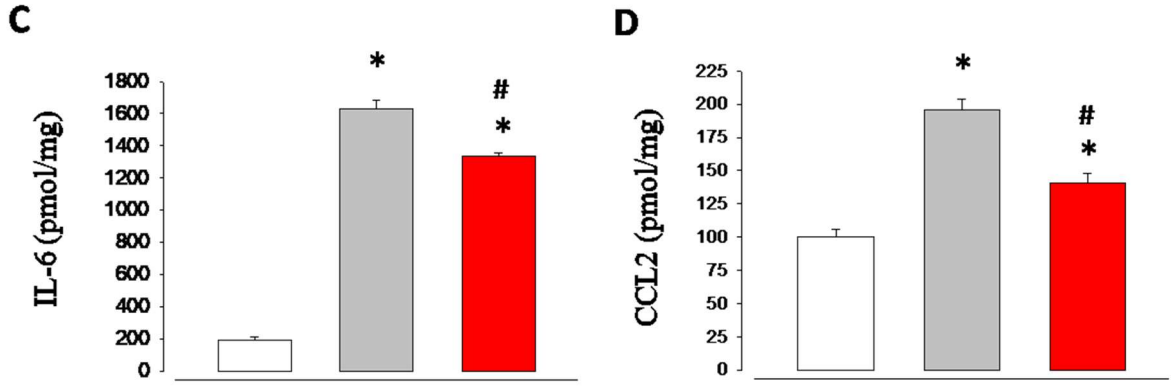

Figure 6. Immuno-enzimatic quantification of TNF-α, IL-1β, IL-6 and CCL2 concentration in the supernatant of primary cultures of spinal cord astrocytes from WT and SOD1^{G93A} adult mice.

Bar plots report the concentration of the pro-inflammatory cytokines TNF-α **(A)**, IL-1β **(B)** IL-6 **(C)** and CCL2 **(D)** in the supernatant of WT astrocytes, untreated SOD1^{G93A} astrocytes, and exosome-treated SOD1^{G93A} astrocyte cultures. Protein concentration was determined as per specific ELISA commercial kits. Data presented are means ± SEM of 3 independent experiments run in triplicate (three analyses for each experimental condition). *$P < 0.001$ vs. WT astrocytes; $^{\#}P < 0.05$ vs. untreated SOD1^{G93A} astrocytes (One-way ANOVA followed by Bonferroni post-hoc test).

4.1.4 Exosome treatment normalizes NLRP3 inflammasome over-expression in SOD1^{G93A} astrocytes

NLRP3 is a protein complex strictly related to the inflammatory environment. Its assembly determines the cleavage through caspase-1 of IL-1β and IL-18 and their conversion in the active form, exacerbating neuroinflammation and promoting cell apoptosis and necroptosis (Mangan et al., 2018).

NLRP3 expression was analysed by Western blot. SOD1^{G93A} astrocytes showed a higher expression of NLRP3 than WT astrocytes [237% increase ($P < 0.05$, $F_{(2,10)}=9.562$)]. SOD1^{G93A} astrocytes treated with MSC-derived exosomes retained a lower expression of

NLRP3 compared to untreated SOD1^{G93A} astrocytes [72% decrease ($P < 0.05$, $F_{(2,10)}=9.562$)] (Figure 7A and 7B).

The same pattern was confirmed by confocal microscopy experiments. In accordance with Western blot data, NLRP3 was up-regulated by 35% ($P < 0.001$, $F_{(2,24)}=80.841$) in SOD1^{G93A} astrocytes compared to WT astrocytes. Upon exposure to MSC-derived exosomes a significant reduction of NLRP3 expression in SOD1^{G93A} astrocytes compared to untreated SOD1^{G93A} astrocytes was detected [77% decrease ($P < 0.001$, $F_{(2,24)}=80.841$)] (Figure 7C and 7D).

FIGURA 7.

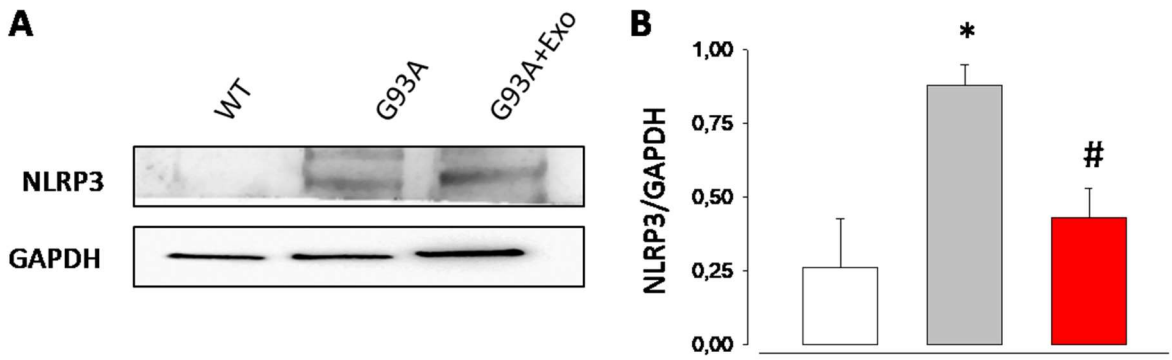

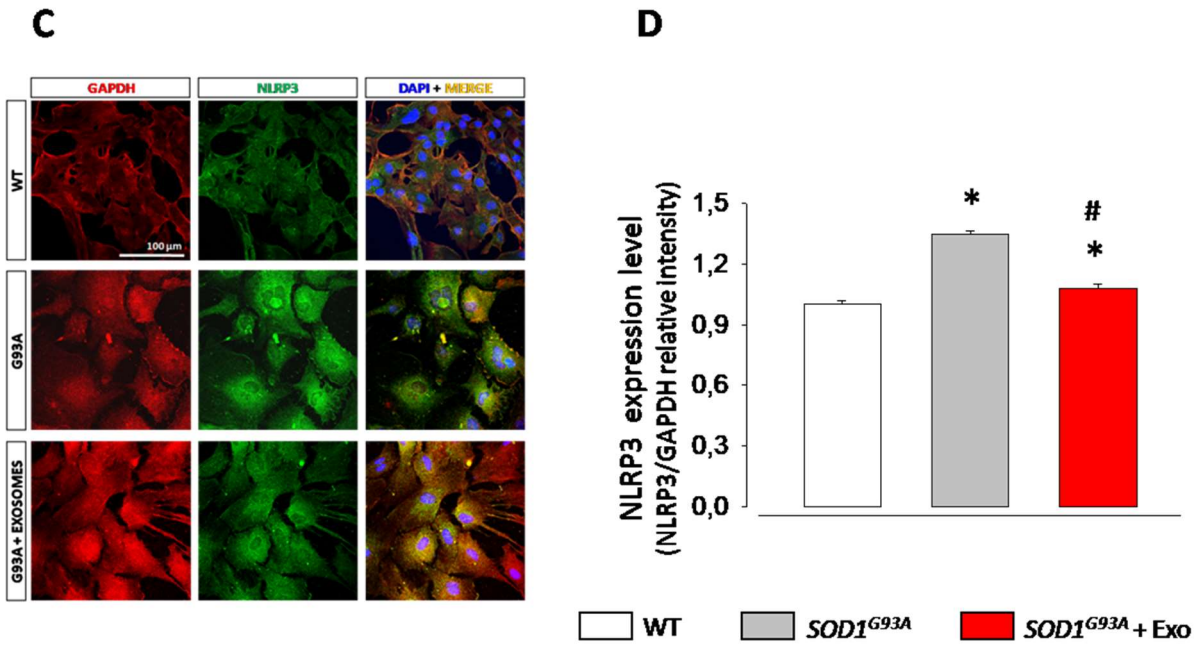

Figure 7. Western blot and immunocytochemical quantification of NLRP3-inflammasome complex expression in primary cultures of spinal cord astrocytes from WT and SOD1^{G93A} adult mice.

(A) Representative immunoreactive bands for NLRP3 inflammasome complex in WT astrocytes, untreated SOD1^{G93A} astrocytes and SOD1^{G93A} astrocytes treated with IFNγ-primed MSC-derived exosomes for 24h. (**B**) Western blot quantification of protein expression as per scanned band density. Protein expression was calculated as relative band density normalized to the housekeeping protein GAPDH. Data presented are means ± SEM of 4 independent experiments. *P <0.05 vs. WT astrocytes; $^{\#}P < 0.05$ vs. untreated SOD1^{G93A} astrocytes (One-way ANOVA followed by Bonferroni post-hoc test). **(C)** Representative confocal microscopy immunocytochemical images for GAPDH (red), NLRP3 (green) and DAPI (blue), in WT astrocytes, untreated SOD1^{G93A} astrocytes and SOD1^{G93A} astrocytes treated with IFNγ-primed MSC-derived exosomes for 24h. The merge panels represent the co-expression of NLRP3 with GAPDH. Scale bar: 100 µm. **(D)** Quantification of protein expression, as per relative fluorescence intensity, was performed calculating the co-localization coefficients (Manders et al., 1992) using Image-J software analyses. Data are expressed as relative fluorescence intensity of NLRP3 normalized to the fluorescence intensity of the housekeeping protein GAPDH. The relative intensity of control WT astrocytes is reported as 1. Data are presented as the means ± SEM of 3 experiments run in triplicate (three different coverslips for each experimental condition). *$P < 0.001$ vs. WT astrocytes; $^{\#}P < 0.001$ vs. untreated SOD1^{G93A} astrocytes (One- way ANOVA followed by Bonferroni post-hoc test).

4.1.5 IL-10 expression is increased by MSC-derived exosomes in SOD1^{G93A} astrocytes

Astrocytes secrete also anti-inflammatory cytokines, that can ameliorate the extracellular milieu and contribute to determine the phenotype of activated astrocytes (Burmeister and Marriott, 2018). It has been shown above that astrocyte produce and secrete a wide panel of pro-inflammatory cytokines; we measured here the expression of the anti-inflammatory cytokine IL-10 as a paradigm of the anti-inflammatory activity of SOD1^{G93A} astrocytes.

Confocal microscopy showed that the total cellular expression of IL-10 was significant decreased, by 27% ($P < 0.001$, $F_{(2,24)}=250.037$), in SOD1^{G93A} astrocytes compared to WT astrocytes. After the treatment with exosomes IL-10 down-regulation was almost completely reversed to control levels compared to untreated SOD1^{G93A} astrocytes ($P < 0.001$, $F_{(2,24)}=250.037$) (Figure 8).

FIGURE 8.

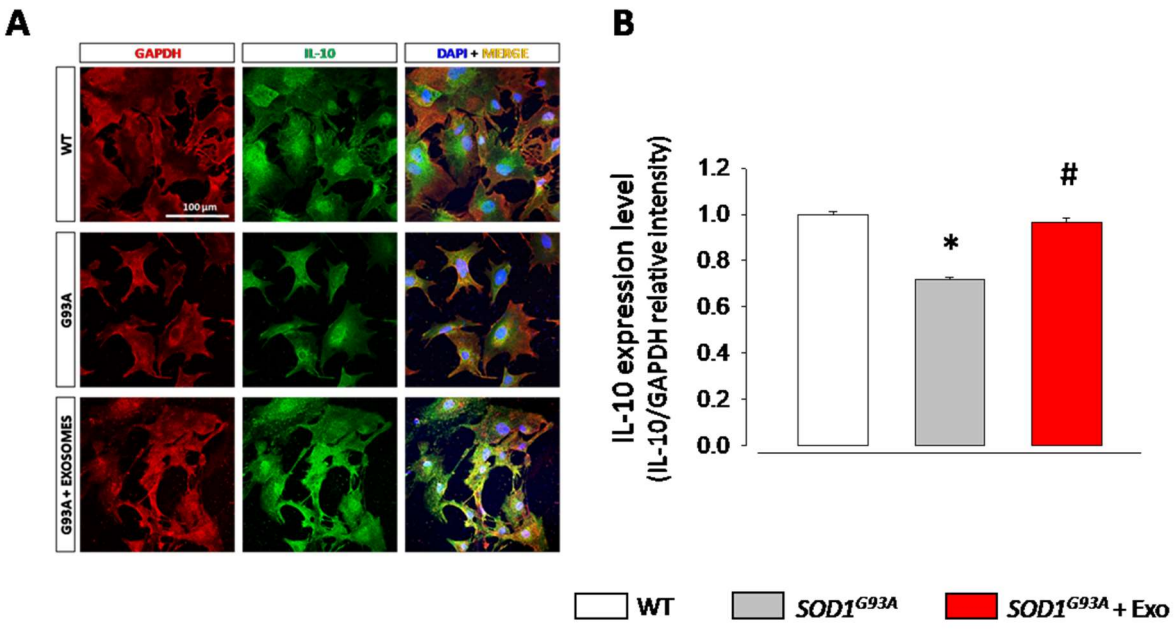

Figure 8. Immunocytochemical quantification of IL-10 expression in primary cultures of spinal cord astrocytes from WT and SOD1^{G93A} adult mice.

(A) Representative confocal microscopy images for GAPDH (red) and IL-10 (green) in WT astrocytes, untreated SOD1^{G93A} astrocytes and SOD1^{G93A} astrocytes treated for 24h with IFNγ-primed MSC-derived exosomes. Nuclei were stained with DAPI (blue). The merge panels represent the co-expression of IL-10 with GAPDH. Scale bar: 100 μm. **(B)** Quantification of protein expression, as per relative fluorescence intensity, was performed calculating the co-localization coefficients (Manders et al., 1992) using Image-J software analyses. Data are expressed as relative fluorescence intensity of IL-10 normalized to the fluorescence intensity of the housekeeping protein GAPDH. The relative intensity of control WT astrocytes is reported as 1. Data presented are means ± SEM of 3 experiments run in triplicate (three different coverslips for each experimental condition). $^{*}P < 0.001$ vs. WT astrocytes; $^{\#}P < 0.001$ vs. untreated SOD1^{G93A} astrocytes (One- way ANOVA followed by Bonferroni post-hoc test).

4.1.6 Exosome treatment boosts the anti-oxidant response that is reduced in SOD1^{G93A} astrocytes

Nrf2 represents a transcriptional factor promoting the transcription of genes that are under the control of ARE, inducing the synthesis of anti-oxidant proteins; therefore, an increased nuclear localization of Nrf2 is potential linked with a stronger activation of pathways protecting the cell to oxidative stress (Petri et al., 2012).

The resistance to oxidative stress was measured by quantifying the total cellular expression and the nuclear fraction of Nrf2 in WT-, SOD1^{G93A}- and exosome-treated SOD1^{G93A} astrocytes by confocal microscopy experiments. Nrf2 expression strongly diminished in SOD1^{G93A} astrocytes, both in the cytosol [32% decrease ($P < 0.001$, $F_{(2,18)}=42.142$)] and nuclei [61% decrease ($P < 0.001$, $F_{(2,18)}=288.227$)], compared to WT astrocytes.

After 24 hours exposure to MSC-derived exosomes, the total cellular expression of Nrf2 was increased by 68% ($P < 0.001$, $F_{(2,18)}=42.142$) compared to untreated SOD1^{G93A}

astrocytes. In addition, the active nuclear fraction of Nrf2 was increased by 77% ($P < 0.001$, $F_{(2,18)}=288.227$) in $SOD1^{G93A}$ astrocytes in response to exosome treatment (Figure 9).

FIGURE 9.

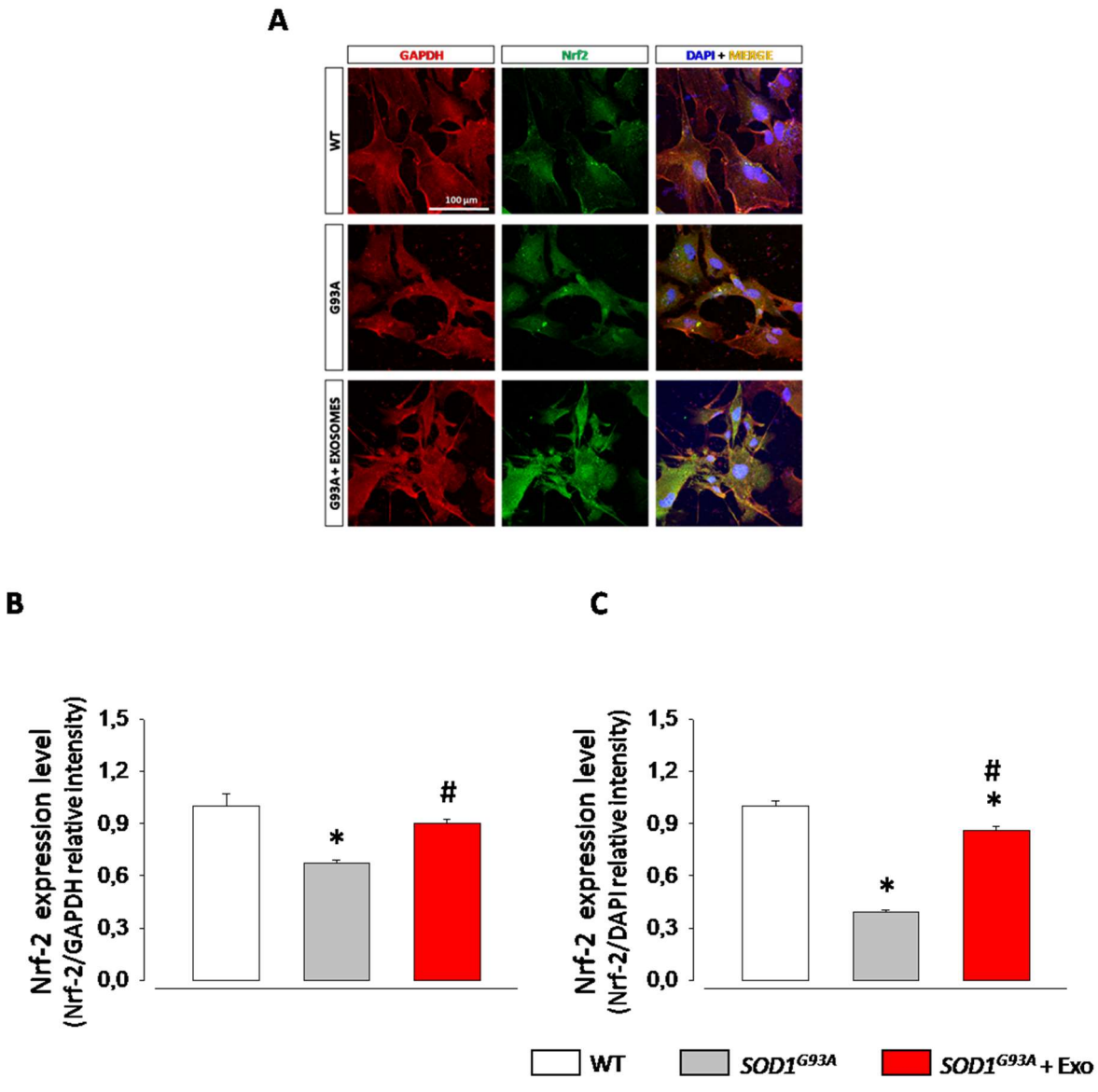

Figure 9. Immunocytochemical quantification of Nrf-2 expression in primary cultures of spinal cord astrocytes from WT and SOD1^{G93A} adult mice.

(A) Representative confocal microscopy immunocytochemical images for GAPDH (red) and Nrf-2 (green) in WT astrocytes, untreated SOD1^{G93A} astrocytes and exosome-treated SOD1^{G93A} astrocytes. Nuclei were stained with DAPI (blue). The merge panels represent the co-expression of Nrf2 and GAPDH. Scale bar: 100 μm. **(B, C)** Quantification of protein expression, as per relative fluorescence intensity, was performed calculating the co-localization coefficients (Manders et al., 1992) using Image-J software analyses. Data are expressed as relative fluorescence intensity of Nrf2 normalized to the fluorescence intensity of the housekeeping protein GAPDH or to the fluorescence intensity of the nuclear staining DAPI. The relative intensity of control WT astrocytes is reported as 1. Data presented are means ± SEM of 3 experiments run in triplicate (three different coverslips for each experimental condition); $^{*}P < 0.001$ vs. WT astrocytes; $^{\#}P < 0.001$ vs. untreated SOD1^{G93A} astrocytes (One- way ANOVA followed by Bonferroni post-hoc test).

4.1.7 Characterization of motor neurons isolated from SOD1^{G93A} mouse embryos

Motor neurons were prepared from SOD1^{G93A} mouse embryos and seeded on mature and confluent SOD1^{G93A} astrocytes, prepared from 120 days-old SOD1^{G93A} mice. A panel of markers selective for motor neurons, were chosen to determine the purity of the preparation. In particular, β-Tubulin III was used as generic neuronal marker, to indentify soma, axon and dendrites, while Hb9 and Islet-1 because they selectively label motor neurons.

As shown in figure 10, the most part of neurons were positive for Hb9 and Islet-1, as well as for β-Tubulin III, confirming that our preparation is enriched in motor neurons. In particular, about 80% of neurons positive for β-Tubulin III were positive also for Hb9 or Islet-1.

FIGURE 10.

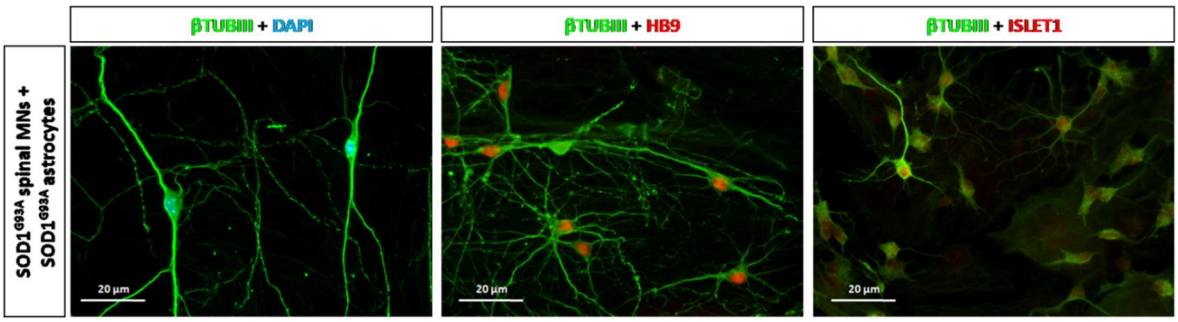

Figure 10. Immunocytochemical characterization of motor neurons isolated from the spinal cord of SOD1^{G93A} embryos (E13.5).

Representative images of spinal cord SOD1^{G93A} MNs co-cultured in the presence of SOD1^{G93A} astrocytes and stained for **(A)** β-tubulin III (green) and DAPI (blue), **(B)** β-tubulin III (green) and HB9 (red), and **(C)** β-tubulin III (green) and Islet1 (red). Scale bar: 20 µm.

4.1.8 SOD1^{G93A} astrocyte phenotype amelioration has a positive impact on motor neuron viability

Experiments on co-cultures of motor neurons isolated from SOD1^{G93A} mouse embryos and adult SOD1^{G93A} astrocytes, treated or not with MSC-derived exosomes, were performed in order to evaluate if the positive modulation exerted by MSC-derived exosomes on the astrocyte phenotype can impact on MN survival.

The viability of MNs were assessed starting 4 days after seeding and for further 10 days. When analyzing the viability of SOD1^{G93A} MNs co-cultured with SOD1^{G93A} astrocytes, we observed a constant and fast decrease of MN number during the experimental time [day 4: 100% viability; day 6: 50% viability; day 8: 33% viability; day 10: 16% viability; day 12: 11% viability; day 14: 5%viability].

The previous exosome treatment of astrocytes had a positive impact on their ability to prevent neuronal degeneration. Again, a constant reduction of MN number was detected, but the amount of MNs was higher at each time point when they were grown on exosome-treated astrocytes [day 4: 100% viability; day 6: 72% viability ($P< 0.001$, $t= -3.710$); day 8: 50% viability ($P<0.01$, $t=-2.854$); day 10: 37% viability ($P < 0.001$, $t= -4.944$); day 12: 19% viability ($P < 0.001$, $t= -3.157$); day 14: 12% viability ($P < 0.01$, $t= -2.983$)]. Significance was calculated vs. survival of MNs co-cultured with untreated $SOD1^{G93A}$ astrocytes at the respective time point (Figure 11).

FIGURE 11.

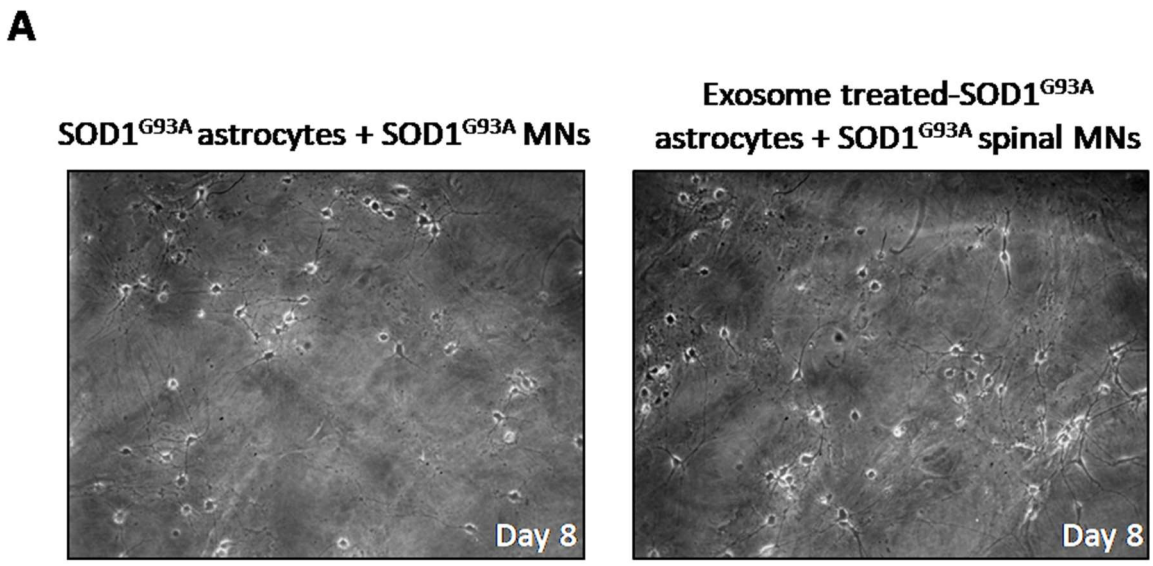

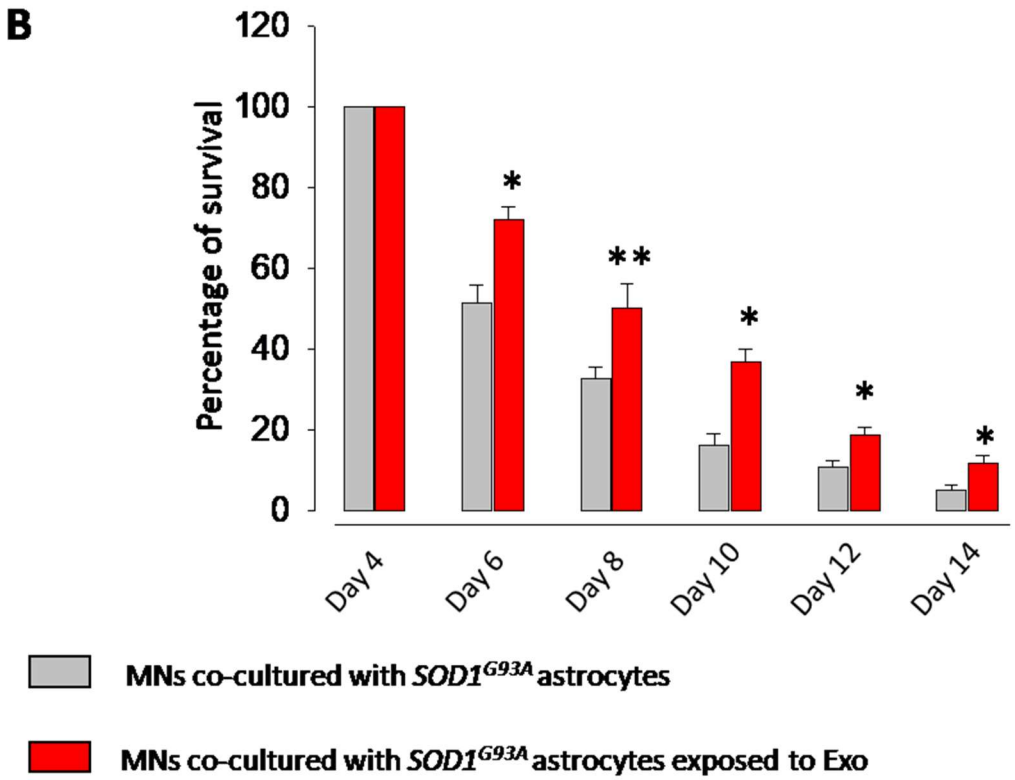

Figure 11. Viability of motor neurons co-cultured in the presence of untreated and exosome-treated spinal cord astrocytes from adult SOD1^{G93A} mice

(**A**) Representative phase-contrast microscopy images (10x) at day 8 after seeding of MNs on SOD1^{G93A} astrocytes (left panel) or on SOD1^{G93A} astrocytes treated with exosomes for 24h (right panel). (**B**) Quantitative analysis of MN viability. The analysis was performed by the direct count of viable MNs in a previously defined area for the analyses (1 square centimeter divided in 100 quadrants). MN viability was expressed as % survival of MNs co-cultured with exosome-treated SOD1^{G93A} astrocytes vs. survival of MNs co-cultured with untreated SOD1^{G93A} astrocytes. Data represent the means ± SEM of 5 independent experiments. *P<0.01, **P<0.001 vs. MN/untreated SOD1^{G93A} astrocyte co-cultures (two-tailed Student's t-test).

4.1.9 Transfection with single synthetic miRNA mimic reduces astrogliosis and inflammation of SOD1^{G93A} astrocytes

As previously described, when MSCs were stimulated with IFN-γ their miRNA expression pattern changed compared to unstimulated MSCs, suggesting a possible role in mediating the immunomodulatory functions of MSCs and MSC-derived exosomes. We hypothesized that miRNAs contained in exosomes could be the mediators of the beneficial effects of exosome treatment. To test our hypothesis we transfected SOD1^{G93A} astrocytes with synthetic miRNAs, which have been found up-regulated in IFN-γ- primed-MSCs and present in exosomes.

After 48 hour transfection we quantified the expression of GFAP, TNF-α and IL-1β by confocal microscopy. All miRNA mimics determined a significant reduction of GFAP, TNF-α and IL-1β, except miR-5126 and miR-467g. The percentage of variation of GFAP ($P < 0.001$, $F_{(11,66)}=17.012$), TNF-α ($P < 0.001$, $F_{(11,78)}=58.167$) and IL-1β ($P < 0.001$, $F_{(11,84)}=42.485$) expression vs. SOD1^{G93A} was summarize in table 4 and in figure 12.

Table 4.

	G93A + Scramble	G93A +466q	G93A +467f	G93A +466m-5p	G93A +466i-5p	G93A +466i-3p	G93A +467g	G93A +5126	G93A +669c-3p	G93A +3082-5p
GFAP	-10%± 5.6	-40% ± 0.9	-57% ±2.7	-68% ± 4.1	-80% ± 2.8	-54% ±3.0	-22% ± 2.7	-18% ± 1.8	-65% ± 2.4	-58% ± 2.4
TNF-α	-11% ± 1.3	-97% ± 1.5	-97% ± 1.8	-100% ± 2.4	-100% ± 1.9	-113% ± 3.0	-22% ± 2.5	-29% ± 1.4	-110% ± 2.5	-97% ± 2.7
IL-1β	-4% ± 2.8	-68% ± 4.2	-68% ± 4.2	-56% ± 1.7	-75% ± 2.9	-69% ± 5.0	-19% ± 3.5	-20% ± 2.1	-74% ± 2.7	-57% ± 2.9

Modifications of GFAP, TNF-α or IL-1β expression are indicated as percentage variation vs. non transfected SOD1^{G93A} astrocytes (100% expression). Data are the mean ± s.e.m. of 3 indipendent experiments run in triplicate (three different coverslips for each experimental condition). There was no significant difference between SOD1^{G93A} astrocytes and SOD1^{G93A} astrocytes transfected with 467g and 5126 miRNAs or with the scramble, confirming the selective action of other tested synthetic miRNAs.

FIGURE 12.

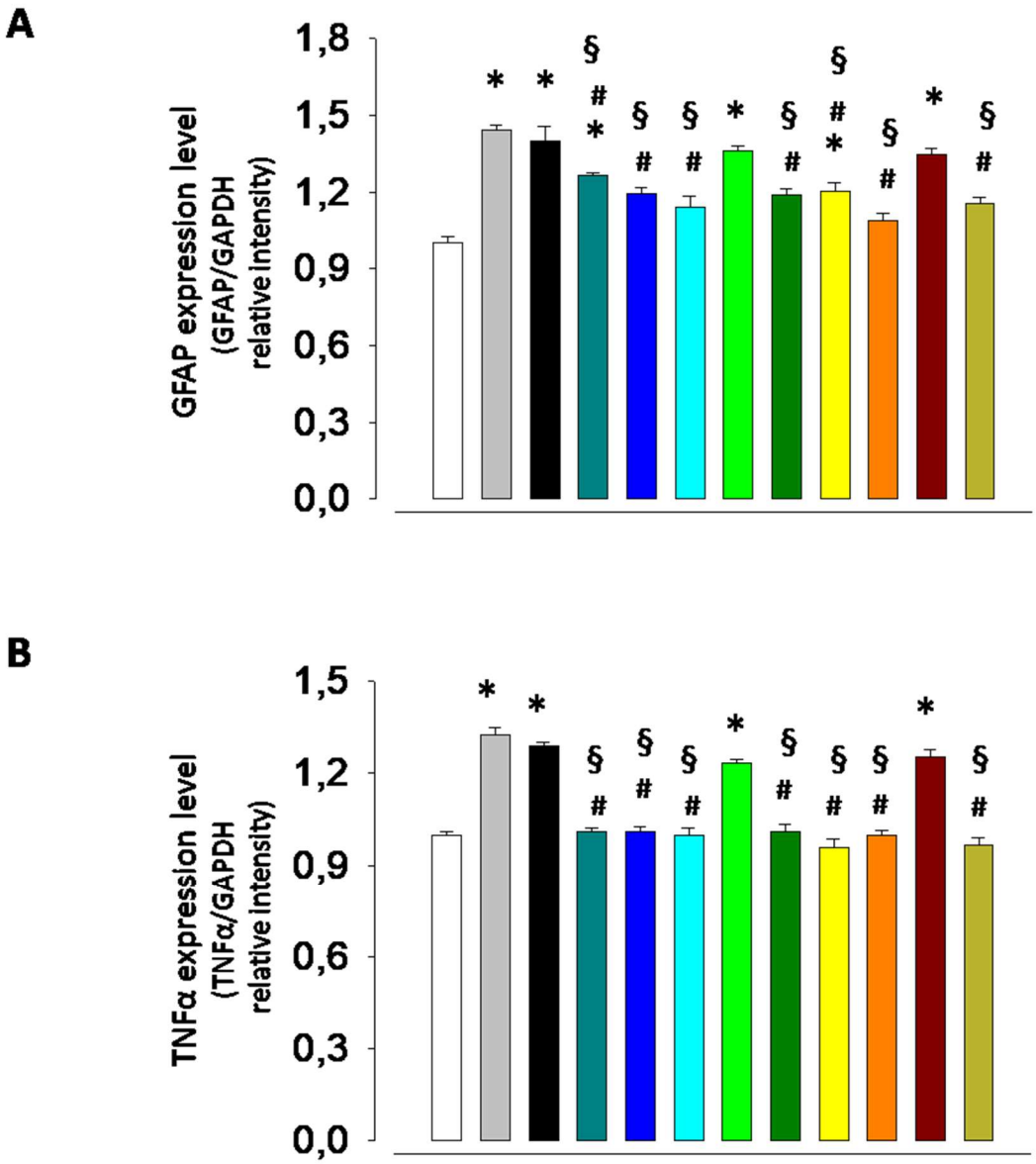

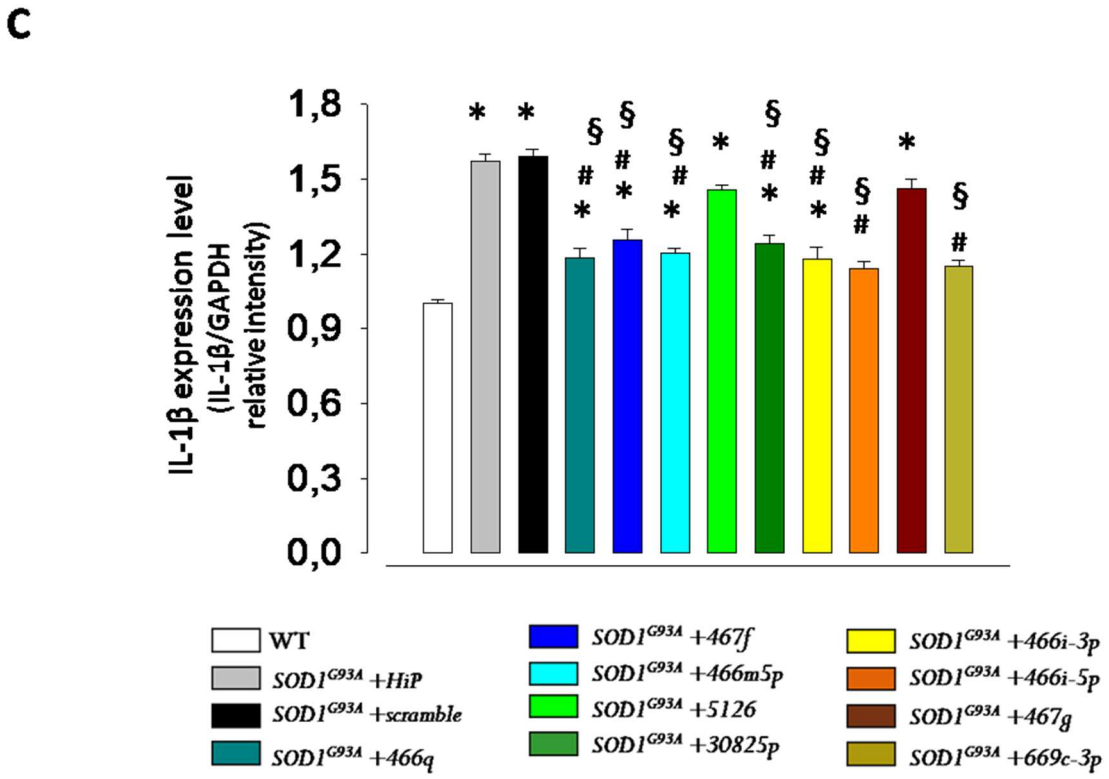

Figure 12. Immunocytochemical quantification of GFAP, IL-1β and TNF-α expression in spinal cord primary cultures of WT and SOD1^{G93A} adult mouse astrocytes exposed to miRNA mimics.

Astrocytes from SOD1^{G93A} mice were cultured as described in the Methods section, and transfected with the single synthetic miRNAs that are mimics of the miRNAs upregulated in IFNγ-primed-MSCs and present in exosomes. After 48h exposure to the miRNA mimics, expression of GFAP **(A)**, TNF-α **(B)** and IL-1β **(C)** was assessed by immunocytochemistry and laser confocal microscopy. The transfection solution (HighPerfect buffer) and a scrambled miRNA were used as controls. Quantification of protein expression, as per relative fluorescence intensity, was performed calculating the co-localization coefficients (Manders et al., 1992) using Image-J software analyses. Data are expressed as relative fluorescence intensity of GFAP, TNF-α or IL-1β normalized to the fluorescence intensity of the housekeeping protein GAPDH (confocal microscopy images not shown). The relative intensity of control WT astrocytes is reported as 1. Data presented are means ± SEM of 3 experiments run in triplicate (three different coverslips for each experimental condition). *$P < 0.001$ vs. WT astrocytes; $^{\#}P < 0.001$ vs. SOD1^{G93A}astrocytes + HighPerfect buffer; $^{\S}P < 0.001$ vs. SOD1^{G93A}astrocytes + scrambled miRNA (two-way ANOVA followed by Bonferroni post-hoc test).

4.1.10 Identification of the pathways targeted by miRNAs

The most effective miRNAs, tested above, were selected for further studies in order to elucidate the pathways affected by the exosome treatment based on their predicted targets. Noteworthy, miR-466q, miR-466m-5p, miR-466i-3p and miR-467f, that were identified as potential messenger molecules, in virtue of their significant effect in ameliorating the phenotype of $SOD1^{G93A}$ astrocytes, were also the four miRNAs up-regulated both in IFN-γ-primed-MSCs and in exosomes derived from IFN-γ-primed-MSCs.

First of all, computational analysis was performed and relevant target pathways, regulating inflammation, cytokine synthesis and oxidative stress, were identified by miRWalk or miRBase database.

In this respect, miR-466m-5p presents a wide range of actions. Indeed, it affects several inflammatory pathways, such as MAPK, NFκB and TLR signalling pathways.

In particular, miR-466m-5p can reduce the translation of Mitogen-Activated Protein *Kinase KinaseKinase* 8 (MAP3K8), which is involved in the phosphorylation and activation of p38 and NFκB, promoting the transcription of cytokine genes (Figure 13A and 13B).

Mitogen-activated protein kinase-11 (MAPK11) is a second target of miR-466m-5p. In stress condition, MAPK11 is in the phosphorylated form and it phosphorylates the Activating Transcription Factor (ATF2), which promotes the transcription of the pro-inflammatory cytokine TNF-α (Mahlknecht et al., 2004) (Figure 13 C).

Moreover, miR-466m-5p is potentially able to reduce the translation of TNF Receptor Associated Factor 6 (TRAF6), TGF-β Activated Kinase 1 and Mitogen-Activated Protein *Kinase KinaseKinase* 7 (MAP3K7) Binding Protein 2 (TAB2) and p65. These three proteins determine the activation of NFκB signalling pathway. TRAF6 and TAB2

assembly with MAP3K7 and TAB1 in response to LPS or pro-inflammatory cytokines and this protein complex phosphorylates downstream kinases, such as IKKB and MAPK, leading to the activation of the transcription factors NFκB and AP-1, respectively (Walsh et al., 2015). In addition, the modulation of p65 expression directly affects NFκB complex assembly; indeed p65 is one of the subunits that form the active complex with pro-inflammatory function (Lawrence, 2009) (Figure 13D).

Moreover, miR-466m-5p is able to increase the resistance to oxidative stress of cells, decreasing the translation of the transcription factor BTB and CNC homology 1 (BACH1), which is a functional inhibitor of Nrf2, by competing for the same binding site of ARE. A reduction of BACH1 facilitates the binding of Nrf2 to the transcription factor ARE and promotes the activation of anti-oxidant mechanisms (Zhang et al., 2018) (Figure 13E).

Some targets of miR-466m-5p are shared with the other selected miRNAs. For instance, miR-467f and miR-466i-3p inhibit the transcription of MAP3K8 (Figure 13A), miR-466i-3p reduces the expression of MAPK11, HDAC3 and ATF2 (Figure 13C). Moreover, miR-466q and miR-466i-3p can act on MAPKAPK2, which phosporylates IκB allowing NFκB translocation into the nucleus and represents a downstream kinase of p38 promoting cytokine expression (Figure 13B).

FIGURE 13.

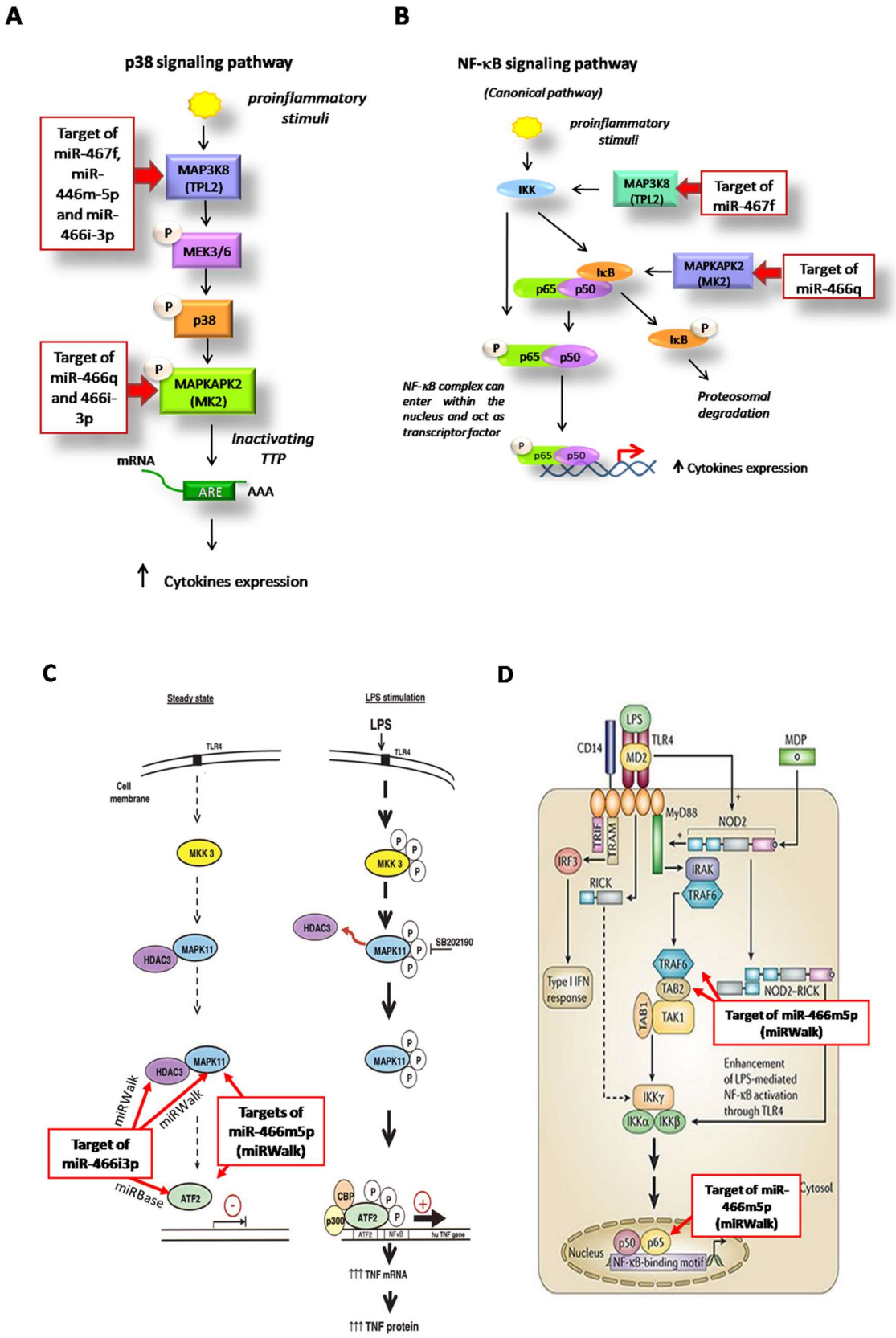
A
p38 signaling pathway
proinflammatory stimuli
Target of miR-467f, miR-446m-5p and miR-466i-3p
MAP3K8 (TPL2)
P
MEK3/6
P
p38
Target of miR-466q and 466i-3p
P
MAPKAPK2 (MK2)
Inactivating TTP
mRNA
ARE
AAA
Cytokines expression
B
NF-κB signaling pathway
(Canonical pathway)
proinflammatory stimuli
IKK
MAP3K8 (TPL2)
Target of miR-467f
IκB
p65 p50
MAPKAPK2 (MK2)
Target of miR-466q
IκB
P
P
p65 p50
NF-κB complex can enter within the nucleus and act as transcriptor factor
Proteosomal degradation
P
p65 p50
Cytokines expression
C
Steady state
LPS stimulation
LPS
TLR4
TLR4
Cell membrane
MKK 3
MKK 3
HDAC3
MAPK11
HDAC3
MAPK11
SB202190
MAPK11
HDAC3
MAPK11
miRWalk
miRWalk
Target of miR-466i3p
Targets of miR-466m5p (miRWalk)
miRBase
ATF2
CBP
p300
ATF2
ATF2
NFκB
hu TNF gene
↑↑↑ TNF mRNA
↑↑↑ TNF protein
D
LPS
CD14
TLR4
MD2
MDP
MyD88
NOD2
TRIF
TRAM
IRF3
IRAK
RICK
TRAF6
Type I IFN response
TRAF6
TAB2
NOD2-RICK
TAB1
TAK1
Target of miR-466m5p (miRWalk)
Enhancement of LPS-mediated NF-κB activation through TLR4
IKKγ
IKKα
IKKβ
Target of miR-466m5p (miRWalk)
Cytosol
Nucleus
p50
p65
NF-κB-binding motif

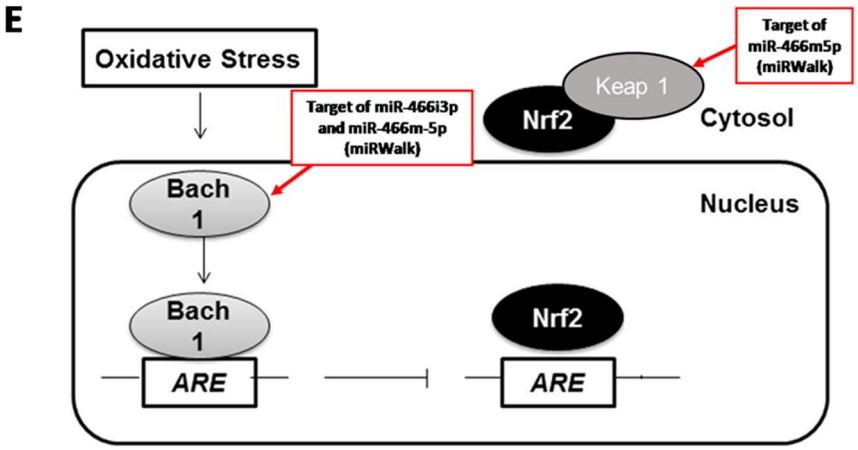

Figure 13. Target pathways of miRNAs shuttled by MSC-derived exosomes

We selected four miRNAs (miR-466q, miR-467f, miR-466m-5p, miR-466i-3p) on the basis of their ability to reduce the activation state of $SOD1^{G93A}$ astrocytes by decreasing GFAP, IL-1β and TNF-α overexpression (see Fig. 10). The selected miRNAs mainly affect pathways related to inflammation, in particular NFκB and MAPK pathways. Interestingly, one of these miRNAs, miR-466m-5p, modulates also pathways that lead to the reduction of the oxidative stress. miRNA targets were identified through miRWalk and miRBase databases. **(A)** Graphical representation of p38 signaling pathway and miRNAs targeting two of the kinases involved in the activation of p38. **(B)** Graphical representation of p65 canonical signaling pathway and miRNAs targeting two of the kinases involved in the phosphorylation and activation of p65. **(C)** Graphical representation of Toll-like receptor (TLR) signaling pathway for Activating Transcription Factor 2 (ATF2) activation and TNF-α synthesis. The indicated miRNAs could affect ATF2 activation through the downregulation of their relevant targets that are components of the pathway, as described in miRWalk and miRBase database. **(D)** Graphical representation of TLR-4 signaling pathway activating p65 translocation to the nucleus and miRNA targets inhibiting some crucial steps of the cascade. **(E)** Graphical representation of Nrf2 pathway and predicted miRNAs modulating transcription of inhibitory factor of Nrf2 binding to Antioxidant Response Element (ARE).

4.1.11 Validation of the pathways targeted by miRNAs

The panel of pathways identified by *in-silico* studies has been validated by qPCR analysis. MAPK-11 showed the most promising results. Indeed it was significantly increased in $SOD1^{G93A}$ astrocytes compared to WT astrocytes [193% increase ($P < 0.05$, t=-3.529)] and transfection of $SOD1^{G93A}$ astrocytes with miR-467f and miR-466q determined a strong reduction of MAPK-11 over-expression [87% decrease ($P < 0.05$, t=2.360); 76% decrease ($P < 0.05$, t=2.312), respectively]. Also miR-466i-3p and miR-466m-5p reduced MAPK11 mRNA, altrough non significantly (20% decrease; n.s., t=0.740; 58% decrease; n.s., t=1.739 respectively) (Figure 14A).

The other selected targets, MAP3K8, MAPKAPK2 and TRAF6, were not affected by miRNA transfection.

MAP3K8 was significantly augmented in $SOD1^{G93A}$ astrocytes compared to control astrocytes (105% increase; $P< 0.05$, t=-3.432). However, any of the tested miRNAs was able to modulate the expression of this kinase (Figure 14B).

Similarly, MAPKAPK2 showed a trend to increase in $SOD1^{G93A}$ astrocytes compared to WT even if not significant (t=-1.589). However, its mRNA expression was not modified in $SOD1^{G93A}$ astrocytes by exposure to miRNA transfection (Figure 14C).

TRAF6 is a target selected only for miR-466m-5p, but the results discouraged its involvement in astrocyte phenotype modulation, since TRAF6 mRNA expression was not different among control-, $SOD1^{G93A}$- and transfected-$SOD1^{G93A}$ astrocytes (Figure 14D).

Finally, the expression of BACH1 was measured in WT and $SOD1^{G93A}$ astrocytes. However, the cycles needed to amplify the gene were too elevated, indicating a too low gene expression in our astrocytes; thus, making it difficult to obtain reliable results (data not shown).

FIGURE 14.

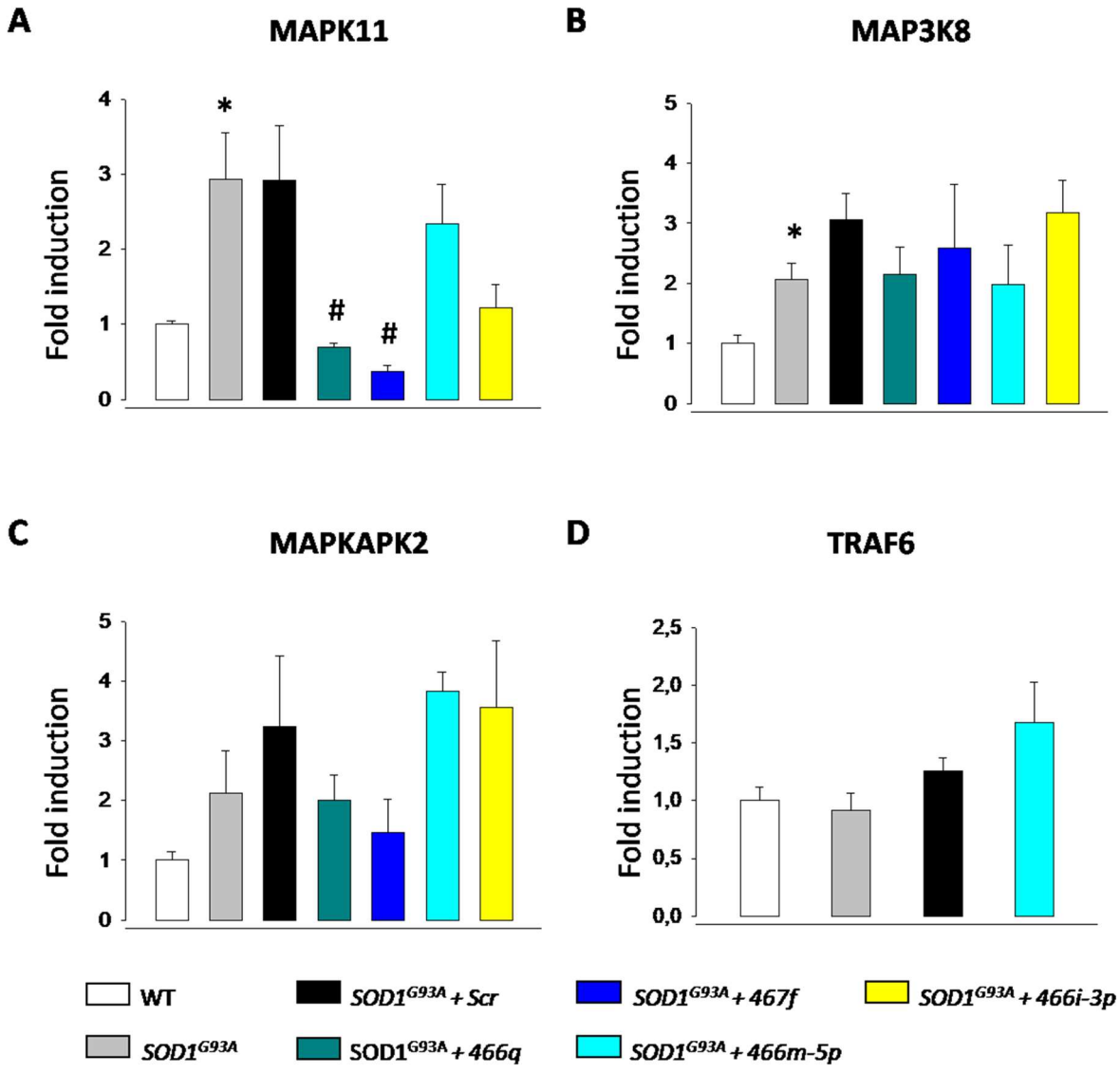

Figure 14. qPCR analysis of MAPK11, MAP3K8, MAPKAPK2 and TRAF6 expression in spinal cord primary cultures of WT and SOD1^{G93A} adult mouse astrocytes exposed to miRNA mimics.

Quantification of (**A**) MAPK11, (**B**) MPA3K8, (**C**) MAPKAPK2 and (**D**) TRAF6 expression by qPCR. The mRNA expression was normalized to the expression of the housekeeping gene GAPDH. The relative expression of control WT astrocytes is reported as 1. Data presented are means ± SEM of 4 experiments run in duplicate. *$P < 0.05$ vs. WT astrocytes; $^{\#}P < 0.05$ vs. untreated SOD1^{G93A} astrocytes (two-tailed Student's t-test).

4.2 Human astrocyte characterization and treatment with human MSC-derived exosomes

4.2.1 Human astrocyte characterization

Human astrocytes were differentiated from fibroblasts derived from two ALS patients carrying the $SOD1^{4AV}$ mutation (patients 100 and 102) and one non-ALS patient (individual 155). After four weeks of differentiation protocol to obtain inducible neuroprogenitor cells (iNPCs), astrocytes were prepared by switching iNPCs medium with astrocyte medium.

To confirm the efficacy of the differentiation protocol, the expression of GFAP, vimentin and CD44, selective markers for astrocytes, was analysed by immunofluorescence. iAstrocytes result highly positive to these markers (Figure 15). These results confirm that after the differentiation protocol an extensiveenrichment toward astrocyte-like cells was obtained.

FIGURE 15.

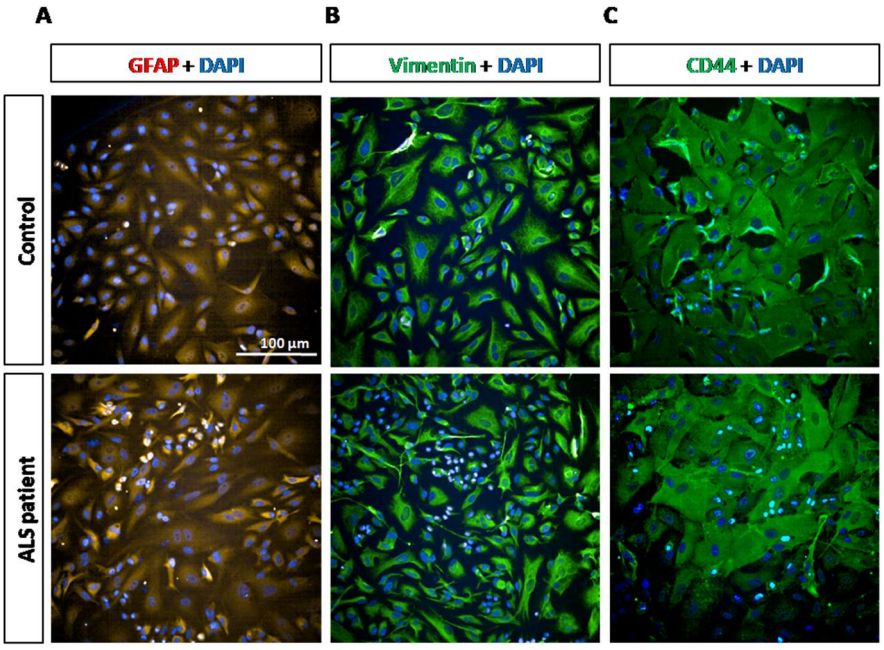

Figure 15. Immunocytochemical characterization of human astrocytes from control and ALS patients.

Representative images of human astrocytes (iAstrocytes) differentiated from fibroblasts derived from control and ALS patients. iAstrocytes were stained for (**A**) GFAP (red) and DAPI (blue), (**B**) Vimentin (green) and DAPI (blue), and (**C**) CD44 (green) and DAPI (blue). Scale bar: 100 μm.

4.2.2 Treatment with exosomes isolated from human MSCs exerts a mild effects on iAstrocytes phenotype

As described above, the experiments were performed on iAstrocytes derived from one non-ALS patient (control astrocytes, n. 155) and on two different lines of $SOD1^{A4V}$ iAstrocytes derived from distinct patients (n. 100 and 102). The expression of p-p65, NLRP3, Nrf2 and NQO1 was analysed by Western blot experiments.

The phosphorylated form of p65 was significantly higher in iAstrocytes from patient 102 compared to control iAstrocytes ($P < 0.05$, $t = -4.668$). No significant difference was detected in patient 100 iAstrocytes vs. control iAstrocytes ($t= -0.573$). Exosome treatment reduced p-p65 expression by 7% (n.s., $t=0.169$) and by 29% (n.s., $t=1.790$) in iAstrocytes derived from patient 100 and patient 102, respectively (Figure 16).

Also NLRP3 expression was not significantly modified between ALS and control iAstrocytes. Upon exposure to exosomes, the trend to a decrease of NLRP3 expression was observed in both patients' iAstrocytes compared to their respective untreated control (patient 100-iAstrocytes= 25% decrease, n.s., $t=0.685$; patient 102-iAstrocytes= 12% decrease, n.s., $t=0.398$) (Figure 16).

FIGURE 16.

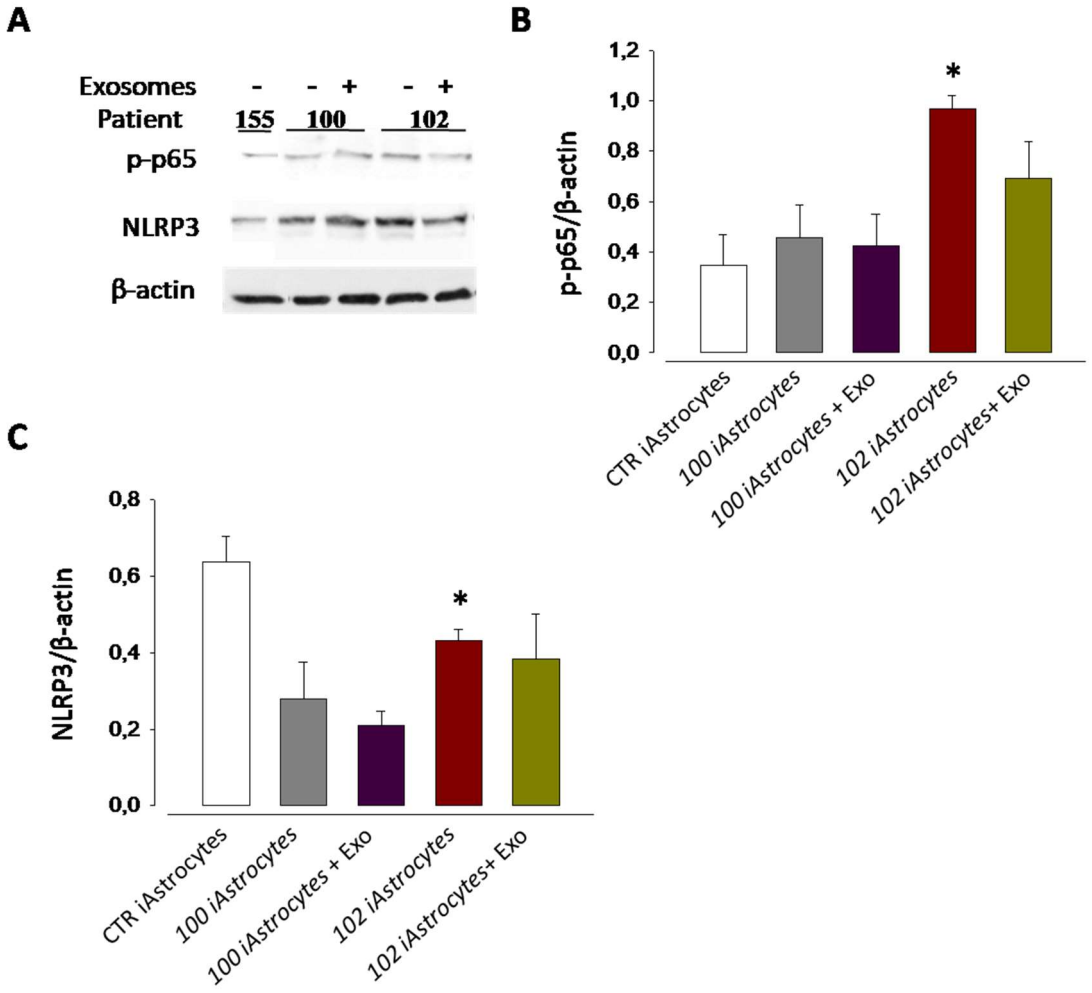

Figure 16. Western blot quantification of phospho-p65 and NLRP3-inflammosome complex expression in cell lysates from cultures of human astrocytes from control and SOD1^{A4V} patients.

(**A**) Representative immunoreactive bands for phospho-p65, NLRP3-inflammosome complex and β-actin in control (individual 155) iAstrocytes, patient-100 and patient-102 untreated SOD1^{4AV} iAstrocytes and patient-100 and patient-102 SOD1^{4AV} iAstrocytes treated with IFNγ-primed MSC-derived exosomes for 24h. (**B**) Quantification of protein expression as per scanned band density in control iAstrocytes, untreated SOD1^{A4V} iAstrocytes and SOD1^{A4V} iAstrocytes treated for 24h with exosomes. Protein expression was calculated as relative band density normalized to the housekeeping protein β-actin. Data presented are means ± SEM of 3 independent experiments. *P <0.05 vs. control iAstrocytes (two-tailed Student's t-test).

In accordance with experiments performed using mouse astrocytes, cell resistance to oxidative stress was measured. Nrf2 was strongly decreased in iAstrocytes from patients 100 and 102 compared to control iAstrocytes (65% decrease, n.s., t= 2.607, and 88% decrease, n.s., t= 2.642, respectively). Exosome treatment significantly reversed the down-regulation of Nrf2 in patient 102 iAstrocytes compared to untreated iAstrocytes (126% increase, $P < 0.05$, t= -7.005). In iAstrocytes derived from patient 100, exosome treatment determined an augmentation of Nrf2 expression by 67% compared to untreated $iAstrocytes_{(100)}$ (n.s., t= -0.552).

Finally, NQO1 expression was significant lower in ALS iAstrocytes compared to control iAstrocytes (patient 100-iAstrocytes= 68% decrease, $P < 0.05$, t = -3.904; patient 102-iAstrocytes= 88% decrease, $P < 0.001$, t= 20.254). The treatment with exosomes determined a trend to amelioration of this parameter since iAstrocytes derived from patient 100 and patient 102 showed an increase of NQO1 expression by 77% (n.s., t = -0.864) and by 104% (n.s., t = -1.598) compared to the respective untreated iAstrocytes (Figure 17).

FIGURE 17.

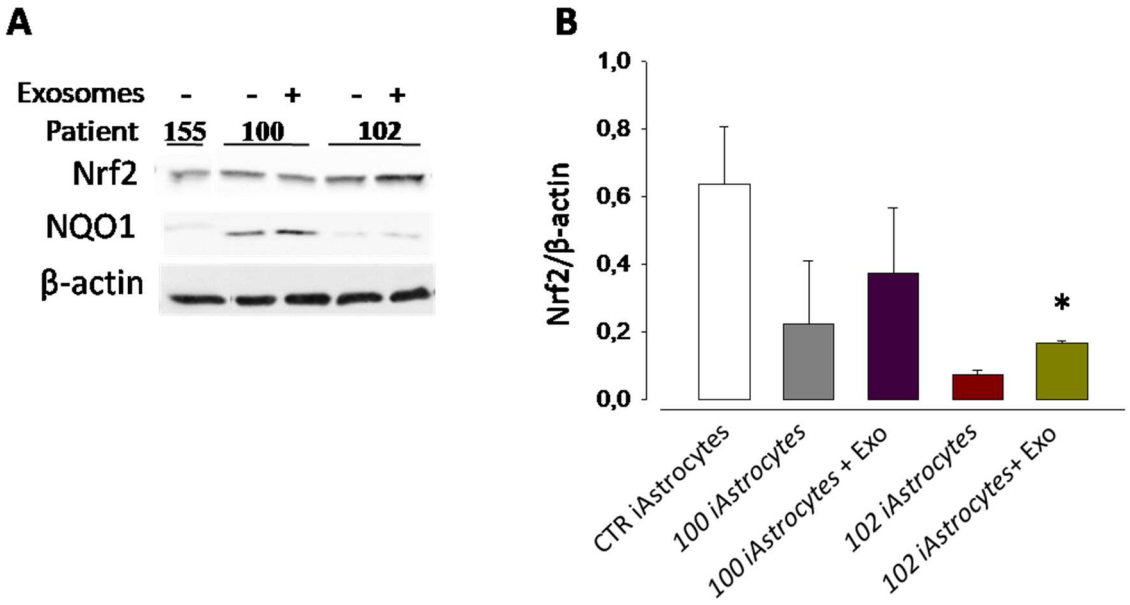

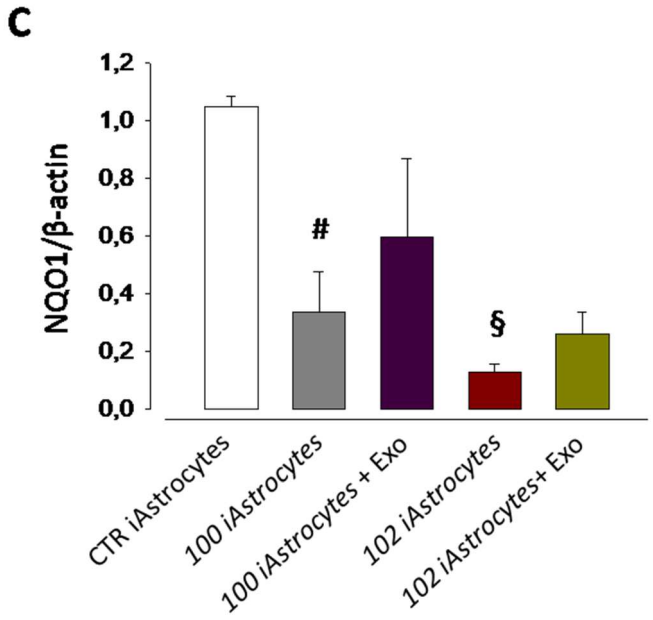

Figure 17. Western blot quantification of Nrf2 and NQO1 expression in cell lysates from cultures of human astrocytes from control and SOD1^{A4V} patients.

(**A**) Representative immunoreactive bands for Nrf2, NQO1 and β-actin in control (individual 155) iAstrocytes, patient-100 and patient-102 untreated SOD1^{A4V} iAstrocytes and patient-100 and patient-102 SOD1^{A4V} iAstrocytes treated with IFNγ-primed MSC-derived exosomes for 24h. (**B**, **C**) Quantification of protein expression as per scanned band density in control iAstrocytes, untreated SOD1^{A4V} iAstrocytes and SOD1^{A4V} iAstrocytes treated for 24h with exosomes. Protein expression was calculated as relative band density normalized to the housekeeping protein β-actin. Data presented are means ± SEM of 3 independent experiments. **P* < 0.05 vs. untreated 102 iAstrocytes, $^{\#}$P < 0.05 or §P < 0.001 vs. control iAstrocytes (two-tailed Student's t-test).

4.2.3 iAstrocytes treated with human MSC-derived exosomes are more supportive for MNs compared to untreated iAstrocytes

MNs, derived from mouse embryonic stem cells and expressing GFP under the MN-specific promoter Hb9, were co-cultured with iAstrocytes from patient 100 and patient 102, treated or not with exosomes derived from human MSCs.

iAstrocytes were treated with exosomes for 24 hours, then MNs were seeded. MNs were counted for 3 days and MN viability was measured as percentage of survival between day 3 and day 1.

When cultured on untreated iAstrocytes, the percentage of MN survival at day 3 was 33% for iAstrocytes from patient 100 and 38% for iAstrocytes from patient 102. The treatment with exosomes was able to partially rescue MN degeneration in the co-culture system. The percentage of MN survival at day 3 was 56% ($P < 0.05$, $t= -2.524$) and 47% (n.s., $t= -1.303$) in treated -patient 100-iAstrocytes and in –patient 102-iAstrocytes, respectively (Figure 18).

As a whole, the experiments with human astrocytes suggest that the treatment with exosomes ameliorates their phenotype and demonstrate that this amelioration would have a positive impact on MN survival. However, more experiments are needed to verify the significance of the modifications measured.

FIGURE 18.

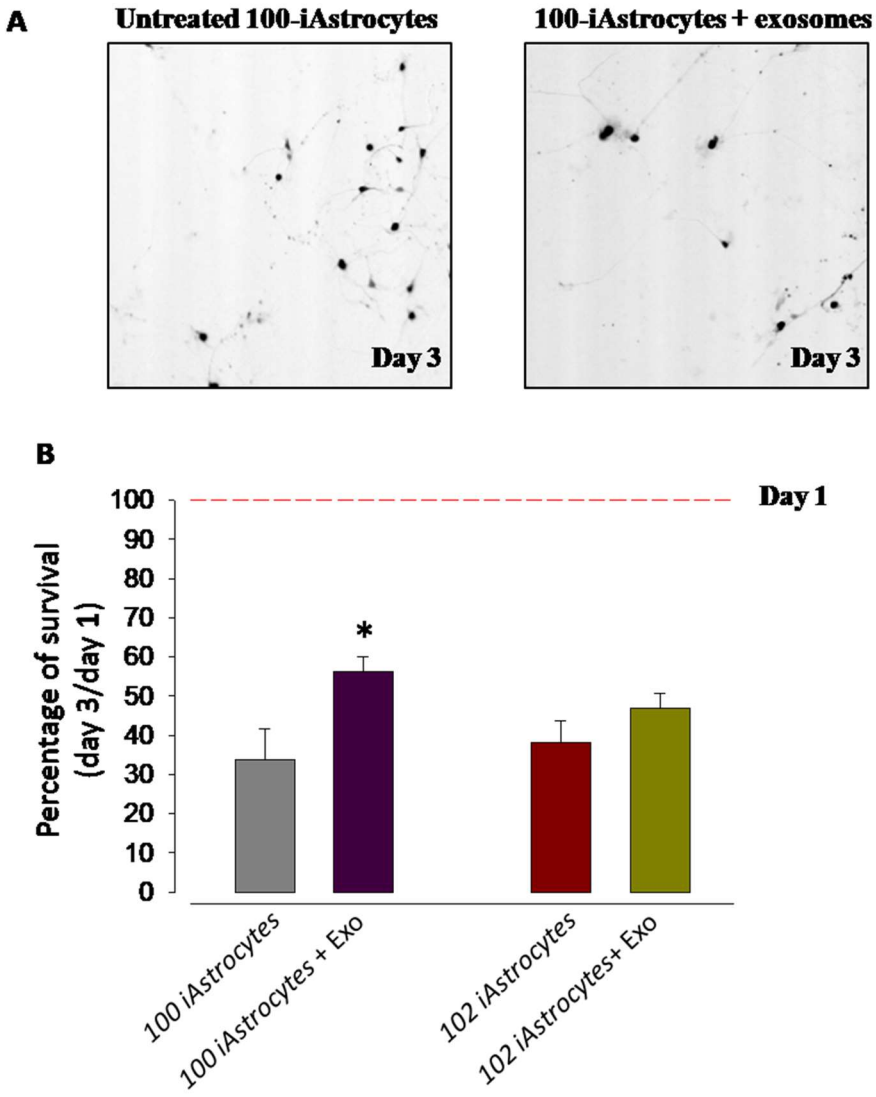

Figure 18. Viability of motor neurons co-cultured in the presence of untreated or exosome-treated iAstrocytes from patients, carrying the A4V ALS-linked SOD1 mutation.

A) Representative phase-contrast microscopy images of MN morphology at day 3 after seeding on patient-100 iAstrocytes treated or not with exosomes. Images obtained with the InCell® were used for semi-automated high throughput analysis with Columbus microscopy software. **B)** Quantitative analysis of MN viability. The number of motor neurons were quantified automatically, and only motor neurons bearing axons were counted. Histograms represent MN survival expressed as percentage of the ratio between the number of MNs at day 3 and that at day 1. Day 1 is considered as 100% survival. Data represent the means ± SEM of 3 independent experiments, run in triplicate. **P*<0.05 vs untreated MN/untreated SOD1^{G93A} iAstrocyte cultures (two-tailed Student's t-test).

5. DISCUSSION

MSCs are largely studied as innovative therapy for ALS and other neurodegenerative diseases. However, the mechanisms of action of MSCs have been only partially elucidated. Initially, it was proposed a direct therapeutic effect of MSCs after infusion, driven by migration to the sites of damage, engraft, differentiation and interaction with other cells. Nowadays, the beneficial effects of MSCs are mostly attributed to paracrine mechanisms rather than differentiation of MSCs in other cellular types (Mendt et al., 2019).

In one of our previous studies, we reported that a single intravenous administration of MSCs in $SOD1^{G93A}$ mice determined an extension of lifespan, an amelioration of motor skills and a reduction of astrogliosis and inflammation in spinal cord (Uccelli et al., 2012). These beneficial effects were not exerted by MSC differentiation; indeed the most part of injected cells were sequestered in lungs and hardly reached the spinal cord, as described later also in several other studies using MSCs as a treatment (Mendt et al., 2019). Thus, in our study we proposed that paracrine mechanisms, implying cell-to-cell communication by diffusing messengers, could be at the basis of the observed effects.

The present study highlights the role of exosomes derived from MSCs as possible mediators of the functions of MSCs themselves. To elucidate the regulatory mechanisms involved in the modulation of ALS characteristics by exosomes, we focused on astrocytes derived from $SOD1^{G93A}$ mice and from ALS patients, because of their relevant function in disease progression. Indeed, it is well recognised that ALS is a non-cell autonomous disease (Lee et al., 2016) and glial cells fulfil a crucial function in MN death, by losing the ability of support of MNs, exerted in physiological conditions through the release of neurotrophic factors and to the maintenance of synapses homeostasis. Instead, they become harmful by releasing neurotoxic factors, such as pro-inflammatory cytokines, chemokines,

complement factors and products derived from oxidative stress (Lee et al., 2016, Yamanaka et al., 2017).

In our mouse model experiments, we utilized astrocytes prepared from 120 days-old $SOD1^{G93A}$ mice, at the late stage of the disease, and age-matched WT mice. In spite of the difficulties to obtain and expand adult astrocytes respect to the new born ones, we decided to use these cells because they represent, in our belief, a more appropriate disease model. Certainly, they matured *in-vivo* during the evolution of the disease, spanning from the pre-symptomatic, low-progressing, to the symptomatic, fast-progressing, stages and are, therefore, activated because exposed to a "true" pathological environment. Adult mouse-derived astrocytes parallel, in a way, the human astrocytes derived from patient's reprogrammed fibroblasts. Accordingly, $SOD1^{G93A}$ astrocytes and human iNPC-derived SOD1-astrocytes showed a stronger reactivity and an inflammatory phenotype compared to control astrocytes. The treatment with exosomes derived from MSCs was able to reduce the toxic activation of $SOD1^{G93A}$ astrocytes and, even if less emphasised, of iAstrocytes.

Several findings support the involvement of paracrine mechanisms as the main mode of action of MSCs. Sun and Colleagues demonstrated that MSCs and MSC conditioned medium exerted a comparable ameliorative effect in different *in vitro* model of ALS. The administration of MSCs or MSC conditioned medium to primary motor neurons, NSC-34 cells and astrocytes was neuroprotective against staurosporine toxicity. In particular, in $SOD1^{G93A}$ neonatal astrocytes, MSC conditioned medium was able to positively modulated MAPK/Erk1/2 and PI3-K/Akt signalling pathways, that are involved in differentiation, proliferation, growth and survival of neuron and astrocytes, to stimulate the synthesis of many neurotrophic and neuroprotective factors and to reduce the inflammatory response upon exposure to LPS through the down-regulation of TNF-α, IL-6 and iNOS gene

expression (Sun et al., 2013). A further study revealed several soluble factors (PGE2, TGF-β, IL-10) and extracellular vesicles released from MSCs, that were able to abolish inflammatory responses and sustain regenerative processes (Zhou et al., 2019).

MSC-derived exosomes were reported to promote the switch of macrophages to M2 anti-inflammatory phenotype in bronchopulmonary dysplasia, to down-regulate the level of inflammatory cytokines (Willis et al., 2018) and to increase the expression of anti-inflammatory factors, such as PGE2 (Hyvärinen et al., 2018). Moreover, they reduced the activation of T cells, B cells and dendritic cells, but promoted the proliferation of Treg (Del Fattore et al., 2015, Budoni et al., 2013, Reis et al., 2018).

Studies on a spinal cord injury rodent model sustain the effectiveness of MSC-derived EVs in protect neurons from degeneration, mainly through the suppression of the NFκB signalling pathway activation in astrocytes and perycites (Wang et al. 2018; Lu et al., 2019).

In our project we wanted to elucidate in depth whether exosomes were able to ameliorate the noxious phenotype of astrocytes prepared from $SOD1^{G93A}$ mice and which are the components of the exosome cargo involved in this positive modulation. Among the molecules contained into exosomes there are miRNAs, non-coding RNAs which modulate the expression of up to 30% of all mammalian protein-encoding genes. Notably, miRNAs are selectively sorted in EVs, suggesting their pivotal role in cell-to-cell communication (Qiu et al., 2018). Therefore, we analysed the miRNA cargo of exosomes and identified four miRNAs that can be potential modulators of inflammatory response in ALS astrocytes.

Exosome treatment determined a decreased expression and release of the pro-inflammatory cytokines TNF-α, IL-1β, IL-6 and of the chemokine CCL2 in $SOD1^{G93A}$ astrocytes. The reduction of cytokine secretion is probably linked to the observed amelioration of MN survival. Kia and Colleagues identified TNF-α as one main toxic factor released from astrocytes, causing MN degeneration through the activation of NFκB signalling pathway but also through the alteration of AMPA receptors (Kia et al., 2018). The correlation between TNF-α and excitotoxicity has been reported by several research groups. It has been observed that TNF-α can exacerbate AMPA receptor-mediated excitotoxicity of lumbar spinal cord MNs, possibly by increasing AMPA permeability to Ca^{2+} (Hermann et al., 2001, Yin et al., 2012). In adding, TNF-α was reported to down-regulate astrocytic EAAT2 expression through the NFκB binding to the EAAT2 promoter (Sitcheran et al., 2005). These findings suggest that a reduction of TNF-α expression could be strongly ameliorative of the ALS astrocytic phenotype, not only for the influence on the inflammatory pattern but also in reducing excitotoxicity, one of the major features of ALS pathogenesis.

Pro-inflammatory stimuli driven by activation of TNF-α receptors (TNFR1 and TNFR2) determine the activation of NFκB, which induces NLRP3 transcription, as well as that of other key pro-inflammatory genes, including that encoding for pro-IL-1β. The activation of NLRP3 leads to the cleavage of pro-IL-1β and pro-IL-18 to the respective active form and, consequently, to their secretion. Moreover, NLRP3 seems involved in necroptosis, a type of inflammatory cell death. Indeed, its assembly can be induced by RIP3 and pseudokinase mixed-lineage kinase domain-like protein (MLKL), the major components of necroptosis pathway, through the activation of caspase 8. These findings suggest a role of NLRP3 in

exacerbating the pro-inflammatory stimuli in cells, which can potentially promote necroptotic cell death.

Because of the relevant role of NLRP3, it turns out to be a possible target in several diseases characterized by an inflammatory component, such as multiple sclerosis, Alzheimer disease, traumatic brain injury, Parkinson's disease (Mangan et al., 2018, Chen et al., 2018). Also in ALS, NLRP3 was reported to be increased (Johann et al., 2015, Gugliandolo et al., 2017). In accordance, we detected an increase of NLRP3 in $SOD1^{G93A}$ astrocytes. Exosome treatment normalized this activation, contributing to the reduction of IL-1β. We hypothesize that a reduction in NLRP3 could also reduce necroptosis-mediated cell death in astrocytes, that reflects in an amelioration of MN viability, due to a lower release of inflammatory toxic factors. To confirm this hypothesis we plan to analyse the expression of RIP3 and MLKL and their phosphorylation state in $SOD1^{G93A}$ MNs co-cultured with $SOD1^{G93A}$ astrocytes treated or not with exosomes.

The ameliorative effects of exosomes affected also the reactive phenotype of $SOD1^{G93A}$ astrocytes. GFAP, vimentin and S100β expression were significantly down-regulated in $SOD1^{G93A}$ exposed to exosomes. In normal condition astrogliosis has a neuroprotective and regenerative scope, however, reactive astrogliosis is often exacerbated in neurodegenerative diseases, including ALS, and astrocytes are subjected to degeneration and gain of toxic function (Verkhratsky and Zorec, 2018). A reduction of astrogliosis markers, together with the increased survival of MNs when grew on exosome-treated astrocytes, strongly suggest that exosome treatment promotes a switch of astrocytes to a less neurotoxic phenotype.

The decrease of S100β could affect also cell injury and the expression of pro-inflammatory genes. S100β was reported to behave as a component of the DAMPs when, released in high concentrations, participates in the cascade of events causing cell injury, and to bind the Receptor for Advanced Glycation End products (RAGE), leading to microglia migration. Serrano and Colleagues demonstrated that silencing of S100β in $SOD1^{G93A}$ astrocytes determined a down-regulation of GFAP, TNF-α, CXCL10 and CCL6 expression. Therefore, the significant reduction of S100β expression, observed upon exposure to exosomes, may determine a synergic action with MSC- derived exosomes in decreasing inflammation in ALS.

In last decades, it has been documented that MSCs have the ability to reduce the toxic effect of oxidative stress, in addition to their immunomodulatory function. MSCs and MSC-derived exosomes were reported to decrease oxidative stress by reducing ROS production and over-expressing anti-oxidant enzymes, and also inhibiting NLRP3 activation following H_2O_2 treatment (Alhazzani et al., 2018; Xia et al., 2019). Further, in our previous study we detected that MSC injection in $SOD1^{G93A}$ mice determined a reduction of oxidative stress condition at the level of spinal cord of these mice through the induction of the glutathione S-transferase (Uccelli et al., 2012).

The modulation of oxidative stress response has been largely studied as a possible therapeutic target in ALS, in part due to the mutation of genes that regulate detoxification of ROS. Nrf2 is a transcription factor that activates ARE, promoting transcription of numerous cytoprotective proteins, such as glutathione S-transferase, NQO1, Heme oxygenase-1, and glutamate-cysteine ligase. The expression of Nrf2 is decreased in ALS patients and rodent model of the disease (Petri et al., 2012).

We found that Nrf2 is down-regulated in SOD1^{G93A} astrocytes compared to WT astrocytes. The Nrf2 impairment was significantly rescued by exosome treatment. By analysing miRNA pathways, we revealed that the up-regulated miRNA miR-466m-5p can exert an anti-oxidant effect abolishing the transcription of BACH1, which inhibits ARE by competing with Nrf2 for the same binding site. In addition, Xia and Colleagues detected the presence in exosomes of antioxidant proteins such as heat shock protein of 75 kDa (HSP75), phospholipid hydroperoxide glutathione peroxidase, and peroxiredoxin-1, suggesting a further synergic mechanism of action of the exosome treatment.

Recent studies showed that the induction of Nrf2-ARE pathway by pharmacological interventions determines an increase of MN survival both *in-vitro* and *in-vivo* models of ALS, possibly by increasing the secretion of glutathione (Mead et al., 2013; Kanno et al., 2012). Also, an interplay between Nrf2 and NFκB has been described, which contributes to worsening the inflammatory state. The down-regulation or ablation of Nrf2 determines an increased activation of NFκB and, consequently, of cytokine production following brain injury, inducing astrogliosis, demyelination and neuronal death (Pan et al., 2012; Neymotin et al., 2011). These findings highlight the contribute of rescuing Nrf2 expression in supporting MN viability in our co-culture system.

To verify whether all the advantageous modifications of the astrocyte phenotype, that led also to a reduction of pro-inflammatory cytokine secretion, observed after exposure to exosomes, were able to positively impact on MN well-being, we measured the survival of MNs when co-cultured with SOD1^{G93A} astrocytes previously exposed to exosomes or to standard culture medium. Results highlighted that the survival was absolutely augmented when MNs were exposed to astrocytes pre-treated with exosomes. Notably, our experimental method allows to unequivocally attribute the increase of MN survival to the

amelioration of astrocyte phenotype. In fact, astrocytes were treated with MSC-derived exosomes, while MNs were added after exosome wash-out. This implies that the diminished expression of pro-inflammatory cytokines and the improved response to oxidative stress in $SOD1^{G93A}$ astrocytes can potentially slowdown MN degeneration.

As already described above, the reduction of the release of pro-inflammatory cytokines, especially TNF-α, exerts a positive impact on MN survival mitigating phenomena linked to chronic and acute inflammation, such as the trigger of apoptosis and necroptosis pathways through TNFR activation, NLRP3 assembly, Caspase 3 activity and complement cascade activation (Zhang et al., 2017). In addition, the increased resistance to oxidative stress, through the normalization of Nrf2 expression, can possibly reduce mitochondria damage and malfunction, such as alteration of the mitochondrial electron transport chain and unpaired oxidative phosphorylation, with consequent lower level of ATP synthesis that has been observed in different ALS models (Ravera et al., 2018, Pharaoh et al., 2019), and restore cellular homeostasis and ROS levels.

Indeed, in response to stress, Nrf2 was reported to modulate the expression of detoxifying enzymes and to regulate the transcription of genes involved in mitochondria biogenesis and proliferation (Hayashi et al., 2017). We can hypothesize that the environment surrounding MNs becomes less toxic upon exposure of astrocytes to MSC-derived exosomes because of the lower production and release of ROS. Interestingly, it has been reported that the overexpression of Nrf2 in astrocytes completely protects MNs from mutant SOD1 toxicity in co-cultures and delays disease onset in the $SOD1^{G93A}$ mouse model (Vargas et al., 2008). At the basis of the improvement of MN survival there was a decrease of the NO-dependent toxicity, mediated by Nrf2 activation, which enhance glutathione biosynthesis, inhibiting, in turn, p75NTR-dependent motor neuron apoptosis (Vargas et al., 2006).

The less toxic astrocyte phenotype can affect also other cellular type involved in ALS. For instance, the decreased release of CCL2 may reduce the recruitment of macrophages and M1 microglia in CNS and the activation of phosphatidylinositol-3 kinase/Akt and MAPK, contributing to alleviate pro-inflammatory response and gliosis (Kawaguchi-Niida et al., 2013). Further, the reduction of TNF-α and IL-1β expression, together with the increased expression of IL-10 in exosome-treated $SOD1^{G93A}$ astrocytes can lead to an overall improvement of CNS environment and determine a shift of M1 microglia to the rest state.

Thus, astrocytes might succeed in supporting MN viability directly, as in our experiments, by reducing the toxicity of the extracellular milieu, and indirectly, by ameliorated the noxious phenotype of microglia and of other cell types. Indeed, in future studies we plan to study in depth the influence of astrocytes on microglia of $SOD1^{G93A}$ mice. Whether the exosome-treated astrocyte conditioned medium is able to modulate the $SOD1^{G93A}$ microglia activation state and the evaluation of the soluble factors released by $SOD1^{G93A}$ astrocytes and regulated by exposure to MSC-derived exosomes will pave the way to these studies.

Astrocytes play a pivotal roles in maintaining BBB integrity through the establishment of tight junctions between endothelial cells. In ALS, it was reported a reduced expression of proteins involved in tight junction formation and the degeneration of astrocyte end-feet, leading to BBB disruption and red blood and immune cell extravasation (Sweeney et al., 2019). Garbuzova-Davis and Colleagues demonstrated that the transplantation of bone marrow MSCs in symptomatic $SOD1^{G93A}$ mice ameliorates the BBB structure and functions. These findings suggest that a rescue of astrocyte activation can contribute to BBB restoration, not only by directly stabilizing tight junctions but also reducing pro-inflammatory stimuli on pericytes and endothelial cells. Indeed, the excessive pericyte

migration, reported in ALS, was decreased following the reduction of NFκB activation (Lu et al., 2019; Garbuzova-Davis et al., 2018).

This evidence hypothesizes positive cross-talk between astrocytes and other cells of CNS and immune system, paving the way to further studies to better understand the essential role of astrocytes in ALS and how their modulation can affect the whole CNS environment.

In the attempt to identify the molecular determinants of the exosome effects, we identified nine up-regulated miRNAs in mouse MSCs after stimulation with IFN-γ. These miRNAs were also present in exosomes but only four were over-expressed, when compared to exosomes isolated from unstimulated MSCs. These four miRNAs can potentially inhibit the translation of several kinase proteins and transcriptional factors involved in NFκB and MAPK pathways, reducing inflammatory response activation. There is evidence in rodent models of spinal cord injury that administration of MSCs or MSC-derived exosomes ameliorates A1 astrocyte phenotype by reducing the expression of phospho-IκBα and, therefore, phospho-p65 translocation into the nucleus (Wang et al., 2018, Lu et al., 2019), supporting the relevance of our identified miRNAs in the modulation of NFκB pathway.

Another identified pathway is p38-ERK, that induces cell apoptosis and resulted altered in ALS (Bendotti et al., 2005). miR-466q, miR-467f and miR-466i-3p can affect the translation of several kinases involved in p38 phosphorylation, determining a lower activation of this pro-apoptotic pathway. Modulation of the p38 pathway was observed also in other models. For instance, increased phosphorylation of p38 and ERK was reported in chondrocytes exposed to IL-1β, that was reversed upon exposure to exosomes

derived from MSCs. The normalization of p38-ERK activation leads also to a reduction of apoptosis (Qi et al., 2018).

Identified targets of miR-466q, miR467f, miR-466m-5p and miR-466i-3p were validated by qPCR. The only significant modification of mRNA expression, upon transfection with single synthetic miRNA mimics, was detected for MAPK11, while the other targets were not significantly affected.

Notably, the strong reduction of MAPK11 is in accordance with the results obtained with exosome treatment. Indeed, MAPK11 phosphorylates ATF2 promoting the synthesis of TNF-α, which was the cytokine mostly affected by exosome treatment in our experiments. This finding strongly supports the modulation of MAPK11 expression by exosome treatment, granting that a direct inhibition of its synthesis can lead to a partial restoration of astrocyte-MN cross-talk , since TNF-α is one of the main neurotoxic factors released from astrocytes.

The phenotype characterization of $SOD1^{A4V}$ iAstrocytes derived from iNPCs did not show strong inflammatory activation compared to control iAstrocytes. However, exosome treatment determined a trend of reduction of p-p65 and NLRP3, specially, in patient 102 iAstrocytes. These results suggest the presence of a modulatory effect on inflammation, even if less substantial, also in human-derived astrocytes.

More consistent positive effects were detected in the anti-oxidative pathways, even if not significant, that deserve further analysis. Most important, in the human model represented by MN-iAstrocytes co-cultures, as seen in companion rodent experiments, we obtained an amelioration of MN viability, supporting the essential role of exosomes in counteract astrocyte toxicity. Thanks to a preliminary analysis of miRNAs contained in exosomes

from human MSCs, we identified miR-29b-3p as a possible mediator of the anti-oxidant effects and MN survival improvement (data not shown).

miR-29b-3p has been found down-regulated in several neurological disorders, including ALS, and the restoration of its levels promotes neuronal survival by down-regulating the expression of the pro-apoptotic proteins of the BH3-only family (Paladino et al., 2018; Klatt et al., 2019). Moreover, miR-29b-3p acts also on Nrf2 pathway by inhibiting the translation of BACH2, a negative competitor of Nrf2 for the ARE binding site, supporting its involvement in Nrf2 expression and regulation. Interestingly, it has been reported that Nrf2 is able to positively regulate miR-29b-3p expression, which can potentially determine an increase in neuronal survival (Paladino et al., 2018). Further studies are request to clarify which pathways are modified by exosome-shuttled miRNAs.

Thanks to the identification of the pathways affected by the miRNA cargo of exosomes, both in human and rodent exosomes from primed MSCs, it is possible to hypothesize the prospective of a treatment with selected miRNAs, through non-viral methods such as lipid-based or polymeric nanoparticle-based delivery systems or viral vectors such as adenovirus vectors and adeno-associated virus (AAV) vectors (Slotaand Booth, 2019). miRNA-based therapeutics have been proposed and largely studied to treat disorders such as cancer, heart diseases and diabetes (Rupaimoole et al., 2017). Currently, miRNA treatment are becoming a promising alternative to classical therapeutic approaches also in neurodegenerative diseases and neurological disorders

A treatment with artificial miR-124a oligonucleotides, that can normalize the increase in EAAT2 expression associated with decreased miR-124a expression, that is observed in mutant SOD1 murine spinal cords, has been already tested in ALS (Morel et al., 2013).

Two other studies reported that the administration of artificial miRNA against mutated SOD1 determined an extension of lifespan of SOD1-linked ALS animal models (Borel et al., 2018; Stoica et al., 2016), supporting not only the role of SOD1 in the disease pathogenesis but also that the administration of artificial miRNA through AAV9 viral vector technology to treat ALS is safe and effective, paving the way to the discovery of other possible targets for a multimodal therapeutic approach.

5.1 Conclusion

In the present work we established that exosomes derived from MSCs are one of the mediators of the therapeutic effect of MSCs, proving a comparable modulatory action on inflammation and oxidative stress. Their action is due also to the transport of miRNAs, that we demonstrated are helpful for the amelioration of astrocyte phenotype and MN survival. These results encourage the develop of MSC-derived exosome-based therapy or miRNA-based therapy, with a wide range of action on different features of ALS.

The administration of MSC-derived exosomes containing modulatory miRNAs instead of MSCs themselves presents some relevant advantages; first of all, the bypass of ethical issues and safety concerns related to fate and long persistence of replicating cells in the host, but also the removal of the high-cost burden of cell expansion for transplantation in patients. However, primary questions concerning the hypothesis of a possible exosome-based therapy are still unsolved: how exosomes can be produce on upscale following good manufacture practice conditions? How exosome-based products can be precisely defined and characterized for purity and exosome number? What are the pharmacodynamic and pharmacokinetic properties of exosomes?

The same questions are applicable also for miRNA-based therapy, although there are already studies on their safety after administration in *in-vivo* models.

In conclusion, to succeed in the design of an effectiveness and safe exosome based-therapy or miRNA-based therapy, it is firstly necessary to define the behaviour of these innovative therapeutic tools in the organism.

6. BIBLIOGRAPHY

Aizawa H, Sawada J, Hideyama T, Yamashita T, Katayama T, Hasebe N, Kimura T, Yahara O, Kwak S. TDP-43 pathology in sporadic ALS occurs inmotor neurons lacking the RNA editing enzyme ADAR2. Acta Neuropathol. 2010 Jul;120(1):75-84. doi: 10.1007/s00401-010-0678-x.

Ajmone-Cat MA, Onori A, Toselli C, Stronati E, Morlando M, Bozzoni I, Monni E, Kokaia Z, Lupo G, Minghetti L, Biagioni S, Cacci E. Increased FUS levels in astrocytes leads to astrocyte and microglia activation and neuronal death. Sci Rep. 2019 Mar 14;9(1):4572. doi: 10.1038/s41598-019-41040-4.

Alami NH, Smith RB, Carrasco MA, Williams LA, Winborn CS, Han SSW, Kiskinis E, Winborn B, Freibaum BD, Kanagaraj A, Clare AJ, Badders NM, Bilican B, Chaum E, Chandran S, Shaw CE, Eggan KC, Maniatis T, Taylor JP. Axonal transport of TDP-43 mRNA granules is impaired by ALS-causing mutations. Neuron. 2014 Feb 5;81(3):536-543. doi: 10.1016/j.neuron.2013.12.018.

Alami NH, Smith RB, Carrasco MA, Williams LA, Winborn CS, Han SSW, Kiskinis E, Winborn B, Freibaum BD, Kanagaraj A, Clare AJ, Badders NM, Bilican B, Chaum E, Chandran S, Shaw CE, Eggan KC, Maniatis T, Taylor JP. Axonal transport of TDP-43 mRNA granules is impaired by ALS-causing mutations. Neuron. 2014 Feb 5;81(3):536-543. doi: 10.1016/j.neuron.2013.12.018.

Alhazzani A, Rajagopalan P, Albarqi Z, Devaraj A, Mohamed MH, Al-Hakami A, Chandramoorthy HC. Mesenchymal Stem Cells (MSCs) Coculture Protects [Ca2+]i Orchestrated Oxidant Mediated Damage in Differentiated Neurons In Vitro. Cells. 2018 Dec 6;7(12). doi: 10.3390/cells7120250.

Allaoua H, Chaudieu I, Krieger C, Boksa P, Privat A, Quirion R. Alterations in spinal cord excitatory amino acid receptors in amyotrophic lateral sclerosis patients. Brain Res. 1992 May 1;579(1):169-72.

Allen SP, Hall B, Castelli LM, Francis L, Woof R, Siskos AP, Kouloura E, Gray E, Thompson AG, Talbot K, Higginbottom A, Myszczynska M, Allen CF, Stopford MJ, Hemingway J, Bauer CS, Webster CP, De Vos KJ, Turner MR, Keun HC, Hautbergue GM, Ferraiuolo L, Shaw PJ. Astrocyte adenosine deaminase loss increases motor neuron toxicity in amyotrophic lateral sclerosis. Brain. 2019 Mar 1;142(3):586-605. doi: 10.1093/brain/awy353.

Al-Saif A, Al-Mohanna F, Bohlega S. A mutation in sigma-1 receptor causes juvenile amyotrophic lateral sclerosis. Ann Neurol. 2011 Dec;70(6):913-9. doi: 10.1002/ana.22534.

Andersen PM. Amyotrophic lateral sclerosis associated with mutations in the Cu/Zn superoxide dismutase gene. Curr Neurol Neurosci Rep. 2006 Jan;6(1):37-46.

Arai T, Hasegawa M, Akiyama H, Ikeda K, Nonaka T, Mori H, Mann D, Tsuchiya K, Yoshida M, Hashizume Y, Oda T. TDP-43 is a component of ubiquitin-positive tau-negative inclusions in frontotemporal lobar degeneration and amyotrophic lateral sclerosis. Biochem. Biophys. Res. Commun. 351, 602–611. doi: 10.1016/j.bbrc.2006.10.093.

Arhzaouy K, Papadopoulos C, Schulze N, Pittman SK, Meyer H, Weihl CC. VCP maintains lysosomal homeostasis and TFEB activity in differentiated skeletal muscle. Autophagy. 2019 Jun;15(6):1082-1099. doi: 10.1080/15548627.2019.1569933.

Ash PE, Bieniek KF, Gendron TF, Caulfield T, Lin WL, Dejesus-Hernandez M, van Blitterswijk MM, Jansen-West K, Paul JW 3rd, Rademakers R, Boylan KB, Dickson DW, Petrucelli L. Unconventional translation of C9ORF72 GGGGCC expansion generates insoluble polypeptides specific to c9FTD/ALS. Neuron. 2013 Feb 20;77(4):639-46. doi: 10.1016/j.neuron.2013.02.004.

Ashkenazi A, Salvesen G. Regulated cell death: signaling and mechanisms. Annu Rev Cell Dev Biol. 2014;30:337-56. doi: 10.1146/annurev-cellbio-100913-013226.

Ayala YM, De Conti L, Avendaño-Vázquez SE, Dhir A, Romano M, D'ambrogio A, Tollervey J, Ule J, Baralle M, Buratti E, Baralle FE. TDP-43 regulates its mRNA levels through a negative feedback loop. EMBO J. 2011 Jan 19;30(2):277-88. doi: 10.1038/emboj.2010.310.

Bach1: Function, Regulation, and Involvement in Disease Oxid Med Cell Longev. 2018; 2018: 1347969. Published online 2018 Oct 2. doi: 10.1155/2018/1347969.

Bar-Peled O, O'Brien RJ, Morrison JH, Rothstein JD. Cultured motor neurons possess calcium-permeable AMPA/kainate receptors. Neuroreport. 1999 Mar 17;10(4):855-9.

Bartolome F, Esteras N, Martin-Requero A, Boutoleau-Bretonniere C, Vercelletto M, Gabelle A, Le Ber I, Honda T, Dinkova-Kostova AT, Hardy J, Carro E, Abramov AY. Pathogenic p62/SQSTM1 mutations impair energy metabolism through limitation of mitochondrial substrates. Sci Rep. 2017 May 10;7(1):1666. doi: 10.1038/s41598-017-01678-4.

Baskaran P, Shaw C, Guthrie S. TDP-43 causes neurotoxicity and cytoskeletal dysfunction in primary cortical neurons. PLoS One. 2018 May 22;13(5):e0196528. doi: 10.1371/journal.pone.0196528.

Basso M, Pozzi S, Tortarolo M, F, Bisighini C, Pasetto L,Spaltro G, Lidonnici D, Gensano F, Battaglia E, Bendotti C,Bonetto V. Mutant Copper-Zinc Superoxide Dismutase (SOD1) InducesProtein Secretion Pathway Alterations and Exosome Releasein Astrocytes. J BIOLCHEM. VOL. 288, NO. 22, pp. 15699–15711, May 31, 2013

Becker LA, Huang B, Bieri G, Ma R, Knowles DA, Jafar-Nejad P, Messing J, Kim HJ, Soriano A, Auburger G, Pulst SM, Taylor JP, Rigo F, Gitler AD. Therapeutic reduction of ataxin-2 extends lifespan and reduces pathology in TDP-43 mice. Nature. 2017 Apr 20;544(7650):367-371. doi: 10.1038/nature22038.

Beeldman E, van der Kooi AJ, de Visser M, van Maarle MC, van Ruissen F, Baas F. A Dutch family with autosomal recessively inherited lower motor neuron predominant motor neuron disease due to optineurin mutations. Amyotroph Lateral Scler Frontotemporal Degener. 2015;16(5-6):410-1. doi: 10.3109/21678421.2015.1066821.

Beers DR, Henkel JS, Xiao Q, Zhao W, Wang J, Yen AA, Siklos L, McKercher SR, Appel SH. Wild-type microglia extend survival in PU.1 knockout mice with familial amyotrophic lateral

sclerosis. Proc Natl Acad Sci U S A. 2006 Oct 24;103(43):16021-6. Doi:10.1073/pnas.0607423103.

Beers DR, Zhao W, Liao B, Kano O, Wang J, Huang A, Appel SH, Henkel JS. Neuroinflammation modulates distinct regional and temporal clinical responses in ALS mice. Brain Behav Immun. 2011 Jul;25(5):1025-35. doi: 10.1016/j.bbi.2010.12.008.

Beers DR, Zhao W, Wang J, Zhang X, Wen S, Neal D, Thonhoff JR, Alsuliman AS, Shpall EJ, Rezvani K, Appel SH. ALS patients' regulatory T lymphocytes are dysfunctional, and correlate with disease progression rate and severity. JCI Insight. 2017 Mar 9;2(5):e89530. doi: 10.1172/jci.insight.89530.

Bellezza I, Grottelli S, Costanzi E, Scarpelli P, Pigna E, Morozzi G, Mezzasoma L, Peirce MJ, Moresi V, Adamo S, Minelli A. Peroxynitrite Activates the NLRP3 Inflammasome Cascade in SOD1(G93A) Mouse Model of Amyotrophic Lateral Sclerosis. Mol Neurobiol. 2018 Mar;55(3):2350-2361. doi: 10.1007/s12035-017-0502-x.

Bendotti C, Bao Cutrona M, Cheroni C, Grignaschi G, Lo Coco D, Peviani M, Tortarolo M, Veglianese P, Zennaro E. Inter- and intracellular signaling in amyotrophic lateral sclerosis: role of p38 mitogen-activated protein kinase. Neurodegener Dis. 2005;2(3-4):128-34.

Benninger F, Glat MJ, Offen D, Steiner I. Glial fibrillary acidic protein as a marker of astrocytic activation in the cerebrospinal fluid of patients with amyotrophic lateral sclerosis. J Clin Neurosci. 2016 Apr;26:75-8. doi: 10.1016/j.jocn.2015.10.008.

Bentmann E, Neumann M, Tahirovic S, Rodde R, Dormann D, Haass C. Requirements for stress granule recruitment of fused insarcoma (FUS) and TAR DNA-binding protein of 43 kDa (TDP-43). J Biol Chem. 2012 Jun 29;287(27):23079-94. doi: 10.1074/jbc.M111.328757.

Bernard-Marissal N, Medard JJ, Azzedine H, Chrast R. Dysfunction inendoplasmic reticulum-mitochondria crosstalk underlies SIGMAR1 loss offunction mediated motor neuron degeneration. Brain. 2015 Apr;138(Pt 4):875-90. doi: 10.1093/brain/awv008.

Bilsland LG, Sahai E, Kelly G, Golding M, Greensmith L, Schiavo G. Deficits in axonal transport precede ALS symptoms in vivo. Proc Natl Acad Sci U S A. 2010 Nov 23;107(47):20523-8. doi: 10.1073/pnas.1006869107.

Blanquer M, Moraleda JM, Iniesta F, Gomez-Espuch J, Meca-Lallana J, Villaverde R, et al. Neurotrophic bone marrow cellular nests prevent spinal motoneuron degeneration in amyotrophic lateral sclerosis patients: a pilot safety study. Stem Cells. 2012;30(6):1277–1285. doi: 10.1002/stem.1080.

Boillée S, Yamanaka K, Lobsiger CS, Copeland NG, Jenkins NA, Kassiotis G, Kollias G, Cleveland DW. Onset and progression in inherited ALS determined by motor neurons and microglia Science. 2006 Jun 2;312(5778):1389-92. doi: 10.1126/science.1123511.

Bonafede R, Brandi J, Manfredi M, Scambi I, Schiaffino L, Merigo F, Turano E, Bonetti B, Marengo E, Cecconi D, Mariotti R. The Anti-Apoptotic Effect of ASC-Exosomes in an In

Vitro ALS Model and Their Proteomic Analysis. Cells. 2019 Sep 14;8(9). doi: 10.3390/cells8091087.

Bonafede R, Mariotti R. ALS Pathogenesis and Therapeutic Approaches: The Role of Mesenchymal Stem Cells and extracellular vsicles. Frontiers in Cell Neurosci 2017 | Volume 11 | Article 80

Bonafede R, Scambi I, Peroni D, Potrich V, Boschi F, Benati D, Bonetti B, Mariotti R. Exosome derived from murine adipose-derved stromal cells: neuroprotective effecr on in vitro model of amyotrophic lateral sclerosis. Exp cell Res.2016: 340, 150-158

Bonifacino T, Cattaneo L, Gallia E, Puliti A, Melone M, Provenzano F, Bossi S, Musante I, Usai C, Conti F, Bonanno G, Milanese M. In-vivo effects of knocking-down metabotropic glutamate receptor 5 in the SOD1G93A mouse model of amyotrophic lateral sclerosis. Neuropharmacology. 2017 Sep 1;123:433-445. doi: 10.1016/j.neuropharm.2017.06.020.

Bonifacino T, Musazzi L, Milanese M, Seguini M, Marte A, Gallia E, Cattaneo L, Onofri F, Popoli M, Bonanno G. Altered mechanisms underlying the abnormal glutamate release in amyotrophic lateral sclerosis at a pre-symptomatic stage of the disease. Neurobiol Dis. 2016 Nov;95:122-33. doi: 10.1016/j.nbd.2016.07.011.

Bonifacino T, Rebosio C, Provenzano F, Torazza C, Balbi M, Milanese M, Raiteri L, Usai C, Fedele E, Bonanno G. Enhanced Function and Overexpression of Metabotropic Glutamate Receptors 1 and 5 in the Spinal Cord of the SOD1G93A Mouse Model of Amyotrophic Lateral Sclerosis during Disease Progression. Int J Mol Sci. 2019 Sep 13;20(18). doi: 10.3390/ijms20184552.

Borel F, Gernoux G, Sun H, Stock R, Blackwood M, Brown RH Jr, Mueller C. Safe and effective superoxide dismutase 1 silencing using artificial microRNA in macaques. Sci Transl Med. 2018 Oct 31;10(465). doi: 10.1126/scitranslmed.aau6414.

Bozzoni V, Pansarasa O, Diamanti L, Nosari G, Cereda C, Ceroni M. Amyotrophic lateral sclerosis and environmental factors. Funct Neurol. 2016 Jan-Mar;31(1):7-19.

Brambilla L, Guidotti G, Martorana F, Iyer AM, Aronica E, Valori CF, Rossi D. Disruption of the astrocytic TNFR1-GDNF axis accelerates motor neuron degeneration and disease progression in amyotrophic lateral sclerosis. Hum Mol Genet. 2016 Jul 15;25(14):3080-3095. Doi: 10.1093/hmg/ddw161.

Brenner D, Yilmaz R, Müller K, Grehl T, Petri S, Meyer T, Grosskreutz J, Weydt P, Ruf W, Neuwirth C, Weber M, Pinto S, Claeys KG, Schrank B, Jordan B, Knehr A, Günther K, Hübers A, Zeller D, Kubisch C, Jablonka S, Sendtner M, Klopstock T, de Carvalho M, Sperfeld A, Borck G, Volk AE, Dorst J, Weis J, Otto M, Schuster J, Del Tredici K, Braak H, Danzer KM, Freischmidt A, Meitinger T, Strom TM, Ludolph AC, Andersen PM, Weishaupt JH; German ALS network MND-NET. Hot-spot KIF5A mutations cause familial ALS. Brain. 2018 Mar 1;141(3):688-697. doi: 10.1093/brain/awx370.

Bristol LA, Rothstein JD. Glutamate transporter gene expression in amyotrophic lateral sclerosis motor cortex. Ann Neurol. 1996 May;39(5):676-9.

Brown HA, Murphy RC. Working towards an exegesis for lipids in biology. Nat Chem Biol. 2009 Sep;5(9):602-6. doi: 10.1038/nchembio0909-602.

Brown RH Jr. Amyotrophic lateral sclerosis: recent insights from genetics and transgenic mice. Cell. 1995 Mar 10;80(5):687-92.

Bruijn LI, Becher MW, Lee MK, Anderson KL, Jenkins NA, Copeland NG, Sisodia SS, Rothstein JD, Borchelt DR, Price DL, Cleveland DW. ALS-linked SOD1 mutant G85R mediates damage to astrocytes and promotes rapidly progressive disease with SOD1-containing inclusions Neuron. 1997 Feb;18(2):327-38. doi: 10.1016/s0896-6273(00)80272-x.

Budini M, Buratti E, Morselli E, Criollo A. Autophagy and its impact on neurodegenerative diseases: new roles for TDP-43 and C9orf72. Front Mol Neurosci. 2017 May 30;10:170. doi: 10.3389/fnmol.2017.00170.

Budoni M, Fierabracci A, Luciano R, Petrini S, Di Ciommo V, Muraca M. The Immunosuppressive Effect of Mesenchymal Stromal Cells on B Lymphocytes is Mediated by Membrane Vesicles. Cell Transplant. 2013;22(2):369-79. doi: 10.3727/096368911X582769.

Buratti E and Baralle FE. Characterization and functional implications of the RNA binding properties of nuclear factor TDP-43, a novel splicing regulator of CFTR exon 9. J. Biol. Chem. 276, 36337–36343. doi: 10.1074/jbc.M104236200.

Buratti E. Chapter one–functional significance of TDP-43 mutations in disease. Adv Genet. 2015;91:1-53. doi: 10.1016/bs.adgen.2015.07.001.

Bursch F, Kalmbach N, Naujock M, Staege S, Eggenschwiler R, Abo-Rady M, Japtok J, Guo W, Hensel N, Reinhardt P, Boeckers TM, Cantz T, Sterneckert J, Van Den Bosch L, Hermann A, Petri S, Wegner F. Altered calcium dynamics and glutamate receptor properties in iPSC-derived motor neurons from ALS patients with C9orf72, FUS, SOD1 or TDP43 mutations. Hum Mol Genet. 2019 Sep 1;28(17):2835-2850. doi: 10.1093/hmg/ddz107.

Carriedo SG, Sensi SL, Yin HZ, Weiss JH. AMPA exposures induce mitochondrial Ca2+ overload and ROS generation in spinal motor neurons in-vitro. J Neurosci. 2000 Jan 1;20(1):240-50.

Carriedo SG, Yin HZ, Weiss JH. Motor neurons are selectively vulnerable to AMPA/kainate receptor-mediated injury in vitro. J Neurosci. 1996 Jul 1;16(13):4069-79.

Cereda C, Leoni E, Milani P, Pansarasa O, Mazzini G, Guareschi S, Alvisi E, Ghiroldi A, Diamanti L, Bernuzzi S, Ceroni M, Cova E. Altered intracellular localization of SOD1 in leukocytes from patients with sporadic amyotrophic lateral sclerosis. PLoS One. 2013 Oct 14;8(10):e75916. doi: 10.1371/journal.pone.0075916.

Chan DC. Fusion and fission: interlinked processes critical formitochondrial health. Annu Rev Genet. 2012;46:265-87. doi: 10.1146/annurev-genet-110410-132529.

Chang YJ, Jeng US, Chiang YL, Hwang IS, Chen YR. The glycine-alanine dipeptide repeat from C9orf72 Hexanucleotide expansions forms toxic amyloids possessing cell-to-cell transmission properties. J Biol Chem. 2016 Mar 4;291(10):4903-11. doi: 10.1074/jbc.M115.694273.

Chen H, Kankel MW, Su SC, Han SWS, Ofengeim D. Exploring the genetics and non-cell autonomous mechanisms underlying ALS/FTLD. Cell Death Differ. 2018 Mar;25(4):648-662. doi: 10.1038/s41418-018-0060-4.

Chen L, Xue L, Zheng J, Tian X, Zhang Y, Tong Q. PPARß/δ agonist alleviates NLRP3 inflammasome-mediated neuroinflammation in the MPTP mouse model of Parkinson's disease. Behav Brain Res. 2019 Jan 1;356:483-489. doi: 10.1016/j.bbr.2018.06.005.Op

Chiarotto GB, Nardo G, Trolese MC, França MC Jr, Bendotti C, Rodrigues de Oliveira AL. The Emerging Role of the Major Histocompatibility Complex Class I in Amyotrophic Lateral Sclerosis. Int J Mol Sci. 2017 Nov 1;18(11). doi: 10.3390/ijms18112298.

Chiò A, Benzi G, Dossena M, Mutani R, Mora G. Severely increased risk of amyotrophic lateral sclerosis among Italian professional football players. Brain. 2005 Mar;128(Pt 3):472-6.

Chio A, Calvo A, Dossena M, Ghiglione P, Mutani R, Mora G.ALS in Italian professional soccer players: the risk is still present and could be soccer-specific. Amyotroph Lateral Scler. 2009 Aug;10(4):205-9. doi: 10.1080/17482960902721634.

Chung MJ, Suh YL. Ultrastructural changes of mitochondria in the skeletal muscle of patients with amyotrophic lateral sclerosis. Ultrastruct Pathol. 2002 Jan-Feb;26(1):3-7.

Ciervo Y, Ning K, Jun X, Shaw PJ, Mead RJ. Advances, challenges and future directions for stem cell therapy in amyotrophic lateral sclerosis. Mol Neurodegener. 2017 Nov 13;12(1):85. doi: 10.1186/s13024-017-0227-3.

Cirulli ET, Lasseigne BN, Petrovski S, Sapp PC, Dion PA, Leblond CS, Couthouis J, Lu YF, Wang Q, Krueger BJ, et al. Exome sequencing in amyotrophic lateral sclerosis identifies risk genes and pathways. Science. 2015;347(6229):1436–41.

Ciura S, Lattante S, Le Ber I, Latouche M, Tostivint H, Brice A, Kabashi E. Loss of function of C9orf72 causes motor deficits in a zebrafish model of amyotrophic lateral sclerosis. Ann Neurol. 2013 Aug;74(2):180-7. doi: 10.1002/ana.23946.

Clausen TH, Lamark T, Isakson P, Finley K, Larsen KB, Brech A, Øvervatn A, Stenmark H, Bjørkøy G, Simonsen A, Johansen T. p62/SQSTM1 and ALFY interact to facilitate the formation of p62 bodies/ALIS and their degradation by autophagy. Autophagy. 2010 Apr;6(3):330-44.

Clement AM, Nguyen MD, Roberts EA, Garcia ML, Boillée S, Rule M, McMahon AP, Doucette W, Siwek D, Ferrante RJ, Brown RH Jr, Julien JP, Goldstein LS, Cleveland DW. Wild-type nonneuronal cells extend survival of SOD1 mutant motor neurons in ALS mice. Science. 2003 Oct 3;302(5642):113-7. Erratum in: Science. 2003 Oct 24;302(5645):568.

Cohen TJ. An acetylation switch controls TDP-43 function and aggregationpropensity. Nat Commun. 2015 Jan 5;6:5845. doi: 10.1038/ncomms6845.

Cooper-Knock J, Walsh MJ, Higginbottom A, Robin Highley J, Dickman MJ, Edbauer D, Ince PG, Wharton SB, Wilson SA, Kirby J, Hautbergue GM, Shaw PJ. Sequestration of multiple RNA

recognition motifcontaining proteins by C9orf72 repeat expansions. Brain. 2014 Jul;137(Pt 7):2040-51. doi: 10.1093/brain/awu120.

Corcia P, Danel V, Lacour A, Beltran S, Andres C, Couratier P, Blasco H, Vourc'h P.A novel mutation of the C-terminal amino acid of FUS (Y526C) strengthens FUS gene as the most frequent genetic factor in aggressive juvenile ALS. Amyotroph Lateral Scler Frontotemporal Degener. 2017 May;18(3-4):298-301. doi: 10.1080/21678421.2016.1265564.

Cox PA, Kostrzewa RM, Guillemin GJ. BMAA and Neurodegenerative Illness. Neurotox Res. 2018 Jan;33(1):178-183. doi: 10.1007/s12640-017-9753-6.

Croese T, FurlanR. Extracellular vesicles in neurodegenerative diseases. Molecular Aspects of Medicine 60 (2018) 52e61

Crugnola V, Lamperti C, Lucchini V, Ronchi D, Peverelli L, Prelle A, Sciacco M, Bordoni A, Fassone E, Fortunato F, Corti S, Silani V, Bresolin N, Di Mauro S, Comi GP, Moggio M. Mitochondrial respiratory chain dysfunction in muscle from patients with amyotrophic lateral sclerosis. Arch Neurol. 2010 Jul;67(7):849-54. doi: 10.1001/archneurol.2010.128.

Cudkowicz ME, Titus S, Kearney M, Yu H, Sherman A, Schoenfeld D, Hayden D, Shui A, Brooks B, Conwit R, Felsenstein D, Greenblatt DJ, Keroack M, Kissel JT, Miller R, Rosenfeld J, Rothstein JD, Simpson E, Tolkoff-Rubin N, Zinman L, Shefner JM; Ceftriaxone Study Investigators. Safety and efficacy of ceftriaxone for amyotrophic lateral sclerosis: a multi-stage, randomised, double-blind, placebo-controlled trial. Lancet Neurol. 2014 Nov;13(11):1083-1091. doi: 10.1016/S1474-4422(14)70222-4.

Damiano M, Starkov AA, Petri S, Kipiani K, Kiaei M, Mattiazzi M, Flint Beal M, Manfredi G. Neural mitochondrial Ca2+ capacity impairment precedesthe onset of motor symptoms in G93A Cu/Zn-superoxide dismutase mutantmice. J Neurochem. 2006 Mar;96(5):1349-61.

Davis BK, Wen H, Ting JP. The inflammasome NLRs in immunity, inflammation, and associated diseases. Annu Rev Immunol. 2011;29:707-35. doi: 10.1146/annurev-immunol-031210-101405.

de Majo M, Topp SD, Smith BN, Nishimura AL, Chen HJ, Gkazi AS, Miller J, Wong CH, Vance C, Baas F, Ten Asbroek ALMA, Kenna KP, Ticozzi N, Redondo AG, Esteban-Pérez J, Tiloca C, Verde F, Duga S, Morrison KE, Shaw PJ, Kirby J, Turner MR, Talbot K, Hardiman O, Glass JD, de Belleroche J, Gellera C, Ratti A, Al-Chalabi A, Brown RH, Silani V, Landers JE, Shaw CE. ALS-associated missense and nonsense TBK1 mutations can both cause loss of kinase function. Neurobiol Aging. 2018 Nov;71:266.e1-266.e10. doi: 10.1016/j.neurobiolaging.2018.06.015.

De Marco N, Buono M, Troise F, Diez-Roux G. Optineurin increases cell survival and translocates to the nucleus in a Rab8-dependent manner upon an apoptotic stimulus. J Biol Chem. 2006 Jun 9;281(23):16147-56.

De Vos KJ and Hafezparast M. Neurobiology of axonal tran sport defects in motor neuron disease: Opportunities for translational research? Neurobiol Dis. 2017 Sep;105:283-299. doi: 10.1016/j.nbd.2017.02.004.

De Vos KJ, Chapman AL, Tennant ME, Manser C, Tudor EL, Lau KF, Brownlees J, Ackerley S, Shaw PJ, McLoughlin DM, Shaw CE, Leigh PN, Miller CCJ, Grierson AJ. Familial amyotrophic lateral sclerosis-linkedSOD1 mutants perturb fast axonal transport to reduce axonal mitochondria content. Hum Mol Genet. 2007 Nov 15;16(22):2720-2728. doi: 10.1093/hmg/ddm226.

DeJesus-Hernandez M, Mackenzie IR, Boeve BF, Boxer AL, Baker M, Rutherford NJ, Nicholson AM, Finch NA, Flynn H, Adamson J, Kouri N, Wojtas A, Sengdy P, Hsiung GY, Karydas A, Seeley WW, Josephs KA, Coppola G, Geschwind DH, Wszolek ZK, Feldman H, Knopman DS, Petersen RC, Miller BL, Dickson DW, Boylan KB, Graff-Radford NR, Rademakers R. Expanded GGGGCC hexanucleotide repeat in noncoding region of C9ORF72 causes chromosome 9p-linked FTD and ALS. Neuron. 2011 Oct 20;72(2):245-56. doi: 10.1016/j.neuron.2011.09.011.

Del Fattore A, Luciano R, Pascucci L, Goffredo BM, Giorda E, Scapaticci M, Fierabracci A, Muraca M. Immunoregulatory Effects of Mesenchymal Stem Cell-Derived Extracellular Vesicles on T Lymphocytes. Cell Transplant. 2015;24(12):2615-27. doi: 10.3727/096368915X687543.

Deng HX, et al. (2011) Mutations in UBQLN2 cause dominant X-linked juvenile and adult-onset ALS and ALS/dementia. Nature 477:211–215.

Deng J, Yang M, Chen Y, Chen X, Liu J, Sun S, Cheng H, Li Y, Bigio EH, Mesulam M, Xu Q, Du S, Fushimi K, Zhu L, Wu JY. FUS interacts with HSP60 to promote mitochondrial damage. PLoS Genet. 2015 Sep 3;11(9):e1005357. doi: 10.1371/journal.pgen.1005357.

Dewil M, dela Cruz VF, Van Den Bosch L, Robberecht W. Inhibition of p38 mitogen activated protein kinase activation and mutant SOD1(G93A)-induced motor neuron death. Neurobiol Dis. 2007 May;26(2):332-41. doi: 10.1016/j.nbd.2006.12.023.

Donnelly CJ, Zhang PW, Pham JT, et al. RNA toxicity from the ALS/FTD C9ORF72 expansion is mitigated by antisense intervention. Neuron. 2013 Oct 16;80(2):415-28. doi: 10.1016/j.neuron.2013.10.015.

Donnelly CJ, Zhang PW, Pham JT, Haeusler AR, Mistry NA, Vidensky S, Daley EL, Poth EM, Hoover B, Fines DM, Maragakis N, Tienari PJ, Petrucelli L, Traynor BJ, Wang J, Rigo F, Bennett CF, Blackshaw S, Sattler R, Rothstein JD. RNA toxicity from the ALS/FTD C9ORF72 expansion is mitigated by antisense intervention. Neuron. 2013 Oct 16;80(2):415-28. doi: 10.1016/j.neuron.2013.10.015.

Duan W, Guo M, Yi L, Zhang J, Bi Y, Liu Y, Li Y, Li Z, Ma Y, Zhang G, Liu Y, Song X, Li C. Deletion of Tbk1 disrupts autophagy and reproduces behavioral and locomotor symptoms of FTD-ALS in mice. Aging (Albany NY) 2019 Apr 30; 11(8): 2457–2476. doi: 10.18632/aging.101936.

Echaniz-Laguna A, Zoll J, Ponsot E, N'guessan B, Tranchant C, Loeffler JP, Lampert E. Muscular mitochondrial function in amyotrophic lateral sclerosis is progressively altered as the disease develops: a temporal study in man. Exp Neurol. 2006 Mar;198(1):25-30.

Ederle H and Dormann D. TDP-43 and FUS en route from the nucleus to the cytoplasm. FEBS Lett. 2017 Jun;591(11):1489-1507. doi: 10.1002/1873-3468.12646.

Endo F, Komine O, Fujimori-Tonou N, Katsuno M, Jin S, Watanabe S, Sobue G, Dezawa M, Wyss-Coray T, Yamanaka K. Astrocyte-Derived TGF-b1 Accelerates Disease Progression in ALS Mice by Interfering with the Neuroprotective Functions of Microglia and T Cells. Cell Rep. 2015 Apr 28;11(4):592-604. doi: 10.1016/j.celrep.2015.03.053.

Engl E and Attwell D. Non-signalling energy use in the brain. J Physiol. 2015 Aug 15;593(16):3417-29. doi: 10.1113/jphysiol.2014.282517.

Ezzi SA, Urushitani M, Julien JP. Wild-type superoxide dismutase acquires binding and toxic properties of ALS-linked mutant forms through oxidation. J Neurochem. 2007 Jul;102(1):170-8.

Farina C, Aloisi F, Meinl E. Astrocytes are active players in cerebral innate immunity. Trends Immunol. 2007 Mar;28(3):138-45.

Ferber EC, Peck B, Delpuech O, Bell GP, East P, Schulze A. FOXO3a regulates reactive oxygen metabolism by inhibitingmitochondrial gene expression. Cell Death Differ. 2012 Jun;19(6):968-79. doi: 10.1038/cdd.2011.179.

Ferguson SW & Nguyen J. Exosomes as therapeutics: The implications of molecular composition and exosomal heterogeneity. J Control Release. 2016 Apr 28;228:179-190. doi: 10.1016/j.jconrel.2016.02.037.

Ferguson SW, Wang J, Lee CJ, Liu M, Neelamegham S, Canty JM, Nguyen J. The microRNA regulatory landscape of MSC-derived exosomes: a systems view. Sci Rep. 2018 Jan 23;8(1):1419. doi: 10.1038/s41598-018-19581-x.

Ferraiuolo L, Meyer K, Sherwood TW, Vick J, Likhite S, Frakes A, Miranda CJ, Braun L, Heath PR, Pineda R, Beattie CE, Shaw PJ, Askwith CC, McTigue D, Kaspar BK. Oligodendrocytes contribute to motor neuron death in ALS via SOD1-dependent mechanism. Proc Natl Acad Sci U S A. 2016 Oct 18;113(42):E6496-E6505. doi: 10.1073/pnas.1607496113.

Ferri A, Cozzolino M, Crosio C, Nencini M, Casciati A, Gralla EB, Rotilio G, Valentine JS, Carrì MT. Familial ALS-superoxide dismutases associate withmitochondria and shift their redox potentials. Proc Natl Acad Sci U S A. 2006 Sep 12;103(37):13860-5.

Finelli MJ, Liu KX, Wu Y, Oliver PL, Davies KE. Oxr1 improves pathogeniccellular features of ALS-associated FUS and TDP-43 mutations. Hum Mol Genet. 2015 Jun 15;24(12):3529-44. doi: 10.1093/hmg/ddv104.

Forsberg K, Andersen PM, Marklund SL, Brännström T.Glial nuclear aggregates of superoxide dismutase-1 are regularly present in patients with amyotrophic lateral sclerosis. Acta Neuropathol. 2011 May;121(5):623-34. doi: 10.1007/s00401-011-0805-3.

Frakes AE, Ferraiuolo L, Haidet-Phillips AM, Schmelzer L, Braun L, Miranda CJ, Ladner KJ, Bevan AK, Foust KD, Godbout JP, Popovich PG, Guttridge DC, Kaspar BK. Microglia induce

motor neuron death via the classical NF-κB pathway in amyotrophic lateral sclerosis. Neuron. 2014 Mar 5;81(5):1009-1023. doi: 10.1016/j.neuron.2014.01.013.

Fratta P, Mizielinska S, Nicoll AJ, Zloh M, Fisher EM, Parkinson G, Isaacs AM. C9orf72 hexanucleotide repeat associated with amyotrophic lateral sclerosis and frontotemporal dementia forms RNA G-quadruplexes. Sci Rep. 2012;2:1016. doi: 10.1038/srep01016.

Freibaum BD, Chitta RK, High AA, Taylor JP. Global analysis of TDP-43 interacting proteins reveals strong association with RNA splicing and translation machinery. J Proteome Res. 2010 Feb 5;9(2):1104-20. doi: 10.1021/pr901076y.

Freischmidt A, Wieland T, Richter B, Ruf W, Schaeffer V, Muller K, Marroquin N, Nordin F, Hubers A, Weydt P, et al. Haploinsufficiency of TBK1 causes familial ALS and fronto-temporal dementia. Nat Neurosci. 2015;18(5):631–6.

Frick P, Sellier C, Mackenzie IRA, Cheng CY, Tahraoui-Bories J, Martinat C, Pasterkamp RJ, Prudlo J, Edbauer D, Oulad-Abdelghani M, Feederle R, Charlet-Berguerand N, Neumann M. Novel antibodies reveal presynaptic localization of C9orf72 protein and reduced protein levels in C9orf72 mutation carriers. Acta Neuropathol Commun. 2018 Aug 3;6(1):72. doi: 10.1186/s40478-018-0579-0.

Fucile S. Ca2+ permeability of nicotinic acetylcholine receptors. Cell Calcium. 2004 Jan;35(1):1-8.

Gagliardi S, Abel K, Bianchi M, Milani P, Bernuzzi S, Corato M, Ceroni M, Cashman JR, Cereda C. Regulation of FMO and PON detoxication systems in ALS human tissues. Neurotox Res. 2013 May;23(4):370-7. doi: 10.1007/s12640-012-9356-1.

Gao FB, Almeida S, Lopez-Gonzalez R. Dysregulated molecular pathways in amyotrophic lateral sclerosis-frontotemporal dementia spectrum disorder. EMBO J. 2017 Oct 16;36(20):2931-2950. doi: 10.15252/embj.201797568.

Garbuzova-Davis S, Haller E, Navarro S, Besong TE, Boccio KJ, Hailu S, Khatib M, Sanberg PR, Appel SH, Borlongan CV. Transplantation of human bone marrow stem cells into symptomatic ALS mice enhances structural and functional blood-spinal cord barrier repair. Exp Neurol. 2018 Dec;310:33-47. doi: 10.1016/j.expneurol.2018.08.012.

Gegelashvili G, Danbolt NC, Schousboe A. Neuronal soluble factors differentially regulate the expression of the GLT1 and GLAST glutamate transporters in cultured astroglia. J Neurochem. 1997 Dec;69(6):2612-5.

Ghosh S, Karin M. Missing pieces in the NF-kappaB puzzle. Cell. 2002 Apr;109 Suppl:S81-96.

Gibbs KL, Kalmar B, Rhymes ER, Fellows AD, Ahmed M, Whiting P, Davies CH, Greensmith L, Schiavo G. Inhibiting p38 MAPK alpha rescues axonal retrograde transport defects in a mouse model of ALS. Cell Death Dis. 2018 May 22;9(6):596. doi: 10.1038/s41419-018-0624-8.

Gijselinck I, Van Mossevelde S, van der Zee J, Sieben A, Engelborghs S, De Bleecker J, Ivanoiu A, Deryck O, Edbauer D, Zhang M, Heeman B, Bäumer V, Van den Broeck M, Mattheijssens M, Peeters K, Rogaeva E, De Jonghe P, Cras P, Martin JJ, de Deyn PP, Cruts M, Van Broeckhoven C. The C9orf72 repeat size correlates with onset age of disease, DNA

methylation and transcriptional downregulation of the promoter. Mol Psychiatry. 2016 Aug;21(8):1112-24. doi: 10.1038/mp.2015.159.

Giribaldi F, Milanese M, Bonifacino T, Anna Rossi PI, Di Prisco S, Pittaluga A, Tacchetti C, Puliti A, Usai C, Bonanno G. Group I metabotropic glutamate autoreceptors induce abnormal glutamate exocytosis in a mouse model of amyotrophic lateral sclerosis. Neuropharmacology. 2013 Mar;66:253-63. doi: 10.1016/j.neuropharm.2012.05.018.

Goldman RD, Khuon S, Chou Y, Opal P, Steinert P. The function of intermediate filaments in cell shape and cytoskeletal integrity. J Cell Biol. 1996 Aug;134(4):971-83. doi:10.1083/jcb.134.4.971.

Gomes C, Cunha C, Nascimento F, Ribeiro JA, Vaz AR, Brites D. Cortical Neurotoxic Astrocytes with Early ALS Pathology and miR-146a Deficit Replicate Gliosis Markers of Symptomatic SOD1G93A Mouse Model. Mol Neurobiol. 2019 Mar;56(3):2137-2158. doi: 10.1007/s12035-018-1220-8.

Gorshkov K, Aguisanda F, Thorne N, Zheng W. Astrocytes as targets for drug discovery. Drug Discov Today. 2018 Mar;23(3):673-680. doi: 10.1016/j.drudis.2018.01.011.

Gruzman A, Wood WL, Alpert E, Prasad MD, Miller RG, Rothstein JD, Bowser R, Hamilton R, Wood TD, Cleveland DW, Lingappa VR, Liu J. Common molecular signature in SOD1 for both sporadic and familial amyotrophic lateral sclerosis. Proc Natl Acad Sci U S A. 2007 Jul 24;104(30):12524-9.

Gugliandolo A, Giacoppo S, Bramanti P, Mazzon E. NLRP3 Inflammasome Activation in a Transgenic Amyotrophic Lateral Sclerosis Model. Inflammation. 2018 Feb;41(1):93-103. doi: 10.1007/s10753-017-0667-5.

Guo W, Naujock M, Fumagalli L, Vandoorne T, Baatsen P, Boon R, Ordovás L, Patel A, Welters M, Vanwelden T, Geens N, Tricot T, Benoy V, Steyaert J, Lefebvre-Omar C, Boesmans W, Jarpe M, Sterneckert J, Wegner F, Petri S, Bohl D, Vanden Berghe P, Robberecht W, Van Damme P, Verfaillie C, Van Den Bosch L. HDAC6 inhibition reverses axonal tran sport defects in motor neurons derived from FUS-ALS patients. Nat Commun. 2017 Oct 11;8(1):861. doi: 10.1038/s41467-017-00911-y.

Gurney ME, Pu H, Chiu AY, Dal Canto MC, Polchow CY, Alexander DD, Caliendo J, Hentati A, Kwon YW, Deng HX, et al. Motor neuron degeneration in mice that express a human Cu,Zn superoxide dismutase mutation. Science. 1994 Jun 17;264(5166):1772-5. doi: 10.1126/science.8209258.

Haeusler AR, Donnelly CJ, Periz G, Simko EA, Shaw PG, Kim MS, Maragakis NJ, Troncoso JC, Pandey A, Sattler R, Rothstein JD, Wang J. C9orf72 nucleotide repeat structures initiate molecular cascades of disease. Nature. 2014 Mar 13;507(7491):195-200. doi: 10.1038/nature13124.

Haidet-Phillips AM, Hester ME, Miranda CJ, Meyer K, Braun L, Frakes A, Song S, Likhite S, Murtha MJ, Foust KD, Rao M, Eagle A, Kammesheidt A, Christensen A, Mendell JR,

Burghes AH, Kaspar BK. Astrocytes fromfamilial and sporadic ALS patients are toxic to motor neurons. Nat Biotechnol. 2011 Aug 10;29(9):824-8. doi: 10.1038/nbt.1957.

Hall CE, Yao Z, Choi M, Tyzack GE, Serio A, Luisier R, Harley J, Preza E, Arber C, Crisp SJ, Watson PMD, Kullmann DM, Abramov AY, Wray S, Burley R, Loh SHY, Martins LM, Stevens MM, Luscombe NM, Sibley CR, Lakatos A, Ule J, Gandhi S, Patani R. Progressive Motor Neuron Pathology and the Role of Astrocytes in a Human Stem Cell Model of VCP-Related ALS. Cell Rep. 2017 May 30;19(9):1739-1749. doi: 10.1016/j.celrep.2017.05.024.

Halliwell B, Gutteridge JMC. Oxygen toxicity, oxygen radicals, transition metals and disease. Biochem J. 1984 Apr 1;219(1):1-14.

Halliwell B. Biochemistry of oxidative stress. Biochem. Soc. Trans. 2007, 35, 1147–1150.

Halliwell B. Reactive Species and Antioxidants. Redox Biology Is a Fundamental Theme of Aerobic Life. Plant Physiol. 2006, 141, 312–322.

Hammond TR, Robinton D, Stevens B. Microglia and the Brain: Complementary Partners in Development and Disease. Annu Rev Cell Dev Biol. 2018 Oct 6;34:523-544. doi: 10.1146/annurev-cellbio-100616-060509.

Han C, Zhang L, Song L, Liu Y, Zou W, Piao H, Liu J. Human adipose-derived mesenchymal stem cells: a better cell source for nervous system regeneration. Chin Med J (Engl). 2014;127(2):329-37.

Hardiman O and van den Berg LH. Edaravone: a new treatment for ALS on the horizon? Lancet Neurol. 2017 Jul;16(7):490-491. doi: 10.1016/S1474-4422(17)30163-1.

Hayashi G, Jasoliya M, Sahdeo S, Saccà F, Pane C, Filla A, Marsili A, Puorro G, Lanzillo R, Brescia Morra V, Cortopassi G. Dimethyl fumarate mediates Nrf2-dependent mitochondrial biogenesis in mice and humans. Hum Mol Genet. 2017 Aug 1;26(15):2864-2873. doi: 10.1093/hmg/ddx167.

He Y, Hara H, Núñez G. 2016. Mechanism and Regulation of NLRP3 Inflammasome Activation. Trends Biochem Sci. 2016 Dec;41(12):1012-1021. doi: 10.1016/j.tibs.2016.09.002.

Heather L. Wilson, Sheila E. Francis, Steven K. Dower and David C. Crossman. Secretion of Intracellular IL-1 Receptor Antagonist (Type 1) Is Dependent on P2X7 Receptor Activation. J Immunol. 2004 Jul 15;173(2):1202-8. doi: 10.4049/jimmunol.173.2.1202.

Hermann GE, Rogers RC, Bresnahan JC, BeattieMS. Tumor necrosis factor-alpha induces cFOS and strongly potentiates glutamate-mediated cell death in the rat spinal cord. Neurobiol Dis. 2001 Aug;8(4):590-9. doi:10.1006/nbdi.2001.0414

Herx LM and Yong VW. Interleukin-1bis required for the early evolution of reactive astrogliosis following CNS lesion. J Neuropathol Exp Neurol. 2001 Oct;60(10):961-71.

Hiji M, Takahashi T, Fukuba H, Yamashita H, Kohriyama T, Matsumoto M. White matter lesions in the brain with frontotemporal lobar degeneration with motor neuron disease: TDP-43-

immunopositive inclusions co-localize with p62, but not ubiquitin. Acta Neuropathol. 2008 Aug;116(2):183-91. doi: 10.1007/s00401-008-0402-2.

Hirano A, Donnenfeld H, Sasaki S, Nakano I. Fine structural observations of neurofilamentous changes in amyotrophic lateral sclerosis. J. Neuropathol. J Neuropathol Exp Neurol. 1984a Sep;43(5):461-70.

Hirano A, Nakano I, Kurland LT, Mulder DW, Holley PW, Saccomanno G. Fine structural study of neurofibrillary changes in a family with amyotrophic lateral sclerosis. J Neuropathol Exp Neurol. 1984b Sep;43(5):471-80.Corbo, M., Hays, A.P., 1992. Peripherin and neurofilament protein coexist in spinal spheroids of motor neuron disease. J. Neuropathol. Exp. Neurol. 51, 531–537.

Hirokawa N, Noda Y, Tanaka Y, Niwa S. Kinesin superfamily motor proteins and intracellular transport. Nat Rev Mol Cell Biol 2009; 10: 682–96.

Hjerpe R, Bett JS, Keuss MJ, Solovyova A, McWilliams TG, Johnson C, Sahu I, Varghese J, Wood N, Wightman M, Osborne G, Bates GP, Glickman MH, Trost M, Knebel A, Marchesi F, Kurz T. UBQLN2 mediates autophagy-independent protein aggregate clearance by the proteasome. Cell. 2016 Aug 11;166(4):935-949. doi: 10.1016/j.cell.2016.07.001.

Hoitzing H, Johnston IG, Jones NS. What is the function of mitochondrial networks? A theoretical assessment of hypotheses and proposal for future research. Bioessays. 2015 Jun;37(6):687-700. doi: 10.1002/bies.201400188.

Holden, C. Astrocytes secrete substance that kills motor neurons in ALS. Science. 2007 Apr 20;316(5823):353. doi:10.1126/science.316.5823.353a

Hosler BA, Siddique T, Sapp PC, Sailor W, Huang MC, Hossain A, Daube JR, Nance M, Fan C, Kaplan J, Hung WY, McKenna-Yasek D, Haines JL, Pericak-Vance MA, Horvitz HR, Brown RH Jr. Linkage of familial amyotrophic lateral sclerosis with frontotemporal dementia to chromosome 9q21-q22. JAMA. 2000 Oct 4; 284(13):1664-9. doi: 10.1001/jama.284.13.1664.

Houi K, Kobayashi T, Kato S, Mochio S, Inoue K. Increased plasma TGF-beta1 in patients with amyotrophic lateral sclerosis. Acta Neurol Scand. 2002 Nov;106(5):299-301. doi: 10.1034/j.1600-0404.2002.01301.x.

Hu Y, Cao C, Qin XY, Yu Y, Yuan J, Zhao Y, Cheng Y. Increased peripheral blood inflammatory cytokine levels in amyotrophic lateral sclerosis: a meta-analysis study. Sci Rep. 2017 Aug 22;7(1):9094. doi: 10.1038/s41598-017-09097-1.

Hyvärinen K, Holopainen M, Skirdenko V, Ruhanen H, Lehenkari P, Korhonen M, Käkelä R, Laitinen S, Kerkelä E.Mesenchymal Stromal Cells and Their Extracellular Vesicles Enhance the Anti-Inflammatory Phenotype of Regulatory Macrophages by Downregulating the Production of Interleukin (IL)-23 and IL-22. Front Immunol. 2018 Apr 12;9:771. doi: 10.3389/fimmu.2018.00771.

Iguchi Y,Eid L, Parent M, Soucy G, Bareil C,Riku Y, Kawai K, Takagi S, Yoshida M, Katsuno M, Sobue J, JulienJ-P. Exosome secretion is a key pathway forclearance of pathological TDP-43. BRAIN 2016: 139; 3187–3201

Ilieva H, Polymenidou M, Cleveland DW. Non-cell autonomous toxicity in neurodegenerative disorders: ALS and beyond. J Cell Biol. 2009 Dec 14;187(6):761-72. doi: 10.1083/jcb.200908164.

Israelson A, Arbel N, Da Cruz S, Ilieva H, Yamanaka K, Shoshan-Barmatz V, Cleveland DW. Misfolded mutant SOD1 directly inhibits VDAC1conductance in a mouse model of inherited ALS. Neuron. 2010 Aug 26;67(4):575-87. doi: 10.1016/j.neuron.2010.07.019.

Iyer A, Zurolo E, Prabowo A, Fluiter K, Spliet WG, van Rijen PC, Gorter JA, Aronica E. MicroRNA-146a: a key regulator of astrocyte-mediated inflammatory response. PLoS One. 2012;7(9):e44789. doi: 10.1371/journal.pone.0044789.

Jaiswal MK. Riluzole and edaravone: A tale of two amyotrophic lateral sclerosis drugs. Med Res Rev. 2019 Mar;39(2):733-748. doi: 10.1002/med.21528.

Jiang J, Zhu Q, Gendron TF, et al. Gain of toxicity from ALS/FTD-linked repeat expansions in C9ORF72 is alleviated by antisense oligonucleotides targeting GGGGCC-containing RNAs. Neuron. 2016 May 4;90(3):535-50. doi: 10.1016/j.neuron.2016.04.006.

Jiang YM, Yamamoto M, Kobayashi Y, Yoshihara T, Liang Y, Terao S, Takeuchi H, Ishigaki S, Katsuno M, Adachi H, Niwa J, Tanaka F, Doyu M, Yoshida M, Hashizume Y, Sobue G. Gene expression profile of spinal motor neurons in sporadic amyotrophic lateral sclerosis. Ann Neurol. 2005 Feb;57(2):236-51.

Johann S, Heitzer M, Kanagaratnam M, Goswami A, Rizo T, Weis J, Troost D, Beyer C. NLRP3 inflammasome is expressed by astrocytes in the SOD1 mouse model of ALS and in human sporadic ALS patients. Glia. 2015 Dec;63(12):2260-73. doi: 10.1002/glia.22891.

Johnson JO, Mandrioli J, Benatar M, Abramzon Y, Van Deerlin VM, Trojanowski JQ, Gibbs JR, Brunetti M, Gronka S, Wuu J, Ding J, McCluskey L, Martinez-Lage M, Falcone D, Hernandez DG, Arepalli S, Chong S, Schymick JC, Rothstein J, Landi F, Wang YD, Calvo A, Mora G, Sabatelli M, Monsurrò MR, Battistini S, Salvi F, Spataro R, Sola P, Borghero G; ITALSGEN Consortium, Galassi G, Scholz SW, Taylor JP, Restagno G, Chiò A, Traynor BJ. Exome sequencing reveals VCP mutations as a cause of familial ALS. Neuron. 2010 Dec 9;68(5):857-64. doi: 10.1016/j.neuron.2010.11.036.

Joseph MS, Bilousova T, Zdunowski S, Wu ZP, Middleton B, Boudzinskaia M, Wong B, Ali N, Zhong H, Yong J, Washburn L, Escande-Beillard N, Dang H, Edgerton VR, Tillakaratne NJ, Kaufman DL. Transgenic mice with enhanced neuronal major histocompatibility complex class I expression recover locomotor function better after spinal cord injury. J Neurosci Res. 2011 Mar;89(3):365-72. doi: 10.1002/jnr.22557.

Jovičić A, Mertens J, Boeynaems S, Bogaert E, Chai N, Yamada SB, Paul JW 3rd, Sun S, Herdy JR, Bieri G, Kramer NJ, Gage FH, Van Den Bosch L, Robberecht W, Gitler AD. Modifiers of

C9orf72 dipeptide repeat toxicity connect nucleocytoplasmic transport defects to FTD/ALS. Nat Neurosci. 2015 Sep;18(9):1226-9. doi: 10.1038/nn.4085.

Kanai K, Kuwabara S, Misawa S, Tamura N, Ogawara K, Nakata M, Sawai S, Hattori T, Bostock H. Altered axonal excitability properties in amyotrophic lateral sclerosis: impaired potassium channel function related to disease stage. Brain 2006 129,953–962.

Kang J, Li Z, Zhi Z, Wang S, Xu G. MiR-21 derived from the exosomes of MSCs regulates the death and differentiation of neurons in patients with spinal cord injury. Gene Ther. 2019 Sep 30. doi: 10.1038/s41434-019-0101-8.

Kang SH, Li Y, Fukaya M, Lorenzini I, Cleveland DW, Ostrow LW, Rothstein JD, Bergles DE. Degeneration and impaired regeneration of gray matter oligodendrocytes in amyotrophic lateral sclerosis. Nat Neurosci. 2013 May;16(5):571-9. doi: 10.1038/nn.3357.

Kanno T, Tanaka K, Yanagisawa Y, Yasutake K, Hadano S, Yoshii F, Hirayama N, Ikeda JE. A novel small molecule, N-(4-(2-pyridyl)(1,3-thiazol-2-yl))-2-(2,4,6-trimethylphenoxy) acetamide, selectively protects against oxidative stress-induced cell death by activating the Nrf2-ARE pathway: therapeutic implications for ALS. Free Radic Biol Med. 2012 Dec 1;53(11):2028-42. doi:10.1016/j.freeradbiomed.2012.09.010.

Karussis D, Karageorgiou C, Vaknin-Dembinsky A, Gowda-Kurkalli B, Gomori JM, Kassis I, et al. Safety and immunological effects of mesenchymal stem cell transplantation in patients with multiple sclerosis and amyotrophic lateral sclerosis. Arch Neurol. 2010;67(10):1187–1194. doi: 10.1001/archneurol.2010.248.

Kawaguchi-Niida M, Yamamoto T, Kato Y, Inose Y, Shibata N. MCP-1/CCR2 signaling-mediated astrocytosis is accelerated in a transgenic mouse model of SOD1-mutated familial ALS. Acta Neuropathol Commun. 2013 Jun 4;1:21. doi: 10.1186/2051-5960-1-21.

Kawahara Y, Ito K, Sun H, Aizawa H, Kanazawa I, Kwak S. Glutamate receptors: RNA editing and death of motor neurons. Nature. 2004 Feb 26;427(6977):801.

Kendrick S and Hurley LH. The role of G-quadruplex/imotif secondary structures as cis-acting regulatory elements. Pure Appl Chem. 2010 Jan 1;82(8):1609-1621.

Keshtkar S, Azarpira N, Ghahremani MH. Mesenchymal stem cell-derived extracellular vesicles: novel frontiers in regenerative medicine. Stem Cell Res Ther. 2018 Mar 9;9(1):63. doi: 10.1186/s13287-018-0791-7.

Kia A, McAvoy K, Krishnamurthy K, Trotti D, Pasinelli P. Astrocytes expressing ALS-linked mutant FUS induce motor neuron death through release of tumor necrosis factor-alpha. Glia. 2018 May;66(5):1016-1033. doi: 10.1002/glia.23298.

Kikuchi S, Shinpo K, Ogata A, Tsuji S, Takeuchi M, Makita Z, Tashiro K. Detection of N-epsilon–(carboxymethyl)lysine (CML) and non–CML advanced glycation end–products in the anterior horn of amyotrophic lateral sclerosis spinal cord. Amyotroph Lateral Scler Other Motor Neuron Disord. 2002 Jun;3(2):63-8.

Kim S, Chung AY, Na JE, Lee SJ, Jeong SH, Kim E, Sun W, Rhyu IJ, Park HC. Myelin degeneration induced by mutant superoxide dismutase 1 accumulation promotes amyotrophic lateral sclerosis. Glia. 2019 Oct;67(10):1910-1921. doi: 10.1002/glia.23669.

Kim SH, Shanware NP, Bowler MJ, Tibbetts RS. Amyotrophic lateral sclerosis-associated proteins TDP-43 and FUS/TLS function in a common biochemical complex to co-regulate HDAC6 mRNA. J Biol Chem. 2010 Oct 29;285(44):34097-105. doi: 10.1074/jbc.M110.154831.

Klatt CL, Theis V, Hahn S, Theiss C, Matschke V.Deregulated miR-29b-3p Correlates with Tissue-Specific Activation of Intrinsic Apoptosis in An Animal Model of Amyotrophic Lateral Sclerosis. Cells. 2019 Sep 12;8(9). doi: 10.3390/cells8091077.

Ko HS, Uehara T, Tsuruma K, Nomura Y. Ubiquilin interacts with ubiquitylated proteins and proteasome through its ubiquitin-associated and ubiquitin-like domains. FEBS Lett. 2004 May 21;566(1-3):110-4.

Koppers M, Blokhuis AM, Westeneng HJ, Terpstra ML, Zundel CA, Vieira de Sá R, Schellevis RD, Waite AJ, Blake DJ, Veldink JH, van den Berg LH, Pasterkamp RJ. C9orf72 ablation in mice does not cause motor neuron degeneration or motor deficits. Ann Neurol. 2015 Sep;78(3):426-38. doi: 10.1002/ana.24453.

Kreiter N, Pal A, Lojewski X, Corcia P, Naujock M, Reinhardt P, Sterneckert J, Petri S, Wegner F, Storch A, Hermann A. Age-dependent neurodegeneration and organelle transport deficiencies in mutant TDP43 patient-derived neurons are independent of TDP43 aggregation. Neurobiol Dis. 2018 Jul;115:167-181. doi: 10.1016/j.nbd.2018.03.010.

Kumar V, Hasan GM and Hassan I. Unraveling the Role of RNA Mediated Toxicity of C9orf72 Repeats in C9-FTD/ALS. Front Neurosci. 2017; 11: 711. doi: 10.3389/fnins.2017.00711.

Kurtzke JF. Epidemiology of amyotrophic lateral sclerosis. Adv Neurol. 1982 36:281–302.

Kuzuhara S, Kokubo Y, Sasaki R, Narita Y, Yabana T, Hasegawa M, Iwatsubo T. Familial amyotrophic lateral sclerosis and parkinsonism-dementia complex of the Kii Peninsula of Japan: Clinical and neuropathological study and tau analysis. Ann Neurol. 2001 Apr;49(4):501-11.

Kwak MK and Kensler TW. Targeting NRF2 signaling for cancer chemoprevention. Toxicol Appl Pharmacol. 2010 Apr 1;244(1):66-76. doi: 10.1016/j.taap.2009.08.028.

Kwiatkowski TJ Jr, Bosco DA, Leclerc AL, Tamrazian E, Vanderburg CR, Russ C, Davis A, Gilchrist J, Kasarskis EJ, Munsat T, Valdmanis P, Rouleau GA, Hosler BA, Cortelli P, de Jong PJ, Yoshinaga Y, Haines JL, Pericak-Vance MA, Yan J, Ticozzi N, Siddique T, McKenna-Yasek D, Sapp PC, Horvitz HR, Landers JE, Brown RH Jr. Mutations in the FUS/TLS Gene on Chromosome 16 Cause Familial Amyotrophic Lateral Sclerosis. Science. 2009 Feb 27;323(5918):1205-8. doi: 10.1126/science.1166066.

Kwon I, Xiang S, Kato M, Wu L, Theodoropoulos P, Wang T, Kim J, Yun J, Xie Y, McKnight SL. Poly-dipeptides encoded by the C9orf72 repeats bind nucleoli, impede RNA biogenesis, and kill cells. Science. 2014 Sep 5;345(6201):1139-45. doi: 10.1126/science.1254917.

Lagiertourenne C, Polymenidou M, Cleveland DW. TDP-43 and FUS/TLS: Emerging roles in RNA processing and neurodegeneration. Hum Mol Genet. 2010 Apr 15;19(R1):R46-64. doi: 10.1093/hmg/ddq137.

Lai C, Xie C, Shim H, Chandran J, Howell BW, Cai H. Regulation of endosomal motility and degradation by amyotrophic lateral sclerosis 2/alsin. Mol Brain. 2009 Jul 24;2:23. doi: 10.1186/1756-6606-2-23.

Lanzillotta A, Pignataro G, Branca C, Cuomo O, Sarnico I, Benarese M, Annunziato L, Spano P, Pizzi M. Targeted acetylation of NF-kappaB/RelA and histones by epigenetic drugs reduces post-ischemic brain injury in mice with an extended therapeutic window. Neurobiol Dis. 2013 Jan;49:177-89. doi: 10.1016/j.nbd.2012.08.018.

Lanzillotta A, Sarnico I, Ingrassia R, Boroni F, Branca C, Benarese M, Faraco G, Blasi F, Chiarugi A, Spano P, Pizzi M. The acetylation of RelA in Lys310 dictates the NF-κB-dependent response in post-ischemic injury. Cell Death Dis. 2010 Nov 4;1:e96. doi: 10.1038/cddis.2010.76.

Laura Ferraiuolo, Adrian Higginbottom, Paul R. Heath, Sian Barber, David Greenald, Janine Kirby and Pamela J. Shaw. Dysregulation of astrocyte–motoneuron cross-talk in mutant superoxide dismutase 1-related amyotrophic lateral sclerosis. Brain 2011: 134; 2627–2641. doi:10.1093/brain/awr193.

Lawrence T. The Nuclear Factor NF-κB Pathway in Inflammation. Cold Spring Harb Perspect Biol. 2009 Dec;1(6):a001651. doi: 10.1101/cshperspect.a001651.

Le MT, Xie H, Zhou B, Chia PH, Rizk P, Um M, Udolph G, Yang H, Lim B, Lodish HF. MicroRNA-125b promotes neuronal differentiation in human cells by repressing multiple targets. Mol Cell Biol. 2009 Oct;29(19):5290-305. doi: 10.1128/MCB.01694-08.

Leal-Lasarte MM, Franco JM, Labrador-Garrido A, Pozo D, Roodveldt C. Extracellular TDP-43 aggregates target MAPK/MAK/MRK overlapping kinase (MOK) and trigger caspase-3/IL-18 signaling in microglia. FASEB J. 2017 Jul;31(7):2797-2816. doi: 10.1096/fj.201601163R

Lee M, Ban JJ,Kim KY, Jeon GS, Im W, Sung JJ, Kim M.Adipose-derived stem cell exosomes alleviate pathology of amyotrophic lateral sclerosis in vitro.BiochemBiophys Res Commun. 2016 Oct 21;479(3):434-439. doi: 10.1016/j.bbrc.2016.09.069.

Lee Y, Morrison BM, Li Y, Lengacher S, Farah MH, Hoffman PN, Liu Y, Tsingalia A, Jin L, Zhang PW, Pellerin L, Magistretti PJ, Rothstein JD. Oligodendroglia metabolically support axons and contribute to neurodegeneration. Nature. 2012 Jul 26;487(7408):443-8. doi: 10.1038/nature11314.

Lee YB, Chen HJ, Peres JN, Gomez-Deza J, Attig J, Stalekar M, Troakes C, Nishimura AL, Scotter EL, Vance C, Adachi Y, Sardone V, Miller JW, Smith BN, Gallo JM, Ule J, Hirth F, Rogelj B, Houart C, Shaw CE. Hexanucleotide repeats in ALS/FTD form length-dependent RNA foci, sequester RNA binding proteins, and are neurotoxic. Cell Rep. 2013 Dec 12;5(5):1178-86. doi: 10.1016/j.celrep.2013.10.049.

Lee J, Hyeon SJ, Im H, Ryu H, Kim Y, Ryu H. Astrocytes and Microglia as Non-cell Autonomous Players in the Pathogenesis of ALS. Exp Neurobiol. 2016 Oct;25(5):233-240.

Leko MB, Župunski V, Kirincich J, Smilović D, Hortobágyi T, Hof PR, Šimić G. Molecular Mechanisms of Neurodegeneration Related to C9orf72 Hexanucleotide Repeat Expansion. Behav Neurol. 2019 Jan 15;2019:2909168. doi:10.1155/2019/2909168

Lepore AC, Rauck B, Dejea C, Pardo AC, Rao MS, Rothstein JD, Maragakis NJ. Focal transplantation-based astrocyte replacement is neuroprotective in a model of motor neuron disease. Nat Neurosci. 2008 Nov;11(11):1294-301. doi: 10.1038/nn.2210.

Li YR, King OD, Shorter J, Gitler AD. Stress granules as crucibles of ALS pathogenesis. J Cell Biol. 2013 Apr 29;201(3):361-72. doi: 10.1083/jcb.201302044.

Liddelow SA, Guttenplan KA, Clarke LE, Bennett FC, Bohlen CJ, Schirmer L, Bennett ML, Münch AE, Chung WS, Peterson TC, Wilton DK, Frouin A, Napier BA, Panicker N, Kumar M, Buckwalter MS, Rowitch DH, Dawson VL, Dawson TM, Stevens B, Barres BA. Neurotoxic reactive astrocytes are induced by activated microglia. Nature. 2017 Jan 26;541(7638):481-487. doi: 10.1038/nature21029.

Lilley BN, Ploegh HL. Viral modulation of antigen presentation: Manipulation of cellular targets in the ER and beyond. Immunol Rev. 2005 Oct;207:126-44.

Lin CL, Bristol LA, Jin L, Dykes-Hoberg M, Crawford T, Clawson L, Rothstein JD. Aberrant RNA processing in a neurodegenerative disease: the cause for absent EAAT2, a glutamate transporter, in amyotrophic lateral sclerosis. Neuron. 1998 Mar;20(3):589-602.

Liu G, Coyne AN, Pei F, Vaughan S, Chaung M, Zarnescu DC, Buchan JR. Endocytosis regulates TDP-43 toxicity and turnover. Nat Commun. 2017 Dec 12;8(1):2092. doi: 10.1038/s41467-017-02017-x.

Liu W, Yamashita T, Tian F, Morimoto N, Ikeda Y, Deguchi K, Abe K. Dynamic changes of mitochondrial fusion and fission proteins in a murinemodel of amyotrophic lateral sclerosis. Curr Neurovasc Res. 2013 Aug;10(3):222-30.

Liu Y, Pattamatta A, Zu T, Reid T, Bardhi O, Borchelt DR, Yachnis AT, Ranum LP. C9orf72 BAC mouse model with motor deficits and neurodegenerative features of ALS/FTD. Neuron. 2016 May 4;90(3):521-34. doi: 10.1016/j.neuron.2016.04.005.

Lorenzini I, Moore S, Sattler R. RNA Editing Deficiency in Neurodegeneration. Adv Neurobiol. 2018;20:63-83. doi: 10.1007/978-3-319-89689-2_3.

Lu Y, Zhou Y, Zhang R, Wen L, Wu K, Li Y, Yao Y, Duan R, Jia Y.Bone Mesenchymal Stem Cell-Derived Extracellular Vesicles Promote Recovery Following Spinal Cord Injury via Improvement of the Integrity of the Blood-Spinal Cord Barrier. Front Neurosci. 2019 Mar 12;13:209. doi: 10.3389/fnins.2019.00209.

Ly CV, Miller TM. Emerging antisense oligonucleotide and viral therapies for amyotrophic lateral sclerosis. Curr Opin Neurol. 2018 Oct;31(5):648-654. doi: 10.1097/WCO.0000000000000594.

Mackenzie IR, Arzberger T, Kremmer E, Troost D, Lorenzl S, Mori K, Weng SM, Haass C, Kretzschmar HA, Edbauer D, Neumann M. Dipeptide repeat protein pathology in C9ORF72 mutation cases: clinico-pathological correlations. Acta Neuropathol. 2013 Dec;126(6):859-79. doi: 10.1007/s00401-013-1181-y.

Mackenzie IR, Rademakers R, Neumann M.TDP-43 and FUS in amyotrophic lateral sclerosis and frontotemporal dementia. Lancet Neurol. 2010 Oct;9(10):995-1007. doi: 10.1016/S1474-4422(10)70195-2.

Maffioli E, Nonnis S, Angioni R, Santagata F, Calì B, Zanotti L, Negri A, Viola A, TedeschiG. Proteomic analysis of the secretome of human bone marrow-derived mesenchymal stem cells primed by pro-inflammatory cytokines. J Proteomics. 2017 Aug 23;166:115-126. doi: 10.1016/j.jprot.2017.07.012.

Magrané J, Cortez C, Gan WB, Manfredi G. Abnormal mitochondrial transport and morphology are common pathological denominators in SOD1and TDP43 ALS mouse models. Hum Mol Genet. 2014 Mar 15;23(6):1413-24. doi: 10.1093/hmg/ddt528.

Magrane, J, Cortez, C, Gan, WB, Manfredi, G. Abnormal mitochondrial transport and morphology are common pathological denominators in SOD1 and TDP-43 ALS mouse models. Hum Mol Genet. 2014 Mar 15;23(6):1413-24. doi: 10.1093/hmg/ddt528.

Maharjan N., Künzli C, Buthey K, and Saxena S. C9ORF72 regulates stress granule formation and its deficiency impairs stress granule assembly, hypersensitizing cells to stress. Mol Neurobiol. 2017 May;54(4):3062-3077. doi: 10.1007/s12035-016-9850-1.

Mahlknecht U, Will J, Varin A, Hoelzer D, Herbein G. Histone deacetylase 3, a class I histone deacetylase, suppresses MAPK11-mediated activating transcription factor-2 activation and represses TNF gene expression. J Immunol. 2004 Sep 15;173(6):3979-90.

Manders EM, Stap J, Brakenhoff GJ, van Driel R, Aten JA. Dynamics of three-dimensional replication patterns during the S-phase, analysed by double labelling of DNA and confocal microscopy. J Cell Sci. 1992 Nov;103 (Pt 3):857-62.

Manfredi G, Kawamata H. Mitochondria and endoplasmic reticulum crosstalk in amyotrophic lateral sclerosis. Neurobiol Dis. 2016 Jun;90:35-42. doi: 10.1016/j.nbd.2015.08.004.

Mangan MSJ, Olhava EJ, Roush WR, Seidel HM, Glick GD, Latz E. Targeting the NLRP3 inflammasome in inflammatory diseases. Nat Rev Drug Discov. 2018 Aug;17(8):588-606. doi: 10.1038/nrd.2018.97.

Markovinovic A, Cimbro R, Ljutic T, Kriz J, Rogelj B, Munitic I. Optineurin in amyotrophic lateral sclerosis: Multifunctional adaptor protein at the crossroads of different neuroprotective mechanisms. Prog Neurobiol. 2017 Jul;154:1-20. doi: 10.1016/j.pneurobio.2017.04.005.

Markovinovic A, Ljutic T, Béland LC, Munitic I. Optineurin Insufficiency Disbalances Proinflammatory and Anti-inflammatory Factors by Reducing Microglial IFN-b Responses. Neuroscience. 2018 Sep 15;388:139-151. doi: 10.1016/j.neuroscience.2018.07.007.

Marrone L, Drexler HCA, Wang J, Tripathi P, Distler T, Heisterkamp P, Anderson EN, Kour S, Moraiti A, Maharana S, Bhatnagar R, Belgard TG, Tripathy V, Kalmbach N, Hosseinzadeh Z, Crippa V, Abo-Rady M, Wegner F, Poletti A, Troost D, Aronica E, Busskamp V, Weis J, Pandey UB, Hyman AA, Alberti S, Goswami A, Sterneckert J. FUS pathology in ALS is linked to alterations in multiple ALS-associated proteins and rescued by drugs stimulating autophagy. Acta Neuropathol. 2019 Apr 1. doi: 10.1007/s00401-019-01998-x.

Martier R, Liefhebber JM, García-Osta A, Miniarikova J, Cuadrado-Tejedor M, Espelosin M, Ursua S, Petry H, van Deventer SJ, Evers MM, Konstantinova P. Targeting RNA-Mediated Toxicity in C9orf72 ALS and/or FTD by RNAi-Based Gene Therapy. Mol Ther Nucleic Acids. 2019a Jun 7;16:26-37. doi: 10.1016/j.omtn.2019.02.001.

Martier R, Liefhebber JM, Miniarikova J, van der Zon T, Snapper J, Kolder I, Petry H, van Deventer SJ, Evers MM, Konstantinova P. Artificial MicroRNAs Targeting C9orf72 Can Reduce Accumulation of Intra-nuclear Transcripts in ALS and FTD Patients. Mol Ther Nucleic Acids. 2019b Mar 1;14:593-608. doi: 10.1016/j.omtn.2019.01.010.

Martínez-Muriana A, Mancuso R, Francos-Quijorna I, Olmos-Alonso A, Osta R, Perry VH, Navarro X, Gomez-Nicola D, López-Vales R. CSF1R blockade slows theprogression of amyotrophic lateral sclerosis by reducing microgliosis and invasionof macrophages into peripheral nerves. Sci Rep. 2016 May 13;6:25663. doi: 10.1038/srep25663.

Maruyama H, Morino H, Ito H, Izumi Y, Kato H, Watanabe Y, Kinoshita Y, Kamada M, Nodera H, Suzuki H, Komure O, Matsuura S, Kobatake K, Morimoto N, Abe K, Suzuki N, Aoki M, Kawata A, Hirai T, Kato T, Ogasawara K, Hirano A, Takumi T, Kusaka H, Hagiwara K, Kaji R, Kawakami H. Mutations of optineurin in amyotrophic lateral sclerosis. Nature. 2010 May 13;465(7295):223-6. doi: 10.1038/nature08971.

Mathis S, Goizet C, Soulages A, Vallat JM, Masson GL. Genetics of amyotrophic lateral sclerosis: A review. J Neurol Sci. 2019 Apr 15;399:217-226. doi: 10.1016/j.jns.2019.02.030.

Mathis S, Couratier P, Julian A, Vallat JM, Corcia P, Le Masson G. Management and therapeutic perspectives in amyotrophic lateral sclerosis. Expert Rev Neurother. 2017 Mar;17(3):263-276. doi: 10.1080/14737175.2016.1227705.

Mavlyutov TA, Epstein ML, Verbny YI, Huerta MS, Zaitoun I, Ziskind- Conhaim L, Ruoho AE. Lack of sigma-1 receptor exacerbates ALS progression in mice. Neuroscience. 2013 Jun 14;240:129-34. doi: 10.1016/j.neuroscience.2013.02.035.

Mazzini L, Fagioli F, Boccaletti R, Mareschi K, Oliveri G, Olivieri C, et al. Stem cell therapy in amyotrophic lateral sclerosis: a methodological approach in humans. Amyotroph Lateral Scler Other Motor Neuron Disord. 2003;4(3):158–161. doi: 10.1080/14660820310014653.

Mazzini L, Ferrari D, Andjus PR, Buzanska L, Cantello R, De Marchi F, Gelati M, Giniatullin R, Glover JC, Grilli M, Kozlova EN, Maioli M, Mitrečić D, Pivoriunas A, Sanchez-Pernaute R, Sarnowska A, Vescovi AL; BIONECA COST ACTION WG Neurology. Advances in stem cell therapy for amyotrophic lateral sclerosis. Expert Opin Biol Ther. 2018 Aug;18(8):865-881. doi: 10.1080/14712598.2018.1503248.

McGown A, McDearmid JR, Panagiotaki N, Tong H, Al Mashhadi S, Redhead N, Lyon AN, Beattie CE, Shaw PJ, Ramesh TM. Early interneuron dysfunction in ALS: insights from a mutant sod1 zebrafish model. Ann Neurol. 2013 Feb;73(2):246-58. doi: 10.1002/ana.23780.

Mead RJ, Higginbottom A, Allen SP, Kirby J, Bennett E, Barber SC, Heath PR, Coluccia A, Patel N, Gardner I, Brancale A, Grierson AJ, Shaw PJS[+] Apomorphine is a CNS penetrating activator of the Nrf2-ARE pathway with activity in mouse and patient fibroblast models of amyotrophic lateral sclerosis. Free Radic Biol Med. 2013 Aug;61:438-52. doi: 10.1016/j.freeradbiomed.2013.04.018.

Meissner F, Molawi K, Zychlinsky A. Mutant superoxide dismutase 1-induced IL-1 accelerates ALS pathogenesis. Proc Natl Acad Sci U S A. 2010 Jul 20;107(29):13046-50. doi: 10.1073/pnas.1002396107..

Mendez EF, Sattler R. Biomarker development for C9orf72 repeat expansion in ALS. Brain Res. 2015 May 14;1607:26-35. doi: 10.1016/j.brainres.2014.09.041.

Mendt M, Rezvani K, Shpall E. Mesenchymal stem cell-derived exosomes for clinical use. Bone Marrow Transplant. 2019 Aug;54(Suppl 2):789-792. doi: 10.1038/s41409-019-0616-z.

Meyer H, Bug M, Bremer S. Emerging functions of the VCP/p97 AAA-ATPase in the ubiquitin system. Nat Cell Biol. 2012 Feb 2;14(2):117-23. doi: 10.1038/ncb2407.

Milanese M, Zappettini S, Onofri F, Musazzi L, Tardito D, Bonifacino T, Messa M, Racagni G, Usai C, Benfenati F, Popoli M, Bonanno G. Abnormal exocytotic release of glutamate in amousemodel of amyotrophic lateral sclerosis. J Neurochem. 2011 Mar;116(6):1028-42. doi: 10.1111/j.1471-4159.2010.07155.x.

Miller RG, Mitchell JD, Moore DH. Riluzole for amyotrophic lateral sclerosis (ALS)/motor neuron disease (MND). Cochrane Database Syst Rev. 2012 Mar 14;(3):CD001447. doi: 10.1002/14651858.CD001447.pub3.

Miller TM, Pestronk A, David W, Rothstein J, Simpson E, Appel SH, Andres PL, Mahoney K, Allred P, Alexander K, Ostrow LW, Schoenfeld D, Macklin EA, Norris DA, Manousakis G, Crisp M, Smith R, Bennett CF, Bishop KM, Cudkowicz ME. An antisense oligo nucleotide against SOD1 delivered intrathecally for patients with SOD1 familial amyotrophic lateral sclerosis: a phase 1, randomised, first-in-man study. Lancet Neurol. 2013 May;12(5):435-42. doi: 10.1016/S1474-4422(13)70061-9.

Moens TG, Mizielinska S, Niccoli T, Mitchell JS, Thoeng A, Ridler CE, Grönke S, Esser J, Heslegrave A, Zetterberg H, Partridge L, Isaacs AM. Sense and antisense RNA are not toxic in Drosophila models of C9orf72-associated ALS/FTD. Acta Neuropathol. 2018 Mar;135(3):445-457. doi: 10.1007/s00401-017-1798-3.

Moller A, Bauer CS, Cohen RN, Webster CP, De Vos KJ. Amyotrophic lateral sclerosis-associated mutant SOD1 inhibits anterograde axonal transport of mitochondria by reducing Miro1 levels. Hum Mol Genet. 2017 Dec 1;26(23):4668-4679. doi: 10.1093/hmg/ddx348.

Morel L, Regan M, Higashimori H, Ng SK, Esau C, Vidensky S, Rothstein J, Yang Y. Neuronal exosomal miRNA-dependent translational regulation of astroglial glutamate transporter GLT1. J Biol Chem. 2013 Mar 8;288(10):7105-16. doi: 10.1074/jbc.M112.410944.

Morita M, Al-Chalabi A, Andersen PM, Hosler B, Sapp P, Englund E, Mitchell JE, Habgood JJ, de Belleroche J, Xi J, Jongjaroenprasert W, Horvitz HR, Gunnarsson LG, Brown RH Jr. A locus on chromosome 9p confers susceptibility to ALS and frontotemporal dementia. Neurology. 2006 Mar 28;66(6):839-44.

Mórotz GM, De Vos KJ, Vagnoni A, Ackerley S, Shaw CE, Miller CC. Amyotrophic lateral sclerosis-associated mutant VAPBP56s perturbscalcium homeostasis to disrupt axonal transport of mitochondria. Hum Mol Genet. 2012 May 1;21(9):1979-88. doi: 10.1093/hmg/dds011.

Moser JM, Bigini P, Schmitt-John T. The wobbler mouse, an ALS animal model. Mol Genet Genomics. 2013 Jun;288(5-6):207-29. doi: 10.1007/s00438-013-0741-0

Muller FL, Song W, Jang YC, Liu Y, Sabia M, Richardson A, Van Remmen H. Denervation-induced skeletal muscle atrophy is associated with increased mitochondrial ROS production. Am J Physiol Regul Integr Comp Physiol. 2007 Sep;293(3):R1159-68.

Nagai M, Re DB, Nagata T, Chalazonitis A, Jessell TM, Wichterle H, Przedborski S. Astrocytes expressing ALS-linked mutated SOD1 release factors selectively toxic to motor neurons. Nat Neurosci. 2007 May;10(5):615-22. Doi: 10.1038/nn1876

Napoli L, Crugnola V, Lamperti C, Silani V, Di Mauro S, Bresolin N, Moggio M. Ultrastructural mitochondrial abnormalities in patients with sporadic amyotrophic lateral sclerosis. Arch Neurol. 2011 Dec;68(12):1612-3. doi: 10.1001/archneur.68.12.1612.

Nardo G, Trolese MC, Bendotti C. Major histocompatibility complex I expression by motor neurons and its implication in amyotrophic lateral sclerosis. Front Neurol. 2016 Jun 13;7:89. doi: 10.3389/fneur.2016.00089.

Nardo G, Trolese MC, Verderio M, Mariani A, de Paola M, Riva N, Dina G, Panini N, Erba E, Quattrini A, Bendotti C. Counteracting roles of MHCI and CD8+ T cells in the peripheral and central nervous system of ALS SOD1-G93A mice. Mol Neurodegener. 2018 Aug 9;13(1):42. doi: 10.1186/s13024-018-0271-7.

Nayak D, Roth TL, McGavern DB. Microglia development and function. Annu Rev Immunol. 2014;32:367-402. doi: 10.1146/annurev-immunol-032713-120240.

Neumann M, Rademakers R, Roeber S, Baker M, Kretzschmar HA, Mackenzie IRA. A new subtype of frontotemporal lobar degeneration with FUS pathology. Brain. 2009 Nov;132(Pt 11):2922-31. doi: 10.1093/brain/awp214.

Neymotin A, Calingasan NY, Wille E, Naseri N, Petri S, Damiano M, Liby KT, Risingsong R, Sporn M, Beal MF, Kiaei M. Neuroprotective effect of Nrf2/ARE activators, CDDO ethylamide and CDDO trifluoroethylamide, in a mouse model of amyotrophic lateral sclerosis. Free Radic Biol Med. 2011 Jul 1;51(1):88-96. doi: 10.1016/j.freeradbiomed.2011.03.027.

Nowicka N, Juranek J, Juranek JK, Wojtkiewicz J. Risk Factors and Emerging Therapies in Amyotrophic Lateral Sclerosis. Int. J. Mol. Sci. 2019, 20, 2616. doi:10.3390/ijms20112616

Oakes JA, Davies MC, Collins MO. TBK1: a new player in ALS linking autophagy and neuroinflammation. Mol Brain. 2017 Feb 2;10(1):5. doi: 10.1186/s13041-017-0287-x.

Oh KW, Moon C, Kim HY, Oh SI, Park J, Lee JH, Chang IY, Kim KS, Kim SH. Phase I trial of repeated intrathecal autologous bone marrow-derived mesenchymal stromal cells in amyotrophic lateral sclerosis. Stem Cells Transl Med. 2015;4(6):590–597. doi: 10.5966/sctm.2014-0212.

Oliveira AL, Thams S, Lidman O, Piehl F, Hökfelt T, Kärre KLAS, Lindå H, Cullheim S. A role for MHC class I molecules in synaptic plasticity and regeneration of neurons after axotomy. Proc Natl Acad Sci U S A. 2004 Dec 21;101(51):17843-8.

Orla Hardiman, Ammar Al-Chalabi, Carol Brayne, Ettore Beghi, Leonard H van den Berg, Adriano Chio, Sarah Martin, Giancarlo Logroscino, James Rooney (2017) The changing picture of amyotrophic lateral sclerosis: lessons from European registers. J Neurol Neurosurg Psychiatry. 2017 Jul;88(7):557-563. doi: 10.1136/jnnp-2016-314495.

Oskarsson B, Gendron TF, Staff NP. Amyotrophic Lateral Sclerosis: An Update for 2018. Mayo Clin Proc. 2018 Nov;93(11):1617-1628. doi: 10.1016/j.mayocp.2018.04.007.

Paladino S, Contea A, Caggiano R, Pierantoni GM, Faraonio R. Nrf2 Pathway in Age-Related Neurological. Cell Physiol Biochem. 2018;47(5):1951-1976. doi: 10.1159/000491465.

Pan H, Wang H, Wang X, Zhu L, Mao L.The Absence of Nrf2 Enhances NF-B-Dependent Inflammation following Scratch Injury in Mouse Primary Cultured Astrocytes Mediators Inflamm. 2012;2012:217580. doi: 10.1155/2012/217580.

Pansarasa O, Bordoni M, Diamanti L, Sproviero D, Gagliardi S, Cereda C. SOD1 in Amyotrophic Lateral Sclerosis: "Ambivalent" Behavior Connected to the Disease. Int J Mol Sci. 2018 May 3;19(5). doi: 10.3390/ijms19051345.

Papadeas ST, Kraig SE, O'Banion C, Lepore AC, Maragakis NJ. Astrocytes carrying the superoxide dismutase 1 (SOD1G93A) mutation induce wild-type motor neuron degeneration in vivo. Proc Natl Acad Sci U S A. 2011 Oct 25;108(43):17803-8. doi: 10.1073/pnas.1103141108.

Parker SJ, Meyerowitz J, James JL, Liddell JR, Crouch PJ, Kanninen KM, White AR. Endogenous TDP-43 localized to stress granules can subsequently form protein aggregates. Neurochem Int. 2012 Mar;60(4):415-24. doi: 10.1016/j.neuint.2012.01.019.

Pasinelli P, Belford ME, Lennon N, Bacskai BJ, Hyman BT, Trotti D, Brown RH Jr. Amyotrophic lateral sclerosis-associated SOD1 mutant proteinsbind and aggregate with Bcl-2 in spinal cord mitochondria. Neuron. 2004 Jul 8;43(1):19-30.

Pellerin L, Bouzier-Sore AK, Aubert A, Serres S, Merle M, Costalat R, et al. Activity-dependent regulation of energy metabolism by astrocytes: an update. Glia 2007; 55: 1251–62.

Pellerin L, Magistretti PJ. Glutamate uptake into astrocytes stimulates aerobic glycolysis: a mechanism coupling neuronal activity to glucose utilization. Proc Natl Acad Sci USA 1994; 91: 10625–9.

Petri S, Körner S, Kiaei M. Nrf2/ARE Signaling Pathway: Key Mediator in Oxidative Stress and Potential Therapeutic Target in ALS. Neurol Res Int. 2012;2012:878030. doi: 10.1155/2012/878030.

Petri S, Krampfl K, Hashemi F, Grothe C, Hori A, Dengler R, Bufler J. Distribution of GABAA receptor mRNA in the motor cortex of ALS patients. J. Neuropathol. Exp. Neurol. 2003 62, 1041–1051.

Petrou P, Gothelf Y, Argov Z, Gotkine M, Levy YS, Kassis I, Vaknin-Dembinsky A, Ben-Hur T, Offen D, Abramsky O, Melamed E, Karussis D. Safety and Clinical Effects of Mesenchymal Stem Cells Secreting Neurotrophic Factor Transplantation in Patients With Amyotrophic Lateral Sclerosis: Results of Phase 1/2 and 2a Clinical Trials. JAMA Neurol. 2016 Mar;73(3):337-44. doi: 10.1001/jamaneurol.2015.4321.

Pharaoh G, Sataranatarajan K, Street K, Hill S, Gregston J, Ahn B, Kinter C, Kinter M, Van Remmen H. Metabolic and Stress Response Changes Precede Disease Onset in the Spinal Cord of Mutant SOD1 ALS Mice. Front Neurosci. 2019 May 31;13:487. doi: 10.3389/fnins.2019.00487.

Philips T, Robberecht W. Neuroinflammation in amyotrophic lateral sclerosis: role of glial activation in motor neuron disease. Lancet Neurol. 2011 Mar;10(3):253-63. doi: 10.1016/S1474-4422(11)70015-1.

Phinney DG, Di Giuseppe M, Njah J, Sala E, Shiva S, St Croix CM, Stolz DB, Watkins SC, Di YP, Leikauf GD, Kolls J, Riches DW, Deiuliis G, Kaminski N, BoregowdaSV, McKenna DH, Ortiz LA. Mesenchymal stem cells use extracellular vesicles to outsource mitophagy and shuttle microRNAs. Nat Commun. 2015 Oct 7;6:8472. doi: 10.1038/ncomms9472.

Pieri M, Carunchio I, Curcio L, Mercuri NB, Zona C. Increased persistent sodium current determines cortical hyperexcitability in a genetic model of amyotrophic lateral sclerosis. Exp Neurol. 2009 Feb;215(2):368-79. doi: 10.1016/j.expneurol.2008.11.002.

Pikkarainen M, Hartikainen P, Alafuzoff I. Neuropathologic Features of Frontotemporal Lobar Degeneration With Ubiquitin-Positive Inclusions Visualized With Ubiquitin-Binding Protein p62 Immunohistochemistry. J Neuropathol Exp Neurol. 2008 Apr;67(4):280-98. doi: 10.1097/NEN.0b013e31816a1da2.

Pinto S, Cunha C, Barbosa M, Vaz AR, Brites D.Exosomes from NSC-34 Cells Transfected with hSOD1-G93A Are Enriched in miR-124 and Drive Alterations in Microglia Phenotype.Front Neurosci.2017 May 17;11:273. doi: 10.3389/fnins.2017.00273.

Poloni M, Facchetti D, Mai R, Micheli A, Agnoletti L, Francolini G, Mora G, Camana C, Mazzini L, Bachetti T. Circulating levels of tumour necrosis factor-alpha and its soluble receptors are increased in the blood of patients with amyotrophic lateral sclerosis. Neurosci Lett. 2000 Jun 30;287(3):211-4. doi: 10.1016/s0304-3940(00)01177-0.

Prasad A, Bharathi V, Sivalingam V, Girdhar A, Patel BK. Molecular mechanisms of TDP-43 misfolding and pathology in Amyotrophic Lateral Sclerosis. Front Mol Neurosci. 2019 Feb 14;12:25. doi: 10.3389/fnmol.2019.00025.

Prause J, Goswami A, Katona I, Roos A, Schnizler M, Bushuven E, Dreier A, Buchkremer S, Johann S, Beyer C, Deschauer M, Troost D, Weis J. Altered localization, abnormal modification and loss of function of Sigma receptor-1 in amyotrophic lateral sclerosis. Hum Mol Genet. 2013 Apr 15;22(8):1581-600. doi: 10.1093/hmg/ddt008.

Puls I, Jonnakuty C, LaMonte BH, Holzbaur EL, Tokito M, Mann E, Floeter MK, Bidus K, Drayna D, Oh SJ, Brown RH Jr, Ludlow CL, Fischbeck KH. Mutant dynactin inmotor neuron disease. Nat Genet. 2003 Apr;33(4):455-6.

Qi H, Liu DP, Xiao DW, Tian DC, Su YW, Jin SF. Exosomes derived from mesenchymal stem cells inhibit mitochondrial dysfunction-induced apoptosis of chondrocytes via p38, ERK, and Akt pathways. In Vitro Cell Dev Biol Anim. 2019 Mar;55(3):203-210. doi: 10.1007/s11626-019-00330-x.

Qiu G, Zheng G, Ge M, Wang J, Huang R, Shu Q, Xu J. Mesenchymal stem cell-derived extracellular vesicles affect disease outcomes via transfer of microRNAs. Stem Cell Res Ther. 2018 Nov 21;9(1):320. doi: 10.1186/s13287-018-1069-9.

Rahimifard M, Maqbool F, Moeini-Nodeh S, Niaz K, Abdollahi M, Braidy N, Nabavi SM, Nabavi SF. Targeting the TLR4 signaling pathway by polyphenols: A novel therapeutic strategy for neuroinflammation. Ageing Res Rev. 2017 Jul;36:11-19. doi: 10.1016/j.arr.2017.02.004. Epub 2017 Feb 21.

Ramaswami M, Taylor JP, Parker R. Altered Ribostasis: RNA-Protein Granules in Degenerative Disorders. Cell. 2013 Aug 15;154(4):727-36. doi: 10.1016/j.cell.2013.07.038.

Rao SD, Banack SA, COX PA, Weiss JH. BMAA selectively injures motor neurons via AMPA/kainate receptor activation. Exp Neurol. 2006 Sep;201(1):244-52.

Rao SD, Yin HZ, Weiss JH. Disruption of glial glutamate transport by reactive oxygen species produced in motor neurons. J Neurosci. 2003 Apr 1;23(7):2627-33.

Raposo G, Stoorvogel W. Extracellular vesicles: exosomes, microvesicles, and friends. J Cell Biol. 2013 Feb 18;200(4):373-83. doi: 10.1083/jcb.201211138.

Rasola A, Sciacovelli M, Pantic B, Bernardi P. Signal transduction to the permeabilità transition pore. FEBS Lett. 2010 May 17;584(10):1989-96. doi: 10.1016/j.febslet.2010.02.022.

Ravera S, Bonifacino T, Bartolucci M, Milanese M, Gallia E, Provenzano F, Cortese K, Panfoli I, Bonanno G. Characterization of the Mitochondrial Aerobic Metabolism in the Pre- and Perisynaptic Districts of the SOD1G93A Mouse Model of Amyotrophic Lateral Sclerosis. Mol Neurobiol. 2018 Dec;55(12):9220-9233. doi: 10.1007/s12035-018-1059-z.

Reddy K, Schmidt MH, Geist JM, Thakkar NP, Panigrahi GB, Wang YH, Pearson CE. Processing of double-R-loops in (CAG)·(CTG) and C9orf72 (GGGGCC)·(GGCCCC) repeats causes instability. Nucleic Acids Res. 2014;42(16):10473-87. doi: 10.1093/nar/gku658.

Redza-Dutordoir M, Averill-Bates DA. Activation of apoptosis signalling pathways by reactive oxygen species. Biochim Biophys Acta. 2016 Dec;1863(12):2977-2992. doi: 10.1016/j.bbamcr.2016.09.012.

Reis M, Mavin E, Nicholson L, Green K, Dickinson AM, Wang XN. Mesenchymal Stromal Cell-Derived Extracellular Vesicles Attenuate Dendritic Cell Maturation and Function. Front Immunol. 2018 Nov 9;9:2538. doi: 10.3389/fimmu.2018.02538.

Rojas F, Cortes N, Abarzua S, Dyrda A, van Zundert B. Astrocytes expressing mutant SOD1 and TDP43 trigger motoneuron death that is mediated via sodium channels and nitroxidative stress. Front Cell Neurosci. 2014 Feb 7;8:24. doi: 10.3389/fncel.2014.00024.

Rosen DR. Mutations in Cu/Zn superoxide dismutase gene are associated with familial amyotrophic lateral sclerosis. Nature. 1993 Jul 22;364(6435):362.

Rossi C, Cusimano M, Zambito M, Finardi A, Capotondo A, Garcia-Manteiga JM, Comi G, Furlan R, Martino G, Muzio L. Interleukin 4 modulates mi-croglia homeostasis and attenuates the early slowly progressive phase of amyo-trophic lateral sclerosis. Cell Death Dis. 2018 Feb 14;9(2):250. doi: 10.1038/s41419-018-0288-4.

Rothstein JD, Dykes-Hoberg M, Pardo CA, Bristol LA, Jin L, Kuncl RW, Kanai Y, Hediger MA, Wang Y, Schielke JP, Welty DF. Knockout of glutamate transporters reveals a major role for astroglial transport in excitotoxicity and clearance of glutamate. Neuron. 1996 Mar;16(3):675-86. doi: 10.1016/s0896-6273(00)80086-0

Rowland LP, How amyotrophic lateral sclerosis got its name: the clinical-pathologic genius of Jean-Martin Charcot, in Arch. Neurol., vol. 58, nº 3, March 2001, pp. 512 5, DOI:10.1001/archneur.58.3.512.

Roy J, Saucier D, O'Connell C, Morin P Jr. Extracellular vesicles and their diagnostic potential in amyotrophic lateralsclerosis. Clinica Chimica Acta 497 (2019) 27–34.

Rupaimoole R and Slack FJ. MicroRNA Therapeutics: Towards a New Era for the Management of Cancer and Other Diseases. Nat Rev Drug Discov. 2017 Mar;16(3):203-222. doi: 10.1038/nrd.2016.246.

Russell AP, Wada S, Vergani L, Hock MB, Lamon S, Léger B, Ushida T, Cartoni R, Wadley GD, Hespel P, Kralli A, Soraru G, Angelini C, Akimoto T. Disruption of skeletal muscle mitochondrial network genes and miRNAs in amyotrophic lateral sclerosis. Neurobiol Dis. 2013 Jan;49:107-17. doi: 10.1016/j.nbd.2012.08.015.

Ryan TA and Tumbarello DA. Optineurin: A Coordinator of Membrane-Associated Cargo Trafficking and Autophagy. Front Immunol. 2018 May 15;9:1024. doi: 10.3389/fimmu.2018.01024.

Saccon RA, Bunton-Stasyshyn RKA, Fisher EMC, Fratta P. Is SOD1 loss of function involved in amyotrophic lateral sclerosis? Brain. 2013 Aug;136(Pt 8):2342-58. doi: 10.1093/brain/awt097.

Saotome M, Safiulina D, Szabadkai G, Das S, Fransson A, Aspenstrom P, Rizzuto R, Hajnóczky G. Aspenstrom, R. Rizzuto, G. Hajnoczky, Bidirectional Ca2+-dependent control of

mitochondrial dynamics by the Miro GTPase. Proc Natl Acad Sci U S A. 2008 Dec 30;105(52):20728-33. doi: 10.1073/pnas.0808953105.

Sarlette A, Krampfl K, Grothe C, Neuhoff Nv, Dengler R, Petri S. Nuclear erythroid 2-related factor 2-antioxidative response element signaling pathway in motor cortex and spinal cord in amyotrophic lateral sclerosis. J Neuropathol Exp Neurol. 2008 Nov;67(11):1055-62. doi: 10.1097/NEN.0b013e31818b4906.

Sasaki S and Iwata M. Mitochondrial alterations in the spinal cord of patientswith sporadic amyotrophic lateral sclerosis. J Neuropathol Exp Neurol. 2007 Jan;66(1):10-6.

Sau D, De Biasi S, Vitellaro-Zuccarello L, Riso P, Guarnieri S, Porrini M, Simeoni S, Crippa V, Onesto E, Palazzolo I, Rusmini P, Bolzoni E, Bendotti C, Poletti A. Mutation of SOD1 in ALS: a gain of a loss of function. Hum Mol Genet. 2007 Jul 1;16(13):1604-18.

Schiaffino L, Bonafede R, Scambi I, Parrella E, Pizzi M, Mariotti R. Acetylation state of RelA modulated by epigenetic drugs prolongs survival and induces a neuroprotective effect on ALS murine model. Sci Rep. 2018 Aug 27;8(1):12875. doi: 10.1038/s41598-018-30659-4

Schiffer D, Cordera S, Cavalla P, Migheli A. Reactive astrogliosis of the spinal cord in amyotrophic lateral sclerosis. J Neurol Sci. 1996 Aug;139 Suppl:27-33. doi:10.1016/0022-510x(96)00073-1.

Schwartz G and Fehlings MG. Secondary injury mechanisms of spinal cord trauma: A novel therapeutic approach for the management of secondary pathophysiology with the sodium channel blocker riluzole. Prog Brain Res.2002; 137:177-90. doi: 10.1016/s0079-6123(02)37016-x.

Serrano A, Donno C, Giannetti S, Perić M, Andjus P, D'Ambrosi N, Michetti F. The Astrocytic S100B Protein with Its Receptor RAGE Is Aberrantly Expressed in SOD1G93A Models, and Its Inhibition Decreases the Expression of Proinflammatory Genes. Mediators Inflamm. 2017;2017:1626204. doi: 10.1155/2017/1626204.

Shan X, Chiang PM, Price DL, Wong PC. Altered distributions of Gemini of coiled bodies and mitochondria in motor neurons of TDP-43 transgenic mice. Proc Natl Acad Sci U S A. 2010 Sep 14;107(37):16325-30. doi: 10.1073/pnas.1003459107.

Sharkey LM, Safren N, Pithadia AS, Gerson JE, Dulchavsky M, Fischer S, Patel R, Lantis G, Ashraf N, Kim JH, Meliki A, Minakawa EN, Barmada SJ, Ivanova MI, Paulson HL.Mutant UBQLN2 promotes toxicity by modulating intrinsic self-assembly. Proc Natl Acad Sci U S A. 2018 Oct 30;115(44):E10495-E10504. doi: 10.1073/pnas.1810522115.

Shibuya K, Misawa S, Arai K, Nakata M, Kanai K, Yoshiyama Y, Ito K, Isose S, Noto Y, Nasu S, Sekiguchi Y, Fujimaki Y, Ohmori S, Kitamura H, Sato Y, Kuwabara S. Markedly reduced axonal potassium channel expression in human sporadic amyotrophic lateral sclerosis: an immunohistochemical study. Exp Neurol. 2011 Dec;232(2):149-53. doi: 10.1016/j.expneurol.2011.08.015.

Shlevkov E, Kramer T, Schapansky J, LaVoie MJ, Schwarz TL. Miro phosphorylation sites regulate Parkin recruitment and mitochondrial motility. Proc Natl Acad Sci U S A. 2016 Oct 11;113(41):E6097-E6106.

Silverman JM, Fernando SM, GradLI, Hill AF, Turner BJ, YerburyJJ. Cashman NR. Disease Mechanisms in ALS: Misfolded SOD1 TransferredThrough Exosome-Dependent and Exosome-IndependentPathways. Cell Mol Neurobiol (2016) 36:377–381.

Singh A, Kukreti R, Saso L, Kukreti S. Oxidative Stress: A Key Modulator in Neurodegenerative Diseases. Molecules. 2019 Apr 22;24(8). pii: E1583. doi: 10.3390/molecules24081583.

Singhal G, Jaehne EJ, Corrigan F, Toben C, Baune BT. Inflammasomes in neuroinflammation and changes in brain function: a focused review. Front Neurosci. 2014 Oct 7;8:315. doi: 10.3389/fnins.2014.00315.

Sitcheran R, Gupta P, Fisher PB, Baldwin AS.Positive and negative regulation of EAAT2 by NF-kappaB: a role for N-myc in TNFalpha-controlled repression. EMBO J. 2005 Feb 9;24(3):510-20.

Skarnes WC, Rosen B, West AP, Koutsourakis M, Bushell W, Iyer V, Mujica AO, Thomas M, Harrow J, Cox T, Jackson D, Severin J, Biggs P, Fu J, Nefedov M, de Jong PJ, Stewart AF, Bradley A. A conditional knockout resource for the genome-wide study of mouse gene function. Nature. 2011 Jun 15;474(7351):337-42. doi: 10.1038/nature10163.

Slota JA and Booth SA. MicroRNAs in Neuroinflammation: Implications in Disease Pathogenesis, Biomarker Discovery and Therapeutic Applications. Noncoding RNA. 2019 Apr 24;5(2). doi: 10.3390/ncrna5020035.

Slowik A, Tomik B, Wolkow PP, Partyka D, Turaj W, Malecki MT, Pera J, Dziedzic T, Szczudlik A, Figlewicz DA. Paraoxonase gene polymorphisms and sporadic ALS. Neurology. 2006 Sep 12;67(5):766-70.

Smith EF, Shaw PJ, De Vos KJ. The role of mitochondria in amyotrophic lateral sclerosis. Neurosci Lett. 2019 Sep 25;710:132933. doi: 10.1016/j.neulet.2017.06.052.

Smith RA, Miller TM, Yamanaka K, et al. Antisense oligonucleotide therapy for neurodegenerative disease. J Clin Invest. 2006 Aug;116(8):2290-6.

So EY, Kang MH, Kim BS. Induction of chemokine and cytokine genes inastrocytes following infection with Theiler's murine encephalomyelitis virus is mediated by the Toll-like receptor 3. Glia. 2006 Jun;53(8):858-67.

Song W, Song Y, Kincaid B, Bossy B, Bossy-Wetzel E. Mutant SOD1-G93A triggers mitochondrial fragmentation in spinal cord motor neurons: neuroprotection by SIRT3 and PGC-1. Neurobiol Dis. 2013 Mar;51:72-81. doi: 10.1016/j.nbd.2012.07.004.

Sreedharan J, Blair IP, Tripathi VB, Hu X, Vance C, Rogelj B, Ackerley S, Durnall JC, Williams KL, Buratti E, Baralle F, de Belleroche J, Mitchell JD, Leigh PN, Al-Chalabi A, Miller CC, Nicholson G, Shaw CE. TDP-43 mutations in familial and sporadic amyotrophic lateral sclerosis. Science. 2008 Mar 21;319(5870):1668-72. doi: 10.1126/science.1154584.

Staats KA, Schönefeldt S, Van Rillaer M, Van Hoecke A, Van Damme P, Robberecht W, Liston A, Van Den Bosch L. Beta-2 microglobulin is important for disease progression in a murine model for amyotrophic lateral sclerosis. Front Cell Neurosci. 2013 Dec 10;7:249. doi: 10.3389/fncel.2013.00249.

Staff NP, Madigan NN, Morris J, Jentoft M, Sorenson EJ, Butler G, Gastineau D, Dietz A, Windebank AJ. Safety of intrathecal autologous adipose-derived mesenchymal stromal cells in patients with ALS. Neurology. 2016 Nov 22;87(21):2230-2234.

Steele J.C. and McGeer G.A. The ALS/PDC syndrome of Guam and the cycad hypothesis. Neurology 2008 70 (21), 1984-90.

Stifanese R, Averna M, De Tullio R, Pedrazzi M, Beccaria F, Salamino F, Milanese M, Bonanno G, Pontremoli S, Melloni E. Adaptive modifications in the calpain/calpastatin system in brain cells after persistent alteration in Ca2+ homeostasis. J Biol Chem. 2010 Jan 1;285(1):631-43. doi: 10.1074/jbc.M109.031674.

Stifanese R, Averna M, De Tullio R, Pedrazzi M, Milanese M, Bonifacino T, Bonanno G, Salamino F, Pontremoli S, Melloni E. Role of calpain-1 in the early phase of experimental ALS. Arch Biochem Biophys. 2014 Nov 15;562:1-8. doi: 10.1016/j.abb.2014.08.006.

Stoica L, Todeasa SH, Cabrera GT, Salameh JS, ElMallah MK, Mueller C, Brown RH Jr, Sena-Esteves M. Adeno-associated virus-delivered artificial microRNA extends survival and delays paralysis in an amyotrophic lateral sclerosis mouse model. Ann Neurol. 2016 Apr;79(4):687-700. doi: 10.1002/ana.24618.

Stoica R, De Vos KJ, Paillusson S, Mueller S, Sancho RM, Lau KF, Vizcay-Barrena G, Lin WL, Xu YF, Lewis J, Dickson DW, Petrucelli L, Mitchell JC, Shaw CE, Miller CC. ER-mitochondria associations are regulated by the VAPB-PTPIP51 interaction and are disrupted by ALS/FTD-associated TDP-43. Nat Commun. 2014 Jun 3;5:3996. doi: 10.1038/ncomms4996.

Stoica R, Paillusson S, Gomez-Suaga P, Mitchell JC, Lau DH, Gray EH, Sancho RM, Vizcay-Barrena G, De Vos KJ, Shaw CE, Hanger DP, Noble W, Miller CC. ALS/FTD-associated FUS activates GSK-3beta to disruptthe VAPB-PTPIP51 interaction and ER-mitochondria associations. EMBO Rep. 2016 Sep;17(9):1326-42. doi: 10.15252/embr.201541726.

Strong MJ, Volkening K, Hammond R, Yang W, Strong W, Leystra-Lantz C, Shoesmith C. TDP43 is a human low molecular weight neurofilament (hNFL) mRNA-binding protein. Mol Cell Neurosci. 2007 Jun;35(2):320-7.

Sudria-Lopez E, Koppers M, de Wit M, van der Meer C, Westeneng HJ, Zundel CA, Youssef SA, Harkema L, de Bruin A, Veldink JH, van den Berg LH, Pasterkamp RJ. Full ablation of C9orf72 in mice causes immune system-related pathology and neoplastic events but no motor neuron defects. Acta Neuropathol. 2016 Jul;132(1):145-7. doi: 10.1007/s00401-016-1581-x.

Sun H, Kawahara Y, Ito K, Kanazawa I, Kwak S. Slow and selective death of spinal motor neurons in vivo by intrathecal infusion of kainic acid: implications for AMPA receptor-mediated excitotoxicity in ALS. J Neurochem. 2006 Aug;98(3):782-91.

Sun H, Bénardais K, Stanslowsky N, Thau-Habermann N, Hensel N, Huang D, Claus P, Dengler R, Stangel M, Petri S. Therapeutic Potential of Mesenchymal Stromal Cells and MSC Conditioned Medium in Amyotrophic Lateral Sclerosis (ALS) - In Vitro Evidence from Primary Motor Neuron Cultures, NSC-34 Cells, Astrocytes and Microglia. PLoS One. 2013 Sep 12;8(9):e72926. doi: 10.1371/journal.pone.0072926.

Sun S, Sun Y, Ling SC, Ferraiuolo L, McAlonis-Downes M, Zou Y, Drenner K, Wang Y, Ditsworth D, Tokunaga S, Kopelevich A, Kaspar BK, Lagier-Tourenne C, Cleveland DW. Translational profiling identifies a cascade of damage initiated in motor neurons and spreading to glia in mutant SOD1-mediated ALS. Proc Natl Acad Sci U S A. 2015 Dec 15;112(50):E6993-7002. doi: 10.1073/pnas.1520639112.

Swanson GT, Kamboj SK, Cull-Candy SG. Single-channel properties of recombinant AMPA receptors depend on RNA editing, splice variation, and subunit composition. J Neurosci. 1997 Jan 1;17(1):58-69.

Swartz KR, Liu F, Sewell D, Schochet T, Campbell I, Sandor M, Fabry Z. Interleukin-6 promotes post-traumatic healing in the central nervous system. Brain Res. 2001 Mar 30;896(1-2):86-95. doi: 10.1016/s0006-8993(01)02013-3.

Swarup V, Phaneuf D, Dupré N, Petri S, Strong M, Kriz J, Julien JP. Deregulation of TDP-43 in amyotrophic lateral sclerosis triggersnuclear factorkB-mediated pathogenic pathways. J Exp Med. 2011 Nov 21;208(12):2429-47. doi: 10.1084/jem.20111313.

Sweeney MD, Zhao Z, Montagne A, Nelson AR, Zlokovic BV. Blood-Brain Barrier: From Physiology to Disease and Back. Physiol Rev. 2019 Jan 1;99(1):21-78. doi: 10.1152/physrev.00050.2017.

Tadić V, Malci A, Goldhammer N, Stubendorff B, Sengupta S, Prell T, Keiner S, Liu J, Guenther M, Frahm C, Witte OW, Grosskreutz J. Sigma 1 receptor activation modifies intracellular calcium exchange in the G93AhSOD1 ALS model. Neuroscience. 2017 Sep 17;359:105-118. doi: 10.1016/j.neuroscience.2017.07.012.

Taes I, Timmers M, Hersmus N, Bento-Abreu A, Van Den Bosch L, Van Damme P, Auwerx J, Robberecht W. Hdac6 deletion delays disease progression in the SOD1G93A mouse model of ALS. Hum Mol Genet. 2013 May 1;22(9):1783-90. doi: 10.1093/hmg/ddt028.

Takuma H, Kwak S, Yoshizawa T, Kanazawa I. Reduction of GluR2 RNA editing, a molecular change that increases calcium influx through AMPA receptors, selective in the spinal ventral gray of patients with amyotrophic lateral sclerosis. Ann Neurol. 1999 Dec;46(6):806-15.

Tardy M, Fages C, Le Prince G, Rolland B, Nunez J. Regulation of the glial fibrillary acidic protein (GFAP) and of its encoding mRNA in the developing brain and in cultured astrocytes. Adv Exp Med Biol. 1990;265:41-52. doi:10.1007/978-1-4757-5876-4_4.

Tateishi T, Yamasaki R, Tanaka M, Matsushita T, Kikuchi H, Isobe N, Ohyagi Y, Kira J. CSF chemokine alterations related to the clinical course of amyotrophic lateral sclerosis. J Neuroimmunol. 2010 May;222(1-2):76-81. doi: 10.1016/j.jneuroim.2010.03.004.

Therrien M, Rouleau GA, Dion PA, Parker JA. Deletion of C9ORF72 results in motor neuron degeneration and stress sensitivity in C. Elegans. PLoS One. 2013 Dec 12;8(12):e83450. doi: 10.1371/journal.pone.0083450.

Thomsen GM, Alkaslasi M, Vit JP, Lawless G, Godoy M, Gowing G, Shelest O, Svendsen CN. Systemic injection of AAV9-GDNF provides modest functional improvements in the SOD1(G93A) ALS rat but has adverse side effects. Gene Ther. 2017 Apr;24(4):245-252. doi: 10.1038/gt.2017.9.

Thomsen GM, Avalos P, Ma AA, Alkaslasi M, Cho N, Wyss L, Vit JP, Godoy M, Suezaki P, Shelest O, Bankiewicz KS, Svendsen CN. Transplantation of Neural Progenitor Cells Expressing Glial Cell Line-Derived Neurotrophic Factor into the Motor Cortex as a Strategy to Treat Amyotrophic Lateral Sclerosis. Stem Cells. 2018 Jul;36(7):1122-1131. doi: 10.1002/stem.2825.

Thomsen GM, Gowing G, Latter J, Chen M, Vit JP, Staggenborg K, Avalos P, Alkaslasi M, Ferraiuolo L, Likhite S, Kaspar BK, Svendsen CN. Delayed disease onset and extended survival in the SOD1G93A rat model of amyotrophic lateral sclerosis after suppression of mutant SOD1 in the motor cortex. J Neurosci. 2014 Nov 19;34(47):15587-600. doi: 10.1523/JNEUROSCI.2037-14.2014.

Ticozzi N, LeClerc AL, Keagle PJ, Glass JD, Wills AM, van Blitterswijk M, Bosco DA, Rodriguez-Leyva I, Gellera C, Ratti A, Taroni F, McKenna-Yasek D, Sapp PC, Silani V, Furlong CE, Brown RH Jr, Landers JE. Paraoxonase gene mutations in amyotrophic lateral sclerosis. Ann Neurol. 2010 Jul;68(1):102-7. doi: 10.1002/ana.21993.

Tognatta R, Miller RH. Contribution of the oligodendrocyte lineage to CNS repair and neurodegenerative pathologies. Neuropharmacology. 2016 Nov;110(Pt B):539-547. doi: 10.1016/j.neuropharm.2016.04.026.

Tortarolo M, Vallarola A, Lidonnici D, Battaglia E, Gensano F, Spaltro G, Fiordaliso F, Corbelli A, Garetto S, Martini E, Pasetto L, Kallikourdis M, Bonetto V, Bendotti C. Lack of TNFalpha receptor type 2 protects motor neurons in a cellular model of amyotrophic lateral sclerosis and in mutant SOD1 mice but does not affect disease progression. J Neurochem. 2015 Oct;135(1):109-24. doi: 10.1111/jnc.13154.

Tripathi P, Rodriguez-Muela N, Klim JR, de Boer AS, Agrawal S, Sandoe J, Lopes CS, Ogliari KS, Williams LA, Shear M, Rubin LL, Eggan K, Zhou Q. Reactive Astrocytes Promote ALS-like Degeneration and Intracellular Protein Aggregation in Human Motor Neurons by Disrupting Autophagy through TGF-b1. Stem Cell Reports. 2017 Aug 8;9(2):667-680. doi: 10.1016/j.stemcr.2017.06.008.

Tripathi VB, Baskaran P, Shaw CE, Guthrie S. Tar DNA-binding protein-43 (TDP-43) regulates axon growth in vitro and in vivo. Neurobiol Dis. 2014 May;65:25-34. doi: 10.1016/j.nbd.2014.01.004.

Trotti D, Volterra A, Lehre KP, Rossi D, Gjesdal O, Racagni G. Danbolt NC. Arachidonic acid inhibits a purified and reconstituted glutamate transporter directly from the water phase and not via the phospholipid membrane. J Biol Chem. 1995 Apr 28;270(17):9890-5.

Uccelli A, Milanese M, Principato MC, Morando S, Bonifacino T, Vergani L, Giunti D, Voci A, Carminati E, Giribaldi F, Caponnetto C, Bonanno G. Intravenous mesenchymal stem cells improve survival and motor function in experimental amyotrophic lateral sclerosis. Mol Med. 2012 Jul 18;18:794-804. doi: 10.2119/molmed.2011.00498.

Uday B, Dipak D, Ranajit BK. Reactive oxygen species: Oxidative damage and pathogenesis. Curr. Sci. 1990, 77, 658–666

Urwin H, Authier A, Nielsen JE, Metcalf D, Powell C, Froud K, Malcolm DS, Holm I, Johannsen P, Brown J, Fisher EM, van der Zee J, Bruyland M; FReJA Consortium, Van Broeckhoven C, Collinge J, Brandner S, Futter C, Isaacs AM. Disruption of endocytic trafficking in frontotemporal dementia with CHMP2B mutations. Hum Mol Genet. 2010 Jun 1;19(11):2228-38. doi: 10.1093/hmg/ddq100.

van Blitterswijk M1, van Vught PW, van Es MA, Schelhaas HJ, van der Kooi AJ, de Visser M, Veldink JH, van den Berg LH. Novel optineurin mutations in sporadic amyotrophic lateral sclerosis patients. Neurobiol Aging. 2012 May;33(5):1016.e1-7. doi: 10.1016/j.neurobiolaging.2011.05.019.

Van Damme P, Bogaert E, Dewil M, Hersmus N, Kiraly D, Scheveneels W, Bockx I, Braeken D, Verpoorten N, Verhoeven K, Timmerman V, Herijgers P, Callewaert G, Carmeliet P, Van Den Bosch L, Robberecht W. Astrocytes regulate GluR2 expression in motor neurons and their vulnerability to excitotoxicity. Proc Natl Acad Sci U S A. 2007 Sep 11;104(37):14825-30.

Van Damme P, Dewil M, Robberecht W, Van Den Bosch L. Excitotoxicity and amyotrophic lateral sclerosis. Neurodegener Dis. 2005;2(3-4):147-59.

Van Den Bosch L, Vandenberghe W, Klaassen H, Van Houtte E, Robberecht W. Ca2+-permeable AMPA receptors and selective vulnerability of motor neurons. J Neurol Sci. 2000 Nov 1;180(1-2):29-34.

van Loo G, De Lorenzi R, Schmidt H, Huth M, Mildner A, Schmidt-Supprian M, Lassmann H, Prinz MR, Pasparakis M. Inhibition of transcription factor NF-kB in the central nervous system ameliorates autoimmune encephalomyelitis in mice. Nat Immunol. 2006 Sep;7(9):954-61.

Vance C, Al-Chalabi A, Ruddy D, Smith BN, Hu X, Sreedharan J, Siddique T, Schelhaas HJ, Kusters B, Troost D, Baas F, de Jong V, Shaw CE. Familial amyotrophic lateral sclerosis with frontotemporal dementia is linked to a locus on chromosome 9p13.2–21.3. Brain. 2006 Apr;129(Pt 4):868-76.

Vance C, Rogelj B, Hortobágyi T, De Vos KJ, Nishimura AL, Sreedharan J, Hu X, Smith B, Ruddy D, Wright P, Ganesalingam J, Williams KL, Tripathi V, Al-Saraj S, Al-Chalabi A, Leigh PN, Blair IP, Nicholson G, de Belleroche J, Gallo JM, Miller CC, Shaw CE. Mutations in FUS, an RNA processing protein, cause familial amyotrophic lateral sclerosis type 6. Science 323, 1208–1211. doi: 10.1126/science.1165942.

Vandenberghe W, Van Den Bosch L, Robberecht W. Glial cells potentiate kainate-induced neuronal death in a motoneuron-enriched spinal coculture system. Brain Res. 1998 Oct 5;807(1-2):1-10. doi: 10.1016/s0006-8993(98)00569-1.

Varcianna A, Myszczynska MA, Castelli LM, O'Neill B, Kim Y, Talbot J, Nyberg S, Nyamali I, Heath PR, Stopford MJ, Hautbergue GM, Ferraiuolo L. Micro-RNAs secreted through astrocyte-derived extracellular vesicles cause neuronal network degeneration in C9orf72 ALS. EBioMedicine. 2019 Feb; 40:626-635. doi: 10.1016/j.ebiom.2018.11.067.

Vargas MR, Pehar M, Cassina P, Beckman JS, Barbeito L. Increased glutathione biosynthesis by Nrf2 activation in astrocytes prevents p75NTR-dependent motor neuron apoptosis. J Neurochem. 2006 May;97(3):687-96.

Verkhratsky A, Zorec R. Astroglial signalling in health and disease. Neurosci Lett. 2019 Jan 10;689:1-4. doi: 10.1016/j.neulet.2018.07.026.

Vigo T, Procaccini C, Ferrara G, Baranzini S, Oksenberg JR, Matarese G, Diaspro A, Kerlero de Rosbo N, Uccelli A. IFN-γ orchestrates mesenchymal stem cell plasticity through the signal transducer and activator of transcription 1 and 3 and mammalian target of rapamycin pathways. J Allergy Clin Immunol. 2017 May;139(5):1667-1676. doi: 10.1016/j.jaci.2016.09.004.

Volk AE, Weishaupt JH, Andersen PM, Ludolph AC, Kubisch C. Current knowledge and recent insights into the genetic basis of amyotrophic lateral sclerosis. Medgen 2018. 30:252-258. https://doi.org/10.1007/s11825-018-0185-3.

Volonté C, Amadio S, Fabbrizio P, Apolloni S. Functional microglia neurotransmitters in amyotrophic lateral sclerosis. Semin Cell Dev Biol. 2019 Oct;94:121-128. doi: 10.1016/j.semcdb.2019.04.014.

Vucic S, Kiernan MC. Novel threshold tracking techniques suggest that cortical hyperexcitability is an early feature of motor neuron disease. Brain 2006 129, 2436–2446.

Wagle-Shukla A, Ni Z, Gunraj CA, Bahl N, Chen R. Effects of short interval intracortical inhibition and intracortical facilitation on short interval intracortical facilitation in human primary motor cortex . J Physiol 2009 587:5665–5678. doi: 10.1113/jphysiol.2009.181446.

Waite AJ, Bäumer D, East S, Neal J, Morris HR, Ansorge O, Blake DJ Reduced C9orf72 protein levels in frontal cortex of amyotrophic lateral sclerosis and frontotemporal degeneration brain with the C9ORF72 hexanucleotide repeat expansion. Neurobiol Aging. 2014 Jul;35(7):1779.e5-1779.e13. doi: 10.1016/j.neurobiolaging.2014.01.016.

Walker CL, Meadows RM, Merfeld-Clauss S, Du Y, March KL, Jones KJ. Adipose-derived stem cell conditioned medium impacts asymptomatic peripheral neuromuscular denervation in the mutant superoxide dismutase (G93A) transgenic mouse model of amyotrophic lateral sclerosis. Restor Neurol Neurosci. 2018;36(5):621-627. doi: 10.3233/RNN-180820.

Walsh MC, Lee J, Choi Y.Tumor necrosis factor receptor- associated factor 6 (TRAF6) regulation of development, function, and homeostasis of the immune system. Immunol Rev. 2015 Jul;266(1):72-92. doi: 10.1111/imr.12302.

Wang L, Pei S, Han L, Guo B, Li Y, Duan R, Yao Y, Xue B, Chen X, Jia Y. Mesenchymal Stem Cell-Derived Exosomes Reduce A1 Astrocytes via Downregulation of Phosphorylated NFκB P65 Subunit in Spinal Cord Injury. Cell Physiol Biochem. 2018;50(4):1535-1559. doi: 10.1159/000494652.

Wang SJ, Wang KY, Wang WC.. Mechanisms underlying the riluzole inhibition of glutamate release from rat cerebral cortex nerve terminals (synaptosomes). Neuroscience. 2004;125(1):191-201. doi: 10.1016/j.neuroscience.2004.01.019.

Wang W, Li L, Lin WL, Dickson DW, Petrucelli L, Zhang T, Wang X. The ALS disease-associated mutant TDP-43 impairs mitochondrial dynamics and function in motor neurons. Hum Mol Genet. 2013 Dec 1;22(23):4706-19. doi: 10.1093/hmg/ddt319.

Wang X, Schwarz TL. The mechanism of Ca2+−dependent regulation of kinesin-mediated mitochondrial motility. Cell. 2009 Jan 9;136(1):163-74. doi: 10.1016/j.cell.2008.11.046.

Wang Z, Wei D, Xiao H. Methods of cellular senescence induction using oxidative stress. Methods Mol Biol. 2013;1048:135-44. doi: 10.1007/978-1-62703-556-9_11.

Wen X, Westergard T, Pasinelli P, Trotti D. Pathogenic determinants and mechanisms of ALS/FTD linked to hexanucleotide repeat expansions in the C9orf72 gene. Neurosci Lett. 2017 Jan 1;636:16-26. doi: 10.1016/j.neulet.2016.09.007.

Westrate LM, Drocco JA, Martin KR, Hlavacek WS, MacKeigan JP. Mitochondrial morphological features are associated with fission and fusion events PLoS One. 2014 Apr 14;9(4):e95265. doi: 10.1371/journal.pone.0095265.

Wiese S, Herrmann T, Drepper C, Jablonka S, Funk N, Klausmeyer A, Rogers ML, Rush R, Sendtner M. Isolation and enrichment of embryonic mouse motoneurons from the lumbar spinal cord of individual mouse embryos. Nat Protoc. 2010 Jan;5(1):31-8. doi: 10.1038/nprot.2009.193.

Williams, D. B., and Windebank, A. J. Motor neuron disease (amyotrophic lateral sclerosis). Mayo Clin. Proc. 1991 65, 54-82.

Williamson TL and Cleveland DW. Slowing of axonal transport is a very early event in the toxicity of ALS-linked SOD1 mutants to motor neurons. Nat Neurosci. 1999 Jan;2(1):50-6.

Willis GR, Fernandez-Gonzalez A, Anastas J, Vitali SH, Liu X, Ericsson M, Kwong A, Mitsialis, SA, Kourembanas S. Mesenchymal Stromal Cell Exosomes Ameliorate Experimental Bronchopulmonary Dysplasia and Restore Lung Function through Macrophage Immunomodulation. Am J Respir Crit Care Med. 2018 Jan 1;197(1):104-116. doi: 10.1164/rccm.201705-0925OC.

Winton MJ, Igaz LM, Wong MM, Kwong LK, Trojanowski JQ, Lee VM-Y. Disturbance of nuclear and cytoplasmic TAR DNA-binding protein (TDP-43) induces disease-like redistribution, sequestration, and aggregate formation. J Biol Chem 2008;283:13302–13309.

Xia C, Zeng Z, Fang B, Tao M, Gu C, Zheng L, Wang Y, Shi Y, Fang C, Mei S, Chen Q, Zhao J, Lin X, Fan S, Jin Y, Chen P. Mesenchymal stem cell -derived exosomes ameliorate intervertebral disc degeneration via anti-oxidant and anti inflammatory effects. Free Radic Biol Med. 2019 Jul 24;143:1-15. doi: 10.1016/j.freeradbiomed.2019.07.026.

Xiao S, MacNair L, McGoldrick P, McKeever PM, McLean JR, Zhang M, Keith J, Zinman L, Rogaeva E, Robertson J. Isoform-specific antibodies reveal distinct subcellular localizations of C9orf72 in amyotrophic lateral sclerosis. Ann Neurol. 2015 Oct;78(4):568-83. doi: 10.1002/ana.24469.

Xu L, Yan J, Chen D, Welsh AM, Hazel T, Johe K, Hatfield G, Koliatsos VE. Human neural stem cell grafts ameliorate motor neuron disease in SOD-1 transgenic rats. Transplantation. 2006 Oct 15;82(7):865-75. doi:10.1097/01.tp.0000235532.00920.7a.

Xu YF, Gendron TF, Zhang YJ, Lin WL, D'Alton S, Sheng H, Casey MC, Tong J, Knight J, Yu X, Rademakers R, Boylan K, Hutton M, McGowan E, Dickson DW, Lewis J, Petrucelli L. Wild-type human TDP-43 expressioncauses TDP-43 phosphorylation, mitochondrial aggregation, motor deficits,and early mortality in transgenic mice. J Neurosci. 2010 Aug 11;30(32):10851-9. doi: 10.1523/JNEUROSCI.1630-10.2010.

Yamanaka K, Boillee S, Roberts EA, Garcia ML, McAlonis-Downes M, Mikse OR, Cleveland DW, Goldstein LS. Mutant SOD1 in cell types other than motor neurons and oligodendrocytes accelerates onset of disease in ALS mice. Proc Natl Acad Sci U S A. 2008 May 27;105(21):7594-9. doi: 10.1073/pnas.0802556105.

Yamanaka K, Chun SJ, Boillee S, Fujimori-Tonou N, Yamashita H, Gutmann DH, Takahashi R, Misawa H, Cleveland DW. Astrocytes as determinants of disease progression in inherited amyotrophic lateral sclerosis. Nat Neurosci. 2008 Mar;11(3):251-3. doi: 10.1038/nn2047.

Yamanaka K, Komine O.The multi-dimensional roles of astrocytes in ALS. Neurosci Res. 2018 Jan;126:31-38. doi: 10.1016/j.neures.2017.09.011.

Yi J, Ma C, Li Y, Weisleder N, Ríos E, Ma J, Zhou J. Mitochondrial calcium uptake regulates rapid calcium transients in skeletal muscle during excitationcontraction (E-C) coupling. J Biol Chem. 2011 Sep 16;286(37):32436-43. doi: 10.1074/jbc.M110.217711.

Yi M, Weaver D, Hajnóczky G. Control of mitochondrial motility and distribution by the calcium signal: a homeostatic circuit. J J Cell Biol. 2004 Nov 22;167(4):661-72.

Yin HZ, Hsu CI, Yu S, Rao SD, Sorkin LS, Weiss JH. TNF-α triggers rapid membrane insertion of Ca(2+) permeable AMPA receptors into adult motor neurons and enhances their susceptibility to slow excitotoxic injury. Exp Neurol. 2012 Dec;238(2):93-102. doi: 10.1016/j.expneurol.2012.08.004.

Yoshihara T, Ishigaki S, Yamamoto M, Liang Y, Niwa J, Takeuchi H, Doyu M, Sobue G. Differential expression of inflammation- and apoptosis-related genes in spinal cords of a mutant SOD1 transgenic mouse model of familial amyotrophic lateral sclerosis. J Neurochem. 2002 Jan;80(1):158-67. doi: 10.1046/j.0022-3042.2001.00683.x

Yu YC, Kuo CL, Cheng WL, Liu CS, Hsieh M. Decreased antioxidant enzyme activity and increate mitochondrial DNA damage in cellular models of Machado Joseph disease. J Neurosci Res. 2009 Jun;87(8):1884-91. doi: 10.1002/jnr.22011.

Yufang Shi, Yu Wang, Qing Li, Keli Liu, Jianquan Hou, Changshun Shao and Ying Wang. Immunoregulatory mechanisms of mesenchymal stem and stromal cells in inflammatory diseases. Nat Rev Nephrol. 2018 Aug;14(8):493-507. doi: 10.1038/s41581-018-0023-5.

Zamanian JL, Xu L, Foo LC, Nouri N, Zhou L, Giffard RG, Barres BA. Genomic analysis of reactive astrogliosis. J Neurosci. 2012 May 2;32(18):6391-410. doi: 10.1523/JNEUROSCI.6221-11.2012.

Zappia E, Casazza S, Pedemonte E, Benvenuto F, Bonanni I, Gerdoni E, Giunti D, Ceravolo A, Cazzanti F, Frassoni F, Mancardi G, Uccelli A. Mesenchymal stem cells ameliorate experimental autoimmune encephalomyelitis inducing T-cell anergy. Blood. 2005 Sep 1;106(5):1755-61. doi: 10.1182/blood-2005-04-1496.

Zhang S, Tang MB, Luo HY, Shi CH, Xu YM. Necroptosis in neurodegenerative diseases: a potential therapeutic target. Cell Death Dis. 2017 Jun 29;8(6):e2905. doi: 10.1038/cddis.2017.286.

Zhang T, Baldie G, Periz G, Wang J. RNA-processing protein TDP-43regulates FOXO-dependent protein quality control in stress response. PLoS Genet. 2014 Oct 16;10(10):e1004693. doi: 10.1371/journal.pgen.1004693.

Zhang YJ, Jansen-West K, Xu YF, Gendron TF, Bieniek KF, Lin WL, Sasaguri H, Caulfield T, Hubbard J, Daughrity L, Chew J, Belzil VV, Prudencio M, Stankowski JN, Castanedes-Casey M, Whitelaw E, Ash PE, DeTure M, Rademakers R, Boylan KB, Dickson DW, Petrucelli L. Aggregation-prone c9FTD/ALS poly(GA) RAN-translated proteins cause neurotoxicity by inducing ER stress. Acta Neuropathol. 2014 Oct;128(4):505-24. doi: 10.1007/s00401-014-1336-5.

Zhao W, Beers DR, Hooten KG, Sieglaff DH, Zhang A, Kalyana-Sundaram S, Traini CM, Halsey WS, Hughes AM, Sathe GM, Livi GP, Fan GH, Appel SH. Characterization of gene expression phenotype in amyotrophic lateral sclerosis monocytes. JAMA Neurol. 2017 Jun 1;74(6):677-685. doi: 10.1001/jamaneurol.2017.0357.

Zhou Y, Yamamoto Y, Xiao Z, Ochiya T. The Immunomodulatory Functions of Mesenchymal Stromal/Stem Cells Mediated via Paracrine Activity. J Clin Med. 2019 Jul 12;8(7). doi: 10.3390/jcm8071025.